The role of auxin transport in the control of shoot branching

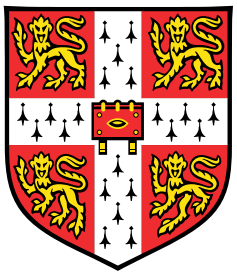

Martin van Rongen

Supervisor: Prof. Ottoline Leyser
Prof. Henrik Jönsson

Department of Plant Sciences
University of Cambridge

This dissertation is submitted for the degree of
Doctor of Philosophy

Clare Hall September 2017

The role of auxin transport in the control of shoot branching

Martin van Rongen

Branching is a highly plastic trait, enabling plants to adapt their growth form in response to environmental stimuli. In flowering plants, shoot branching is regulated through the activity of axillary buds, which grow into branches. Several classes of plant hormones have been shown to play pivotal roles in regulating bud outgrowth. Auxin derived from the primary shoot apex and active branches inhibits bud outgrowth, whereas cytokinin promotes it. Strigolactones also inhibit bud outgrowth, by changing properties of the auxin transport network, increasing the competition between buds. This occurs by modulating access to the polar auxin transport stream (PATS) in the main stem. The PATS provides directional, long distance transport of auxin down the stem, involving basal localisation of the auxin transporter PIN-FORMED1 (PIN1). Buds need to export their auxin across the stem towards the PATS in order to activate, but since PIN1 is mainly expressed in narrow files of cells associated with the stem vasculature, PIN1 itself it is unlikely to facilitate this connectivity.

This thesis re-examines the role of auxin transport in the stem, showing that, besides the PIN1-mediated PATS, other auxin transport proteins constitute a more widespread and less polar auxin transport stream, allowing auxin exchange between the PATS and surrounding tissues. Disruption of this transport stream is shown to reduce bud-bud communication and to partially rescue the increased branching observed in strigolactone mutants. Furthermore, it is shown that distinct classes of auxin transport proteins within this stream can differentially affect bud outgrowth mediated by *BRANCHED1* (*BRC1*). BRC1 is a transcription factor proposed to determine bud activation potential. Taken together, the data presented here provide a more comprehensive understanding of the shoot auxin transport network and its role in shoot branching regulation.

To Sarah.

Declaration

This dissertation is the result of my own work and includes nothing which is the outcome of work done in collaboration except as declared in the Preface and specified in the text. It is not substantially the same as any that I have submitted, or, is being currently submitted for a degree or diploma or other qualification at the University of Cambridge or any other University or similar institution except as declared in the Preface and specified in the text. I further state that no substantial part of my dissertation has already been submitted for any such degree, diploma or other qualification at the University of Cambridge or any other University or similar institution except as declared in the Preface or specified in the text. It does not exceed the prescribed word limit of 60,000 words excluding bibliography, figures, tables and appendices.

Martin van Rongen
September 2017

Acknowledgements

Many people have supported me in the past years during my Ph.D, for which I am very grateful. Although I cannot thank everybody involved individually, I would like to acknowledge some people in particular. Foremost, I would like to thank Ottoline for her continuous support and advice. Her interest in my research and the freedom she has given me to pursue some of my own research interests have made the last few years very enjoyable. Her advice has helped me become a better scientist by taking my ability to think critically and write clearly to a new level. Lastly, her supportive attitude towards combining science and family life gave me the confidence to start a family during my Ph.D, something I would have been very unsure of doing in any other lab. Further thanks also go to Henrik Jönsson and Siobhan Braybrook, whose supervision and support have enabled me to do this research.

All the people in the Leyser lab, past and present, have been very supportive. In particular I would like to thank Tom Bennett for his great support, on more than one occasion helping me find direction when I felt I had lost the plot. A special mention to Genevieve Hines, whose computational modelling and resulting discussions have contributed so much to understanding the sometimes complicated results. I would also like to thank Sally Ward, Maddy Seale, Fabrizio Ticchiarelli, Tanya Waldie, Devin O'Connor and Graeme Mitchison for their help and discussions. Thanks also go to Hugo Tavares, for his help with and discussions on data analysis and statistics.

There has been a lot of technical assistance over the years. First, I would like to thank Ruth Stephens for her technical support in setting up some experiments and looking after plants. Also, Rebecca Butler and Alice Thomas for their help with the nitrate experiments. General support within the Sainsbury Laboratory has been exceptional. I would like to thank Ray Wightman for his microscopy support, the Horticulture staff for their great work on keeping the plant growth facilities going and the Support staff for keeping the lab running so smoothly.

All the experiments were designed and carried out by myself, but I received general technical assistance from Ruth with sowing out experiments and, specifically, setting up the jar assays (Fig. 4.6; 4.10; 5.9). The nitrate experiments were sown out and looked after by Rebecca and Alice (Fig. 5.10). All primary data were collected by myself. The following data,

or part thereof, have been published in Bennett et al. (2016a): Fig. 3.4; 3.8A; 4.2B; 4.5C; 4.8A. Plant lines have been received from various people, as indicated in Appendix A, for which I am grateful.

Lastly, I would like to thank my family. At times the hardest parts, but the ones which also brought the greatest sense of achievement, were mammalian in nature rather than plant-based. For sure, my lovely little girls Lily and Tess have helped me keep things in perspective. Finally, I would like to thank Sarah for her amazing support which enabled me to get to this exciting new starting point. Sarah, we are a far cry from our life as diving instructors in Egypt and I am grateful for every step along the way.

Table of contents

List of figures

List of tables

Chapter 1

Introduction

This thesis concerns the hormonal control of shoot branching and, specifically, the role of transport of the plant hormone auxin.

1.1 Plant architecture

The sessile nature of plants means that they are unable to escape from unfavourable habitats. Instead they need to adapt to the prevailing environmental conditions. Plants are able to do so by changing their body architecture. The root system can change its architecture in response to soil nutrient availability and increases nutrient foraging when there is a shortage of nutrients. The shoot system has to cope with a range of biotic and abiotic factors, such as herbivory and optimising photosynthetic input.

The ability of plants to adapt their body architecture lies in the indeterminate nature of their development. The general body plan is determined very early in the plant's life cycle, during embryogenesis. Here the apical-basal axis is formed, with a shoot apical meristem at the apex and a root apical meristem at the base. The shoot apical meristem determines the subsequent growth of all above ground parts of the plant. It does so in a modular manner by forming phytomers. A phytomer is a repeating unit, which consists of a node and its associated leaf or leaves and axillary meristem, and an internode connecting the phytomer to the next node (Fig. 1.1). Axillary meristems have the same growth potential as the primary shoot apical meristem and can give rise to higher order plant structures. Axillary meristems can form axillary buds, which can either remain dormant or continue to grow and form a branch. The number of phytomers formed, and the activity of the axillary buds thus make an important contribution to determining shoot architecture.

The regulation of axillary bud outgrowth is important because it can influence the reproductive success of the plant. Lateral branches provide a new source of growth when the

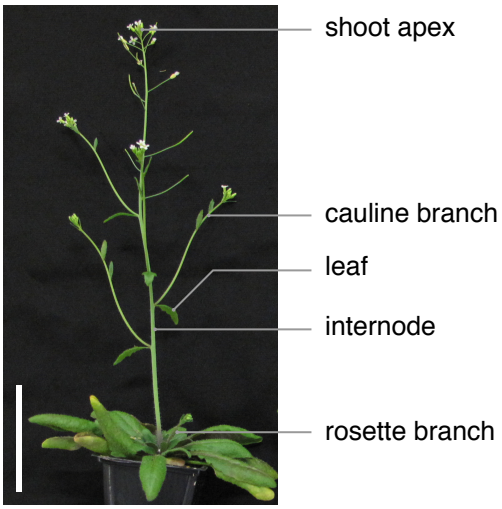

Fig. 1.1 Arabidopsis plant architecture.
Photograph of a 5-week old Arabidopsis plant, grown under long day conditions. The main architecture of the plant is indicated. Bar = 50 mm.

plant is damaged. Lateral branches also produce flowers, which in turn can determine the number of seeds the plant produces in its life. Furthermore, lateral branches can optimise light capture for photosynthesis. All these factors are strongly affected by environmental conditions, making the axillary bud a crucial integrator for the plant's growth response to its environment.

The outgrowth of lateral branches is strongly affected by the activity of the primary shoot apex which, when active, is able to prevent lateral branches from growing. This process is called apical dominance and prevents excessive proliferation of lateral branches when the primary shoot is growing. Directing growth at the shoot apex can have adaptive advantages to the plant, since concentrating growth in the vertical axis can optimise light capture for photosynthesis and allows the plant to outcompete neighbouring plants. The mechanism of apical dominance also ensures rapid activation of lateral branches when, for example due to herbivory, the primary shoot is damaged and the degree of apical dominance is reduced.

The inhibitory effect of the primary shoot apex on lateral branch outgrowth would suggest that branches activate in a basal to apical pattern, since the lateral buds closest to the apex would experience the strongest inhibition. Axillary meristems are formed in the rosette leaf axils when they are approximately 17 nodes removed from the primary shoot apex (Stirnberg et al., 1999). This normally only occurs during prolonged vegetative growth, since under standard long day growth conditions the plant transitions to flowering and at this transition the formation of rosette leaves normally stops. During prolonged vegetative growth lateral buds activate in a basal to apical pattern (Grbic and Bleecker, 1996). However, after floral

transition lateral branches activate rapidly along the primary shoot axis in an apical to basal pattern (Hempel and Feldman, 1994; Stirnberg et al., 1999).

Branching patterns are highly influenced by plant hormones, which change their distribution and activity throughout development and according to growth conditions. As such, they enable the plant to regulate its growth. The role of several hormones in this process is discussed in the following section.

1.2 Plant hormones in shoot development

Plant hormones are substances that affect plant growth and are able to do so at very low concentrations. Hormones are active throughout the entire life cycle of the plant and can have major effects on the shoot architecture of the plant. Transition from a dormant to an active state in axillary buds is strongly influenced by the activity of plant hormones. Three hormones, auxin, cytokinin and strigolactone, appear to be particularly important in the switch to activation and are the focus of the following discussion.

1.2.1 Auxin

Auxins are a class of plant hormones of which indole-3-acetic acid (IAA) is the most abundant. The two main sources of free IAA are de novo synthesis of IAA and release of IAA from stores of conjugates. Synthesis of IAA in plants can occur via different biosynthetic pathways. In most pathways the aromatic amino acid tryptophan is used as a precursor, but mechanisms independent of tryptophan also exist (reviewed in Zhao, 2010). The main biosynthetic pathway for IAA in Arabidopsis uses the intermediate indole-3-pyruvate (IPA), which is catalysed from tryptophan by TAA1 (TRYPTOPHAN AMINOTRANSFERASE of ARABIDOPSIS) and several other closely related proteins (Stepanova et al., 2008; Tao et al., 2008). Members of the YUCCA protein family then catalyse the conversion of IPA to IAA (Mashiguchi et al., 2011; Stepanova et al., 2011; Won et al., 2011; Zhao, 2012).

Auxin conjugates are formed when amino acids or sugars are added to IAA. Auxin conjugates are thought to be inactive, providing a pool of auxin that can be released into its biologically active form (Bartel and Fink, 1995; Jakubowska and Kowalczyk, 2005; Rampey et al., 2004; Östin et al., 1998). The addition of amino acids to IAA is facilitated by the GH3 (GRETCHEN HAGEN3) family of proteins (Staswick et al., 2005). Sugar addition to IAA is catalysed by UGTs (UDP GLUCOSYL TRANSFERASE) (Jackson et al., 2001; Szerszen et al., 1994). Auxin is also degraded and the oxidised form of IAA, 2-oxindole-3-acetic acid

(oxIAA), is a primary catabolite in Arabidopsis (Peer et al., 2013; Pěnčík et al., 2013; Östin et al., 1998).

Perception of auxin occurs through an Skp1-Cullin-F-box (SCF) E3 ubiquitin ligase complex. In Arabidopsis, ASK1 (ARABIDOPSIS SKIP-LIKE1) and CUL1 (CULLIN1) form the Skp1 and Cullin subunits, respectively. Target specificity is mediated by the F-box protein subunit, of which the TIR1 (TRANSPORT INHIBITOR RESPONSE1) protein is an important member (Dharmasiri et al., 2005; Gray et al., 2001; Kepinski and Leyser, 2005; Ruegger et al., 1998). The SCF complex targets proteins for ubiquitination, which marks them for degradation via the 26S proteasome. The TIR1 protein is related to a family of F-box proteins, called AFBs (AUXIN RESPONSE F-BOX) and collectively these proteins mediate transcriptional auxin responses (Dharmasiri et al., 2005). Upon binding with auxin, TIR1/AFBs interact with Aux/IAA (AUXIN/INDOLE-3-ACETIC ACID) proteins, which act as co-receptors. Aux/IAAs contain the conserved DII domain, which forms a lid-like structure upon binding to auxin and TIR1/AFBs (Tan et al., 2007). Auxin affinity is largely determined by the differential auxin sensing properties which arise from the different TIR1/AFB - Aux/IAA combinations (Calderón Villalobos et al., 2012). Through these interactions, auxin brings the Aux/IAAs to the SCF complex, resulting in their ubiquitination and degradation via the 26S proteasome pathway (Gray et al., 2001; Maraschin F dos et al., 2009). Aux/IAAs act as transcriptional repressors and in the absence of auxin they bind to AUXIN RESPONSE FACTOR (ARF) transcription factors, which prevents the ARFs from activating the transcription of auxin-inducible genes (Guilfoyle and Hagen, 2007; Guilfoyle et al., 1998; Ulmasov et al., 1997).

Transport of auxin occurs predominantly through the activity of specialised transport proteins. The function of these proteins is discussed in Section 1.3.

1.2.2 Cytokinin

Cytokinins are a class of plant hormones that induce cytokinesis, or cell division, in the presence of auxin. Several natural cytokinins occur in plants, of which *trans*-zeatin (tZ) and isopentenyladenine (iP) are most abundant in angiosperms. The initial step of iP and tZ cytokinin synthesis is mediated through the activity of *ADENYLATE ISOPENTENYL-TRANSFERASE* (*IPT*) genes (reviewed in Kudo et al., 2010), which are expressed throughout the plant (Miyawaki et al., 2004). Active cytokinin is formed by conversion of iP and tZ nucleotides by LONELY GUY (LOG) family members (Kurakawa et al., 2007; Kuroha et al., 2009).

Degradation of cytokinins in Arabidopsis is catalysed by the members of the *CYTOKININ OXIDASE/DEHYDROGENASE* (*CKX*) gene family. Overexpression of *CKX* genes results in

enhanced breakdown of cytokinins and the catabolism of cytokinins contribute to the correct regulation of cytokinin function in development (Werner et al., 2003).

Perception of cytokinin occurs through a two-component phosphorelay system (reviewed in Hwang et al., 2012). The ARABIDOPSIS HIS KINASE (AHK) receptors are membrane localised and autophosphorylate upon binding with cytokinin. The phosphate is relayed to the ARABIDOPSIS HIS PHOSPHOTRANSFER PROTEINS (AHP), which then move from the cytoplasm into the nucleus. Within the nucleus there are two types of ARABIDOPSIS RESPONSE REGULATORS (ARRs), type A and type B. The type B ARRs act as DNA-binding transcription factors, promoting cytokinin signalling responses. They directly promote the expression of type A ARRs. Type A ARRs are positively regulated by cytokinin and complete a negative feedback loop through their ability to negatively regulate the activity of the type B ARRs, although the mechanism by which they do this is still unclear. Downstream, CYTOKININ RESPONSE FACTORS (CRFs) can mediate further the cytokinin response (Rashotte et al., 2006).

Transport of cytokinins can take place in multiple ways. Movement of tZ can occur from the root towards the shoot, via the xylem. In the opposite direction iP can move in the phloem (reviewed in Kudo et al., 2010). To date, three different protein families involved in cytokinin transport have been identified, PUP, ENT and ABCG. The first member of the *PURINE PERMEASE1* (*PUP*) family was shown to be able to transport kinetin and zeatin in adenine-deficient yeast mutants that were complemented with Arabidopsis cDNA libraries (Gillissen et al., 2000). Recently, PUP14 was shown to localise to the plasma membrane in Arabidopsis embryos, removing apoplastic cytokinin and regulating development by inhibiting perception of cytokinin by plasma membrane-localised cytokinin sensors (Zurcher et al., 2016). However, it is unlikely that much plasma membrane perception of cytokinin occurs, because the AHK receptors are predominantly localised on the endoplasmic reticulum (Wulfetange et al., 2011). Another family of putative cytokinin transporters are the EQUILIBRATIVE NUCLEOTIDE TRANSPORTER (ENT) proteins. The ENTs are thought to transport inactive forms of cytokinin (reviewed in Hirose et al., 2008), but are also able to transport many non-cytokinin compounds, suggesting that they might not act specifically in cytokinin transport. Both the PUP and ENT proteins have been shown to affect the uptake of cytokinin. Cytokinin export has been reported for the ABCG14 protein, which belongs to a sub-clade of the ATP-binding cassette family. Loss-of-function *abcg14* mutants show reduced long distance cytokinin transport of root-derived *trans*-zeatin and use of radiolabelled tZ shows that the protein acts as an efflux pump (Ko et al., 2014; Zhang et al., 2014).

1.2.3 Strigolactone

Strigolactones are a class of cartenoid-derived hormones that were first discovered as a germination stimulant for parasitic plants, such as *Striga* (Cook et al., 1966). Strigolactones are exuded from roots into the rhizosphere. They promote hyphal branching of arbuscular mycorrhizal (AM) fungi, which form symbioses with most land plants, and enhance the efficiency of AM colonisation (Akiyama et al., 2005; Besserer et al., 2006). They have only been identified recently as important regulators of shoot branching control (Gomez-Roldan et al., 2008; Umehara et al., 2008) and have been shown to influence other plant developmental processes, such as cambial growth (Agusti et al., 2011) and leaf shape (Stirnberg et al., 2002).

Strigolactone synthesis in Arabidopsis occurs in sequential steps catalysed by DWARF27 (D27), MORE AXILLARY GROWTH3 (MAX3), MAX4 and MAX1, where all-*trans*-β-carotene is converted into carlactone, a common precursor of diverse strigolactones (Alder et al., 2012). In Arabidopsis, MAX1 converts carlactone into carlactonoic acid, which is then methylated to produce MeCLA (Abe et al., 2014). LATERAL BRANCHING OXIDOREDUCTASE (LBO) further converts MeCLA into an unidentified strigolactone-like compound (Brewer et al., 2016).

Similar to the auxin hormone signalling pathway in Section 1.2.1, strigolactone signalling is based on targeted protein degradation via an SCF complex (Fig. 1.2). The F-box protein determines the specificity of the complex, which in strigolactone signalling is mediated by the MAX2 protein (Stirnberg et al., 2007, 2002). Mutants lacking functional MAX2 are unable to respond to the synthetic strigolactone, GR24, suggesting that MAX2 is involved in strigolactone signalling (Gomez-Roldan et al., 2008; Umehara et al., 2008). The SCF^{MAX2} complex leads to polyubiquitination of SUPPRESSOR OF MORE AXILLARY GROWTH2-LIKE (SMXL) proteins SMXL6, SMXL7, SMXL8, which act as growth regulators, and whose activity is suppressed by strigolactone signalling (Soundappan et al., 2015; Wang et al., 2015).

Recent advances have shown that strigolactone perception occurs through the α/β-hydrolase superfamily protein DWARF14 (D14), which has been identified in different species, such as Arabidopsis, petunia and rice (Hamiaux et al., 2012; Kagiyama et al., 2013; Waters et al., 2012; Zhao et al., 2013). D14 proteins function as strigolactone receptors by cleaving strigolactone, and retain one of the hydrolysis products, leading to a conformational change that allows interaction with MAX2 (de Saint Germain et al., 2016; Yao et al., 2016).

Strigolactone binding enhances the physical interaction of D14 and MAX2, with the latter named D3 in rice, which apparently destabilises D14 (Chevalier et al., 2014; Hamiaux et al., 2012; Zhao et al., 2015). The structure of the D14-D3-ASK1 complex showed that during strigolactone hydrolysis the lid-like structure collapses, reducing the volume of the

hydrophobic cavity and triggering strigolactone signalling (Yao et al., 2016). The D3-ASK1 complex apparently stabilises the closed state of D14, which provides an explanation for the failure to capture D14 in its active signalling state. The *d14-5* mutant retains its ability to hydrolyse strigolactone, but is unable to interact with MAX2/D3 and fails to act as a strigolactone receptor, demonstrating that the enzymatic activity and signalling functions of D14 can be uncoupled (Yao et al., 2016).

Movement of strigolactones in Arabidopsis occurs from the root towards the shoot, but not vice versa, as demonstrated by grafting experiments (Turnbull et al. 2002; Booker et al. 2002). Strigolactones have recently been discovered in the xylem sap from tomato and Arabidopsis, which provides further support for their unidirectional movement (Kohlen et al., 2011). To date, the only characterised strigolactone transporter is the ABC transporter PLEIOTROPIC DRUG RESISTANCE1 (PDR1) in petunia (Kretzschmar et al., 2012). Strigolactone excretion into the soil in petunia *pdr1* mutants is strongly compromised, and overexpression of *PDR1* in Arabidopsis confers increased tolerance to high concentrations of GR24 (Kretzschmar et al., 2012). No other strigolactone transporters have been identified to date, and there is no orthologue of *PDR1* in Arabidopsis, so the role of strigolactone transport and any possible contribution to shoot branching control remains unclear.

1.3 The auxin transport network

Hormonal movement through stems is tightly regulated and plays an important role in the regulation of many plant developmental processes, including the control of shoot branching. A key example of tightly controlled hormone movement is the transport of auxin. Because auxin movement plays a central role in the regulation of shoot branching (see Section 1.5), its transport is explained in more detail below.

1.3.1 The mechanism of auxin transport

Transport of auxin can occur both passively and actively. Auxin is a weak acid and the pH of the environment determines whether it exists as a negatively charged anion (IAA^-) or as an uncharged proton-associated molecule (IAAH). The pH of the apoplast is acidic (pH ~5.5), and here a relatively large proportion of auxin molecules will exist in their uncharged, protonated state. In this state the auxin molecule can passively cross the plasma membrane. The pH within the cell is higher than in the apoplast, usually around 7, which results in disassociation and formation of IAA^-, which is unable to passively cross the plasma membrane. This traps the auxin inside the cell and transporters are required to move auxin out

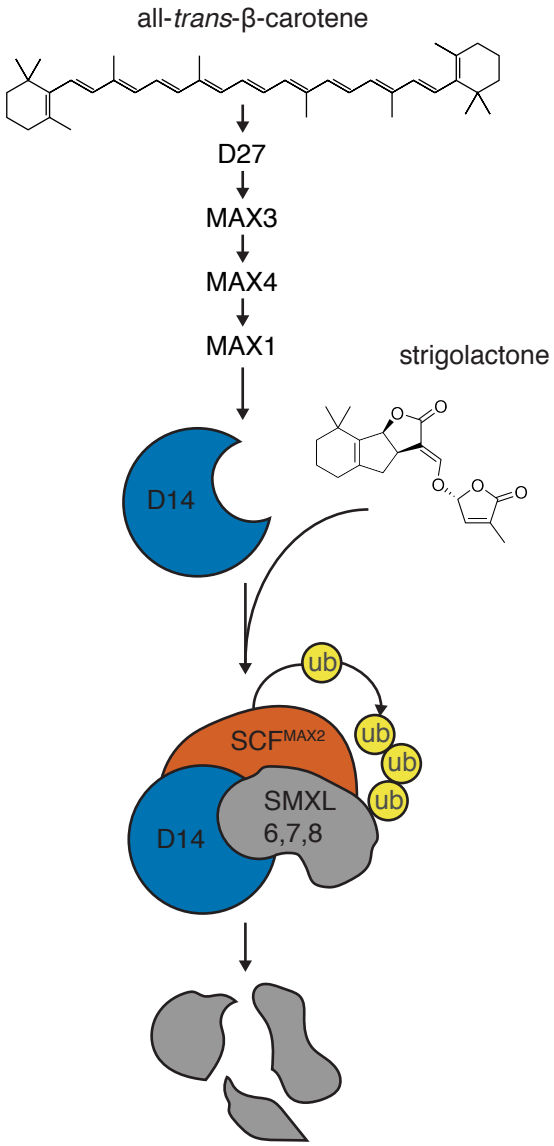

Fig. 1.2 The strigolactone signalling pathway in Arabidopsis.
Strigolactones are synthesised from all-*trans*-β-carotene, which is converted into strigolactones by sequential action of D27, MAX3, MAX4 and MAX1. Perception occurs through D14, which cleaves strigolactone and retains one of the hydrolysis products. The resulting conformational change enables interaction with the MAX2 F-box protein. MAX2 forms part of an SCF-complex which enables ubiquitination and targeted protein degradation of SMXL6,7,8. This allows growth responses to strigolactones. Redrawn and adapted from Morffy et al. (2016).

of the cell. This mechanism is known as the chemiosmotic model of auxin transport (Raven, 1975; Rubery and Sheldrake, 1974).

The ability of auxin to move passively across the plasma membrane suggests that active import into the cell might not be important. However, there is a family of four closely related auxin importers, which in Arabidopsis are the AUXIN RESISTANT1 (AUX1) and three LIKE-AUXIN RESISTANT1 (LAX1-3) proteins (Bennett et al., 1996; Peret et al., 2012; Swarup et al., 2001). Measurements on auxin influx in protoplasts show that auxin influx mediated by AUX1 is of a comparable magnitude as that of auxin efflux, suggesting active AUX1-mediated import may dominate auxin influx into the cell (Rutschow et al., 2014).

Auxin efflux from cells is mediated by several protein families, of which the PIN-FORMED (PIN) family is of particular importance. The PIN family of proteins in Arabidopsis consists of 8 members. The PIN1 protein plays an important role in the movement of auxin down the stem and the regulation of auxin distribution at the shoot apex (Bennett et al., 1995; Gälweiler et al., 1998; Okada et al., 1991). Three other members, PIN3, PIN4 and PIN7, cluster closely together phylogenetically and share the most similarity with PIN1 (Krecek et al., 2009; Paponov et al., 2005). These four proteins often polarise to particular plasma membranes of cells, giving directionality to the auxin movement across tissues. Other members, such as PIN5, PIN6 and PIN8 appear to affect mainly auxin movement within cells (Dal Bosco et al., 2012; Mravec et al., 2009; Sawchuk et al., 2013).

Auxin transport has also been shown to depend on another class of proteins, the ATP-BINDING CASSETTE (ABC) transporters, sub-class B (Geisler et al., 2005; Noh et al., 2001). These proteins localise predominantly in a non-polar manner, although localisation can be polar (Geisler et al., 2005). Apart from their role in auxin export, some ABCB proteins are able to act as both importers and exporters (Kamimoto et al., 2012; Kubes et al., 2012).

Active auxin export can be blocked through pharmacological inhibitors. Two commonly used inhibitors are 1-N-naphthylphthalamic acid (NPA) and 2,3,5-triiodobenzoic acid (TIBA). How they function exactly remains unclear, but both inhibitors appear to have a rather general effect on protein transport (Geldner et al., 2001).

1.3.2 Energising auxin transport through proton ATPase activity

In order to function, transport proteins need energy. In ABCB proteins, the protein itself is able to generate the required energy. ABC transporters have cytoplasmic ATP-binding domains which are able to bind to ATP and the subsequent hydrolysis of ATP drives the transport. Proteins without such ATP-binding domains, like PIN and AUX1/LAX proteins, rely on the proton motive force to energise their transport. The proton motive force across the plasma membrane consists of a membrane potential and a pH gradient, both of which

are generated through the activity of H^+-ATPases. The H^+-ATPases are proton pumps which pump positive charges (H^+) out of the cell. This creates a membrane potential and the increase in protons also acidifies the apoplast. The pH of the apoplast is typically between 5 and 6, whereas the pH of the cytoplasm inside the cell is around 7, and this difference results in a pH gradient across the plasma membrane.

There are 11 isoforms of the Arabidopsis H^+-ATPase (AHA). These proteins are a subfamily of the P-type ATPase superfamily of ion pumps (Axelsen and Palmgren, 2001), which appear to be the only members to specifically catalyse the ATP-dependent efflux of protons across the plasma membrane (Haruta et al., 2010). Two of the genes encoding these proteins, *AHA1* and *AHA2*, are expressed at high levels throughout the plant. Relatively more *AHA1* transcript is found in shoots, whereas *AHA2* transcript is more abundant in roots (Haruta et al., 2010). They play an important role in plant growth, since mutants carrying mutations in both these genes are embryo-lethal (Haruta et al., 2010).

1.3.3 Feedback between auxin and proton ATPase regulation

The activity of H^+-ATPases is at least in part regulated by auxin, since auxin promotes plasma membrane H^+-ATPase activity (Takahashi et al., 2012). This can affect auxin transport and growth. An increase in plasma membrane H^+-ATPase activity increases the proton gradient across the plasma membrane, which is predicted to enhance the accumulation of auxin within the cell and increase both the influx and efflux of auxin (Steinacher et al., 2012).

Auxin-induced H^+-ATPase activity also leads to acidification of the cell wall, which can loosen the cell wall and result in cell expansion (Hager, 2003). This mechanism underlies the acid growth theory, which predicts that growth can occur through rapid elongation of cells in response to an acidic environment (reviewed in Rayle and Cleland, 1992). The molecular mechanism underlying auxin-induced H^+-ATPase activity has only recently been uncovered. In etiolated hypocotyls, auxin application is able to phosphorylate a critical Thr-947 residue in the auto-inhibitory domain of AHAs, activating the proton pump (Takahashi et al., 2012). This effect is mediated through the transcriptional upregulation of members of the *SMALL AUXIN UP-RNA* (*SAUR*) gene family, which are primary auxin response genes. SAUR proteins are highly unstable, but use of stabilised proteins has shown that a cluster of these proteins, including SAUR19, can positively regulate cell expansion (Spartz et al., 2012, 2014, 2017). Stabilised SAUR19 plants exhibit increased plasma membrane H^+-ATPase activity, which results from increased phosphorylation at the critical Thr-947 residue (Spartz et al., 2014). SAUR19 and several other SAUR proteins mediate this effect by physically interacting with the PP2C.D subfamily of protein phosphatases, which negatively regulate plasma membrane H^+-ATPase activity and Thr-947 phosphorylation status (Spartz

et al., 2014). Upon binding to SAURs, PP2C.D phosphatase activity is inhibited, leading to auxin-mediated cell expansion (Spartz et al., 2014, 2017).

Although cell expansion contributes to growth, sustained growth also requires plants to transport their auxin effectively from the shoot towards the root. The vasculature in the stem is important for this, as discussed below.

1.3.4 Auxin transport in stems

Active auxin transport is also strongly associated with the vasculature. The polar auxin transport stream (PATS) in stems makes a major contribution to the transport of auxin from the shoot towards the root. The PATS is associated with the vascular bundles, particularly the xylem parenchyma and the cambium (Goldsmith, 1977) and the composition and number of vascular bundles within the stem is likely to affect auxin transport. The arrangement of tissues within a stem can vary greatly between species. In the majority of higher plants the vascular system is organised in discrete vascular bundles, which have a collection of xylem cells, with phloem cells opposite them. The xylem and phloem are set in the ground tissue, or parenchyma cells, and are separated by the cambium, which consists of meristematic cells that give rise to the xylem and phloem cells. In monocots, the arrangement of the vascular bundles is more or less irregular whereas in dicots the discrete vascular bundles are arranged in a ring. In dicots in the mature stem the cambium can extend between the vascular bundles, forming a complete ring of vascular tissue. This can give rise to extensive xylem and phloem development, which is most obvious in woody plants, such as trees (reviewed in Scarpella and Meijer, 2004).

The stem anatomy in Arabidopsis follows the general arrangement of dicot stems and the different tissues in Arabidopsis stems can be distinguished in cross sections (Fig. 1.3). Following the tissues from the outside towards the centre of the stem at the position of a vascular bundle, there is the epidermis, cortex, phloem, cambium, xylem and xylem parenchyma. Surrounding the vascular bundles, the sclerenchyma cells have very thick cells walls and form a fibrous tissue that provides support to the plant. The inner tissue of the stem is comprised of pith parenchyma cells.

Auxin in the stem moves in a basipetal manner, from the apex towards the root. The bulk of the auxin transport occurs through the PATS, to which the PIN1 protein makes a major contribution (Gälweiler et al., 1998). In the stem, PIN1 is localised predominantly on the basal plasma membrane of xylem parenchyma and cambium cells (Gälweiler et al., 1998). In accordance with this role, the bulk movement of radiolabelled auxin through *pin1* mutants stems is strongly decreased (Bennett et al., 1995; Okada et al., 1991). Conversely, stem auxin

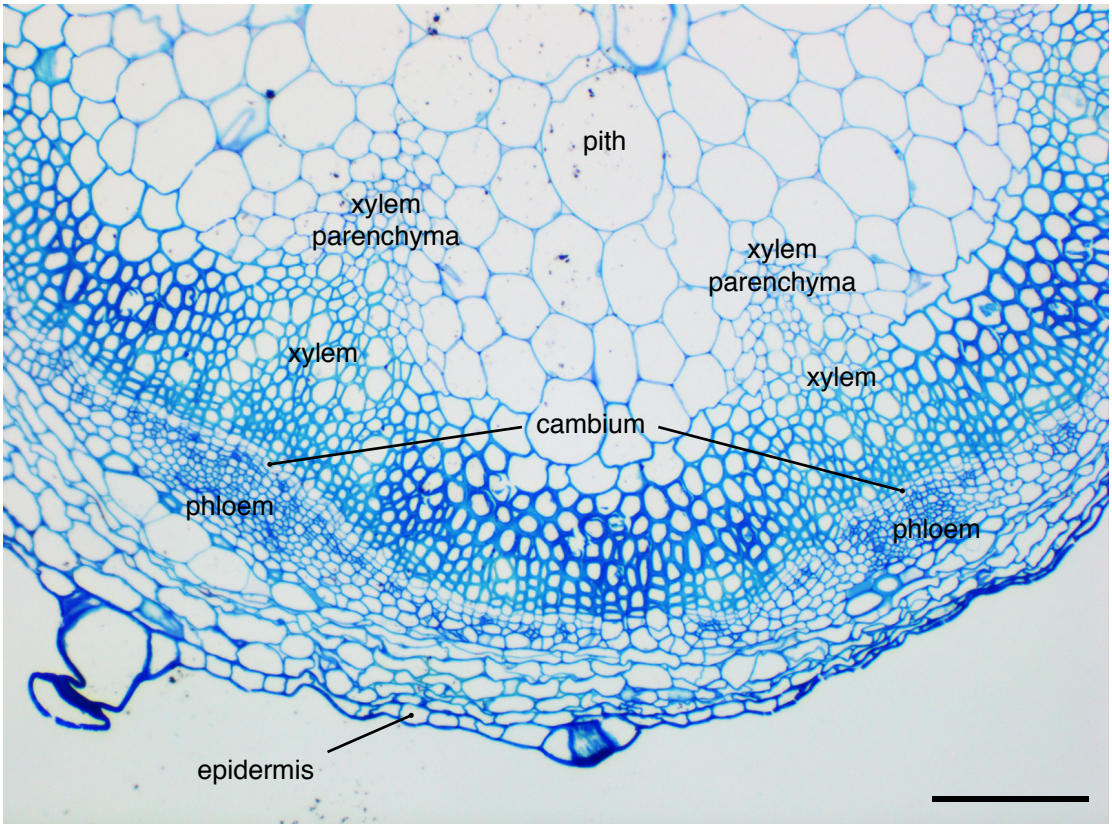

Fig. 1.3 Arabidopsis stem anatomy.
Cross section through the basal internode an Arabidopsis inflorescence stem, grown under long day growth conditions, at terminal flowering. Cell walls are stained with toluidine blue. The main types of tissues discussed in the text are indicated. Bar = 100 µm.

transport in *max* mutants, which show high levels of PIN1 in the stem, is increased (Bennett et al., 2006; Crawford et al., 2010; Shinohara et al., 2013).

Other PIN proteins also contribute to stem auxin transport (Bennett et al., 2016a; Boot et al., 2016). Furthermore, ABCBs, which are expressed in much broader domains in the stem than PINs (Bennett et al., 2016a) can also contribute to stem auxin transport (Noh et al., 2001). The presence of many different auxin efflux proteins in the stem suggests that stem auxin transport dynamics are likely to be complex. In accordance with this, auxin pulses applied to stems generally show a degree of spreading (e.g. Brewer et al., 2009; Rashotte et al., 2003), which would not be expected if auxin moved simply from shoot to root with linear kinetics. Interestingly, the rate of spreading of a pulse over time can provide information about the underlying transport mechanism (Mitchison, 2015) and auxin pulse dynamics suggest that stem auxin transport is likely comprised of multiple auxin transport regimes with different transport properties (Bennett et al., 2016a; Boot et al., 2016; Mitchison, 2015).

1.4 Development and regulation of shoot apices

The capability of long term growth in lateral branches lies at the axillary meristem. Meristematic cells in the axillary meristem give rise to all the tissues that make up the branch and, for branches to grow, these meristematic cells must be formed, maintained and regulated. The regulation of meristems is under tight genetic control. The three hormones discussed above, auxin, cytokinin and strigolactone, all affect axillary meristem activity and their roles are discussed below.

1.4.1 Formation of shoot apices

All aerial parts of the plant derive from the primary shoot apical meristem (SAM). In Arabidopsis, the SAM is a dome of cells with a specific spatial arrangement. The outer L1 layer of cells divides predominantly anticlinally, forming the shoot epidermis. Immediately subtending the L1, the L2 also typically acts as a single layer of cells contributing to sub-epidermal tissues. Further inwards, the L3 divides in both anticlinal and periclinal directions and cells derived from it form core tissues in leaves and stems. Radially, distinct functional zones can be distinguished in the SAM with, at the centre of the dome, a central zone which contains slow dividing meristematic cells, which give rise to the surrounding tissues. Adjacent to this is the peripheral zone, where an increased rate of division amplifies cell

populations and new organs are initiated. Underlying these two zones is the rib zone, where division and elongation contribute to the stem tissues.

Axillary meristems in Arabidopsis exhibit the same cellular and functional organisation as the primary SAM. The SAM is initiated very early in embryogenesis, whereas axillary meristems form post-embryonically in leaf axils. Axillary meristem formation is under the control of at least two hormones, auxin and cytokinin. Their role is discussed below.

1.4.2 Hormonal control of shoot meristem initiation and activity

Recent analyses have characterised the role of plant hormones in the specification of axillary meristem formation (Wang et al., 2014a,b). Low auxin levels in leaf axils precede the initiation of axillary meristems and artificially elevating auxin concentration in this region disrupts axillary meristem formation (Wang et al., 2014a,b). Axillary meristem formation is also impaired when auxin transport is disrupted. Mutants lacking PIN1 form significantly fewer axillary meristems than wild type plants and a similar effect is seen in plants lacking PINOID, an important regulator of PIN1 activity (Wang et al., 2014a,b). Axillary meristem formation is not only compromised in backgrounds where auxin export is impaired, but also in *aux1lax1lax2* auxin importer mutants (Wang et al., 2014a).

Axillary meristem formation is also dependent on cytokinin. Cytokinin signalling, perception and biosynthesis are increased during axillary meristem formation (Wang et al., 2014b) and mutants impaired in these processes show decreased levels of axillary meristem formation (Muller et al., 2015; Wang et al., 2014b).

Apart from their roles in meristem formation, auxin and cytokinin also play important roles in the regulation of meristem activity. The initiation of new organs at the SAM coincides with the accumulation of high concentrations of auxin (Benkova et al., 2003; Heisler et al., 2005; Vernoux et al., 2011). These auxin maxima correspond to the polarisation pattern of PIN1 in the SAM. Here, PIN1 localisation in the L1 layer is polar, and directed towards sites of inferred high auxin accumulation (Bayer et al., 2009; Benkova et al., 2003; Heisler et al., 2005; Reinhardt et al., 2003). Using computational models, the phyllotactic patterns at the shoot apex can largely be reproduced using a system where PIN1-mediated auxin accumulation controls patterning (Jönsson et al., 2006; Smith et al., 2006). Mutants lacking PIN1 provide further evidence. The Arabidopsis *pin1* mutant fails to produce flowers, and applying pharmacological inhibitors of auxin transport to wild type plants can mimic this effect (Bennett et al., 1995; Okada et al., 1991). Conversely, exogenous application of auxin to such barren meristems can trigger flower production, but only when applied to the peripheral zone of the meristem, suggesting that the role of auxin maxima in organ initiation is highly tissue specific (Reinhardt et al., 2003).

The formation of auxin maxima at the SAM depends on the correct localisation of auxin exporters, but it is also influenced by auxin importers. The *aux1lax1lax2lax3* quadruple mutant, lacking all four known auxin import proteins, displays disrupted phyllotactic patterning (Bainbridge et al., 2008). The formation of auxin maxima, as well as PIN polarisation is disrupted in this mutant background and it appears that auxin importers are necessary to stabilise PIN-mediated patterning mechanisms (Bainbridge et al., 2008). Further evidence for this comes from the observation that PIN1 expression in the L1 alone is not sufficient to restore a normal phyllotactic pattern in *pin1aux1lax1* mutants, and that in these mutants PIN1 is ectopically expressed in the L2 (Kierzkowski et al., 2013).

1.5 Models for shoot branching control

The outgrowth of branches is a coordinated interaction between the shoot apices and the stem. It is likely that systemic and local effects are involved in the regulation of bud outgrowth and models which attempt to explain this are discussed below.

1.5.1 The effect of auxin on lateral bud outgrowth

Auxin produced by the shoot apex has an inhibitory effect on the outgrowth of underlying axillary buds. Experiments conducted in the 1930s showed that when the shoot apex is removed through decapitation, axillary buds which were previously inhibited were able to activate. Application of auxin to the decapitated stump was shown to restore bud outgrowth inhibition, demonstrating that auxin is the signal responsible for the inhibition (Thimann and Skoog, 1933). However, the inhibitory effect of auxin is indirect, since auxin itself does not enter the bud (Booker et al., 2003; Prasad et al., 1993). Auxin movement through the stem occurs in a basipetal manner, which precludes upward movement into the bud. Interestingly, this basipetal movement of auxin does not only result in inhibition of buds located basally to the growing shoot, but more apical buds can also be inhibited (Ongaro et al., 2008; Snow, 1929). Together, these observations suggest that auxin inhibits bud outgrowth in an indirect manner.

Two main non-exclusive hypotheses have been proposed to explain the indirect effect of auxin on bud inhibition. One model predominantly takes into account the manner in which auxin transport is dynamically regulated in the context of bud outgrowth. The other model suggests that second messengers relay the inhibitory effects of auxin. Both models are discussed next.

1.5.2 The auxin transport canalisation model for shoot branching control

The auxin transport canalisation model for shoot branching control proposes that buds need to efficiently export their auxin in order to activate and that this export occurs through a process called canalisation. The concept of auxin transport canalisation was proposed to explain patterns of vascular strand formation in response to wounding and describes the process where an initial auxin flow from an auxin source towards an auxin sink is upregulated and polarised, and becomes limited to increasingly narrower files of auxin transporting cells, and thus becomes 'canalised' (Sachs, 1981). This process relies on a positive feedback between auxin flux and transport. Auxin flux upregulates and polarises its own transport in the direction of the flux (Sachs, 1981). Although the concept of canalisation was proposed prior to the molecular genetic era, observations on PIN auxin efflux proteins have confirmed the positive feedback auxin exerts on its own transport, as well as the importance of auxin transport in vascular patterning (Paciorek et al., 2005; Sauer et al., 2006; Sawchuk et al., 2013; Scarpella et al., 2006). Furthermore, when PIN localisation was traced in experiments comparable to Sachs', the dynamic behaviour was consistent with the early predictions (Balla et al., 2011; Sauer et al., 2006).

In the context of shoot branching, canalisation is thought to play an important role in enabling buds to establish efficient and sustained auxin export into the stem. Inactive buds are potential sources of auxin which produce and export auxin upon activation (Balla et al., 2011; Li and Bangerth, 1999; Morris, 1977; Thimann and Skoog, 1933). Auxin export from buds is correlated with their growth (Li and Bangerth, 1999; Morris, 1977; Prusinkiewicz et al., 2009). An explanation for this export requirement might be that it allows continued leaf initiation and expansion (Bayer et al., 2009).

The ability of buds to canalise their auxin transport into the stem is predicted to be influenced by the sink strength of the main stem for auxin, relative to the auxin source strength of the bud. Crucial in this process is the initial auxin flux from the bud towards the stem, which, as a result of the positive feedback between auxin flux, and the upregulation and polarisation its auxin transport, is amplified to establish a polar auxin transport stream out of the bud. It is important to note that the initial flux out of the bud depends on relative, not absolute differences between auxin sources and sinks, as well as the strength of the feedback between auxin flux and its upregulation and polarisation (Prusinkiewicz et al., 2009). For example, auxin concentrations at an auxin source may remain constant in absolute terms, but become relatively stronger if the sink strength is reduced. This situation could arise if less auxin is exported into the sink. In the context of the main stem, this would occur following

decapitation of the primary shoot apex, or when other sources of auxin reduce their auxin export into the sink.

A key determinate of sink strength is the amount of auxin that is present in the main stem. Catabolism and synthesis of auxin in the main stem typically appears to be limited (discussed in Kramer and Ackelsberg, 2015). Therefore the auxin concentration in the main stem is primarily determined by the amount of auxin fed into it and the amount of auxin that is transported away towards the root. Growing shoot apices produce auxin and feed this into the stem. The amount of auxin produced by each active apex is not necessarily constant, so the individual source strength of each active apex can vary. However, each actively growing apex feeds auxin into the stem, thereby affecting the sink strength. The rate at which auxin is transported towards the root also affects the sink strength, since high levels of polar auxin transport away to the root will result in a stronger sink. The resulting relative balance between any given source and sink then determines how readily a bud is able to activate. A bud acting as a strong auxin source, combined with a stem providing a strong sink will enable a bud to canalise its auxin export easily and activate. In contrast, a bud which produces little auxin will find it more difficult to establish an initial auxin flux towards a comparable sink, and would be predicted to remain dormant. Importantly, this system assumes dynamic modulation of the auxin transport network as buds activate. All buds feed into a common sink and as such they compete for access to the polar auxin transport stream in the main stem that constitutes an important part of this sink. As one bud activates, it reduces the stem auxin sink strength by exporting auxin into it. In turn, this makes it harder for other buds to activate. This provides an explanation for the indirect inhibitory effect of auxin in this process, and also explains how buds are able to prevent other buds from activating (Prusinkiewicz et al., 2009).

1.5.3 The role of strigolactones in auxin transport canalisation

The importance of the relative differences between auxin source and sink, as well as the dynamic properties of the auxin transport network, can be used to explain the action of strigolactone on shoot branching. Mutants impaired in strigolactone signalling or biosynthesis show high levels of branching (Booker et al., 2004; Sorefan et al., 2003; Stirnberg et al., 2002; Waters et al., 2012). The high degree of branching in these mutants results at least in part from reduced competition for outgrowth between buds. Competition between buds can be measured by taking young inflorescences bearing two cauline buds and removing the primary shoot apex to release these buds from inhibition (Ongaro et al., 2008). After decapitation, both buds can activate or only one bud grows out and subsequently inhibits the activation of the other bud. Interestingly, the top and the bottom bud are both capable

of inhibiting outgrowth (Ongaro et al., 2008). In strigolactone mutants both buds grow out, but exogenous application of strigolactone enhances competition between shoot apices, such that the ability of one bud to inhibit the outgrowth of another bud is enhanced (Crawford et al., 2010). Applying strigolactone to isolated single buds at physiologically meaningful concentrations has no effect on bud outgrowth. However, when an additional auxin source is provided through apical application of auxin to the decapitated stump, the inhibitory effect of apical auxin is enhanced by basal application of strigolactones, a process that is strigolactone signalling dependent (Crawford et al., 2010). Strigolactones are able to enhance bud-bud competition at least in part by affecting the PIN1 accumulation on the basal plasma membrane. In strigolactone mutants, levels of PIN1 on the basal plasma membrane of xylem parenchyma cells are increased and, consistent with this, *max* mutants show increased levels of stem auxin transport (Bennett et al., 2006; Crawford et al., 2010). The branchy phenotype of these mutants is correlated with the increased auxin transport, since applying low levels of NPA, an auxin transport inhibitor, is able to reduce stem auxin transport to wild type levels and results in a subsequent decrease in branching (Bennett et al., 2006; Lazar and Goodman, 2006). Strigolactones promote PIN1 endocytosis from the plasma membrane and in the *max* mutants this process is impaired, resulting in the observed overaccumulation of PIN1 (Shinohara et al., 2013). PIN1 endocytosis by strigolactones is dependent on strigolactone signalling through MAX2, since the response is abolished in *max2* mutants. Furthermore, it occurs independent of new protein synthesis, suggesting that strigolactone acts post-transcriptionally on PIN1 (Shinohara et al., 2013).

In the context of auxin transport canalisation, the reduced removal of PIN1 from the plasma membrane in strigolactone mutants may contribute to higher sink strength in the stem, because more basal PIN1 is able to transport auxin towards the root. In the bud, the elevated PIN1 levels may enable the bud to export and canalise its auxin more easily towards the stem, influencing source strength. Perhaps most significantly, reduced removal of PIN1 from the plasma membrane will enhance the positive feedback between auxin flux and the polarisation and upregulation of auxin transport, such that a very small initial flux of auxin from the bud to the stem will be sufficient to drive auxin transport canalisation (Prusinkiewicz et al., 2009). This combined effect allows strigolactone mutants to activate their branches more readily, resulting in increased levels of branching (Bennett et al., 2006; Prusinkiewicz et al., 2009; Shinohara et al., 2013). Thus, strigolactone is able to regulate the levels of shoot branching at least partially through its effect on the auxin transport network.

1.5.4 The second messenger model for shoot branching control

Another model for auxin-mediated inhibition of shoot branching has been proposed in which auxin acts through one or more second messengers. In this model, auxin in the stem regulates the production of a second messenger that moves directly into the bud to regulate its activity (Sachs and Thimann, 1967; Snow, 1929). Both cytokinin and strigolactone fit well within this model.

In the second messenger model, cytokinin and strigolactone are thought to act antagonistically, with cytokinin promoting and strigolactone inhibiting bud outgrowth. Consistent with these roles, direct application of cytokinin to inhibited buds is able to activate them, even in the presence of apical auxin (Chatfield et al., 2000; Wickson and Thimann, 1958). Similarly, direct application of strigolactone to buds is able to inhibit outgrowth (Brewer et al., 2009; Gomez-Roldan et al., 2008; Umehara et al., 2008). Furthermore, strigolactone is able to reduce the stimulatory effect of cytokinin on bud outgrowth (Dun et al., 2012).

The indirect effect of auxin on bud outgrowth in this model is proposed to occur via transcriptional regulation of cytokinin and strigolactone biosynthesis. Here, auxin has been shown to act through the AXR1-AFB (AUXIN RESISTANCE PROTEIN1-AUXIN SIGNALLING F-BOX PROTEIN)-dependent auxin signalling pathway (Hayward et al., 2009; Nordstrom et al., 2004). Through this pathway auxin is able to negatively regulate transcription of members of the *IPT* gene family which are involved in cytokinin synthesis, leading to decreased cytokinin production (Nordstrom et al., 2004; Tanaka et al., 2006). Upon decapitation, repression is reduced, and cytokinin produced at the stem-bud node is thought to enter the bud, stimulating bud outgrowth.

Conversely, AXR1-AFB-dependent auxin signalling is likely to positively affect the production of strigolactones, because strigolactone biosynthesis genes are upregulated by auxin (Brewer et al., 2009; Foo et al., 2005; Hayward et al., 2009; Sorefan et al., 2003). In accordance with this, reducing auxin in the main stem through decapitation or NPA treatment decreases transcript levels of these genes (Foo et al., 2005; Hayward et al., 2009). Movement of auxin from the shoot to the root could thus stimulate strigolactone production in the root, which would lead to increased movement of strigolactone from the root to the shoot, where they could modulate bud activity. Strigolactone levels in the shoot are not only determined by synthesis in the root. Grafting experiments have demonstrated that wild type shoots grafted to strigolactone deficient roots can still suppress branching (Booker et al., 2005), suggesting that strigolactones are also synthesised in the shoot at sufficient levels to modulate bud outgrowth. Therefore it is possible that auxin is able to locally upregulate strigolactone production in the shoot, which enables the movement of strigolactone into the bud, where it can inhibit bud outgrowth.

1.5.5 The role of *BRC1* in shoot branching

A proposed mechanism by which cytokinin and strigolactone are able to inhibit bud outgrowth is via the transcriptional regulation of *BRANCHED1* (*BRC1*). The *BRC1* gene belongs to the TCP family of transcription factors. These transcription factors contain a TCP domain, named after the first characterised members TEOSINTE BRANCHED1 in maize, CYCLOIDEA in snapdragon and PCF1 and PCF2 in rice. In Arabidopsis, *BRC1* is closely related to *TEOSINTE BRANCHED1* (*TB1*) in maize (Aguilar-Martinez et al., 2007). During domestication of maize from its wild relative teosinte, a mutation which confers overexpression of TB1 has been selected, resulting in reduced branching and different flowering patterns in the shoot. Loss-of-function mutants in TB1 display increased branching phenotypes, resembling teosinte (Doebley et al., 1997), suggesting that *TB1* negatively regulates branching. Consistent with this, *TB1*-like mutants in Arabidopsis, such as *brc1* and, to a lesser extent *brc2*, show increased levels of branching (Aguilar-Martinez et al., 2007; Finlayson, 2007). *TB1* in maize and *BRC* genes in Arabidopsis are predominantly expressed in the axillary buds (Aguilar-Martinez et al., 2007; Doebley et al., 1997), correlating well with a possible function in regulating axillary bud activity. Although the function of BRC1 is not specifically known, other TCP transcription factors include cell cycle regulators genes among their transcriptional targets (Kosugi and Ohashi, 2002; Li et al., 2005; Schommer et al., 2014; Trémousaygue et al., 2003). This has led to the assumption that BRC1 regulates cell cycle progression in buds, although there are many other transcriptional targets for this gene family (reviewed in Li, 2015).

Hormones can regulate the transcript levels of *BRC1*. In pea, the *PsBRC1* orthologue is positively regulated by cytokinin, and negatively by strigolactone (Braun et al., 2012; Dun et al., 2012), consistent with the stimulatory and inhibitory effects of these hormones on bud outgrowth. *BRC1* transcript levels frequently correlate with bud activity, with high *BRC1* levels correlating with bud outgrowth inhibition, and vice versa (Aguilar-Martinez et al., 2007; Finlayson, 2007; Seale et al., 2017). However, this correlation can be broken. For example, strigolactone mutants in maize constitutively express high levels of *TB1*, but still exhibit high levels of branching (Guan et al., 2012). In Arabidopsis, *brc1* buds can remain inhibited and buds with high levels of *BRC1* transcript can be active, suggesting that the role of *BRC1* is more complex than that of a straightforward bud outgrowth regulator (Seale et al., 2017).

1.5.6 Reconciling models for shoot branching control

Although the second messenger model is able to account for many shoot branching responses, some data are not easily explained. Application of physiologically meaningful concentrations of strigolactone to single buds has no effect on bud outgrowth (Crawford et al., 2010), which is difficult to explain if strigolactones are direct inhibitors of bud outgrowth. Moreover, the ability of buds to compete for outgrowth is difficult to reconcile with the direct effects predicted by the second messenger model. Following decapitation, the buds on stems with two nodes are delayed in their outgrowth, compared to a bud on stem segments bearing only one node (Crawford et al., 2010). This means that the presence of the more basal bud in the two-node situation is able to affect the outgrowth of the more apical bud, even though it is located further away from the decapitation site (Crawford et al., 2010). Auxin concentration changes at the apical node, with the presumed effects on cytokinin and strigolactone concentration, would not be able to affect bud-bud competition in this manner. Even more difficult to explain with the second messenger model is the effect of basal application of strigolactone on two-node bud outgrowth. Here, strigolactone mostly reduces the growth of only one bud (Crawford et al., 2010), which is not easy to reconcile with a direct effect of strigolactone on bud inhibition.

The auxin transport canalisation model for shoot branching readily explains these observations. Here, the main stem provides a common auxin transport pathway for all the growing shoot apices. Branching patterns arise from the dynamic properties of the network, which changes the ability of shoot apices to export their auxin into the stem - a requirement for activation. In this context strigolactone does not directly regulate bud outgrowth, but instead affects the auxin transport network, in turn affecting the ability of buds to export their auxin by dampening polar auxin transport in the stem, leading to enhanced competition (Crawford et al., 2010; Prusinkiewicz et al., 2009; Shinohara et al., 2013). This dynamic regulation of auxin transport can also account for the striking observation that strigolactones can actually promote branching in some instances, such as in the *transport inhibitor3* (*tir3*) auxin transport mutant, which has increased levels of branching associated with reduced levels of auxin transport (Ruegger et al., 1997; Shinohara et al., 2013).

Arguing against the auxin transport canalisation model are recent suggestions that strigolactone acts independently of auxin (Brewer et al., 2015). Here, application of the auxin transport inhibitor NPA to pea buds was unable to fully prevent bud outgrowth in both wild type and strigolactone-deficient mutants. Application of strigolactone to NPA-treated buds was able to inhibit bud outgrowth to a greater extent than NPA alone. This suggests that a bud activation mechanism may exist that is not correlated with auxin transport (Brewer

et al., 2015), but the limited understanding of the mechanism by which NPA works makes interpretation of these results difficult.

It is important to note that the auxin transport canalisation and second messenger models for shoot branching are not mutually exclusive. Both mechanisms could act in parallel, with the contribution of each varying depending on the circumstances.

1.6 Aims

The aim of this thesis is to increase the understanding of the components of the auxin transport network that may underlie the auxin transport canalisation hypothesis for shoot branching control. Specifically, the aim was to answer the following questions:

- How does auxin move down the stem?
  - Which auxin exporters contribute to stem auxin transport?
  - How is auxin distributed in the stem?
  - Do auxin importers affect stem auxin transport?
- To what extent does auxin transport regulate bud-bud communication?
  - Which auxin exporters are involved in communication between shoot apices?
  - Do auxin exporters other than PIN1 act in the strigolactone signalling pathway?
  - Does auxin influx play a role in bud outgrowth regulation?
- What is the relationship between the regulation of shoot branching by *BRC1* and auxin transport?
  - In what way does the auxin transport network affect *BRC1*-mediated bud outgrowth?
- Does H^+-ATPase activity affect shoot branching?
  - Do H^+-ATPases affect auxin transport in the stem?
  - Can H^+-ATPase activity affect bud outgrowth?

Chapter 2

Materials and methods

2.1 Materials and methods

2.1.1 Plant lines

Arabidopsis thaliana ('Arabidopsis' hereafter) plants were all in the Col-0 ecotype. Wild type refers to the Col-0 ecotype. Details of the plant lines used are shown in Appendix A. The physical location on the chromosomes of the most commonly used genes in this study can be found in Fig. 2.1.

2.1.2 Growth conditions

Arabidopsis seeds were stratified on wet filter paper at 4 °C for two to five days prior to sowing. Plants were grown on Levington's F2 compost pre-treated with Intercept at 0.02 g/l or Exemptor at 0.03 g/l (Levington Horticulture, Ipswich, UK). Plants were grown in P40 cellular trays (16 cm^2 per pot) or P24 cellular trays (25 cm^2 per pot). Plants were grown in glasshouses or in controlled environment rooms according to the growth conditions and light regimes shown in Table 2.1.

2.1.3 Growth substrates

Arabidopsis thaliana salt (ATS) solution was used for in vitro growth (Wilson et al., 1990). Sucrose was added at 1 % and agar was added at 0.8 % to solidify the media, where stated.

Nitrate experiments were conducted on a mixture of sand and terra green, as described in de Jong et al. (2014). Each pot was supplied with 25 ml ATS with nitrate solution at the start of the experiment. An additional 10 ml ATS with nitrate solution was added weekly after the

Table 2.1 Plant growth conditions

Condition	Light/dark	Temperature day/ night	Light level	Humidity
Glasshouse	16/8 h	15-31 °C range	min. 88 $W\,m^{-2}$, shading at 500 $W\,m^{-2}$	ambient
Long days	16/8 h	21/17 °C	170 $\mu mol\,m^{-2}\,s^{-1}$	65 %
Short days	8/16 h	21/17 °C	170 $\mu mol\,m^{-2}\,s^{-1}$	65 %
Tissue culture	16/8 h	21/17 °C	85 $\mu mol\,m^{-2}\,s^{-1}$	ambient

first two weeks. Lids were kept on the trays for the first two weeks to maintain high humidity and prevent desiccation. Nitrate concentrations were 1.8 mM for low nitrate availability or 9 mM for high nitrate availability.

2.1.4 Seed sterilisation

Liquid surface sterilisation of seeds was done by washing seeds with 70 % ethanol (w/v) for 15 minutes, followed by treatment with 5 % bleach and 0.005 % Silwet for 25 minutes. Seeds were washed three times with sterile distilled water.

Alternatively, vapour sterilisation was conducted using chlorine gas. Seeds were kept in a sealed box for 6 to 18 hours, containing a jar with 100 ml bleach to which 3 ml of 37 % hydrochloric acid was added to generate chlorine gas.

2.1.5 Crosses

Young flowers were selected where petals were just started to show. Sepals, petals and stamens were removed from the flower and the style and stigma were left to develop for approximately 24 hours. Ripe pollen was selected from donor plants for hand pollination.

2.1.6 Hormone solutions

1-NnNaphthylphthalamic acid (NPA, SigmaAldrich) was dissolved in 70 % ethanol (w/v) and stored at −20 °C. GR24 (LeadGen Labs LLC) was dissolved in 90 % acetone and stored at −80 °C.

2.2 Physiological assays

2.2.1 One- and two-node explant setup

Plants were grown under glasshouse conditions in P40 cellular trays, with one plant per pot as described in Section 2.1.2. Liquid ATS was added to 1.5 ml micro centrifuge tubes and the tubes were covered with parafilm to make ATS tubes. Where applicable, hormones were added to the ATS solution, prior to making the ATS tubes. The parafilm was pierced to make a small hole for the inflorescence stem. When the plant inflorescences reached 1-2 cm, stem segments bearing the primary shoot apex and two axillary buds were harvested. Only segments with axillary buds smaller than 1 mm were selected. To generate one-nodes, the primary shoot apex and the uppermost axillary bud were removed under a stereo microscope, using the tip of a hypodermic needle. To generate two-nodes, only the primary apex was removed. The resulting explants were placed through the hole in the ATS tubes and kept in micro centrifuge blocks. The blocks were kept in trays with a layer of water and tight-fitting lids to provide a high humidity environment and avoid wilting. The ATS tubes were topped up daily with the appropriate growth solution.

Bud outgrowth in one-node explants was tracked by measuring the branch length for 10 consecutive days post decapitation.

Bud outgrowth in two-node explants was tracked by measuring the branch length of both buds, either for 10 consecutive days or at 10 days post decapitation only. The level of competition was determined by using the relative growth index, defined as the length of the longest branch divided by the sum of the length of both branches (Ongaro et al., 2008).

2.2.2 Jar assays

For jar assays Arabidopsis seeds were sterilised as described above. Weck jars were sterilised at 200 °C for at least 24 hours. Each jar was supplemented with 50 ml ATS, containing sucrose and agar. Plants were sown at a density of 7 plants per jar and kept in tissue culture growth conditions.

Primary branch number was scored 8 weeks after sowing. Primary branch number was defined as the sum of cauline branches arising from the primary inflorescence and the number of rosette branches arising from the rosette. A branch was considered active if it was longer than 5 mm.

Dry weight per sample was determined at the end of the experiment by removing the plant from the agar and carefully removing any agar from the root system. Each whole plant

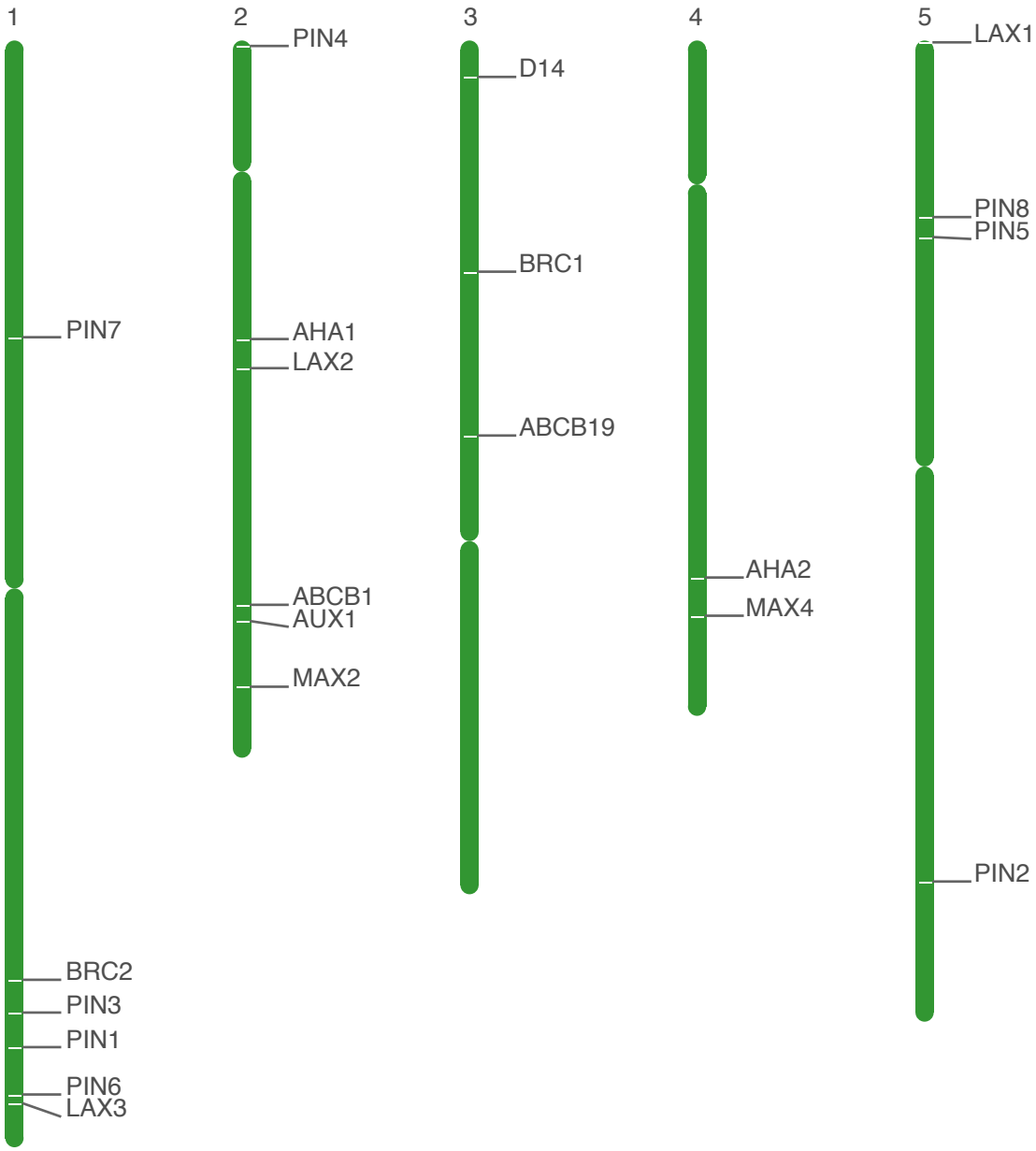

Fig. 2.1 Arabidopsis chromosome map with genes commonly used in this study.
Arabidopsis chromosome map with the five chromosomes numbered from left to right. The physical locations of genes used in this study are indicated on each chromosome. The centromeric region on each chromosome are indicated by the indentations.

was placed in an individual petri dish and dried in an oven at 50 °C for 24 hours. Samples were weighed using a laboratory scale balance (Sartorius CPA124S, d = 0.1 mg).

2.2.3 Intact branching assays

Arabidopsis seeds were grown on soil in P24 pots. Growth conditions are as stated in the figure legends. Primary branch number was scored at terminal flowering, which was defined as the point where all inflorescences stopped flowering. Primary branch number was defined as the sum of cauline branches arising from the primary inflorescence, and the number of rosette branches arising from the rosette. A branch was considered active if it was longer than 5 mm.

2.2.4 Decapitation assay

Rosette branch activation was measured using a modified version of the decapitation assay described in Greb et al. (2003). Arabidopsis seeds were grown on soil in P24 pots. Plants were grown for 4 weeks under short day growth conditions. Plants were then moved to long day growth conditions to induce flowering. The primary inflorescence was removed once it reached 10-15 cm. The number of active rosette branches was counted at various time points, as stated in the figure legends. A rosette branch was considered active if it was longer than 5 mm.

2.2.5 Plant height

The length of the primary inflorescence was used as a measure for plant height. The primary inflorescence length was determined in long day grown plants at terminal flowering, using a ruler.

2.2.6 Branch angle

The branch angle was determined by measuring the angle between the adaxial side of a cauline branch and the primary inflorescence of long day grown plants at the terminal flowering stage. Photos were taken of the two most basal cauline branches and the angle was determined using ImageJ. The branch angle of each sample was defined as the average of these two measurements.

2.2.7 Stem diameter

Stem diameter was determined by measuring the diameter of the basal internode of the primary inflorescence of long day grown plants at the terminal flowering stage. The diameter of the stem at its widest and narrowest point was measured using a digital calliper (Mitutoyo 150 mm digital calliper, 0.01 mm accuracy). The stem diameter of each sample was defined as the average of these two measurements.

2.2.8 Bulk auxin transport assay

Bulk auxin transport assays were modified from those described in Crawford et al. (2010). Plants were grown for 6 weeks under long day growth conditions. The most basal internode was harvested (unless stated otherwise in the figure legend) and from this the basal 15 mm was excised. The apical end of each segment was submerged in a PCR tube with 30 µl ATS (pH = 5.6) and 20 µM 14C-IAA (American Radiolabeled Chemicals). Stems were incubated for 6 or 18 hours, as indicated. Afterwards, the most basal 5 mm of the segment was excised, cut in half and placed in 200 µl MicroScint-20 scintillation liquid (PerkinElmer). Samples were shaken overnight at 400 RPM on MixMate microplate shakers (Eppendorf). Scintillation counting was carried out for 1 minute per well on a MB2 scintillation counter (PerkinElmer). The counts per minute (CPM) were used as a measure for the auxin content of each measured sample.

2.2.9 Auxin pulse assay

Pulse assays were conducted using the method described in van Rongen et al. (2013) and Bennett et al. (2016a). Briefly, the apical ends of 24 mm stem segments from 6-week old basal internodes were submerged for 10 minutes in 20 µl ATS (pH = 5.6) containing 5 µM 14C-IAA and 0.005 % Triton X-100. After 10 minutes samples were transferred to fresh ATS buffer solution without radiolabel and left for various time periods to allow the radiolabelled auxin to move through the segments. Samples were cut into 2 mm segments using stacked razor blades with 2 mm spacers. The radiolabeled content was measured using the scintillation method described in Section 2.2.8.

2.2.10 Auxin uptake assay

Auxin uptake was measured by modifying the method for measuring bulk auxin transport, as described in Section 2.2.8. Samples were incubated for 0.5, 1, 3 or 5 hours. Afterwards the

Table 2.2 DNA extraction buffer

Component	Final concentration
Tris-HCl (pH = 7.5)	200 mM
NaCl	250 mM
EDTA	25 mM
SDS	0.5 %

samples were cut into 2.5 mm segments and the radiolabeled content of each segment was measured using the scintillation method described in Section 2.2.8.

2.3 Molecular biology

2.3.1 DNA extraction

DNA for genotyping was extracted using a high salt-based protocol. The protocol was modified from a method used in the Wigge lab (Sainsbury Laboratory, Cambridge University, UK). Young rosette leaves or part of a young cauline branch were collected and placed in 1.2 ml collection micro tubes containing 3 mm tungsten beads (both from Qiagen). Tissue samples were left at −80 °C for at least 30 minutes prior to homogenisation with a TissueLyser II (Qiagen) for 40 seconds at 27 Hz. Afterwards 300 µl extraction buffer (Table 2.2) was added to the ground samples. Samples were mixed by inverting the tubes and centrifuged at 2,500 x *g* for 20 minutes. Afterwards, 200 µl supernatant was transferred to 96-well collection plates, 200 µl isopropanol was added and samples were mixed. Samples were centrifuged at 6,000 x *g* for 35 minutes. The solution was discarded and samples were air dried for at least 1 hour prior to resuspension of the dry pellet in 75 µl milliQ water by shaking the plate at 450 RPM on MixMate microplate shakers (Eppendorf) at room temperature for at least 1 hour. The quantity and quality of the DNA was verified using the NanoDrop 1000 spectrophotometer (NanoDrop Instruments).

DNA for cloning was extracted using the NucleosSpin Plant II kit (Macherey-Nagel) according to the instructions. The quantity and quality of the DNA was verified using the NanoDrop 1000 spectrophotometer (NanoDrop Instruments).

2.3.2 PCR

The PCR conditions were varied according to the primers used and the expected product size. For genotyping OneTaq (NEB) DNA polymerase was used. For cloning Platinum SuperFi

Table 2.3 PCR conditions

	Component	Quantity
	OneTaq buffer (NEB)	2.5 µl
	10 mM each dNTPs	0.5 µl
	10 µM primers	1 µl
	5 $U\mu l^{-1}$ OneTaq DNA polymerase	0.25 µl
	DNA template	100 ng
	Sterile dH_2O	up to 25 µl
	Temperature °C	Time
	95	1 min
	95	20 s
35 cycles	Primer T_m (50-60)	20 s
	72	1 min per kb product
	72	5 min

(Thermo Fisher Scientific) high fidelity DNA polymerase was used and PCR conditions were according to manufacturer's recommendations. All PCR mixes were made according to manufacturer's recommendations.

Typical PCR conditions followed those using the parameters shown in Table 2.3.

2.3.3 Restriction digests

Restriction digests were conducted using restriction enzymes from New England Biolabs (NEB). All digests were incubated at 37 °C. Reactions were conducted according to the manufacturer's guidelines. When digesting PCR fragments, the buffer and restriction enzyme were added directly to the PCR mix. Digests using high fidelity restriction enzymes were incubated for 5 to 10 minutes, while digests with regular restriction enzymes were incubated for 2 hours. Digests were analysed using gel electrophoresis.

2.3.4 Gateway cloning

The genomic DNA sequence of interest was amplified using PAGE-purified (polyacrylamide gel electrophoresis) primers with Gateway adaptors (SigmaAldrich). PCR fragments were cleaned using the NucleoSpin II kit (Macherey-Nagel). The 5' fragment was recombined into the pDONR-P4-P1R vector and the 3' fragment was recombined into the pDONR-P2r-P3 vector using BP II Clonase (all from Invitrogen), according to the manufacturer's protocol. A

pDONR221 vector (Invitrogen) containing the coding sequence for the citrine fluorescent protein was kindly provided by Dr. Devin O'Connor.

The final vector was constructed using the Multisite Gateway technology (Invitrogen), recombining the pDONR vectors with the pH7m34GW vector (VIB, Ghent) using LR Clonase II (Invitrogen), according to manufacturer's instructions.

2.3.5 Plasmid isolation

Plasmids were isolated using the GeneElute Plasmid MiniPrep Kit (SigmaAldrich), according to the manufacturer's instructions.

2.3.6 Sequencing and analysis

Sanger sequencing reactions (SourceBioscience) were carried out to verify relevant gene sequences. Sequence data were analysed using CLC Main Workbench 6. Raw sequence data were assembled to reference sequences obtained from NCBI GenBank and the Arabidopsis Information Resource (TAIR).

2.3.7 Transformation

Vectors were transformed into electrocompetent DH5α *E. coli* cells by adding 1 µl of the BP or LR reaction mix to 40 µl competent cells. Cells were electroporated using an Eppendorf Multiporator (Eppendorf) at 1,500 V for 5 ms. Cells were placed back on ice for 2 minutes and allowed to recover for 1 hour in 1 ml of SOC medium (Invitrogen) in a 37 °C shaker. Afterwards, cells were plated on LB-agar (lysogeny broth) plates containing the relevant antibiotics and grown at 37 °C. Viable colonies were selected after 16 to 24 hours and cultured in 5 ml of LB, with addition of relevant antibiotics. *E. coli* selection was carried out using 50 µg ml^{-1} kanamycin for pDONR vectors and 100 µg ml^{-1} spectinomycin for the pH7m34GW vector.

For transformation into *Agrobacterium*, 100 µg of vector was added to 40 µl of electrocompetent GV3101 cells. Electroporation was carried out as described above. Cells were allowed to recover as described before, but at 28 °C. Cells were plated and grown at 28 °C. Viable colonies were selected after 48-72 h and cultured at 28 °C. *Agrobacterium* selection was carried out using 100 µg ml^{-1} spectinomycin, 50 µg ml^{-1} gentomycin and 10 µg ml^{-1} rifampicin. Constructs were transformed into Arabidopsis using the floral dip method (Clough and Bent, 1998).

2.3.8 Plant selection

Seeds of transformed plants (T1) were sterilised using vapour sterilisation and plated on ATS medium containing agar, with addition of 25 µg ml^{-1} hygromycin. Plates were stratified for 4-5 days at 4 °C and then subjected to a 6-hour light treatment. Plates were kept horizontal and seeds were allowed to grow in the dark at room temperature. Resistant plants were selected based on their elongated hypocotyl phenotype (Harrison et al., 2006). Resistant plants were transferred to soil, grown to maturity and a segregation analysis was performed in the following T2 generation based on the resistance to antibiotic selection of least 100 seedlings. Individual lines that showed a 3:1 segregation based on the χ^2 statistical test were selected and homozygous offspring of these lines were selected in the T3 generation.

2.4 Microscopy

2.4.1 Fluorescence microscopy

Screening for the presence of fluorescent constructs in segregating populations following crossing was carried out using a Zeiss V12 stereo fluorescence microscope, using a GFP filter. Seeds were vapour sterilised, stratified and plants were grown vertically for 4 days on ATS plates containing agar prior to screening.

2.4.2 Confocal microscopy

Confocal microscopy was carried out using a Zeiss LSM700 confocal microscope, using a 40x water-dipping objective. Laser intensities were varied according to conditions, but kept constant within an experiment. For GFP excitation the 488 nm laser intensity was typically between 5 % to 10 %. Background fluorescence and chloroplasts were obtained using the 639 nm laser at a laser intensity range between 2 % to 6 %. Transmitted light images were recorded to verify tissue anatomy. The pinhole was optimised for the objective and Z-stacks were obtained where necessary.

Image analysis was carried out using ImageJ. Fluorescence levels on basal plasma membranes were quantified according to the method described in Shinohara et al. (2013).

2.5 Bioinformatics and primer design

2.5.1 Statistics

All statistical tests were carried out using R, version 3.3.2 and RStudio version 1.0.136. For most analyses linear models were fitted to the data. The simplest model was initially assumed and additional factors and interactions were implemented if they contributed to a statistically significant better model and were biologically relevant.

Diagnostic plots for linear regression analysis were used to check the assumptions of the underlying model, e.g. checking for normal distribution of the residuals. If the model did not violate the underlying assumptions, the least-square means of the model were calculated with the *lsmeans* package in R. Afterwards, Tukey's HSD test was carried out and different letters were used to indicate statistically significant results at a threshold of $p < 0.05$.

If the linear model appeared to violate its underlying assumptions, the data were analysed using a non-parametric comparison approach. Pairwise Wilcoxon rank-sum tests were carried out and, where applicable, Holm-Bonferroni corrections were made to account for the family-wise error rate arising from making multiple comparisons.

Where box plots are shown, the box spans the first to third quartile and the whiskers show the locations of the minimum and maximum. The line in the box represents the median value, whereas outliers are indicated by individual points.

The error bars in bar plots and line plots indicate the 95 % confidence interval, unless noted otherwise in the figure legend. The 95 % confidence interval was calculated as 1.96 times the standard error of the mean.

2.5.2 Primer design

Primers for genotyping were designed using the CLC Main Workbench 6 sequence analysis software (CLC Bio), unless published primer sequences were available. In the 'Design Primers' function in 'Standard PCR' mode, regions for primers were selected with primer lengths of 18 to 22 base pairs and a melting temperature range of 50 °C to 62 °C. Primers with a high score value and low secondary structures were selected. The primer sequences and genotyping strategies can be found in Appendix B.

Sequencing primers were designed using the CLC Main Workbench 6 sequence analysis software. In the 'Design Primers' function in 'Sequencing' mode, regions for primers were selected with primer lengths of 18 to 22 base pairs and a melting temperature range of 48 °C to 58 °C. Primers with the highest score value were selected.

2.5.3 Graphs and figures

Graphs were plotted using R, version 3.3.2 and RStudio version 1.0.136 and the *ggplot2* package. Figures were compiled using Adobe Illustrator CC, version 18.1.1 and Adobe Photoshop CC, version 2014.2.2. The chromosome map in Fig. 2.1 was generated using the Chromosome Map Tool (www.arabidopsis.org).

Chapter 3

The auxin transport network in stems

3.1 Introduction

The auxin transport network in the stem plays a pivotal role in the regulation of shoot branching. Outgrowth of buds appears to depend on their ability to establish canalised auxin export into the main stem. This is determined by the sink strength of the main stem for auxin relative to the source strength of the bud, in combination with the positive feedback between auxin flux and auxin transporter upregulation and polarisation that drives the canalization process (see Section 1.5.2). An important determinant of stem auxin sink strength is the PATS, which carries auxin away, down the stem to the root. The PIN1 auxin efflux protein makes a major contribution to auxin transport in the PATS (Bennett et al., 1995; Okada et al., 1991). PIN1 is localised to the basal plasma membrane of xylem parenchyma cells surrounding the vasculature, as well as in the cambium (Gälweiler et al., 1998). Since PIN1 is not expressed in the outer cell layers of the stem, PIN1 is unlikely to be directly involved in the movement of auxin from an activating bud towards the PATS. It is therefore likely that the initial movement of auxin between the bud and the stem involves other auxin efflux proteins.

The aim of the work described in this chapter was to characterise the stem auxin transport system in more detail. This includes identification of transporters that contribute to stem auxin transport, and the analysis of their roles in delivering the properties of the network. This was primarily achieved by measuring movement of radiolabelled auxin through isolated stem segments of mutants impaired in auxin export or import proteins. Two main assays were used; a well-established method which measures bulk auxin transport through the stem over a prolonged period (Bennett et al., 2006), and a newly developed method that measures dynamic movement of auxin along the stem, by following the progression of an auxin pulse over time (Bennett et al., 2016a; van Rongen, 2013). Using these two methods, a more

detailed understanding emerged of the components that make up the auxin transport network in the stem, which served as a basis to understand its role in shoot branching.

3.2 Results

3.2.1 The role of PIN proteins in auxin movement in the stem

The PIN1 protein has been shown to be a crucial component of the PATS, since auxin transport is strongly decreased in the *pin1* mutant stems. However, if wild type stems are treated with pharmacological inhibitors of active auxin export, auxin transport is even further reduced (Bennett et al., 1995; Okada et al., 1991), suggesting that additional auxin efflux proteins are active in the stem. With respect to the PIN family, there are eight PIN proteins in Arabidopsis, PIN1 to PIN8. Phylogenetically the PIN3, PIN4 and PIN7 proteins cluster together closely, sharing the most similarity with PIN1 (Krecek et al., 2009; Paponov et al., 2005). Although the function and localisation of PIN3, PIN4 and PIN7 has been reported in many different tissues, only recent data show that they are also expressed in the stem (Bennett et al., 2016a; Boot et al., 2016). All three proteins are expressed in partially overlapping domains with PIN1 (Bennett et al., 2016a), suggesting that they could contribute to stem auxin transport. Given the structural similarities and overlapping expression domains, the three proteins are likely to act redundantly, so to investigate their relative contribution to stem auxin transport, double and triple combinations of mutants lacking functional PIN3, PIN4 or PIN7 were created through crossing.

To assess the role of this clade in auxin transport down the stem, bulk auxin transport in stems of these mutant plants was measured. Inverted isolated 15 mm stem segments were incubated for 6 hours with their apical ends in a buffer solution containing 1 µM 14C-IAA radiolabelled auxin. The accumulation of the auxin in the basal 5 mm of the segments was then measured by scintillation (see Section 2.2.8). Compared to wild type Col-0, the *pin3pin4pin7* mutant showed a significant reduction in bulk auxin transport, whereas no consistent changes were detected in the various double mutant combinations (Fig. 3.1A).

Localisation of PIN1 in roots and floral primordia is known to respond to exogenous auxin application (Benkova et al., 2003; Heisler et al., 2005). Furthermore, in the xylem parenchyma cells of the stem auxin promotes retention of PIN1 on the basal plasma membrane (Bennett et al., 2016a). Therefore, it is possible that the reduced bulk auxin transport in the *pin3pin4pin7* mutant results in part from a reduction or relocation of basal PIN1 in the xylem parenchyma cells of the stem, rather than being directly caused by the loss of PIN3, PIN4 and PIN7. To test this, a *PIN1::PIN1:GFP* reporter construct (Xu et al., 2006)

was crossed into the *pin3pin4pin7* mutant background to investigate PIN1 levels in mutant stems. The level of basal PIN1-GFP accumulation in the basal plasma membrane of xylem parenchyma cells of basal internodes was measured as previously reported (Shinohara et al., 2013). Stems at a comparable stage to the internodes used in the bulk auxin transport assay were selected. Basal PIN1-GFP accumulation in *pin3pin4pin7* mutant stems was comparable to wild type (Fig. 3.1B).

Together, these data show that PIN3, PIN4 and PIN7 contribute to stem auxin transport, and that loss of these PINs does not change basal PIN1 levels in the stem.

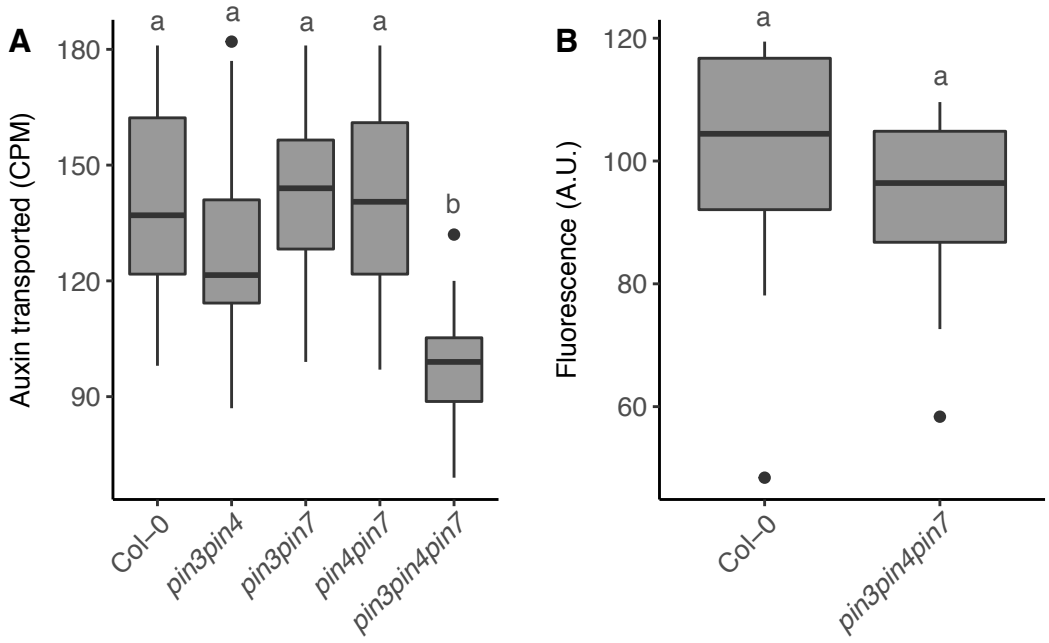

Fig. 3.1 Bulk auxin transport and PIN1 levels in *pin3/pin4/pin7* mutant stems.
(A) Bulk auxin transport in 6-week old basal internodes of plants lacking PIN3, PIN4 and PIN7 functionality in two or three genes. Data are representative of at least two independent experiments, depending on the genotype tested, $n = 24$. **(B)** Quantification of PIN1 levels at the basal plasma membrane of xylem parenchyma cells in basal internodes, at comparable stages as those used in **A**. For each genotype analysed, $n = 40$ membranes (mean of 5 per sample, 8 individual samples per line). Data are representative for two independent experiments. For **A** and **B**, Tukey's HSD test was carried out after obtaining the least-square means for a linear model fitting the data and different letters indicate statistically significant results at $p < 0.05$.

To assess the relative contributions of PIN1, PIN3, PIN4 and PIN7 to stem auxin transport, mutant combinations between *pin1*, *pin3*, *pin4* and *pin7* were created by crossing single or double mutant plants. The *pin1pin4* and *pin1pin7* double mutants were recovered in segregating F2 populations and the *pin1pin4pin7* triple mutant was generated by crossing these double mutants. Combinations involving *pin1* and *pin3* were not recovered despite

screening several hundred plants in a segregating F2 population. This is not surprising since these genes are closely linked on chromosome 1 (Fig. 2.1). Bulk auxin transport was measured in the available *pin1/pin4/pin7* mutant combinations and, as expected, the *pin1* single mutant transported markedly less auxin down their stems than wild type plants (Fig. 3.2). Additional loss of PIN4 and/or PIN7 function in the *pin1* mutant background did not lead to a further reduction of bulk auxin transport and these mutants still transported significantly more auxin than wild type plants treated with the auxin transport inhibitor NPA (Fig. 3.2). Given the lack of *pin1pin3* mutant combinations it is difficult to interpret these data, since the PIN3 protein in these lines could compensate for the lack of PIN4 and PIN7. However, since the *pin1pin3pin4pin7* is reported to be embryo lethal (Blilou et al., 2005), assessing the role of PIN3 would in any case be challenging.

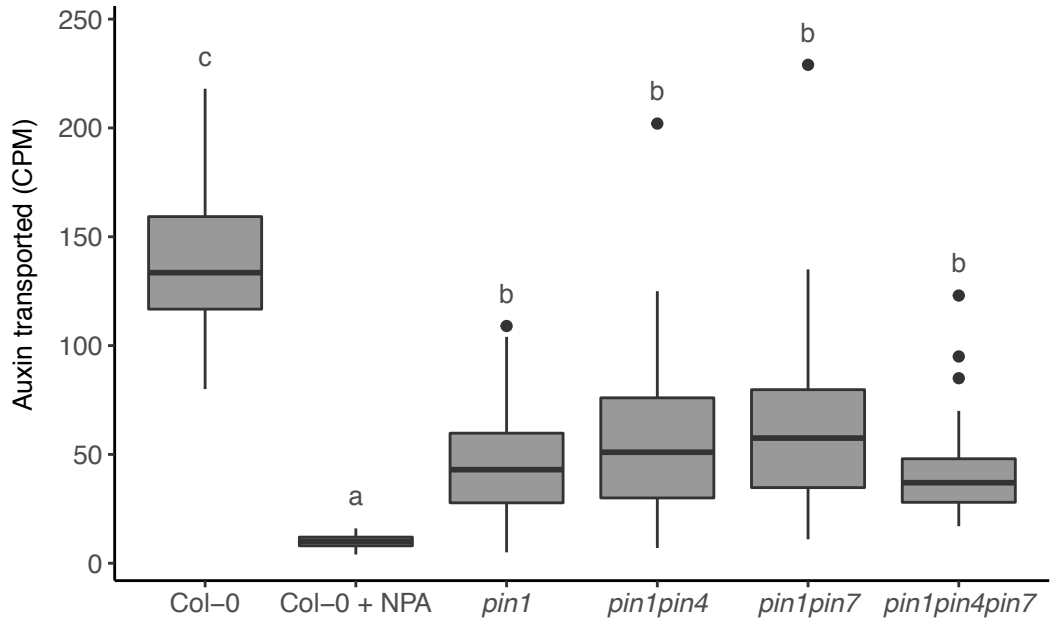

Fig. 3.2 Bulk auxin transport in *pin1/pin4/pin7* mutant stems.
Bulk auxin transport in 6-week old basal internodes of plants lacking PIN1, PIN4 and/or PIN7 functionality. The *pin1pin4pin7* mutant combination was included in three, and the other genotypes were included in two independent experiments, $n = 24$. Tukey's HSD test was carried out after obtaining the least-square means for a linear model fitting the data and different letters indicate statistically significant results at $p < 0.05$.

In addition to PIN1, PIN3, PIN4 and PIN7, PIN2 is also expressed in stems where it accumulates in a weakly polar pattern in xylem parenchyma cells (Bennett et al., 2016a). In addition, PIN6 and PIN8 are expressed mainly in the cambium (Bennett et al., 2016a). To test if these proteins could also play a role in auxin transport down the stem, bulk auxin

transport was measured in mutants lacking functional PIN2, PIN6 or PIN8 proteins. No PIN5 localisation data have been reported for the stem, but a mutant lacking functional PIN5 protein was available and included in the assay for completeness. No significant differences were found in bulk auxin transport between any of these mutants and wild type (Fig. 3.3).

Taken together, these data show that the bulk auxin transport phenotype in *pin1* mutants is not further exacerbated by loss of PIN4 and PIN7. On their own, the PIN2, PIN5, PIN6 and PIN8 proteins do not appear to contribute to bulk auxin transport in the stem.

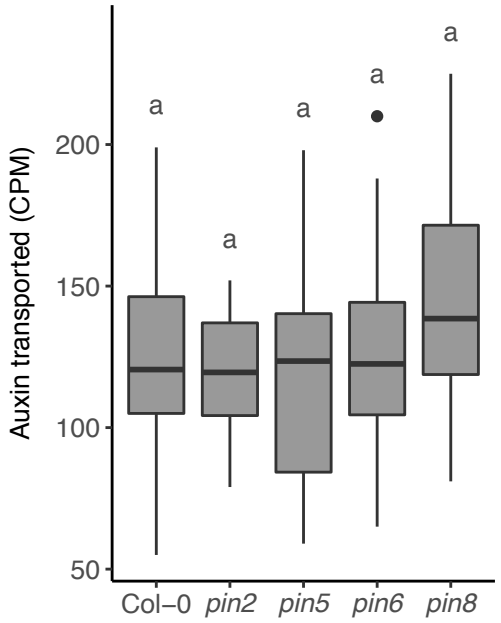

Fig. 3.3 Bulk auxin transport in *pin2, pin5, pin6* and *pin8* mutant stems.
Bulk auxin transport in 6-week old basal internodes of plants lacking PIN2, PIN5, PIN6 or PIN8 functionality. Data are representative of three independent experiments, $n = 24$. Tukey's HSD test was carried out after obtaining the least-square means for a linear model fitting the data and different letters indicate statistically significant results at $p < 0.05$.

3.2.2 The role of PIN proteins in auxin transport dynamics in the stem

The data above show that auxin transport in the stem is facilitated by at least PIN1, PIN3, PIN4 and PIN7. How exactly they contribute to this movement is less clear. The bulk auxin transport assay measures basal accumulation of radiolabelled IAA over a 6-hour time window and as such does not provide any information about how auxin is distributed as it moves through the stem. To get a better understanding of the dynamics of stem auxin movement, an assay was previously developed to track the progression of a pulse of auxin moving

through the stem (Bennett et al., 2016a; van Rongen, 2013). In this assay, basal internodes are incubated with their apical ends in a buffer containing radiolabelled auxin for 10 minutes, providing a pulse of labelled auxin, after which they are transferred to a buffer without auxin. Samples can be left in this buffer for varying amounts of time. The distribution of auxin in the stem can be assayed by cutting the stem into 2 mm segments and determining the radiolabelled auxin content in each segment individually by scintillation (see Section 2.2.9). In this way, the distribution of the auxin in the original pulse can be tracked over time. It has been established that this assay measures active auxin transport, since application of NPA blocks the movement of auxin along the stem (Bennett et al., 2016a; van Rongen, 2013).

In wild type stems, the auxin distribution shows a clear peak after 30 minutes, which becomes shallower and broader at later time points, making it difficult to discern a clear peak (Fig. 3.4A; Bennett et al., 2016a; van Rongen, 2013). At later time points auxin increasingly accumulates at the basal end of the sample. The broadening of the pulse, together with the finding that endogenous auxin drains in a non-linear manner from stem segments (Bennett et al., 2016a), suggests that auxin does not move with simple linear dynamics as would be expected if it moved solely through the PATS. For example, even for the 30-minute time point, it is clear that there is a wide range of rates of movement for auxin, while the speed of the main peak is only 1 cm per hour (Fig. 3.4A; Bennett et al., 2016a). It suggests that there may be significant exchange of auxin between the PATS and the tissues surrounding it, where auxin transport has different kinetics. A computational model that can capture these properties suggests that the auxin transport network in the stem is multimodal, with a high conductance polar component (such as the PATS), and a less polar and lower conductance component surrounding it, which has been termed Connective Auxin Transport (CAT) (Bennett et al., 2016a). The experimental pulse assay data (Fig. 3.4) are best captured if exchange of auxin between the PATS and CAT is incorporated into the model (Bennett et al., 2016a).

The expression pattern of PIN3, PIN4 and PIN7 in the tissues surrounding the PATS, as well as the reduction of bulk auxin transport in *pin3pin4pin7* suggests that these proteins may act as less polar and lower conductance components in the auxin transport network predicted for CAT. To test this idea, an auxin pulse was applied to *pin3pin4pin7* stems to further investigate the contribution of the PIN3/PIN4/PIN7 proteins to auxin transport through the stem. If the pulse was allowed to progress for 30 or 90 minutes, the distribution of the radiolabelled auxin was largely comparable to wild type (Fig. 3.4A). However, if the pulse was allowed to progress for an intermediate period of time, 60 minutes, a proportion of the apical (segment 1) and medial segments (segments 7-10) of the *pin3pin4pin7* samples accumulated higher levels of auxin than wild type ($p < 0.05$ for unadjusted Student's t-test; Holm-Bonferroni adjusted t-tests were not significant)(Fig. 3.4A; Bennett et al., 2016a). Auxin

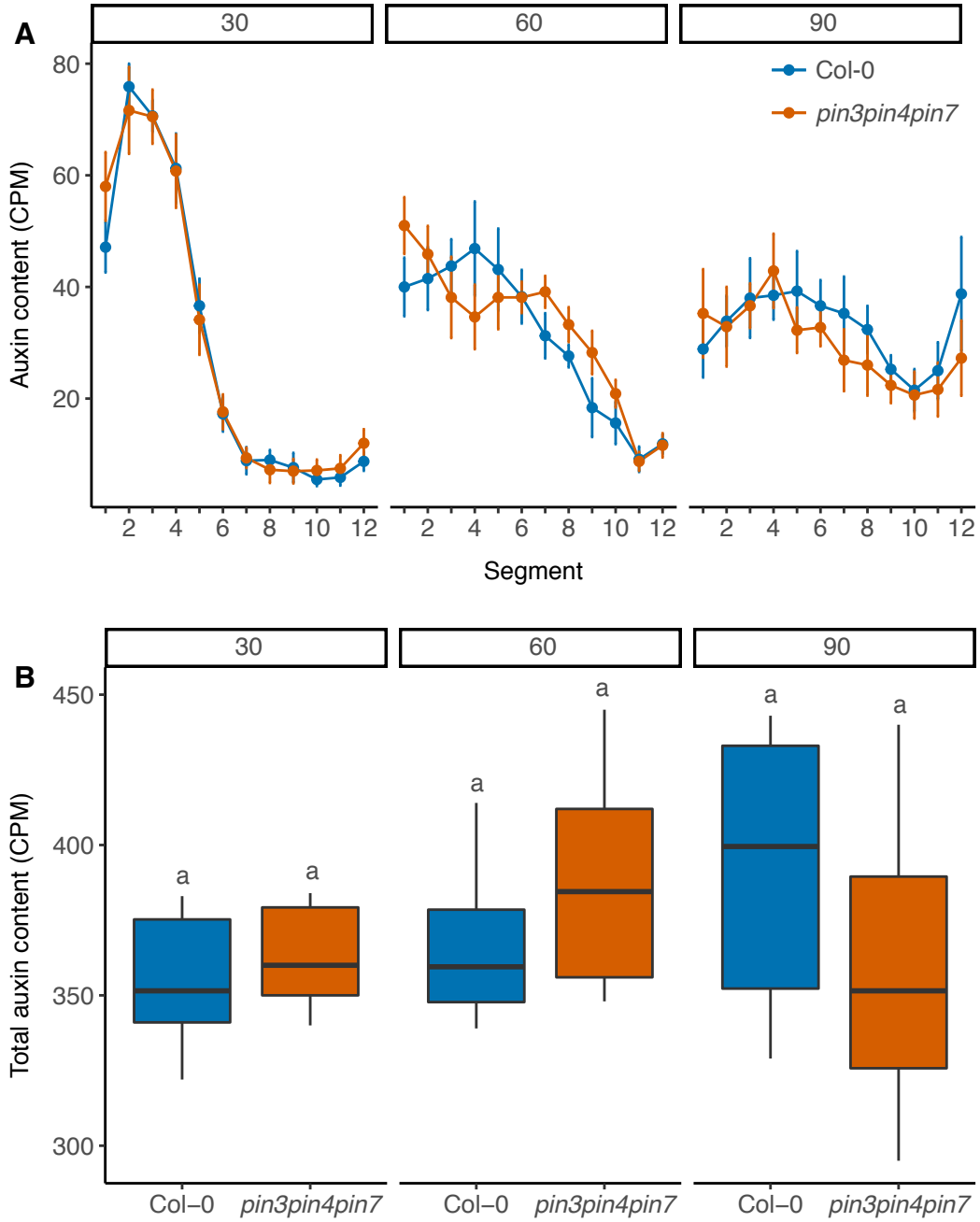

Fig. 3.4 Movement of an auxin pulse in *pin3pin4pin7* mutant stems.
(A) Progression of a 10-minute pulse of 5 µM 14C-IAA through 24 mm long basal internodes of Col-0 and *pin3pin4pin7* stems at 30, 60 and 90 minutes after application (left to right), measured as counts per minute (CPM) in 2 mm segments. The error bars represent the 95 % confidence interval of the mean. **(B)** Total auxin content per sample, equalling the sum of the counts of all segments within one sample. Tukey's HSD test was carried out after obtaining the least-square means for a linear model fitting the data and different letters indicate statistically significant results at $p < 0.05$. Data are representative of three independent experiments, $n = 8$.

uptake into the stems was comparable between wild type and *pin3pin4pin7* stems (Fig. 3.4B), showing that auxin can enter *pin3pin4pin7* stems normally and that the differences in dynamics are not due to differential uptake of auxin. The altered auxin distribution in the *pin3pin4pin7* stems is consistent with a reduced exchange of auxin between the PATS and its surrounding tissues. Specifically, if auxin in the PATS is less likely to move out of the PATS, it will continue to move efficiently down the stem, in the highly polar high capacity PATS. Auxin that takes a more circuitous route via the surrounding tissues, where transport is less polar and of lower capacity, will be less efficient in progress down the stem, and thus take longer to reach more basal stem regions, resulting in a spreading of the auxin distribution. Similarly, at the site of auxin application at the apex, reduced exchange between the PATS and CAT will reduce the rate at which auxin reaches the PATS, resulting in apical accumulation of auxin. The same model used to simulate the wild type pulse dynamics is able to capture the *pin3pin4pin7* pulse data by reducing the permeability of the lateral membranes in each channel, which reduces the exchange of auxin between the channels (Bennett et al., 2016a).

To test the model further, auxin movement in the *max2* mutant was investigated. The *max2* mutant has high levels of basal PIN1, correlating with higher levels of bulk auxin transport in its stems (Bennett et al., 2006; Crawford et al., 2010). To test if the high levels of PIN1 qualitatively affect the distribution of an auxin pulse in the stem, a pulse assay experiment was conducted. No clear difference could be found between wild type and *max2* at any of the sampled time points suggesting that, despite the high levels of PIN1, the overall exchange of auxin between the PATS and its surrounding tissues is unchanged (Fig. 3.5A). Auxin uptake was comparable between genotypes and consistent across the different time points (Fig. 3.5B). The computational model used to capture the pulse dynamics observed in Bennett et al. (2016a) is able to reproduce the *max2* pulse dynamics if the lateral exchange between the PATS and CAT is increased (Dr. G. Hines, pers. comm.).

If the distribution of an auxin pulse in *max2* is indeed comparable to wild type due to an increase in lateral exchange of auxin between the PATS and CAT, then impairing the CAT in this background is expected to lead to changes in distribution of an auxin pulse. To test this, the *pin3pin4pin7* mutations were introduced into a *max2* background through crossing and an auxin pulse assay was conducted using *max2pin3pin4pin7* stems. These data are from a single experiment, so should be treated with caution. No clear difference could be detected after 30 minutes, but after 60 and 90 minutes a greater proportion of auxin can be found in the more apical segments (Fig. 3.6A). The qualitative difference between the wild type and *max2pin3pin4pin7* pulses is most obvious when the individual pulse traces are plotted, particularly in the 90-minute time point. In wild type the pulse traces are mostly flat, consistent with the broadening of the initial pulse (Fig. 3.6B, top). However,

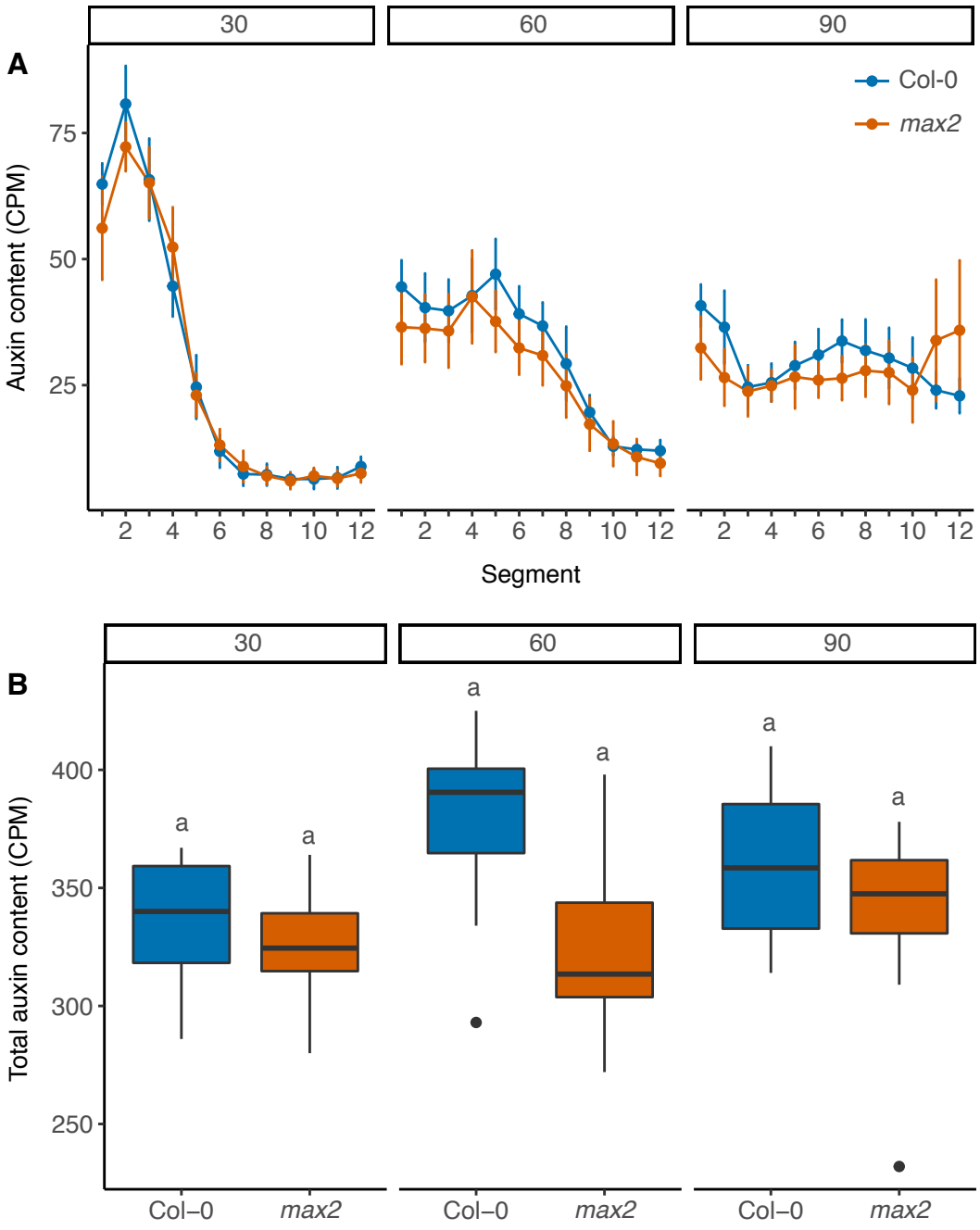

Fig. 3.5 Movement of an auxin pulse in *max2* mutant stems.
(A) Progression of a 10-minute pulse of 5 µM 14C-IAA through 24 mm long basal internodes of Col-0 and *max2* stems at 30, 60 and 90 minutes after application (left to right), measured as counts per minute (CPM) in 2 mm segments. The error bars represent the 95 % confidence interval of the mean. **(B)** Total auxin content per sample, equalling the sum of the counts of all segments within one sample. Tukey's HSD test was carried out after obtaining the least-square means for a linear model fitting the data and different letters indicate statistically significant results at $p < 0.05$. Data are representative of two independent experiments, $n = 8$.

in the *max2pin3pin4pin7* mutant the pulse traces retain their pulse shape much more clearly (Fig. 3.6B, bottom), but the position of the peaks between the different traces is large, with some peaks found in the more apical part of the sample and others at the more basal part. This effect was also noticeable using a slightly modified setup, where the pulse length was increased to 15 minutes to allow for an increased sample size (Fig. 3.7). These data suggest that maintenance of the auxin peak is affected by auxin exchange between tissues of the PATS and CAT.

3.2.3 The role of ABCB proteins in auxin transport in the stem

The bulk auxin transport in Arabidopsis stems has been shown to further depend on a non-PIN class of transport proteins, the B-subfamily of ATP-binding cassette (ABC) transporters. Loss of two closely related homologues, *ABCB1* and *ABCB19*, leads to severe developmental defects and strongly reduced auxin transport in hypocotyls and apical parts of the inflorescence (Geisler et al., 2003; Noh et al., 2001). Under normal growth conditions, no clear phenotypic defects can be found in young or mature *abcb1* single mutant plants (Geisler et al., 2003; Noh et al., 2001). The *abcb19* single mutant has wavy hypocotyl growth in the dark and cotyledons are epinastic (Lin and Wang, 2005; Noh et al., 2001). Phenotypes in the *abcb1abcb19* double mutant are strongly synergistic of both single mutants. The *abcb1abcb19* mutant plants produce wrinkly and severely curved leaves, grow very slowly and are very stunted (Noh et al., 2001). Root and hypocotyl growth is wavy and the cotyledon epinasty is increased, compared to *abcb19* single mutants (Noh et al., 2001).

Localisation of these proteins is predominantly non-polar (Bennett et al., 2016a; Blakeslee et al., 2007; Geisler et al., 2005; Wu et al., 2007), suggesting that they may contribute to the non-polar component of the auxin transport network in the stem. Given the importance of non-polar transport in the stem auxin transport dynamics described above, the contribution of ABCB1 and ABCB19 to stem auxin transport was assessed. Because of the strong developmental defects reported for the *abcb1abcb19* mutant, both single mutants were also included in the analysis. Null alleles for *abcb1* and *abcb19* (Lin and Wang, 2005) were obtained and crossed, allowing the recovery of the cognate *abcb1abcb19* double mutant.

The published bulk auxin transport phenotypes for these *abcb* mutants were obtained by measuring auxin transport in much younger and more apical tissues than those used standardly here (Noh et al., 2001). When assessed in this standard assay, bulk auxin transport in *abcb1abcb19* stems was strongly reduced compared to wild type and both single mutants but, somewhat surprisingly, the *abcb19* single mutant did not show a reduction in auxin transport, contrary to earlier reports(Fig. 3.8A; Noh et al., 2001. Over the course of this study, the *abcb19* mutant was included in 13 bulk auxin transport assays, in which a significant

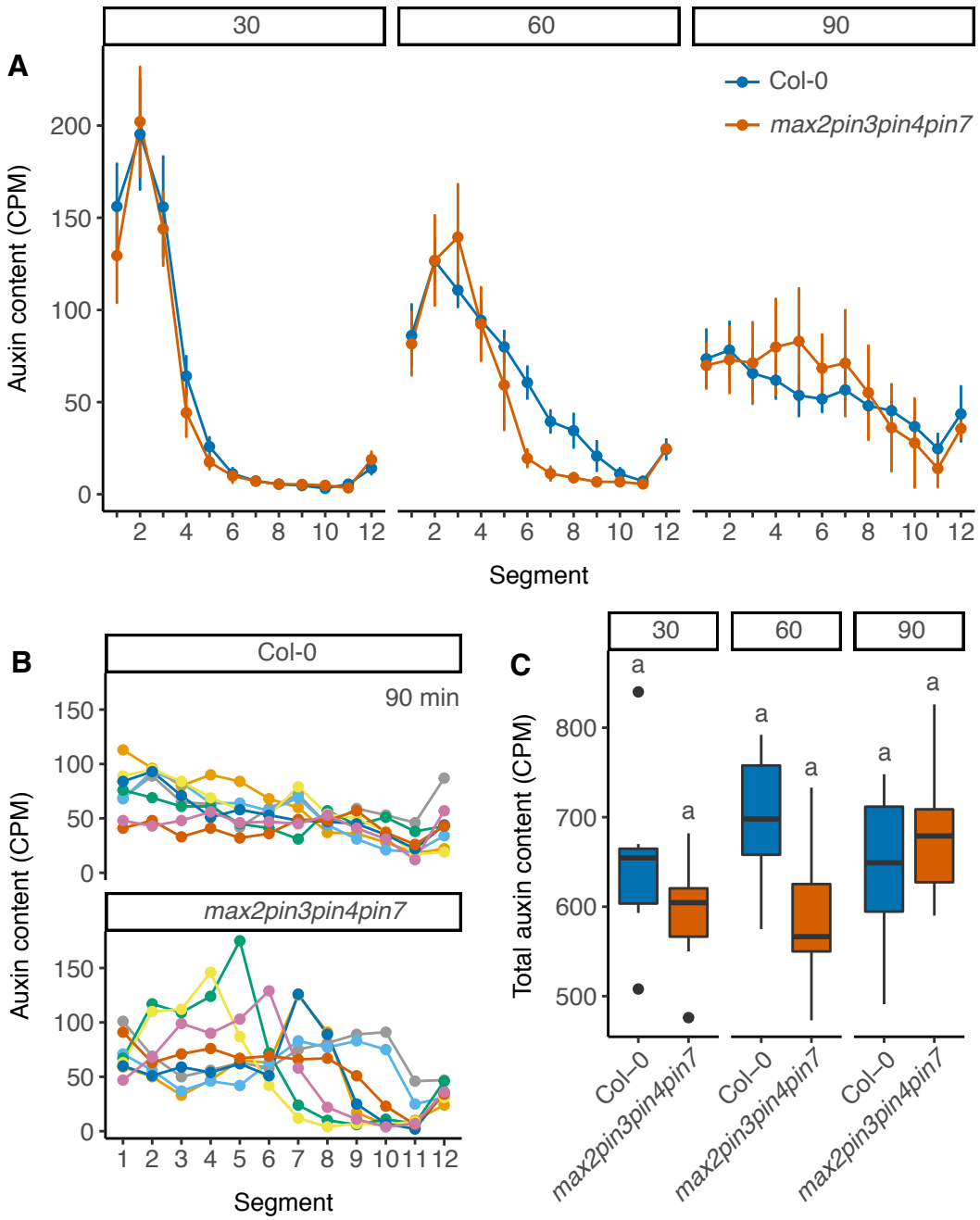

Fig. 3.6 Movement of an auxin pulse in *max2pin3pin4pin7* mutant stems.
(A) Progression of a 10-minute pulse of 5 µM 14C-IAA through 24 mm long basal internodes of Col-0 and *max2pin3pin4pin7* stems at 30, 60 and 90 minutes after application (left to right), measured as counts per minute (CPM) in 2 mm segments. The error bars represent the 95 % confidence interval of the mean. **(B)** Individual pulse traces, 90 minutes after application of the pulse. **(C)** Total auxin content per sample, equalling the sum of the counts of all segments within one sample. Tukey's HSD test was carried out after obtaining the least-square means for a linear model fitting the data and different letters indicate statistically significant results at $p < 0.05$. Data are from a single experiment, $n = 8$.

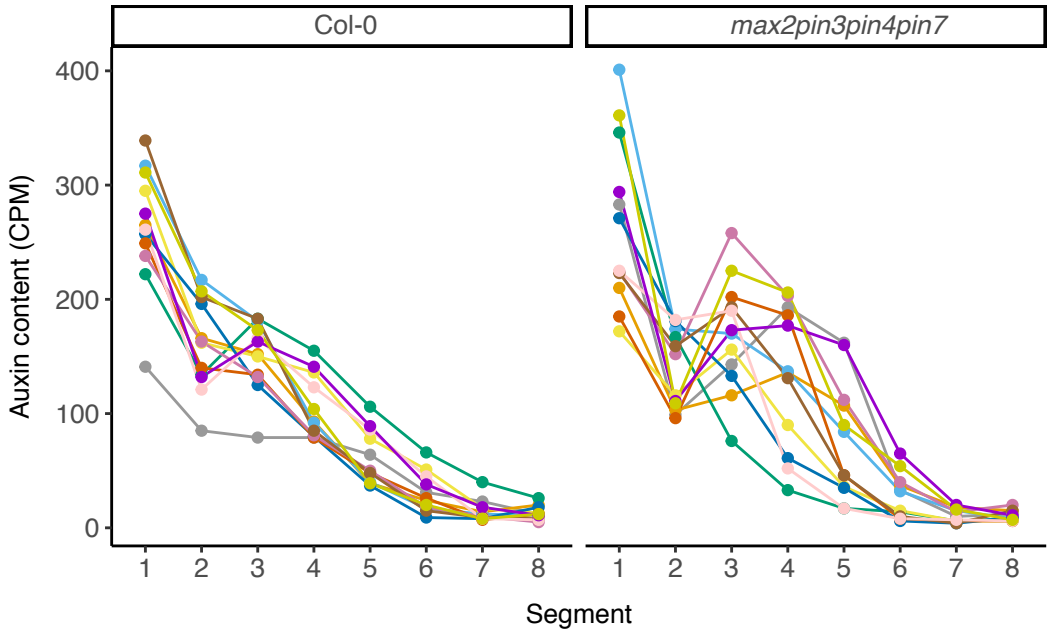

Fig. 3.7 Individual auxin pulse traces in *max2pin3pin4pin7* mutant stems.
Individual auxin pulse traces in 20 mm long Col-0 and *max2pin3pin4pin7* stem segments, following a 15-minute pulse of 250 nM 3H-IAA. Auxin distribution was measured as counts per minute (CPM) in 2.5 mm segments, 45 minutes after application of the pulse.

reduction compared to wild type was observed in eight experiments. Several attempts were made to identify the cause of this variability. Since the original bulk auxin transport assays were conducted on much younger tissues, bulk auxin transport was measured using the standard assay, but on apical segments taken 10 cm below the apex. The amount of auxin transported in these segments was markedly lower than in basal internodes, but no difference was detected between wild type and *abcb19* stems (Fig. 3.8B). To assess whether the 6-hour assay period was insufficient to detect robustly a small difference between wild type and *abcb19*, an 18-hour incubation time was used. In this setup *abcb19* consistently transported less auxin than wild type in two independent experiments (Fig. 3.8C). How this incubation time relates to the published bulk auxin transport data is not clear, since the incubation time was not provided (Noh et al., 2001).

An additional possible source of variation is plant age. In the original experiments, younger inflorescence stems were used than standardly used in the bulk auxin transport assay. The variation in bolting time between wild type and *abcb19* mutant plants is not noticeably different than the variation observed within either genotype, so the developmental stage of the bolting stem was considered comparable when harvested. To assess the effect of plant age on bulk auxin transport rates stems were harvested at 35 days, the earliest time point when all plants had bolted, 42 days, the standard time point used for the bulk auxin transport assay, and 49 days, when most plants had reached the terminal flowering stage. Only a single experiment was carried out, so the results should be treated with caution. In this experiment the *abcb19* mutants showed decreased levels of auxin transport compared to wild type at all ages, using the 6-hour assay period (Fig. 3.8D). Interestingly, auxin transport rates increased in both wild type and *abcb19* mutant plants between 39 and 42 days. No significant further increase was detected at 49 days. Taken together, these data show that the *abcb19* mutant transports less auxin than wild type, but that the ability to detect this difference is sensitive to the length of time over which the transport is measured.

PIN1 has been shown to relocalise in *abcb19* hypocotyls and both ABCB1 and ABCB19 can co-localise with PIN1, suggesting that PIN1-ABCB interactions can affect auxin transport (Blakeslee et al., 2007; Noh et al., 2003). Since changes in PIN1 levels in the stem can result in altered stem auxin transport, PIN1-GFP levels at the basal plasma membrane of xylem parenchyma cells were measured in the *abcb* mutant backgrounds. A *PIN1::PIN1:GFP* reporter construct (Xu et al., 2006) was crossed into *abcb1* and *abcb19* single mutants and homozygous lines were recovered and crossed to generate the *abcb1abcb19 PIN1::PIN1:GFP* line. Accumulation of basal PIN1-GFP in xylem parenchyma cells in *abcb19* mutants was not different to wild type, whereas a small but significant decrease was observed in the *abcb1* mutant background (Fig. 3.9). Despite several attempts to measure PIN1-GFP accumulation

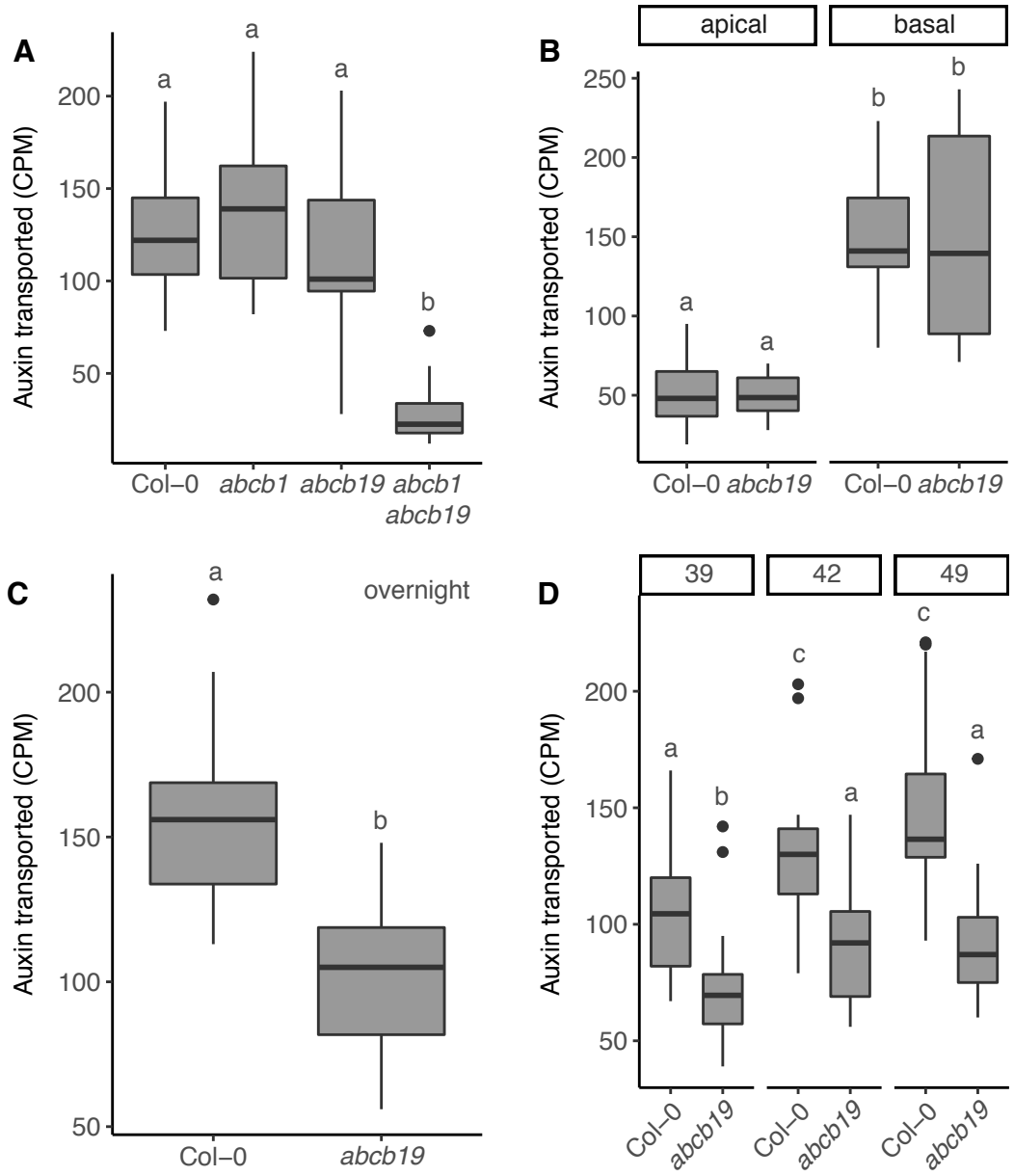

Fig. 3.8 Bulk auxin transport in *abcb1/abcb19* mutant stems.
(A) Bulk auxin transport in 6-week old basal internodes of plants lacking ABCB1, ABCB19 functionality or both. Transport in the *abcb1* and *abcb19* single mutants was measured in at least 7 individual experiments, whereas the *abcb1abcb19* was included once, $n = 24$. **(B)** Effect of segment location on bulk auxin transport in *abcb19* mutants, with 'apical' referring to the stem 10 cm below the apex and 'basal' denoting the most basal internode. Data are representative for two independent experiments, $n = 24$. **(C)** Auxin transport in basal internodes, incubated for 18 hours. Data are representative for two independent experiments, $n = 23$-24. **(D)** Effect of plant age on bulk auxin transport, measured in the basal internodes of plants 39, 42 or 49 days after sowing. Data are from a single experiment, $n = 17$-20. For **A**-**D**, Tukey's HSD test was carried out after obtaining the least-square means for a linear model fitting the data and different letters indicate statistically significant results at $p < 0.05$.

in *abcb1abcb19* double mutant stems, no data could be collected for this mutant. The extreme dwarfism and altered vasculature made it impossible to gather comparable data.

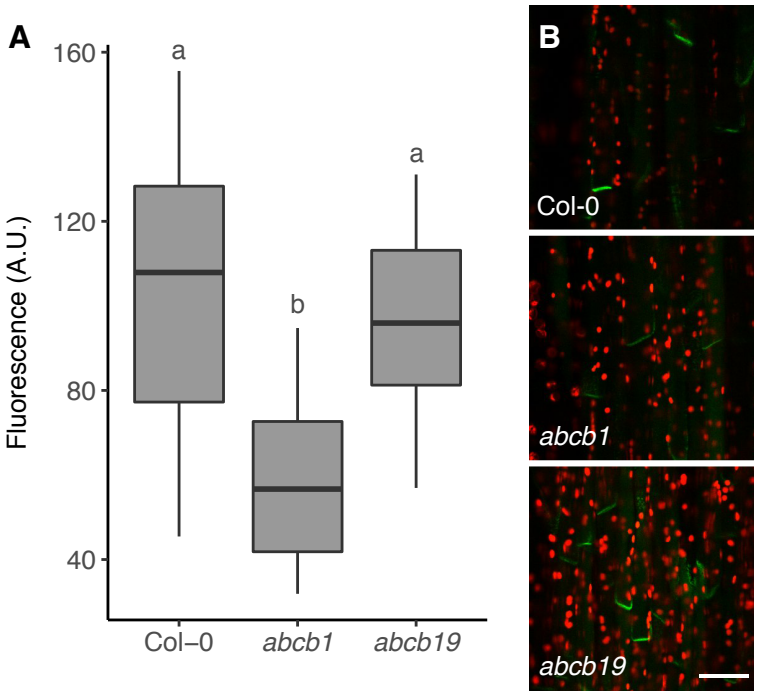

Fig. 3.9 PIN1-GFP levels in *abcb1/abcb19* stems.
(A) Quantification of PIN1-GFP at the basal plasma membrane of xylem parenchyma cells in basal internodes of 6-week old inflorescence stems. For each genotype analysed, $n = 40$ membranes (mean of 5 per sample, 8 individual samples per line). Data are representative of two independent experiments. Tukey's HSD test was carried out after obtaining the least-square means for a linear model fitting the data and different letters indicate statistically significant results at $p < 0.05$. **(B)** PIN1-GFP expression in xylem parenchyma cells, as quantified in **A**. Green signal indicates GFP, red chloroplast auto fluorescence. Images are from longitudinally hand-sectioned basal internodes. Bar = 25 µm.

The non-polar expression of ABCB19 across most tissues in the stem (Bennett et al., 2016a) suggests that ABCB19 might contribute to auxin movement between the PATS and the surrounding tissues. If this is the case, then the movement of an auxin pulse along stems over time may show significant differences between *abcb19* mutants and wild type. However, no clear differences in auxin distribution could be detected between *abcb19* and wild type at any of the investigated time points (Fig. 3.10A), and uptake of the radiolabel was also similar to wild type (Fig. 3.10B). These data suggest that loss of ABCB19 function alone does not markedly change the dynamics of auxin transport through the stem and that auxin is still able to exchange efficiently between the different tissues in the stem.

The overlap in expression domains between ABCB19 and PIN3, PIN4 and PIN7 raises the possibility that the PINs might be able to compensate for any auxin transport defects caused

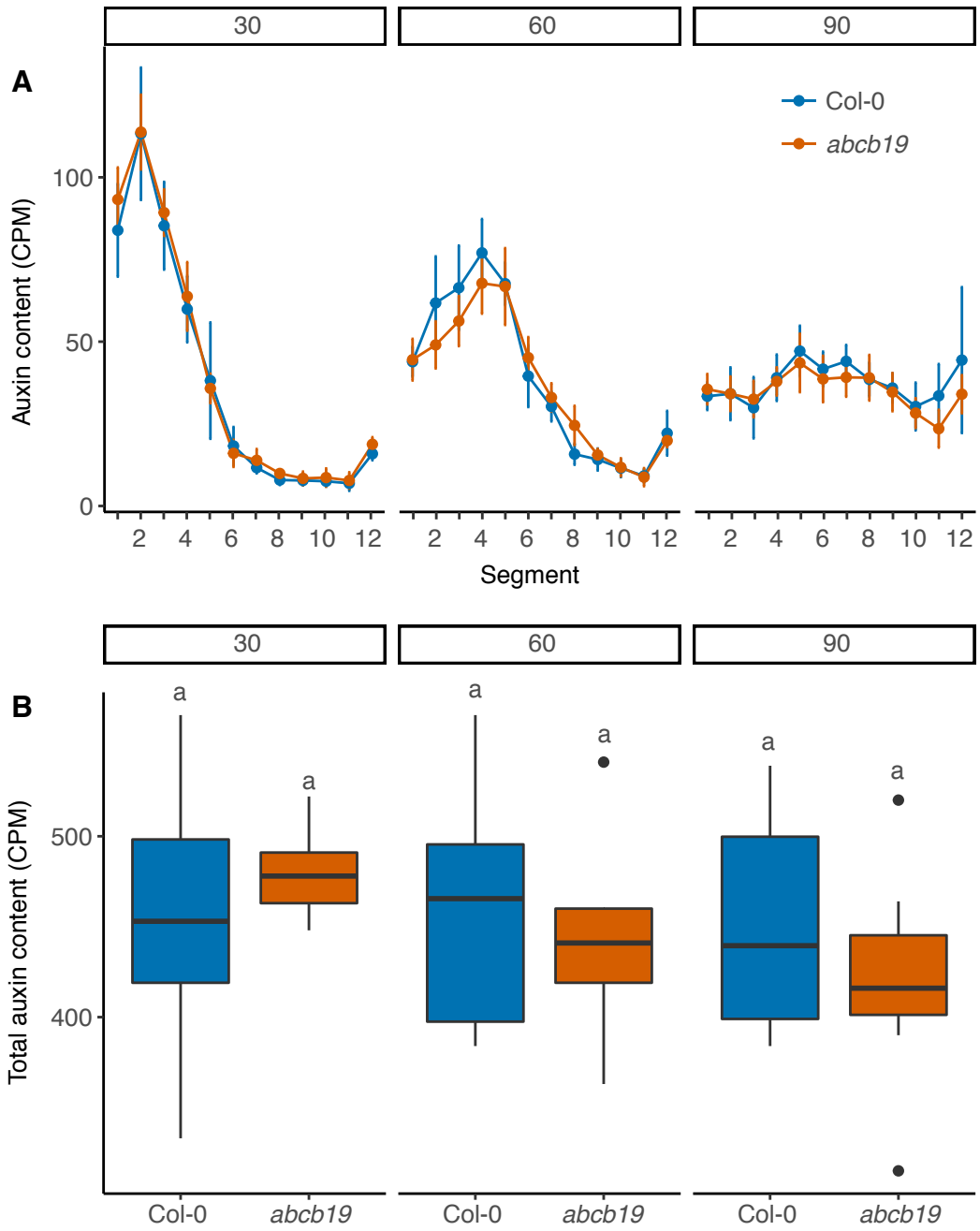

Fig. 3.10 Movement of an auxin pulse in *abcb19* mutant stems.
(A) Progression of a 10-minute pulse of 5 µM 14C-IAA through 24 mm long basal internodes of Col-0 and *abcb19* stems at 30, 60 and 90 minutes after application (left to right), measured as counts per minute (CPM) in 2 mm segments. The error bars represent the 95 % confidence interval of the mean. **(B)** Total auxin content per sample, equalling the sum of the counts of all segments within one sample. Tukey's HSD test was carried out after obtaining the least-square means for a linear model fitting the data and different letters indicate statistically significant results at $p < 0.05$. Data are representative of two independent experiments, $n = 8$.

by loss of ABCB19 function. To address this question, the *abcb19* mutation was introduced into the *pin3pin4pin7* mutant background and bulk auxin transport was measured in the *abcb19pin3pin4pin7* quadruple mutant after a 6-hour incubation period. Consistent with previous experiments, the *pin3pin4pin7* mutant showed decreased levels of auxin transport, but additional loss of *abcb19* did not appear to have any discernible further effect on bulk auxin transport (Fig. 3.11). These data suggest that *pin3pin4pin7* and *abcb19* do not have a synergistic effect on bulk auxin transport in the stem.

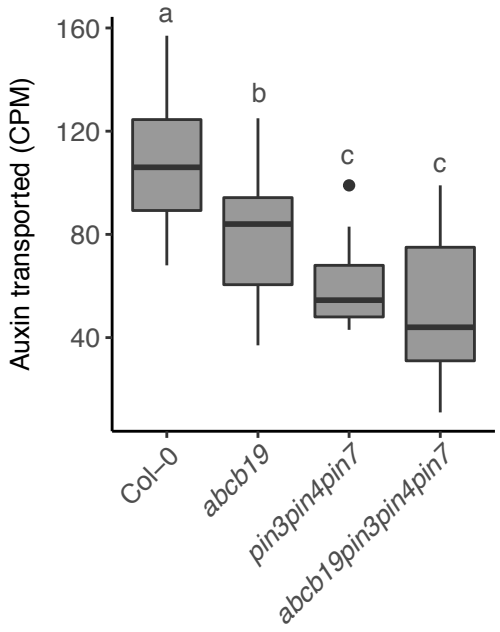

Fig. 3.11 Bulk auxin transport in *abcb19/pin3pin4pin7* mutant stems.
Bulk auxin transport in 6-week old basal internodes of plants lacking ABCB19, PIN3, PIN4 and PIN7 functionality. Data are representative of three independent experiments, $n = 24$. Tukey's HSD test was carried out after obtaining the least-square means for a linear model fitting the data and different letters indicate statistically significant results at $p < 0.05$.

Although no data are available on ABCB1 expression and localisation in the stem, the strong additive effects of ABCB1 and ABCB19 suggest that ABCB1 may play a role in stem auxin transport. To further investigate this, attempts were made to investigate possible synergistic effects of ABCB1 and PIN3, PIN4, PIN7 by creating higher-order mutants lacking functionality for these proteins. However, the *abcb1pin4* double mutant combination was not recovered after screening several hundred plants in a segregating F2 population. Although ABCB1 and PIN4 are on the same chromosome, they are not located in close proximity to one another (Fig. 2.1), suggesting that genetic linkage is unlikely. Regardless, the lack of *abcb1pin4* combinations made further investigation challenging.

3.2.4 The role of AUX1/LAX proteins in auxin transport in the stem

Auxin import in Arabidopsis is facilitated by a family of four closely related auxin import proteins, AUX1 and three LIKE-AUX1 (LAX1-3) proteins (Bennett et al., 1996; Peret et al., 2012; Swarup et al., 2001). Loss of all four *AUX1/LAX* genes results in strongly reduced stem auxin movement (Boot et al., 2016). To explore the contribution of auxin import to the bulk movement of auxin in the stem, a bulk auxin transport assay was performed on plants lacking either *AUX1* or *AUX1* in combination with its three closest homologues *LAX1*, *LAX2* and *LAX3*. Bulk auxin transport was significantly reduced in the *aux1* mutant, with a further decrease in transport observed in the *aux1lax1lax2lax3* quadruple mutant (Fig. 3.12).

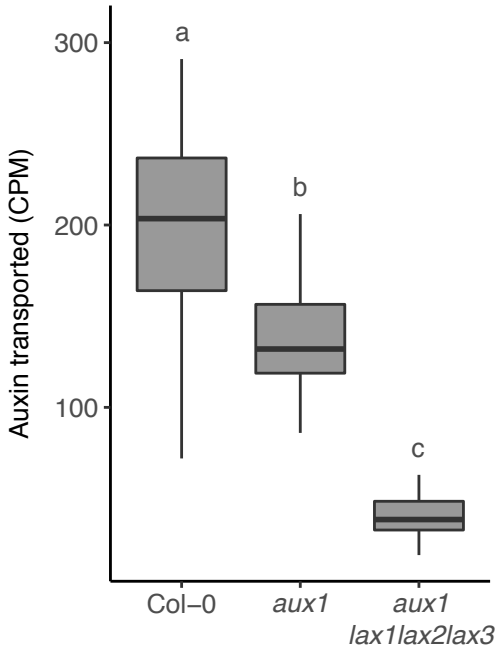

Fig. 3.12 Bulk auxin transport in *aux1/lax* mutant stems.
Bulk auxin transport in 6-week old basal internodes of Col-0, *aux1* and *aux1lax1lax2lax3* plants. Data are representative of two independent experiments, $n = 24$. Tukey's HSD test was carried out after obtaining the least-square means for a linear model fitting the data and different letters indicate statistically significant results at $p < 0.05$.

Since these mutants are highly likely to be impaired in their uptake of auxin at the site of application, the observed reduction in the bulk auxin movement could be the result of reduced uptake of radiolabelled auxin over the course of the experiment, rather than a reduced rate of movement of auxin along the stem. To test this, auxin uptake in basal stem segments was measured by incubating the apical end of the segments in radiolabelled auxin for 3 hours and analysing the auxin content in small segments of each sample (Fig. 3.13A). The

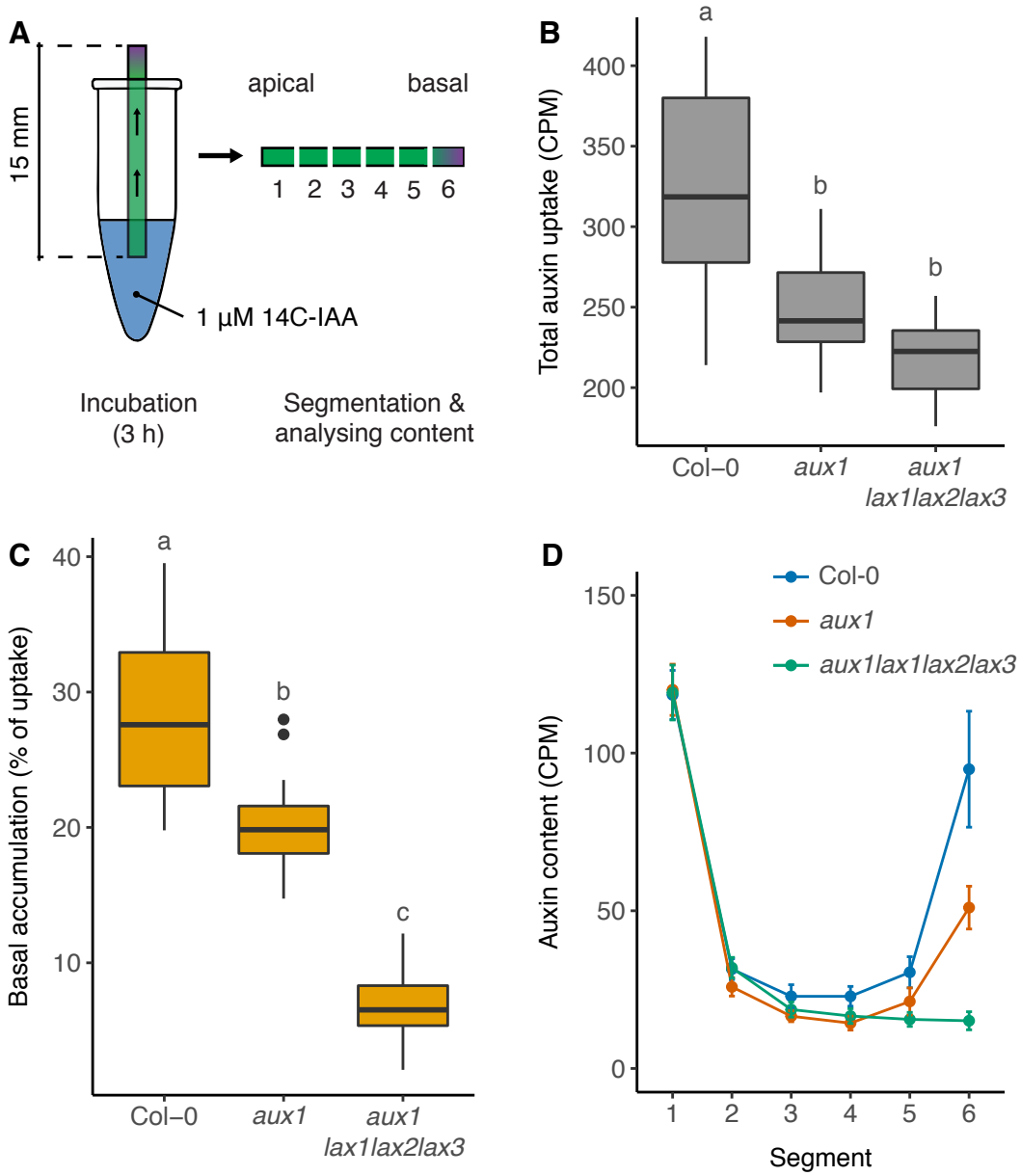

Fig. 3.13 Auxin uptake and movement in *aux1/lax* mutant stems.
(A) Experimental setup for measuring auxin uptake in stems. The apical end of the most basal 15 mm of the primary inflorescence was submerged in 1 µM 14C-IAA for 3 hours, cut into 2.5 mm segments and the radiolabelled content of each individual segment was determined. **(B)** Total auxin uptake, determined by summing the counts of the six segments of each sample. **(C)** Accumulation in the most basal segment, calculated as a percentage of the total uptake. **(D)** Mean auxin content per segment for each genotype. The error bars represent the 95 % confidence interval of the mean. For **B** and **C**, Tukey's HSD test was carried out after obtaining the least-square means for a linear model fitting the data and different letters indicate statistically significant results at $p < 0.05$. Data are representative of two independent experiments, $n = 16$.

total auxin uptake, determined as the sum of all the counts recovered from each sample, was reduced in both *aux1* and *aux1lax1lax2lax3* mutants, compared to wild type, consistent with a reduction of auxin uptake (Fig. 3.13B). Accumulation of auxin at the basal end was significantly reduced in *aux1* and *aux1lax1lax2lax3* mutants, relative to the total uptake of auxin (Fig. 3.13C). This was also evident when analysing the auxin content of each individual segment. The most apical segments of both the *aux1* and *aux1lax1lax2lax3* mutants in contact with the radiolabelled buffer solution were still able to take up radiolabelled auxin at levels comparable to wild type (Fig. 3.13D, segment 1). This suggests that auxin is able to enter the sample, for example accumulating in the apoplast, but that subsequent movement of auxin down *aux1* and *aux1lax1lax2lax3* stems is reduced compared to wild type, resulting in reduced basal accumulation in both mutants (Fig. 3.13B, D, segment 6).

Together, these data show that AUX1/LAX proteins contribute to stem auxin transport.

3.3 Summary

- PIN3, PIN4 and PIN7 contribute to bulk auxin transport in the stem.
- Stem auxin transport in *pin1* mutants is not further decreased by loss of PIN4 and PIN7.
- Auxin transport profiles along the stem suggest a high capacity highly polar auxin transport mode (PATS) as well as a less polar lower capacity transport mode (CAT) with exchange between them.
- PIN3, PIN4 and PIN7 contribute to CAT, and to auxin exchange between PATS and CAT.
- The similarities in auxin transport dynamics between *max2* and wild type stems can be attributed to compensatory changes in the PATS and CAT.
- ABCB1 and ABCB19 contribute to stem auxin transport, but the individual contributions of the transporters are small.
- Auxin importers contribute to stem auxin transport.

Chapter 4

The role of connective auxin transport in the control of shoot branching

4.1 Introduction

The data from the previous chapter show stem auxin transport to be multimodal, with a high conductance polar component (PATS), and a less polar, lower conductance component surrounding it (CAT), as well as exchange of auxin between them. These findings have implications for how the auxin transport network could operate in the control of shoot branching. It has previously been proposed that the PATS could function as an information source, integrating the combined activity of auxin sources across the shoot (Bennett and Leyser, 2014). In terms of shoot branching control, auxin sink strength in the PATS provides long-distance information about the number and status of active apices, since all active buds export their auxin into the PATS. This information, however, needs to be conveyed at a more local level between buds. Connective auxin transport could facilitate this, since it provides an interface between tissues of the PATS and the bud (Bennett et al., 2016a).

The aim of this chapter was to investigate the functional significance of CAT and auxin exchange between tissues in the regulation of shoot branching. This was primarily achieved by assessing the role of broadly expressed auxin export and import proteins in bud outgrowth responses. Bud outgrowth responses were measured in mutants impaired in auxin export or import function using mainly two types of experiments. First, the ability of plants to activate rosette buds was assessed by using a well-established method where rosette buds are released from inhibition following decapitation of the primary shoot apex (Greb et al., 2003). Here, plants are grown under short day conditions for four weeks, which increases the number of rosette leaves. Plants are then transferred to long days to induce flowering

and decapitation takes place once the primary shoot apex reaches around 10 cm (Greb et al., 2003). Using this short day/long day decapitation assay, the progression of bud activation was followed by counting the number of active rosette branches over time, following decapitation. Second, bud outgrowth was assessed in a more isolated manner, using a two-node setup. Here two young, small cauline buds on an isolated inflorescence explant are left to compete for outgrowth following decapitation. It has previously been shown that in this setup buds are able to communicate with each other across the stem and compete for outgrowth, with one bud able to inhibit outgrowth of the other bud (Ongaro et al., 2008). Using mutants impaired in auxin export or import, the contributions of these proteins to bud activation dynamics and bud-bud competition was assessed.

The role of CAT and auxin exchange in shoot branching control was further investigated in the context of strigolactones. Mutants impaired in the perception or synthesis of strigolactone show high levels of branching (Booker et al., 2004; Sorefan et al., 2003; Stirnberg et al., 2002; Waters et al., 2012). This is at least in part caused by reduced removal of PIN1 from the plasma membrane which, in the stem, results in a higher sink strength and, in the bud, enables buds to canalise their auxin from the bud more easily than in wild type plants. Combined, this allows strigolactone mutants to activate their buds more readily than in wild type, resulting in increased levels of branching (Bennett et al., 2006; Prusinkiewicz et al., 2009; Shinohara et al., 2013). Mutants impaired in CAT were introduced into strigolactone mutant backgrounds to investigate their contribution to the shoot branching network.

4.2 Results

4.2.1 The role of PIN3/PIN4/PIN7 in communication between apices

In the previous chapter, the PIN3, PIN4 and PIN7 proteins were shown to contribute to CAT and auxin exchange in the stem. To further investigate their functional significance in the context of shoot branching, bud outgrowth was assessed in *pin3/pin4/pin7* double mutant combinations, and the *pin3pin4pin7* triple mutant. A short day/long day decapitation assay was performed and the number of active branches was counted 10 days post decapitation, the time point standardly used (Greb et al., 2003). Rosette branch numbers were significantly reduced in the *pin3pin4* and *pin3pin4pin7* mutants, compared to wild type, but no clear difference could be found in the *pin3pin7* and *pin4pin7* mutants (Fig. 4.1A; Bennett et al., 2016a).

The reduced rosette bud activation in the *pin3pin4* and *pin3pin4pin7* mutants could result from either a delay or a complete inhibition of bud activation. To test this, rosette branches

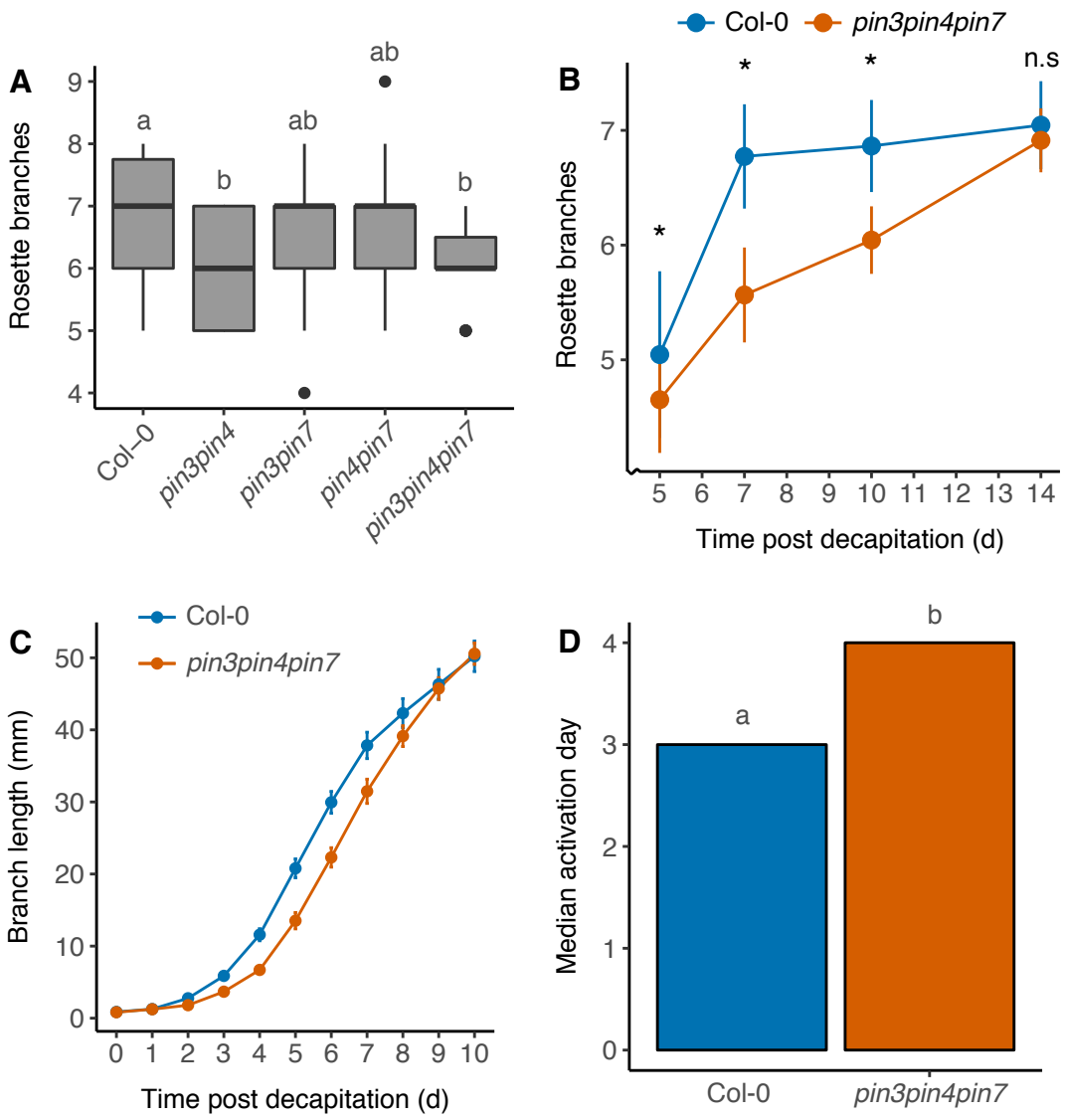

Fig. 4.1 Bud outgrowth dynamics in *pin3/pin4/pin7* mutants.
(A) Rosette branch number of short day to long day shifted plants, 10 days after decapitation, n = 21-24. Tukey's HSD test was carried out after obtaining the least-square means for a linear model fitting the data and different letters indicate statistically significant results at $p < 0.05$. Data are representative for at least two independent experiments depending on the genotype assayed. **(B)** Rosette branch activation dynamics in wild type and the *pin3pin4pin7* mutant, scored 5, 7, 10 and 14 days post decapitation. The data for the 10-day time point in **B** are from the same data set as presented in **A**. Bars represent the 95 % confidence interval of the mean. Asterisks indicate statistically significant differences per time point ($p < 0.05$ for Holm-Bonferroni adjusted pairwise Wilcoxon rank-sum tests); n.s. 'not significant'. Data are representative for three independent experiments. **(C)** Branch length of one-node Col-0 and *pin3pin4pin7* explants, followed for 10 days after decapitation. Data are representative of two independent experiments, n = 19-23. **(D)** Median day where buds first reached 5 mm or more for the data presented in **C**. A comparison with the Wilcoxon rank-sum test was carried out. Different letters indicate statistically significant results at $p < 0.05$.

were counted at earlier and later time points than 10 days post decapitation. Branch numbers were assessed at 5, 7, 10 and 14 days post decapitation in wild type and in the *pin3pin4pin7* triple mutant. In wild type, most rosette branches had activated by 7 days and the number of growing rosette branches stayed constant during the remainder of the experiment (Fig. 4.1B). In contrast, the number of growing rosette branches in the *pin3pin4pin7* mutant continued to increase over time and reached wild type levels towards the end of the experiment (Fig. 4.1B; Bennett et al., 2016a). This delayed outgrowth was also observed in single isolated cauline buds. Young inflorescences bearing two or three cauline buds were collected and transferred to microcentrifuge tubes containing a liquid growth solution. The most basal bud was allowed to activate by removing the primary shoot apex and the axillary buds above it. Buds of the *pin3pin4pin7* mutant tended to activate slower than wild type buds (Fig. 4.1C). Branch length of *pin3pin4pin7* explants was lower than wild type during most of the experiment (Fig. 4.1C). Buds are generally irreversibly active once they reach around 5 mm in length. Determining the median day where each explant reached this threshold showed that *pin3pin4pin7* buds took significantly longer to activate than wild type (Fig. 4.1D). The ability of *pin3pin4pin7* buds to grow was not impaired, since branch length was comparable to wild type in the later stages of the experiment (Fig. 4.1C).

When cauline buds on a two-node explant are released from apical dominance following removal of the primary shoot apex, buds compete for outgrowth (Ongaro et al., 2008). In wild type two-node explants, often only one bud activates, with either the top or the bottom bud dominating and inhibiting outgrowth of the other bud. In a small proportion of two-node explants, both buds are able to activate simultaneously (Fig. 4.2A; Ongaro et al., 2008). The degree of dominance between the buds is best captured using a relative growth index (RGI), defined as the length of the longest branch divided by the summed length of both branches (Ongaro et al., 2008). The buds on such two-node explants vascularise into different vascular bundles and communication between the buds is therefore unlikely to occur directly via the PATS (Ongaro et al., 2008). The contribution of PIN3, PIN4 and PIN7 to auxin exchange between the PATS and CAT suggests that these PINs may contribute to bud-bud communication. To test this, competition between two buds in *pin3pin4pin7* mutant explants was analysed in a two-node assay. In a large proportion of wild type two-node explants, one bud dominated the other, resulting in a high relative growth index (Fig. 4.2B). In contrast, in *pin3pin4pin7* two-node explants both buds tended to activate, resulting in a significantly reduced RGI compared to wild type (Fig. 4.2B; Bennett et al., 2016a).

Taken together, these data show that PIN3, PIN4 and PIN7 play an important role in the activation of buds. Rosette bud activation in the *pin3pin4pin7* mutant is delayed. Furthermore, competition between two isolated buds is reduced in *pin3pin4pin7* mutants, supporting the

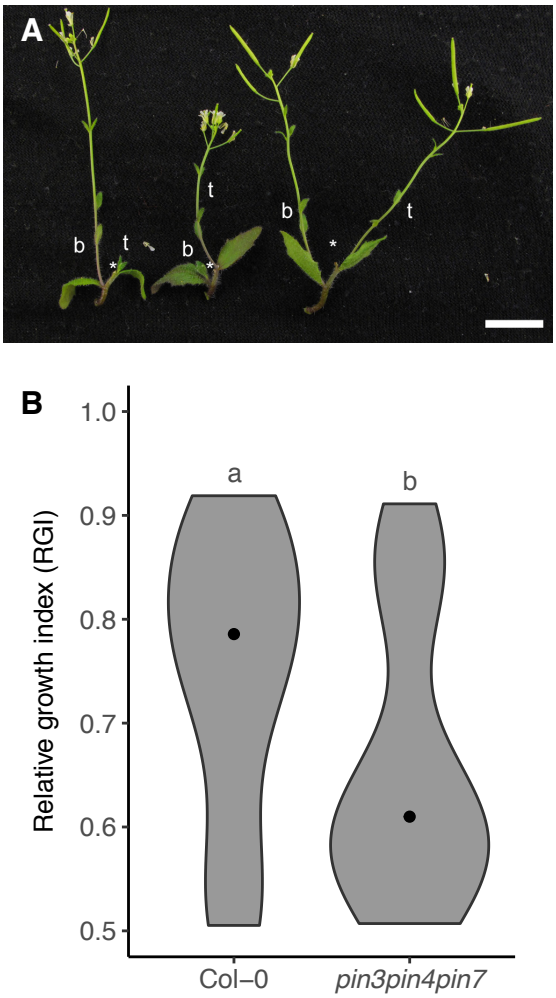

Fig. 4.2 Bud competition in *pin3pin4pin7* mutant two-node explants.
(A) Explants showing the potential outcomes of bud-bud competition in a two-node assay, 10 days post decapitation. The top (t), bottom (b) or both buds can activate. Asterisks indicate the point of decapitation. Bar = 10 mm. **(B)** Violin plot for the relative growth index (RGI) of Col-0 and *pin3pin4pin7* two-nodes, 10 days post decapitation, $n = 24$. The RGI is the proportion of branch length in the longest branch. Black dots indicate the median value and the area of each plot represents the probability distribution of the values. A comparison with the Wilcoxon rank-sum test was carried out. Different letters indicate statistically significant results at $p < 0.05$. Data are representative of three independent experiments and have been published in Bennett et al. (2016a).

notion that these PIN proteins contribute to lateral communication between shoot apices across the stem.

4.2.2 The relationship between strigolactones and PIN3/PIN4/PIN7

The reduced removal of PIN1 from the plasma membrane of strigolactone mutants results in a higher sink strength of the PATS and, in the bud, allows for easier canalisation of auxin across the stem (Prusinkiewicz et al., 2009). The evidence on PIN3, PIN4 and PIN7 presented thus far suggests that loss of these PINs reduces auxin exchange between the PATS and CAT and that this impairs communication between buds. It is therefore possible that PIN3, PIN4 and PIN7 contribute to strigolactone-mediated shoot branching control through their effect on auxin transport. To further investigate this relationship, the *pin3pin4pin7* mutations were introduced into a *max4* strigolactone synthesis deficient background through crossing. The *max2pin3pin4pin7* strigolactone perception mutant has been described in Chapter 3. Bulk auxin transport is reduced in *pin3pin4pin7* mutant stems (Fig. 3.1) and *max2pin3pin4pin7* auxin pulse data show that auxin moves in a qualitatively different manner in these mutant stems, compared to wild type (Fig. 3.6, 3.7). To test whether loss of PIN3, PIN4 and PIN7 also affects bulk auxin transport in a strigolactone mutant background, a bulk auxin transport assay was performed on *max2pin3pin4pin7* and *max4pin3pin4pin7* stems (Fig. 4.3A). Bulk auxin transport was reduced to wild type levels in stems of both *maxpin3pin4pin7* mutants (Fig. 4.3A), whereas the *max* mutants transported significantly higher levels of auxin than wild type, consistent with earlier reports (Fig. 4.3A; Bennett et al., 2006; Crawford et al., 2010; Prusinkiewicz et al., 2009). Consistent with the data presented earlier, the *pin3pin4pin7* mutant had lower-than-wild-type levels of bulk auxin transport (Fig. 3.1, 4.3A).

Basal PIN1 accumulation on the plasma membrane of xylem parenchyma cells is increased in *max* mutants (Crawford et al., 2010; Shinohara et al., 2013). To test whether the reduced transport phenotypes in the *maxpin3pin4pin7* mutants are the result of changes in PIN1 accumulation, a *PIN1::PIN1:GFP* reporter construct (Xu et al., 2006) was introduced into the *max2pin3pin4pin7* background. Basal PIN1-GFP accumulation at the basal plasma membrane of xylem parenchyma cells was determined in basal internodes. Only a single experiment was carried out, so these results should be treated with caution. Basal PIN1-GFP levels were significantly increased in *max2pin3pin4pin7* mutant stems, compared to wild type. However, as reported previously, basal PIN1-GFP levels were also increased in the *max2* background, compared to wild type (Fig. 4.3B; Crawford et al., 2010; Shinohara et al., 2013) and no difference could be detected between *max2* and *max2pin3pin4pin7* mutant stems (Fig. 4.3B). Basal PIN1-GFP levels in *pin3pin4pin7* were indistinguishable from wild type (Fig. 4.3B), consistent with data presented earlier (Fig. 3.1B).

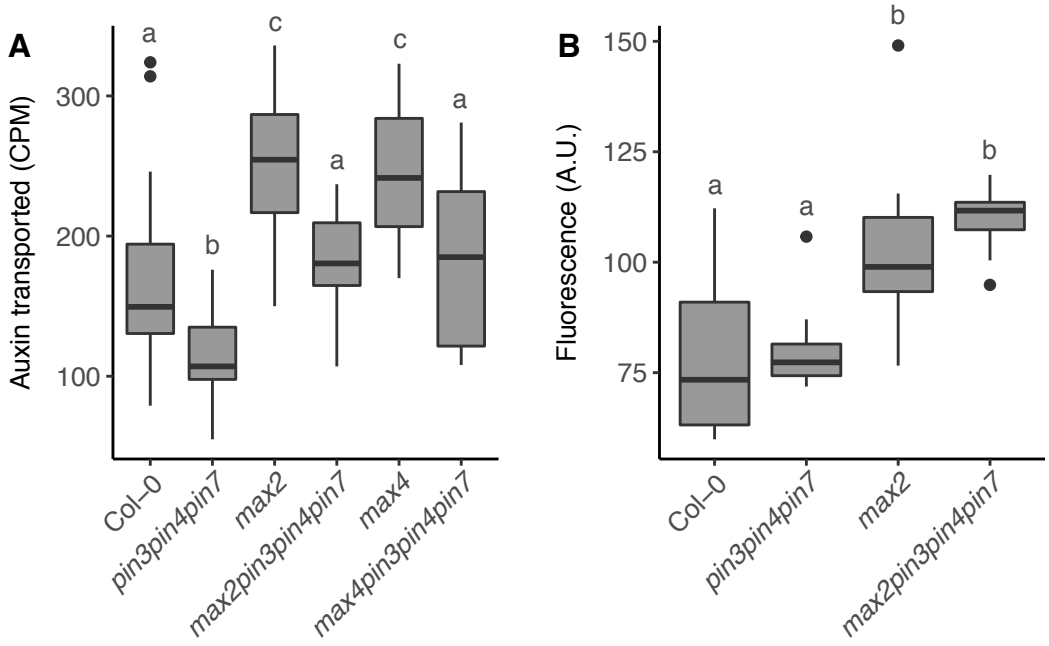

Fig. 4.3 Bulk auxin transport and PIN1 levels in *maxpin3pin4pin7* mutant stems.
(A) Bulk auxin transport measured in 6-week old basal internodes of strigolactone mutants lacking functional PIN3, PIN4 and PIN7. Data are representative of three independent experiments, $n = 24$. **(B)** Quantification of PIN1 levels at the basal plasma membrane of xylem parenchyma cells in basal internodes, at comparable stages as those used in **A**. For each genotype analysed, $n = 40$ membrane (mean of 5 per sample, 8 individual samples per line). Data are from a single experiment. For **A** and **B** Tukey's HSD test was carried out after obtaining the least-square means for a linear model fitting the data and different letters indicate statistically significant results at $p < 0.05$.

Taken together, these data show that loss of PIN3, PIN4 and PIN7 in *max* mutants reduces bulk auxin transport in the stem. Basal PIN1 accumulation in these mutants appears to remain elevated.

To assess whether bud activation in the *maxpin3pin4pin7* mutants was altered, rosette branch activation was measured in a short day/long day decapitation assay. At 10 days post decapitation, both *max2pin3pin4pin7* and *max4pin3pin4pin7*mutants had activated significantly fewer rosette branches than their *max2* and *max4* controls, but still markedly more than wild type (Fig. 4.4A). Rosette branch activation is delayed in *pin3pin4pin7* mutants (Fig. 4.1A). To test if this delay in branch activation also occurs in a strigolactone-deficient background, rosette bud activation was followed over time for the *maxpin3pin4pin7* mutants. At 5 days post decapitation, the first time point sampled, *max2pin3pin4pin7* and *max4pin3pin4pin7* had activated significantly fewer branches than *max2* and *max4*, respectively ($p < 0.05$, Holm-Bonferroni adjusted pairwise Wilcoxon rank-sum tests). Both *max2pin3pin4pin7* and *max4pin3pin4pin7* mutants continued to activate additional rosette branches over the course of the experiment, but activated significantly fewer rosette branches than *max2* and *max4* mutants, respectively, at every time point sampled ($p < 0.05$, Holm-Bonferroni adjusted pairwise Wilcoxon rank-sum tests) (Fig. 4.4B).

The number of buds which grow into branches is determined by how many buds are released from inhibition, but also by the number of buds available for activation. To investigate whether the reduced branching in the *maxpin3pin4pin7* mutants was caused by a reduction in axillary bud formation, plants were grown under the same regime as used for the short day/long day decapitation assay. Rosette axils were dissected at the time point where plants are normally decapitated and the presence or absence of an axillary bud was noted. Given the similarities in response of both *maxpin3pin4pin7* mutants, only the *max2pin3pin4pin7* mutant was sampled. Although only one data set is available for the *max2* and *max2pin3pin3pin7* genotypes, there was very little variation within each genotype, indicating robustness in the result. Whereas both wild type and *pin3pin4pin7* plants usually had several empty axils per plant, no empty axils could be found in either *max2* or *max2pin3pin4pin7* plants (Fig. 4.4C). The total number of rosette axils formed in the *max2pin3pin4pin7* mutant was not different to the number of rosette axils found in either wild type or *max2* (Holm-Bonferroni-adjusted Wilcoxon rank-sum tests, not significant) (Fig. 4.4D).

Taken together, these data show that *pin3pin4pin7* partially suppress rosette branch activation in the *max2* and *max4* mutant backgrounds. The branch suppression is not caused by a reduction in axillary bud formation.

To further characterise the shoot phenotypes of the *maxpin3pin4pin7* mutants, plants were grown under standard long day growth conditions. The level of branching under these

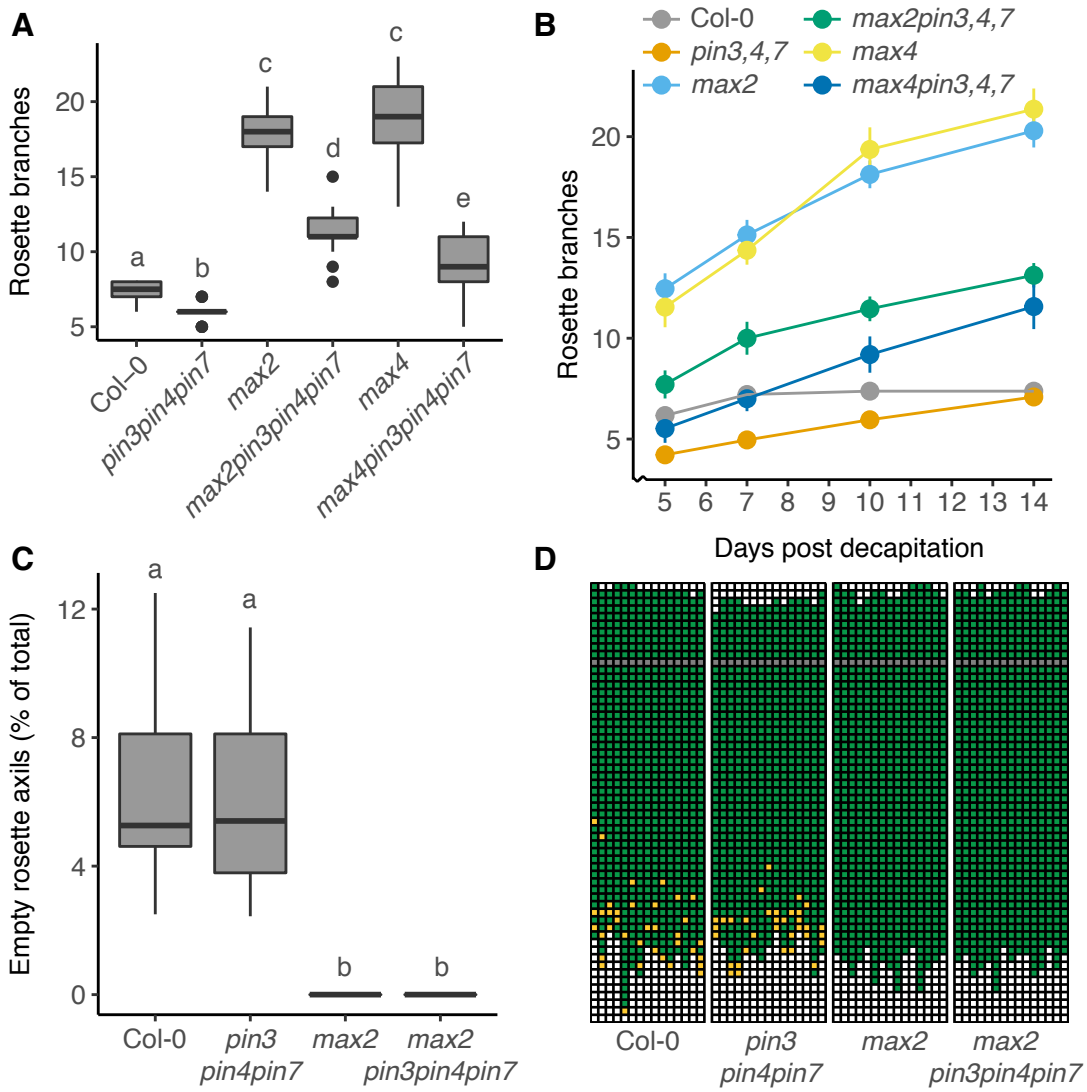

Fig. 4.4 Bud formation and activation dynamics in *maxpin3pin4pin7* mutants.
(A) Rosette branch number of short day to long day shifted plants, 10 days after decapitation. Data are representative for three independent experiments, n = 21-24. **(B)** Rosette branch activation dynamics of the genotypes presented in **A**, scored 5, 7, 10 and 14 days post decapitation. The data for the 10-day time point in **B** are from the same data set as presented in **A**. Bars represent the 95 % confidence interval of the mean. **(C)** Number of empty rosette axils of short day/long day shifted plants at the point of decapitation, calculated as a percentage of the total number of rosette axils for a subset of genotypes shown in **A**. **(D)** Schematic representation of axillary bud formation in the cauline and rosette leaf axils of the plants from **C**. Each column represents an individual plant, and each square a single leaf axil. Axils are scored from top to bottom, with the oldest leaf axils at the bottom. Green denotes the presence and orange the absence of an axillary bud. The grey square represents the border between cauline and rosette leaf axils, with cauline axils above and rosette axils below. Data are from a single experiment, n = 15. For **A** and **B** Tukey's HSD test was carried out after obtaining the least-square means for a linear model fitting the data and different letters indicate statistically significant results at $p < 0.05$.

conditions was determined at the terminal flowering stage. At this stage flower production ceases simultaneously at all inflorescence branches and activity at the meristems stops (Hensel et al., 1994). This makes terminal flowering a useful developmental stage to assess end-point levels of branching. Branching was scored by counting the number of active primary branches, defined as branches arising from the axils of rosette leaves, and cauline branches arising from the main inflorescence. A branch was considered active if it was longer than 5 mm. Under these conditions, branching in both *max2pin3pin4pin7* and *max4pin3pin4pin7* mutants was significantly reduced compared to *max2* and *max4*, respectively (Fig. 4.5A). Branching in both quadruple mutants was still increased relative to wild type (Fig. 4.5A).

Strigolactone mutants display a reduced stature and their primary inflorescence is shorter than in wild type plants (Booker et al., 2004; Stirnberg et al., 2002). Plant height is a phenotype associated with auxin status, since auxin strongly affects cell elongation (reviewed in Perrot-Rechenmann, 2010), thus in part determining stem elongation and plant height. To test whether *pin3pin4pin7* would affect plant height in the *max2* and *max4* background, plant height was determined at terminal flowering by measuring the primary inflorescence length. Loss of PIN3, PIN4 and PIN7 increased plant height in both *max2* and *max4* mutant backgrounds (Fig. 4.5B), partially rescuing their reduced stature. Plant height in the *pin3pin4pin7* mutant was not significantly different from wild type (Fig. 4.5B).

A striking phenotype of the *pin3pin4pin7* mutant is the angle at which its cauline branches emerge from the primary inflorescence. Cauline branches in *pin3pin4pin7* mutants emerge at wider angles to the primary inflorescence than in wild type (Fig. 4.5C, F; Bennett et al., 2016a). The opposite effect is seen in *max* mutants, where cauline branches emerge at more acute angles to the primary inflorescence than in wild type (Fig. 4.5C, F). To test whether *pin3pin4pin7* could affect the branch angle phenotype in the *max2* and *max4* mutant backgrounds, the branch angle was determined at terminal flowering in *max2pin3pin4pin7* and *max4pin3pin4pin7* mutants. In both quadruple mutant backgrounds the branch angle was reduced to wild type levels (Fig. 4.5C, F).

Cambial activity in strigolactone mutant stems is reduced, leading to reduced secondary growth (Agusti et al., 2011). In accordance with this, *max* mutants stems are thinner than in wild type (Bennett et al., 2016b). Local cambial activity is regulated by auxin, so it is possible that reduced radial auxin transport in strigolactone mutants affects stem diameter. To test this, the effect of *pin3pin4pin7* on stem diameter was assessed by measuring the diameter of the most basal internode at terminal flowering, as an average of the narrowest and widest point of each sampled stem. As reported previously, both *max2* and *max4* stems are thinner than wild type (Fig. 4.5D; Bennett et al., 2016b), but loss of PIN3, PIN4 and PIN7

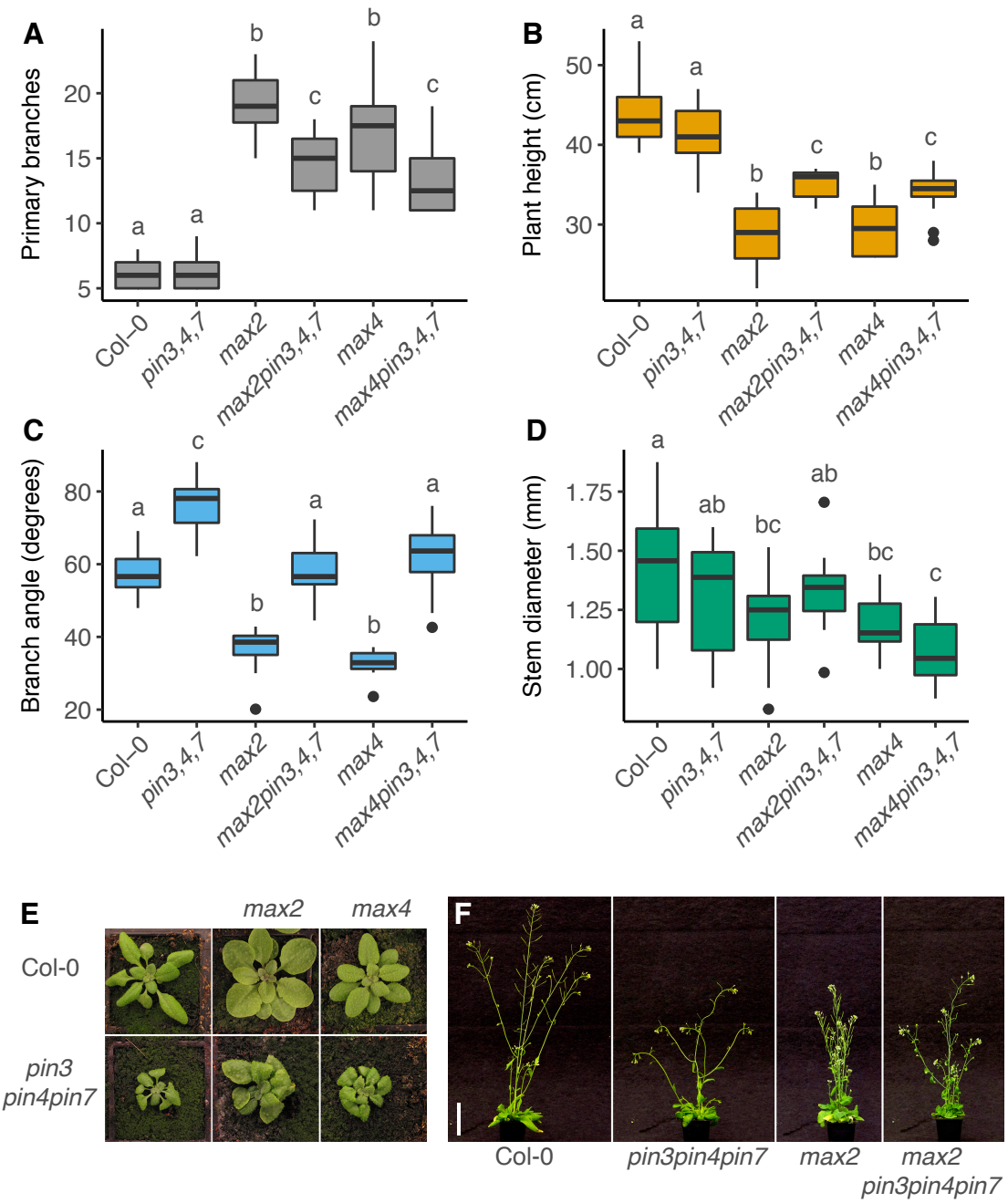

Fig. 4.5 Shoot phenotypes of *maxpin3pin4pin7* mutants.
(A) Primary branch number of plants grown under long days, scored at terminal flowering. **(B)** Plant height at terminal flowering. **(C)** Branch angle at terminal flowering. **(D)** Stem diameter at terminal flowering. **(E)** Photographs of 4-week old plants from **A**-**D**. **(F)** Photographs of a subset of genotypes from **A**-**D** at 6 weeks. Bar = 50 mm. For **A**-**D** Tukey's HSD test was carried out after obtaining the least-square means for a linear model fitting the data and different letters indicate statistically significant results at $p < 0.05$. Data are representative of at least three independent experiments, depending on the genotype. n = 12-20. Branch angle data for *pin3pin4pin7* have been published in Bennett et al. (2016a).

in these mutants had no measurable effect on stem diameter (Fig. 4.5D). The stem diameter of *pin3pin4pin7* triple mutant plants was comparable to wild type (Fig. 4.5D).

Leaf shape in the *pin3pin4pin7* mutant differs markedly from wild type, with leaf blades appearing both shorter and twisted (Fig. 4.5E; Bennett et al., 2016a). The *max* mutants also display altered leaf shapes, with rounder leaves than observed in wild type, due to a reduction in leaf blade length (Stirnberg et al., 2002). Leaf defects in *max2pin3pin4pin7* and *max4pin3pin4pin7* appeared to be additive; displaying rounder leaves which were shorter and more twisted than either wild type or *max2* and *max4*, respectively (Fig. 4.5E).

Together, these data show that PIN3, PIN4 and PIN7 contribute to the increased branching phenotype in strigolactone mutants. Furthermore, *pin3pin4pin7* is able to partially rescue the reduced plant height and completely overcome the increased branch angle of strigolactone mutants. PIN3, PIN4 and PIN7 do not appear to affect stem diameter, neither in a wild type background nor in strigolactone mutants. Leaf phenotypes associated with *pin3pin4pin7* are also evident in strigolactone mutants, and vice versa.

The reduced branching in *maxpin3pin4pin7* mutants suggests that shoot branching control by strigolactones depends at least in part on PIN3, PIN4 and PIN7 function. Branching in strigolactone synthesis mutants can be rescued by supplementing the growth medium with GR24, a synthetic mixture of racemic strigolactones (Crawford et al., 2010; Shinohara et al., 2013). To test whether strigolactone mutants lacking PIN3, PIN4 and PIN7 would still respond to exogenous GR24, plants were grown under long day growth conditions in sterile Weck jars containing agar-solidified ATS medium supplemented with 5 µM GR24 or solvent control. Branching was defined as the total number of primary branches longer than 5 mm. Determining the terminal flowering stage under these conditions is difficult, because plants grow against the lid of the jar. Therefore the number of primary branches was counted 8 weeks after sowing, when all plants appeared to have stopped growing. Consistent with soil-grown plants, *max2pin3pin4pin7* and *max4pin3pin4pin7* mutants grown under control conditions produced fewer branches compared to *max2* and *max4*, respectively (Fig. 4.6A,C). Supplementing the growth media with exogenous GR24 had no effect on *max2* and *max2pin3pin4pin7* mutants, whereas branching was significantly decreased in *max4* and *max4pin3pin4pin7* mutant backgrounds (Fig. 4.6A,C). These data are consistent with the roles of *max2* and *max4* in strigolactone perception and biosynthesis, respectively (see Section 1.2.3). The response to exogenous GR24 of the *pin3pin4pin7* mutant was comparable to wild type (Fig. 4.6A,C).

When mutants are hypersensitive to GR24, this can lead to a reduction in overall plant growth, which can affect the number of branches that activate (Shinohara et al., 2013). To test whether overall vigour of the different genotypes in this assay was comparable, the dry weight

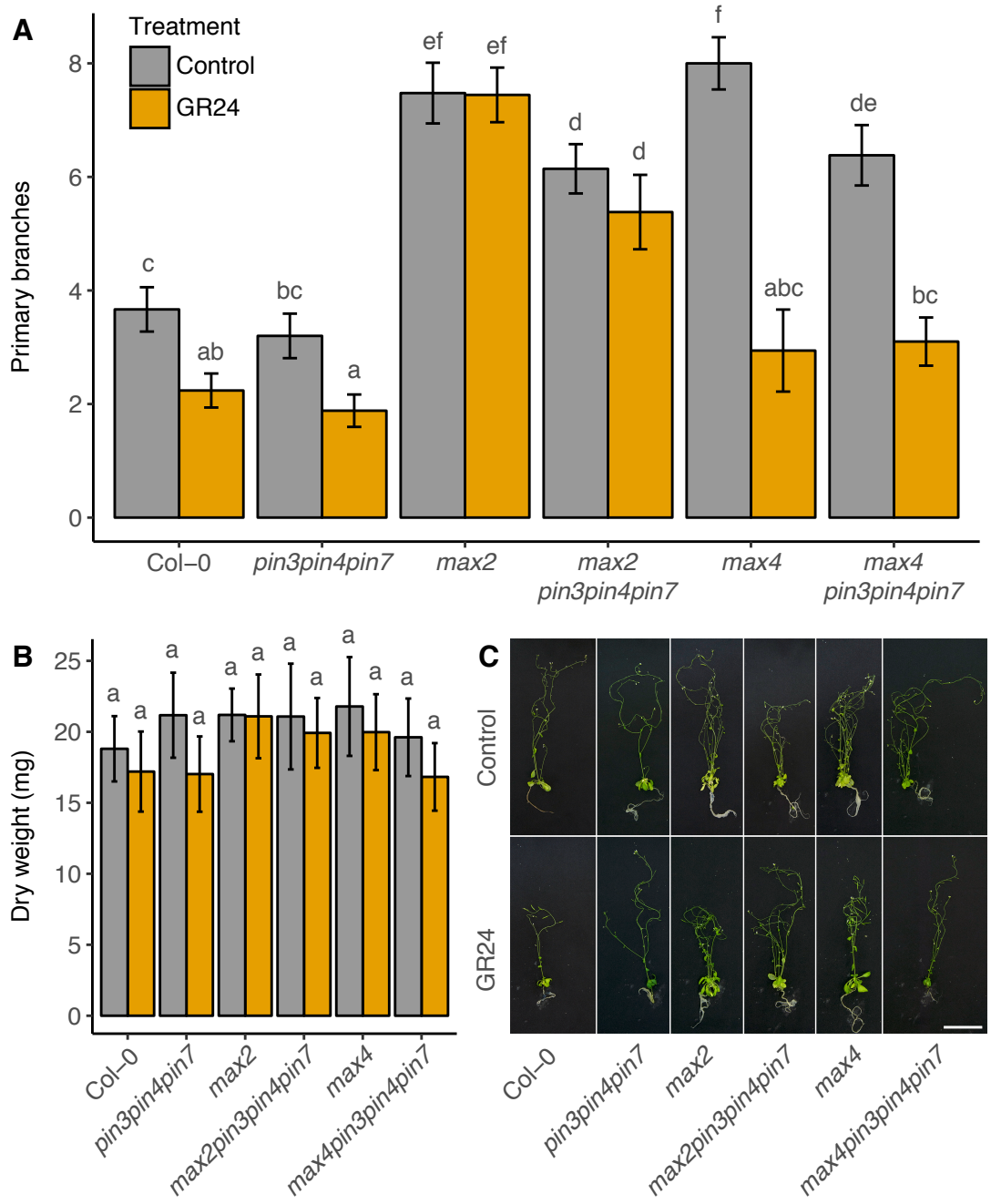

Fig. 4.6 Whole-plant responses of *maxpin3pin4pin7* mutants to GR24.
(A) Primary branch number of plants grown under axenic, long day growth conditions in jars, supplemented with ATS ± 5 µM GR24, scored after 8 weeks. **(B)** Plant dry weight of the plants represented in **A**. For **A** and **B** Tukey's HSD test was carried out after obtaining the least-square means for a linear model fitting the data and different letters indicate statistically significant results at $p < 0.05$. Data are representative of two independent experiments, n = 14-21. Bars represent the 95 % confidence interval of the mean. **(C)** Photographs of representative plants from **A** and **B**, with control treatment (top row) and GR24 treatment (bottom row) for each genotype. Bar = 50 mm.

of the individual plants at the end of the experiments was determined (see Section 2.2.2). Whole plants, containing both the shoot and the root, were oven-dried and weighed. No difference in dry weight was detected between the genotypes tested, nor did supplementing the media with exogenous GR24 affect the dry weight biomass (Fig. 4.6B). This demonstrates that the reduction in branching in response to GR24 is not caused by an overall reduction in plant growth.

The reduction in branching in whole plants in response to exogenous GR24 lacking PIN3, PIN4 and PIN7 shows that these plants are still able to respond to strigolactone, if strigolactone perception is unperturbed (Fig. 4.6). To test bud outgrowth responses to GR24 in a more sensitive and dynamic setup, a two-node assay was used. The assay was performed as described earlier, but here two-nodes were supplemented with either 5 µM GR24 or solvent control, applied basally. The degree of competition between buds was determined by calculating the relative growth index 10 days post decapitation. Previous research shows that basal GR24 increases the competition between buds in strigolactone-sensitive two-node explants, increasing the frequency with which one bud dominates the other (Crawford et al., 2010). This response was also clear in this experiment, where bud-bud competition in wild type two-node explants increased upon GR24 treatment, as reflected in the higher relative growth index (Fig. 4.7). Untreated *pin3pin4pin7* mutant two-nodes have reduced bud-bud competition, compared to wild type (Fig. 4.2; Bennett et al., 2016a), which was also evident in this assay (Fig. 4.7). Although *pin3pin4pin7* two-nodes were still able to respond to basal GR24, their response was significantly less than in wild type (Fig. 4.7). As expected, *max2* and *max4* mutants showed a strong reduction in bud-bud competition under control conditions and GR24 treatment was able to increase competition to wild type levels for *max4*, but not *max2*, consistent with earlier reports (Fig. 4.7; Crawford et al., 2010). Loss of PIN3, PIN4 and PIN7 in the *max2* background did not lead to a further decrease in bud-bud competition under control conditions (Fig. 4.7). Adding basal GR24 to *max2pin3pin4pin7* two-nodes had no effect compared to the control (Fig. 4.7). Under control conditions, competition between *max4pin3pin4pin7* buds did not differ from *max4*, whereas GR24 treatment increased competition, but to a significantly lesser extent than in the *max4* mutant (Fig. 4.7).

Together, these data show that plants lacking PIN3, PIN4 and PIN7 are still able to respond to strigolactone. However, in the bud-bud competition assay this response is compromised, in both wild type and *max4* backgrounds. This suggests bud-bud competition in strigolactone-deficient mutants is at least in part dependent on PIN3, PIN4 and PIN7. Consistent with this idea, the highly branched phenotype of *max2* and *max4* mutants is partially suppressed by *pin3pin4pin7*.

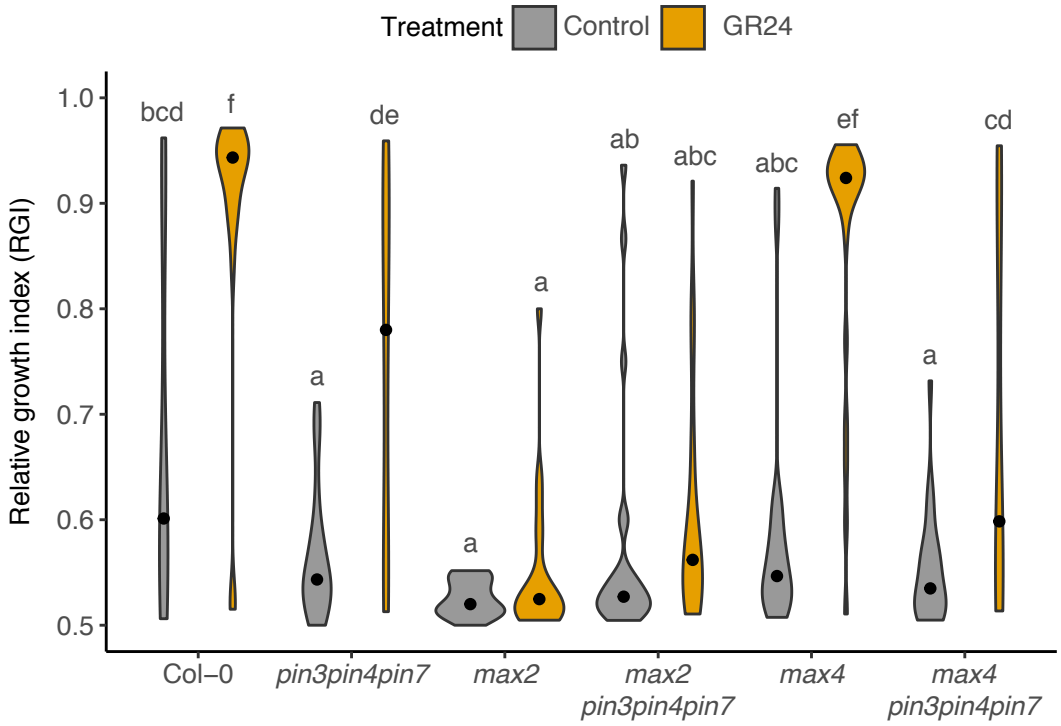

Fig. 4.7 Bud competition in *maxpin3pin4pin7* mutant two-node explants in response to GR24. Violin plot for the relative growth index (RGI) of two-node explants, treated ± 5 µM basal GR24, 10 days post decapitation, n = 20-23. The RGI is the proportion of branch length in the longest branch. Black dots indicate the median value and the area of each plot represents the probability distribution of the values. Tukey's HSD test was carried out after obtaining the least-square means for a linear model fitting the data and different letters indicate statistically significant results at $p < 0.05$. Different letters indicate statistically significant results at $p < 0.05$. Data are representative of two independent experiments.

4.2.3 The role of ABCB1/19 in communication between apices

The severe reduction in stem auxin transport of the *abcb1abcb19* double mutant shows that, at least combined, *ABCB1* and *ABCB19* are able to strongly affect stem auxin movement (Fig. 3.8; Bennett et al., 2016a; Noh et al., 2001). The strong reduction of stem auxin transport in *abcb1abcb19* mutants could affect shoot branching and indeed this mutant is reported to have high levels of branching (Noh et al., 2001). To further explore the effect of ABCB1 and ABCB19 on shoot branching, bud activation was assessed in *abcb1abcb19*. For comparison, the *abcb1* and *abcb19* single mutants were also included in the analyses.

Rosette bud activation for wild type, *abcb1*, *abcb19* and *abcb1abcb19* was investigated using a short day/long day decapitation assay. The number of rosette branches was scored 5, 7, 10 and 14 days post decapitation, to follow bud activation dynamics (Fig. 4.8A). No significant difference in the number of rosette branches between wild type, *abcb1* or *abcb19* was detected at any of the time points sampled (Holm-Bonferroni-adjusted pairwise Wilcoxon rank-sum tests, not significant). In contrast, branching was strongly reduced in the *abcb1abcb19* double mutant at all sampled time points ($p < 0.001$ for Holm-Bonferroni-adjusted pairwise Wilcoxon rank-sum tests).

When the *abcb* mutants were grown under long day conditions, the *abcb1abcb19* double mutant combination used here showed strong developmental defects, consistent with published data (Fig. 4.8D; Lin and Wang, 2005; Noh et al., 2001). Double mutants grown for the short day/long day decapitation assay also showed strong growth defects, and *abcb1abcb19* plants took markedly longer to reach the decapitation stage compared to wild type. To test whether the defects in the *abcb1abcb19* mutant affect axillary bud formation, plants were scored for the absence or presence of axillary buds in the rosette leaf axils at the decapitation stage (Fig. 4.8B). The number of axils containing axillary buds was strongly decreased in *abcb1abcb19* plants, compared to wild type and both *abcb* single mutants ($p < 0.001$ for Holm-Bonferroni-adjusted pairwise Wilcoxon rank-sum tests). Double mutants also produced markedly fewer leaves, compared to the other tested genotypes ($p < 0.001$ for Holm-Bonferroni-adjusted pairwise Wilcoxon rank-sum tests). The *abcb1* and *abcb19* single mutants showed wild type levels of axillary bud formation (Holm-Bonferroni-adjusted pairwise Wilcoxon rank-sum tests were not significant).

Taken together, these data show that, contrary to earlier reports, branching in *abcb1abcb19* double mutants is decreased. Furthermore, axillary bud formation is reduced in *abcb1abcb19* mutants, which makes meaningful comparisons with other genotypes difficult. As such, the *abcb1abcb19* was excluded from further experiments.

The ABCB19 protein has an non-polar localisation across a broad range of tissues in the stem, with exception of the xylem and phloem (Bennett et al., 2016a). As such, ABCB19

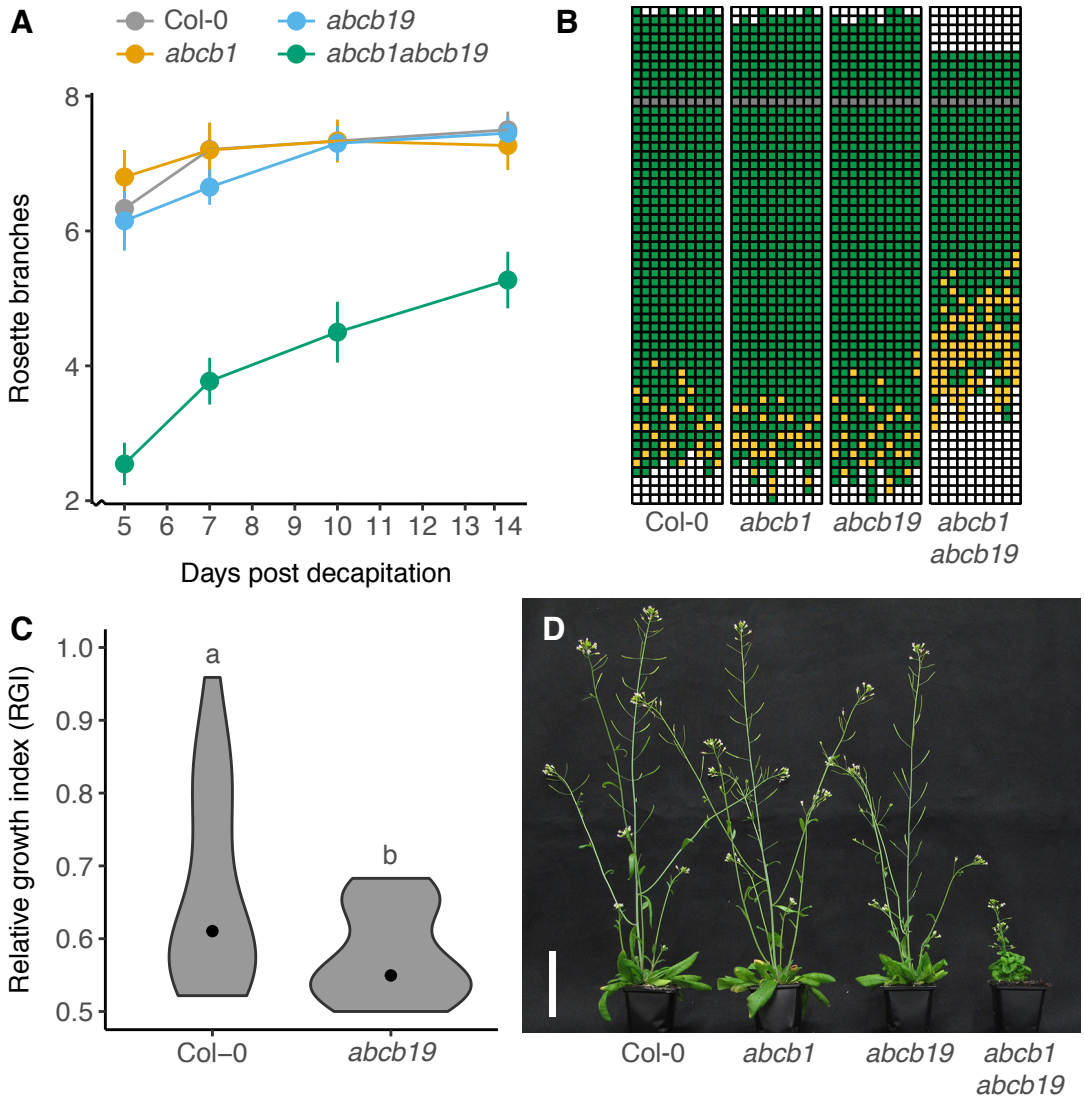

Fig. 4.8 Bud formation and branching responses in *abcb1/abcb19* mutants.
(A) Rosette branch number of short day to long day shifted plants, scored 5, 7, 10 and 14 days post decapitation. Data are representative for two independent experiments, n = 15-24. **(B)** Schematic representation of axillary bud formation in the cauline and rosette leaf axils of the genotypes from **A**. Each column represents an individual plant, and each square a single leaf axil. Axils are scored from top to bottom, with the oldest leaf axils at the bottom. Green denotes the presence and orange the absence of an axillary bud. The grey square represents the border between cauline and rosette leaf axils, with cauline axils above and rosette axils below. Data are from a single experiment, n = 10. **(C)** Violin plot for the relative growth index (RGI) of Col-0 and *abcb19* two-nodes, 10 days post decapitation, n = 18-21. The RGI is the proportion of branch length in the longest branch. Black dots indicate the median value and the area of each plot represents the probability distribution of the values. A comparison with the Wilcoxon rank-sum test was carried out. Different letters indicate statistically significant results at $p < 0.05$. Data are representative of three independent experiments. **(D)** Photograph of mature plants of the genotypes from **A**, grown under long day growth conditions. Bar = 50 mm.

could play a role in communicating auxin status across the stem. Although rosette bud activation in *abcb19* was unchanged in the short day/long day decapitation assay (Fig. 4.8A), it is possible that its effect was too subtle to detect. Therefore, bud-bud communication was assessed in the sensitive two-node bud competition assay. In this setup, *abcb19* two-node explants showed significantly decreased bud-bud competition, compared to wild type (Fig. 4.8C). These data show that ABCB19 is able to affect communication between buds.

4.2.4 The relationship between strigolactones and ABCB1/19

The effect of ABCB19 on auxin transport and shoot branching appears to be subtle. To test whether the role of ABCB19 is more pronounced in a high-branching background, the *abcb19* mutant was introduced into the *max2* and *max4* strigolactone mutant backgrounds. For completeness, *abcb1* was also introduced into these *max* backgrounds.

Shoot phenotypes of the resulting *max/abcb* double combinations were characterised by growing plants under long day growth conditions and scoring phenotypes at the terminal flowering stage. The number of primary branches was significantly decreased in *max2abcb19* and *max4abcb19* mutants, compared to *max2* and *max4*, respectively (Fig. 4.9A, F). No change was detected in *max2abcb1* and *max4abcb1* mutants (Fig. 4.9A, F). Plant height in *abcb1* and *abcb19* was similar to wild type, and loss of ABCB1 or ABCB19 did not affect plant height in the *max* mutants (Fig. 4.9B). The branch angle of *abcb1* and *abcb19* was unchanged from wild type (Fig. 4.9C). Loss of ABCB1 did not affect *max* mutant branch angles, but loss of ABCB19 led to a small, significant increase in branch angle in both *max* backgrounds (Fig. 4.9C). Stem diameters were unchanged in *abcb1* and *abcb19* mutants, compared to wild type (Fig. 4.9D). Furthermore, *abcb1* and *abcb19* did not affect stem diameter in the *max* mutant backgrounds (Fig. 4.9D). Lastly, *abcb1* did not have any apparent effect on rosette leaf shape, neither in wild type or *max* mutant backgrounds (Fig. 4.9E). In contrast, rosette leaves in *abcb19* were shorter, and more wrinkled in both wild type and *max* mutant backgrounds. The rosette in *abcb19* mutants appeared more compact than in wild type, possibly due to reduced petiole length (Fig. 4.9E).

The reduced branching phenotype of *max2abcb19* and *max4abcb19* suggests that shoot branching control mediated by strigolactone depends, at least partially, on ABCB19 function. To test whether *abcb19* mutants are still able to respond to strigolactone, plants were grown in sterile Weck jars containing agar-solidified ATS growth medium supplemented with 5 µM GR24, or solvent control (Fig. 4.10A). When primary branches were counted 8 weeks after sowing, *abcb19* mutants had activated significantly fewer branches compared to wild type under control conditions. Addition of exogenous GR24 reduced branching in both wild type and *abcb19*, with GR24-treated *abcb19* plants again activating significantly fewer branches

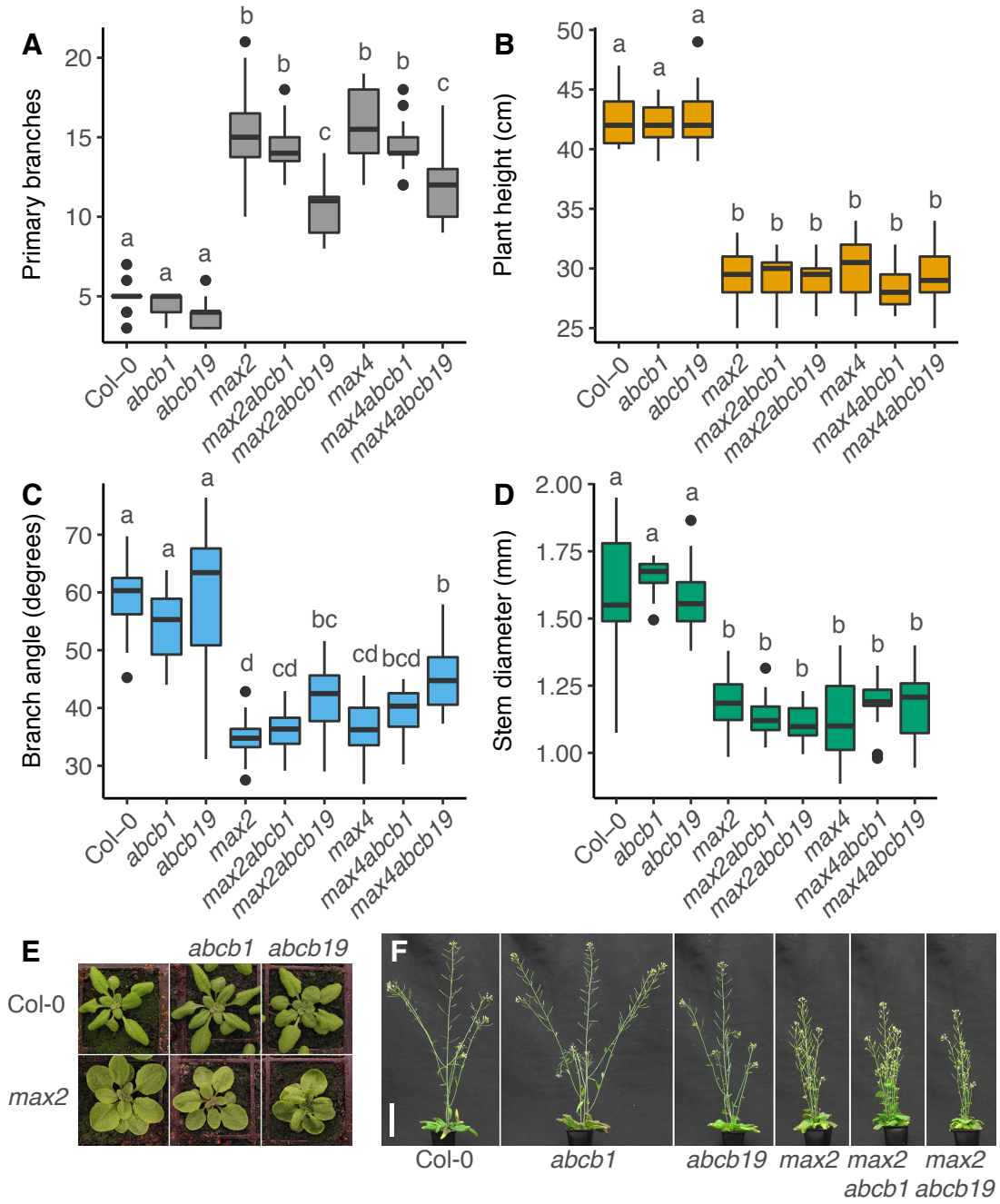

Fig. 4.9 Shoot phenotypes in *maxabcb1* and *maxabcb19* mutants.
(A) Primary branch number of plants grown under long days, scored at terminal flowering. **(B)** Plant height at terminal flowering. **(C)** Branch angle at terminal flowering. **(D)** Stem diameter at terminal flowering. **(E)** Photographs of a subset of genotypes from **A**-**D** at 4 weeks. The Col-0 and *max2* images are the same as shown in Fig. 4.5E. **(F)** Photographs of a subset of genotypes of **A**-**D** at 6 weeks. Bar = 50 mm. For **A**-**D** Tukey's HSD test was carried out after obtaining the least-square means for a linear model fitting the data and different letters indicate statistically significant results at $p < 0.05$. Data are representative of at least three independent experiments, depending on the genotype. n = 20-24.

than treated wild type plants (Fig. 4.10A). The branching response of *abcb19* to GR24 treatment, calculated as the difference in the mean number of branches formed under the different treatments, was comparable to wild type. Wild type plants formed on average (mean ± standard error of the difference between the means of each two samples) of 1.47 ± 0.23 fewer branches upon treatment with GR24, whereas *abcb19* mutant plants reduced their branching by 1.31 ± 0.25.

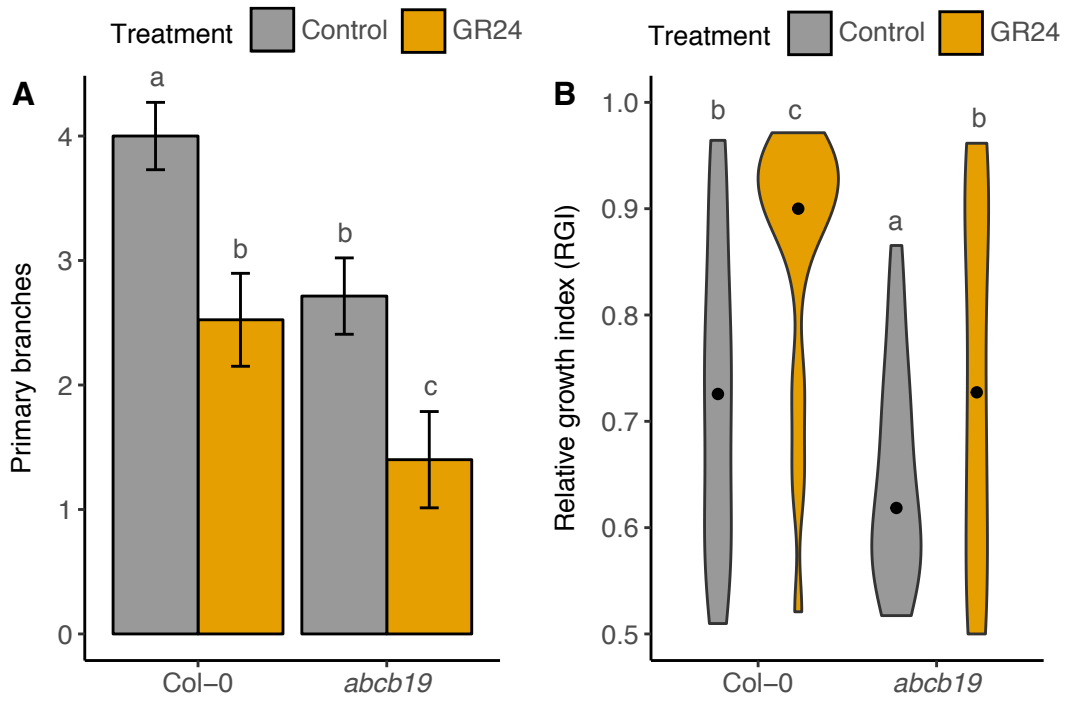

Fig. 4.10 Whole-plant and bud competition responses of *abcb19* mutants to GR24.
(A) Primary branch number for plants grown under axenic, long day growth conditions in jars, in agar-solidified ATS ± 5 µM GR24, scored after 8 weeks. Data are representative of three independent experiments, n = 20-21. **(B)** Violin plot for the relative growth index (RGI) of two-nodes, treated ± 5 µM basal GR24, 10 days post decapitation, n = 21-24. The RGI is the proportion of branch length in the longest branch. Black dots indicate the median value and the area of each plot represents the probability distribution of the values. Data are representative for two independent experiments. For **A** and **B** Tukey's HSD test was carried out after obtaining the least-square means for a linear model fitting the data and different letters indicate statistically significant results at $p < 0.05$. Bars represent the 95 % confidence interval of the mean.

The data above show that *abcb19* plants are able to respond to GR24. Bud-bud competition in the *abcb19* background is reduced compared to wild type (Fig. 4.8C). To assess whether exogenous GR24 can restore the reduced competition in *abcb19* two-node explants, a two-node experiment was performed (Fig. 4.10B). Here, competition between *abcb19* buds without GR24 was significantly decreased compared to wild type, consistent with earlier

experiments (Fig. 4.8C). Addition of GR24 to *abcb19* two-node explants increased bud-bud competition, as captured by the increased relative growth index (Fig. 4.10B). However, the degree of competition was significantly less than in GR24-treated wild type two-node explants (Fig. 4.10B).

Together, these data show that loss of ABCB19 results in reduced branching in strigolactone mutants. ABCB19-deficient plants are still able to respond to exogenous strigolactone, but competition between two cauline buds in *abcb19* mutants can only be partially restored by addition of strigolactone.

4.2.5 The relationship between PIN3/PIN4/PIN7 and ABCB19

The data above show that there are striking similarities between PIN3/PIN4/PIN7 and ABCB19 in the control of shoot branching. Loss of the PINs or ABCB19 both results in reduced bud-bud communication (Fig. 4.2B, 4.8C), and a partial rescue of the increased branching phenotype of strigolactone mutants (Fig. 4.5A, 4.9A). Other phenotypes appear to be more PIN or ABCB19-specific. For example, rosette buds in *pin3pin4pin7* show delayed activation upon decapitation (Fig. 4.1B), whereas *abcb19* rosette bud activation dynamics are similar to wild type (Fig. 4.8A). To explore in more detail the similarities and differences between the PINs and ABCB19, shoot phenotypes and branching responses of the *abcb19*, *pin3pin4pin7* and *abcb19pin3pin4pin7* mutants were investigated.

To test for potential synergistic effects of PIN3/PIN4/PIN7 and ABCB19 on rosette bud activation dynamics, rosette bud activation was followed in a short day/long day decapitation assay (Fig. 4.11A). Consistent with previous results, the *pin3pin4pin7* mutant was delayed in its rosette bud activation, with fewer active branches present at 7 and 10 days post decapitation, compared to wild type ($p < 0.05$, Holm-Bonferroni adjusted Wilcoxon rank-sum tests). Rosette bud activation in *abcb19* was indistinguishable from wild type, as expected (Holm-Bonferroni adjusted Wilcoxon rank-sum tests, not significant). Loss of both *abcb19* and *pin3pin4pin7* had a clear synergistic effect (Fig. 4.11A). The number of rosette branches in the *abcb19pin3pin4pin7* quadruple mutant was comparable to the other tested genotypes at 5 days post decapitation, but where wild type, *abcb19* and *pin3pin4pin7* continued to activate additional rosette buds during the remainder of the experiment, the quadruple mutant did not ($p < 0.001$ at day 14, Holm-Bonferroni adjusted Wilcoxon rank-sum tests).

To investigate whether the reduced activation of rosette branches in the quadruple mutant is caused by a reduction in axillary bud formation, axillary bud formation was assessed in *abcb19pin3pin4pin7* mutant plants. Plants were grown under the same regime as those grown for short day/long day decapitation assay and scored at the point of decapitation (Fig. 4.11B).

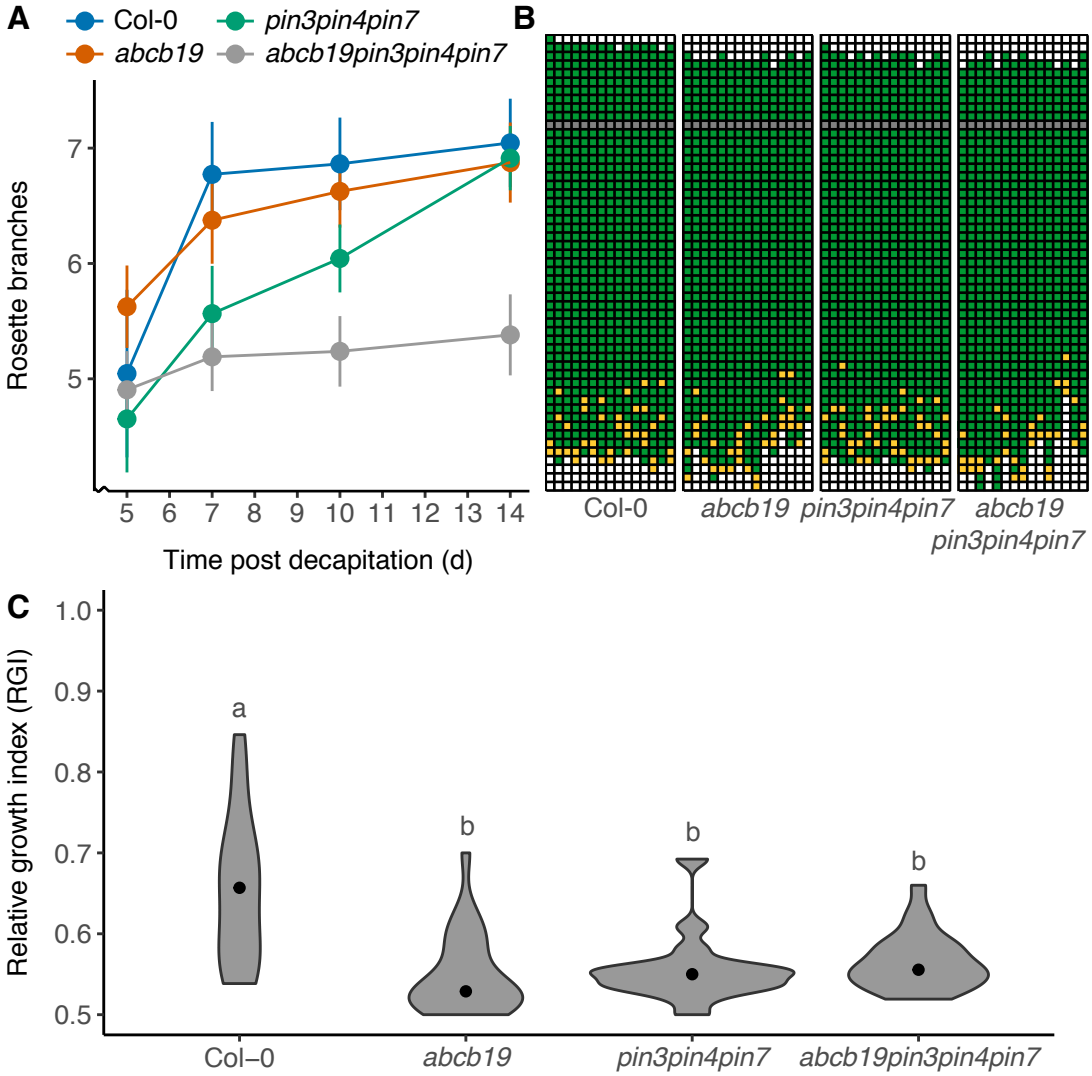

Fig. 4.11 Bud activation dynamics and bud formation in *abcb19pin3pin4pin7* mutants. **(A)** Rosette branch activation dynamics of Col-0, *abcb19*, *pin3pin4pin7* and *abcb19pin3pin4pin7* plants, scored 5, 7, 10 and 14 days post decapitation, n = 21-24. Data are representative for three independent experiments. **(B)** Schematic representation of axillary bud formation in the cauline and rosette leaf axils of the plants from **A**. Each column represents an individual plant, and each square a single leaf axil. Axils are scored from top to bottom, with the oldest leaf axils at the bottom. Green denotes the presence and orange the absence of an axillary bud. The grey square represents the border between cauline and rosette leaf axils, with cauline axils above and rosette axils below. Data are from a single experiment, n = 20 (only 15 samples shown). **(C)** Violin plot for the relative growth index of Col-0, *abcb19*, *pin3pin4pin7* and *abcb19pin3pin4pin7* two-nodes, 10 days post decapitation, n = 17-24. The RGI is the proportion of branch length in the longest branch. Black dots indicate the median value and the area of each plot represents the probability distribution of the values. A comparison with the Wilcoxon rank-sum test was carried out. Different letters indicate statistically significant results at $p < 0.05$. Data are representative of two independent experiments.

Data are from a single experiment, but the *abcb19* and *pin3pin4pin7* controls have been assessed previously (Fig. 4.4D, 4.8B). The number of empty axils in the *abcb19pin3pin4pin7* quadruple mutant did not differ from wild type, *abcb19* and *pin3pin4pin7* mutants (Holm-Bonferroni-adjusted Wilcoxon rank-sum tests, not significant). No difference in total number of rosette leaves was detected between any of the genotypes (Holm-Bonferroni-adjusted Wilcoxon rank-sum tests, not significant).

The reduced activation of rosette buds in the *abcb19pin3pin4pin7* quadruple mutant (Fig. 4.11A) suggests that these PINs and ABCB19 can have synergistic effects on bud outgrowth. Bud-bud communication is impaired in *pin3pin4pin7* and *abcb19* mutants (Fig. 4.2B, 4.8C). To assess whether PIN3, PIN4, PIN7 and ABCB19 are also able to synergistically affect bud-bud competition, a two-node experiment was conducted with *abcb19pin3pin4pin7* mutant explants (Fig. 4.11C). Compared to wild type, bud-bud communication was significantly reduced in the quadruple mutant, indicated by the reduced relative growth index. No significant difference was detected between the quadruple and the *abcb19* or *pin3pin4pin7* mutants (Fig. 4.11C).

To characterise the shoot phenotypes of the *abcb19pin3pin4pin7* quadruple in more detail, plants were grown under long day growth conditions and scored at the terminal flowering stage. Primary branching was not significantly different between any of the tested genotypes (Fig. 4.12A). Plant height was unchanged in the *abcb19* and *pin3pin3pin7* mutants compared to wild type, consistent with earlier results (Fig. 4.5B, 4.9B), but significantly reduced in *abcb19pin3pin4pin7* mutant plants (Fig. 4.12B). Cauline branches in *abcb19pin3pin4pin7* emerged at wider angles from the primary inflorescence than in wild type (Fig. 4.12C, F), and to the same degree as seen in the *pin3pin4pin7* mutant (Fig. 4.12C, F). Stem diameter in *abcb19pin3pin4pin7* mutants was significantly decreased compared to wild type (Fig. 4.12D), whereas stem diameter was unchanged in *abcb19* and *pin3pin4pin7* mutants, as previously shown (Fig. 4.5D, 4.9D). Rosette leaves in the *abcb19pin3pin4pin7* showed a very strong phenotype (Fig. 4.12E). Rosettes were very compact, and leaf blades were short, curled and twisted, compounding phenotypes from both *abcb19* and *pin3pin4pin7* mutants.

Together, these data show that PIN3/PIN4/PIN7 and ABCB19 have synergistic effects on the activation dynamics of rosette buds, following decapitation. These changes are not caused by a reduction in axillary buds available for activation. Plant height, stem diameter and leaf shape are also synergistically affected by loss of PIN3/PIN4/PIN7 and ABCB19.

4.2.6 The role of auxin importers in communication between apices

The data presented in Chapter 3 show that auxin importers contribute to stem auxin transport (Fig. 3.12, 4.13). To further investigate the functional significance of auxin importers in

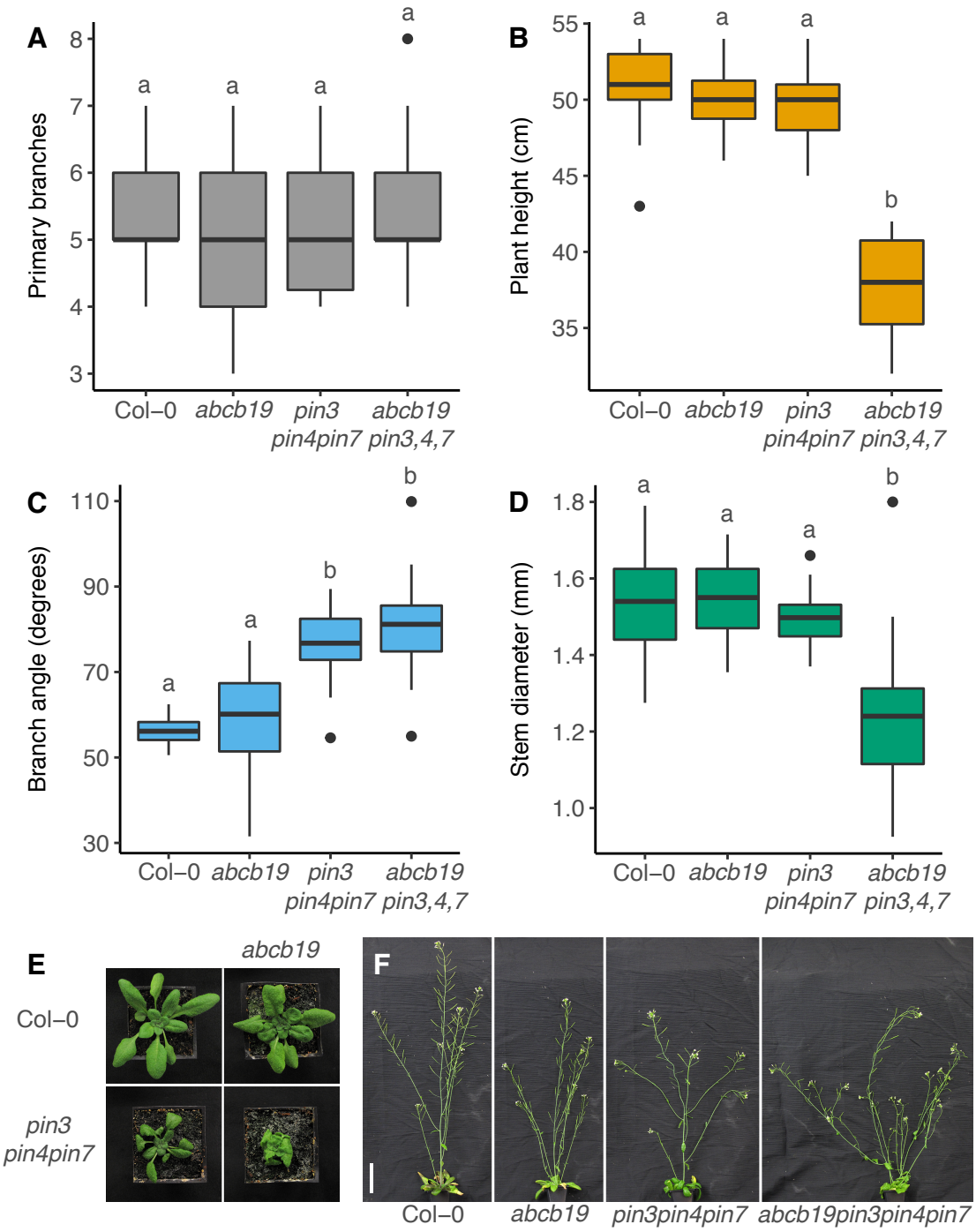

Fig. 4.12 Shoot phenotypes in *abcb19pin3pin4pin7* mutants.
(A) Primary branch number of plants grown under long days, scored at terminal flowering. **(B)** Plant height at terminal flowering. **(C)** Branch angle at terminal flowering. **(D)** Stem diameter at terminal flowering. **(E)** Photographs of the genotypes from **A**-**D** at 4 weeks. **(F)** Photographs of the genotypes from **A**-**D** at 6 weeks. Bar = 50 mm. For **A**-**D** Tukey's HSD test was carried out after obtaining the least-square means for a linear model fitting the data and different letters indicate statistically significant results at $p < 0.05$. Data are representative of three independent experiments. n = 18-24.

the context of shoot branching, bud outgrowth responses were assessed in the *aux1* and *aux1lax1lax2lax3* auxin importer mutants.

To assess rosette bud activation dynamics in *aux1* and *aux1lax1lax2lax3* mutants, a short day/long day decapitation assay was performed. Bud activation was scored at 5, 7, 10 and 14 days post decapitation (Fig. 4.13A). Consistent with previous experiments, wild type plants activated most of their buds 7 days after decapitation, with only a few additional buds activating during the remainder of the experiment. Bud activation dynamics of the *aux1* mutant did not differ from wild type at any of the sampled time points (Holm-Bonferroni adjusted Wilcoxon rank-sum tests, not significant). In contrast, the number of active buds in the *aux1lax1lax2lax3* quadruple mutant was significantly lower to both wild type and *aux1* at all sampled time points ($p < 0.001$, Holm-Bonferroni adjusted Wilcoxon rank-sum tests). Axillary meristem formation in short-day-grown *aux1lax1lax2* triple mutant plants has previously been shown to be highly impaired (Wang et al., 2014a), so it is likely that axillary bud formation in the *aux1lax1lax2lax3* is impaired. To test this, axillary bud formation was assessed by scoring the absence/presence of axillary buds in the rosette leaf axils of short day/long day grown plants, at the point of decapitation (Fig. 4.13B). The number of empty rosette leaf axils was significantly increased in *aux1lax1lax2lax3* plants, compared to wild type ($p < 0.001$, Holm-Bonferroni adjusted Wilcoxon rank-sum tests). The number of empty axils in *aux1* was unaffected (Holm-Bonferroni adjusted Wilcoxon rank-sum tests, not significant). The total number of rosette leaf axils formed in *aux1* and *aux1lax1lax2lax3* mutants was comparable to wild type (Holm-Bonferroni adjusted Wilcoxon rank-sum tests, not significant).

To investigate shoot branching in a potentially less compromised situation, *aux1* and *aux1lax1lax2lax3* mutant plants were grown under long day growth conditions. The number of primary branches was scored at terminal flowering. No significant differences in branching could be found between the *aux1/lax* mutants and wild type (Fig. 4.13C). Under these conditions, no apparent phenotypic differences between wild type and *aux1* plants could be detected (Fig. 4.13E). In contrast, the *aux1lax1lax2lax3* plants showed clear defects in leaf shape and were almost entirely sterile (Fig. 4.13E).

The effect of auxin import on bud activation was further explored using a bud-bud competition assay. Using the two-node assay, *aux1* buds were left to compete following decapitation. The degree of competition was measured by determining the relative growth index 10 days post decapitation. No difference in the relative growth index was found between *aux1* and wild type two-node explants (Fig. 4.13D).

Together, these data show that auxin importers do not appear to contribute to the regulation of bud activity. Although rosette branch activation appears to be reduced in the

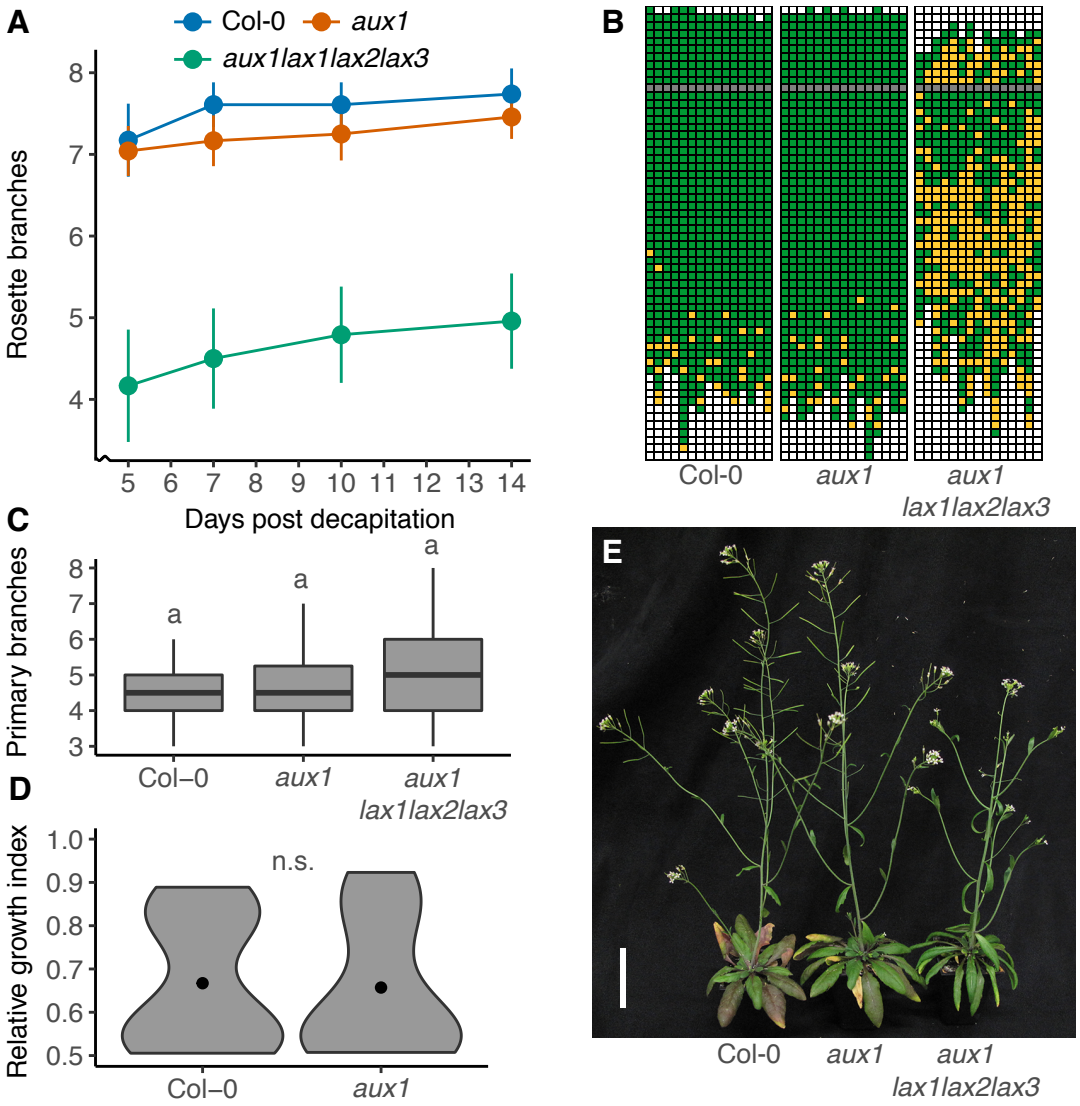

Fig. 4.13 Bud formation and branching responses in *aux1/lax* mutants.
(A) Rosette branch activation dynamics of Col-0, *aux1* and *aux1lax1lax2lax3* plants scored 5, 7, 10 and 14 days post decapitation, n = 23-24. **(B)** Schematic representation of axillary bud formation in the cauline and rosette leaf axils of the genotypes from **A**. Each column represents an individual plant, and each square a single leaf axil. Axils are scored from top to bottom, with the oldest leaf axils at the bottom. Green denotes the presence and orange the absence of an axillary bud. The grey square represents the border between cauline and rosette leaf axils, with cauline axils above and rosette axils below. Data are from a single experiment and the Col-0 data are the same as presented in Fig. 4.4D, n = 15. **(C)** Primary branch number of plants grown under long days, scored at terminal flowering, n = 28-30. **(D)** Violin plot for the relative growth index (RGI) of Col-0 and *aux1* two-nodes, 10 days post decapitation. The RGI is the proportion of branch length in the longest branch. Black dots indicate the median value and the area of each plot represents the probability distribution of the values. A comparison with the Wilcoxon rank-sum test was carried out; n.s. (not significant), n = 18-22. **(E)** Photograph of mature plants of the genotypes from **C**. Bar = 50 mm. Data in **A**, **C** and **D** are representative of two independent experiments.

aux1lax1lax2lax3 quadruple mutant, axillary bud formation is also impaired. This makes assessing the combined role of these auxin importers on branching challenging.

4.3 Summary

- PIN3, PIN4 and PIN7 affect rosette bud activation dynamics.
- PIN3, PIN4 and PIN7 contribute to communication between buds across the stem.
- Shoot branching control by strigolactones is partially dependent on PIN3, PIN4 and PIN7.
- Branching in the *abcb1abcb19* mutant is decreased.
- ABCB19 contributes to communication between buds across the stem.
- Shoot branching control by strigolactones is partially dependent on ABCB19.
- PIN3, PIN4, PIN7 and ABCB19 have synergistic effects on rosette bud activation.
- Auxin importers do not appear to contribute to the regulation of bud activation.

Chapter 5

Interplay between *BRC1* and auxin transport in the control of shoot branching

5.1 Introduction

Historically, the role of *BRC1* in the control of shoot branching has been viewed as that of an integrator of bud outgrowth regulating signals. Bud outgrowth inhibition is in many cases correlated to *BRC1* expression. Supportive of this, in Arabidopsis, *brc1* mutants display a high degree of shoot branching. In maize the orthologue of *BRC1*, *TEOSINTE BRANCHED1* (*TB1*), is constitutively overexpressed and here axillary bud activity is inhibited, resulting in suppression of branches (Doebley et al., 1997; Hubbard et al., 2002). Hormones can regulate *BRC1* expression, because in pea *BRC1* transcript levels are positively regulated by cytokinin, whereas strigolactone has a negative effect (Braun et al., 2012; Dun et al., 2012). These effects are consistent with the stimulatory and inhibitory effect of these hormones on bud outgrowth, respectively. Recent advances show that, at least in Arabidopsis, the role of *BRC1* as a straightforward regulator of bud outgrowth is questionable. In a variety of contexts the correlation between *BRC1* transcript levels and bud activity is broken, suggesting that *BRC1* is neither necessary nor sufficient for bud outgrowth inhibition (Seale et al., 2017). Buds lacking *BRC1* expression can remain inhibited and sensitive to strigolactone, while buds with high levels of *BRC1* can be active (Seale et al., 2017). Instead, it is proposed that *BRC1* acts as a modulator of bud activation potential and that it operates within a larger framework of bud activity control, mediated through an auxin transport-based mechanism (Seale et al., 2017).

The main aim of this chapter was to further explore the relationship between the auxin transport network and *BRC1*-mediated shoot branching control. Another important aim was to investigate the relationship between strigolactone and both of these bud-regulating processes. In the previous chapter, PIN3/PIN4/PIN7 and ABCB19 were shown to mediate communication between buds, and both the PINs and ABCB19 were shown to be important for strigolactone-mediated shoot branching control. To investigate whether *BRC1* might act through the PINs and ABCB19, branching responses were assessed in *brc1brc2* mutants lacking PIN3/PIN4/PIN7 or ABCB19 functionality.

To compare shoot branching control in *brc1brc2* and strigolactone mutant backgrounds, branching was investigated using a different growth regime than used thus far. The level of branching in *brc1brc2* and strigolactone mutants is almost indistinguishable under long day growth conditions (Bennett et al., 2016b; Seale et al., 2017). Under these conditions, virtually all nodes produce an active branch. However, differences in branching between these mutants become increasingly clear when the number of vegetative nodes is increased. When plants are grown exclusively under short day conditions, *brc1brc2* mutants activate significantly fewer branches than strigolactone mutants (Seale et al., 2017). From a practical point of view, working with exclusively short-day-grown plants is not ideal. Plants can take many months to reach terminal flowering and the long life span increases chances of plants succumbing to diseases. To find a suitable middle ground for assessing differences between *brc1brc2* and strigolactone mutant branching patterns, plants were grown under short day conditions for four weeks, then shifted to long day growth conditions and scored at terminal flowering.

In this chapter a mutant impaired in D14 function is used as a strigolactone signalling mutant, as opposed to MAX2. The D14 protein has recently been shown to act as a strigolactone receptor (Hamiaux et al., 2012; Yao et al., 2016). MAX2 is involved in strigolactone signalling, but it also acts in the karrikin signalling pathway, which results in phenotypic defects in *max2* mutants that are unrelated to strigolactone (Bennett et al., 2016b; Soundappan et al., 2015). As such, the *d14* mutant provides a cleaner genetic background in which to study the effects of strigolactone on shoot branching (see Fig. 1.2).

5.2 Results

5.2.1 The effect of PIN3/PIN4/PIN7 on shoot branching in *brc1brc2* and strigolactone mutants

To better distinguish between branching in *brc1brc2* and strigolactone mutants, a new growth regime was used where the number of vegetative nodes was increased by growing plants under short day conditions for four weeks, prior to shifting them to long day growth conditions. To assess whether these conditions distinguish sufficiently between *brc1brc2* and strigolactone mutant branching phenotypes, wild type, *brc1brc2* and *d14* mutant plants were grown under these conditions and branching was assessed at terminal flowering (Fig. 5.1). Under these conditions branching in the *brc1brc2* mutant was significantly increased compared to wild type, but was lower than in the *d14* mutant (Fig. 5.1A). This is consistent with data for these genotypes when grown exclusively under short day growth conditions (Seale et al., 2017). To test whether these growth conditions compromise axillary bud formation, plants were dissected at the terminal flowering stage and the presence and developmental stage of the axillary bud in each primary axis leaf axil was assessed (Fig. 5.1B). Where present, buds were categorised into vegetative and reproductive stage, using a slightly simplified classification scheme adapted from Aguilar-Martinez et al. (2007), as indicated in the figure legend. The total number of rosette leaves formed was comparable between wild type, *brc1brc2* and *d14* plants (Fig. 5.1B, C). The type and developmental stage of the meristems differed between the genotypes. Whereas wild type plants generally had a few empty axils, none could be detected in either *brc1brc2* or *d14* plants (Fig. 5.1B, D). In all genotypes some axillary buds remained in a vegetative state, but most had transitioned into reproductive floral buds (Fig. 5.1B, D). In *d14* plants all reproductive floral buds activated, whereas in wild type and *brc1brc2* mutant plants a proportion of reproductive buds remained dormant (Fig. 5.1A, B).

Together, these data show that axillary bud formation in *brc1brc2* and *d14* mutants is little changed from wild type. In *brc1brc2* plants a proportion of floral buds remains dormant, whereas in *d14* plants all floral buds activate. This accounts for the difference in primary branching observed between *brc1brc2* and *d14* plants.

The data from Chapter 4 show that loss of PIN3, PIN4 and PIN7 in strigolactone mutants is able to partially rescue their increased branching phenotype (Fig. 4.4). To test whether loss of these PINs can also suppress the increased branching of *brc1brc2* mutants, the *pin3pin4pin7* mutations were introduced into the *brc1brc2* mutant background through crossing. To assess differences between *brc1brc2* and *d14*-mediated branching, the *pin3pin4pin7* mutations were also introduced into the *d14* mutant background through crossing and the *d14pin3pin4pin7* was included in the branching assays. Branching was

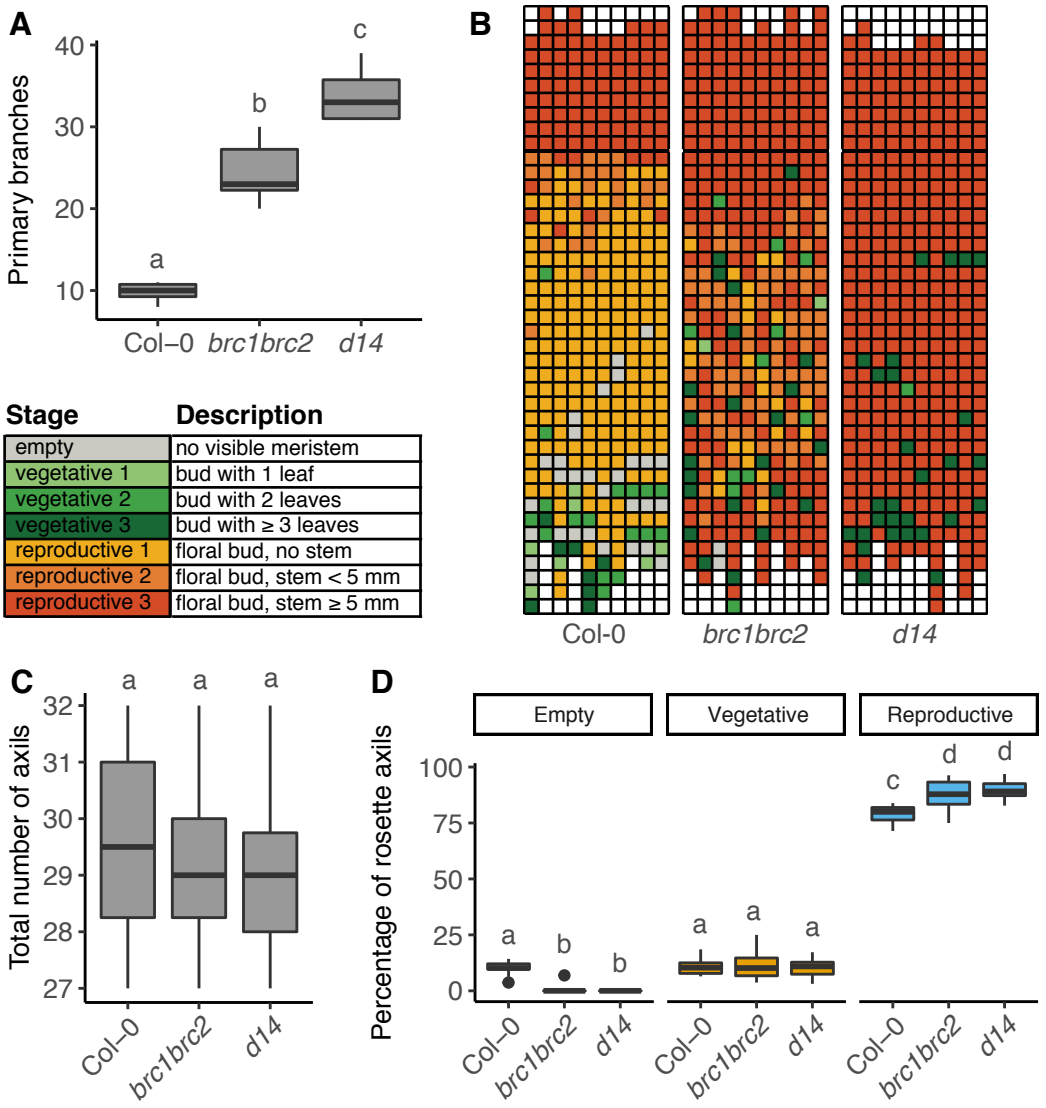

Fig. 5.1 Meristem stages at terminal flowering of wild type, *brc1brc2* and *d14* plants after short day to long day growth.
(A) Primary branch number at terminal flowering, after a 4-week short day growth period, followed by growth under long days. **(B)** Schematic representation of axillary bud formation in the cauline and rosette leaf axils of the plants from **A**, determined by classifying the meristem stages according to the conditions stated in the legend. Each column represents an individual plant, with and each square within a column indicates a single leaf axil. Axils are scored from top to bottom, with the oldest leaf axils at the bottom. The thick black line represents the border between cauline and rosette leaf axils, with cauline axils above and rosette axils below. **(C)** Total number of rosette axils. **(D)** Percentage of rosette axils which were empty, or contained axillary buds with vegetative (vegetative 1, 2 or 3) or reproductive (reproductive 1, 2 or 3) meristems, determined as a percentage of the total number of rosette axils. Data are from a single experiment, $n = 10$. For **A**, **C** and **D** Tukey's HSD test was carried out after obtaining the least-square means for a linear model fitting the data and different letters indicate statistically significant results at $p < 0.05$.

assessed by scoring the number of primary branches at the terminal flowering stage in plants subjected to two growth regimes (Fig. 5.2A). Plants were either grown under long day growth conditions alone, or grown under short day/long day growth conditions as described earlier (Fig. 5.1). Branching was increased in *brc1brc2* plants compared to wild type, irrespective of the growth regime used. Short day/long day shifted plants produced significantly more primary branches than long day grown plants alone (Fig. 5.2A). The number of primary branches was increased for all genotypes after growth under short day conditions (Fig. 5.2A). Loss of PIN3, PIN4 and PIN7 in the *brc1brc2* mutant background did not affect branching in either growth condition (Fig. 5.2A). Plants lacking D14 function produced significantly more branches than *brc1brc2* under both growth conditions (Fig. 5.2A), with the difference between these mutants becoming increasingly clear in short day/long day shifted plants (Fig. 5.2B). Loss of PIN3, PIN4 and PIN7 in the *d14* mutant background significantly reduced branching, irrespective of the growth regime (Fig. 5.2A). This is consistent with the reduction of branching observed in the *maxpin3pin4pin7* mutants (Fig. 4.4, 4.5).

Together, these data show that there are quantitative differences in branch activation between *brc1brc2* and *d14* mutants. These differences become increasingly clear when plants have increased numbers of primary axis leaves and therefore axillary buds. The *pin3pin4pin7* mutations reduce branching in the *d14* strigolactone perception mutant, whereas *pin3pin4pin7* does not affect branching in *brc1brc2* mutants. This suggests that PIN3/PIN4/PIN7-mediated shoot branching control is independent of *BRC1*, and vice versa.

To further explore the effect of PIN3, PIN4 and PIN7 on *brc1brc2* and *d14* plants, additional shoot phenotypes were characterised at the terminal flowering stage in *brc1brc2* and *d14* mutant plants lacking PIN3, PIN4 and PIN7, grown under long day conditions (Fig. 5.3). Primary branching was reduced by *pin3pin4pin7* in the *d14* background, but not in *brc1brc2* mutants (Fig. 5.3A, E, reproduced from the same data set used for the branching under long days in Fig. 5.2A). Plant height was slightly and significantly reduced in *brc1brc2* mutants (Fig. 5.3B), consistent with earlier findings (Bennett et al., 2016b; Seale et al., 2017). The height of *brc1brc2pin3pin4pin7* was not significantly different from *brc1brc2* (Fig. 5.3B). The *d14* mutant displayed a much stronger stunted stature than *brc1brc2*, consistent with earlier findings (Bennett et al., 2016b; Seale et al., 2017). Loss of PIN3, PIN4 and PIN7 in the *d14* mutant background was able to partially rescue this phenotype (Fig. 5.3B), in agreement with the *maxpin3pin4pin7* data presented in Chapter 4 (Fig. 4.5B). The wider branch angle in the *pin3pin4pin7* mutant was visible in both *brc1brc2* and *d14* mutant backgrounds, and was even significantly increased compared to wild type in the latter (Fig. 5.3C). Stem diameter was unchanged in *pin3pin4pin7* mutants, and the *pin3pin4pin7* mutations did not have any significant effect on stem diameter in the *brc1brc2* or *d14* mutant backgrounds (Fig. 5.3D).

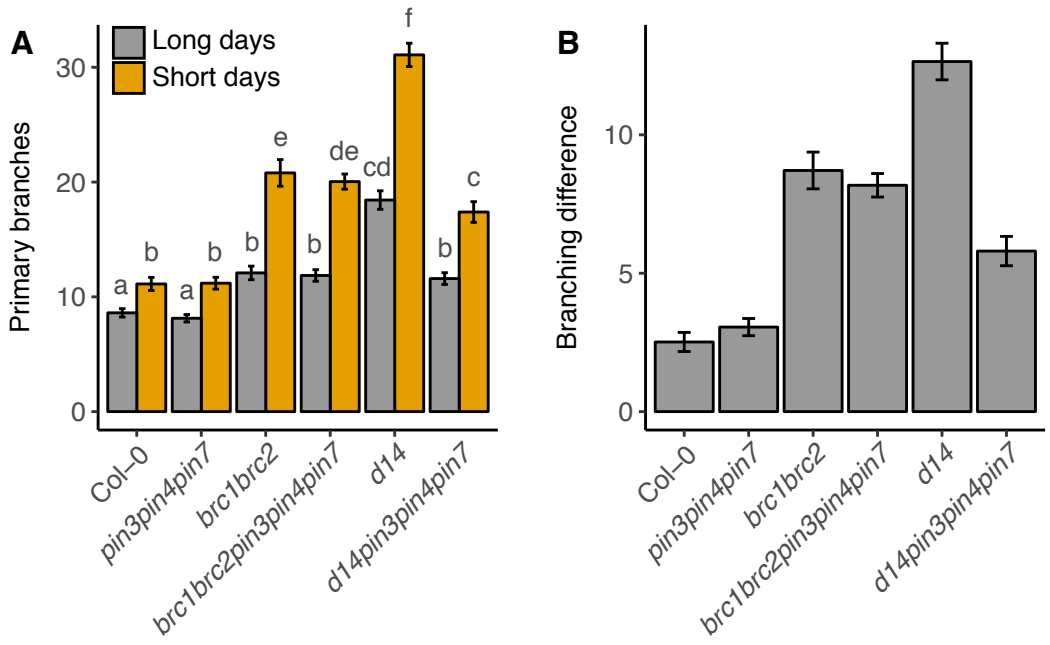

Fig. 5.2 Effect of growth conditions on branching in *brc1brc2* and *d14* mutants lacking PIN3/PIN4/PIN7.

(A) Branching in *brc1brc2* and *d14* mutants lacking functional PIN3, PIN4 and PIN7, scored at terminal flowering. Plants were grown under long day growth conditions (grey bars) or under short day growth conditions for four weeks, prior to shifting to long day growth conditions (orange bars), n = 21-24. Data are representative for two independent experiments. Tukey's HSD test was carried out after obtaining the least-square means for a linear model fitting the data and different letters indicate statistically significant results at $p < 0.05$. **(B)** Difference in the mean number of branches between the different growth regimes of the plants depicted in **A**. Error bars indicate the standard error of the difference between the means of each two samples.

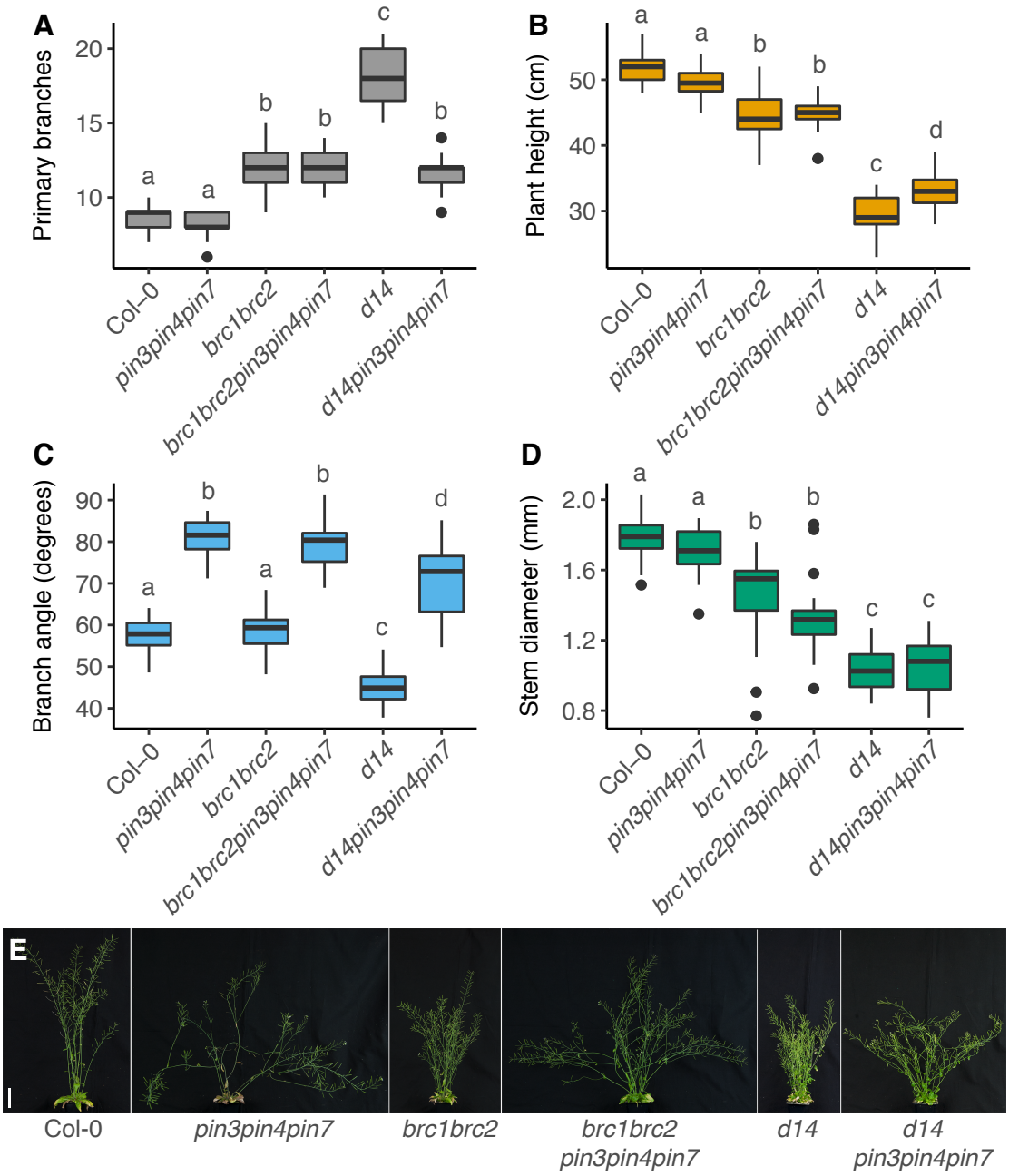

Fig. 5.3 Shoot phenotypes of *brc1brc2* and *d14* mutants lacking PIN3/PIN4/PIN7.
(A) Primary branch number of plants grown under long days, scored at terminal flowering. Data are the same as the long day branching data presented in Fig. 5.2A. **(B)** Plant height at terminal flowering. **(C)** Branch angle at terminal flowering. **(D)** Stem diameter at terminal flowering. **(E)** Photographs of the genotypes shown in **A**-**D** at terminal flowering. Bar = 50 mm. For **A**-**D** Tukey's HSD test was carried out after obtaining the least-square means for a linear model fitting the data and different letters indicate statistically significant results at $p < 0.05$. Data are representative of at least three independent experiments, depending on the genotype. $n = 22$-23.

Taken together, these data show that PIN3, PIN4 and PIN7 affect shoot branching and plant height independently of *BRC1*. Branch angles are unaffected by loss of BRC1 and BRC2, but reduced by loss of D14. Branch angles are increased by *pin3pin4pin7* in all the tested genotypes. Both *brc1brc2* and *d14* mutant plants have thinner stems than wild type, but loss of PIN3, PIN4 and PIN7 has no effect on stem diameter in any of the genotypes tested. Thus several aspects of the phenotypic syndrome resulting from strigolactone loss are partially dependent on PIN3, PIN4 and PIN7, whereas there is no evidence for any interaction between BRC1 and BRC2, and PIN3 PIN4 and PIN7 with respect to these phenotypes.

To test whether stem auxin transport is reduced by loss of PIN3, PIN4 and PIN7 in *brc1brc2* and *d14* mutant backgrounds, bulk auxin transport was measured in these mutant backgrounds. Consistent with published data, bulk auxin transport in *brc1brc2* is comparable to wild type, whereas transport is increased in *d14* mutant stems (Fig. 5.4; Bennett et al., 2016b). Auxin transport in *brcbrc2pin3pin4pin7* and *d14pin3pin4pin7* was significantly decreased compared to *brc1brc2* and *d14*, respectively (Fig. 5.4). These data show that PIN3, PIN4 and PIN7 contribute to stem auxin transport in both *brc1brc2* and *d14* mutant backgrounds.

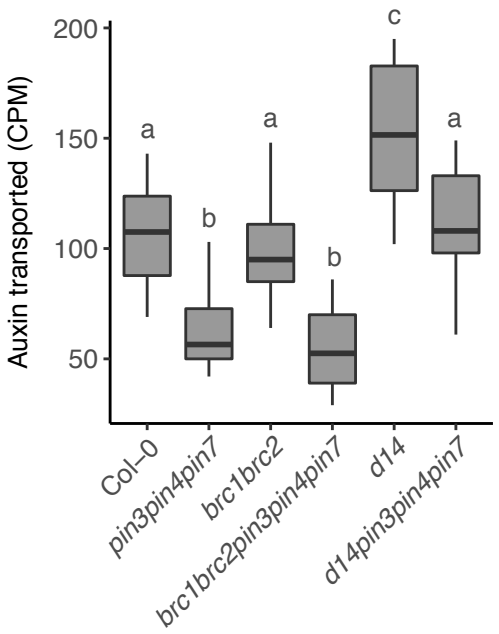

Fig. 5.4 Bulk auxin transport in *brc1brc2* and *d14* mutants lacking PIN3/PIN4/PIN7.
Bulk auxin transport in 6-week old basal internodes of *brc1brc2* and *d14* plants lacking PIN3/PIN4/PIN7 functionality. Data are representative of two independent experiments, n = 17-24. Tukey's HSD test was carried out after obtaining the least-square means for a linear model fitting the data and different letters indicate statistically significant results at $p < 0.05$.

5.2.2 The effect of ABCB1, ABCB19 on shoot branching in *brc1brc2* and strigolactone mutants

Shoot branching in strigolactone mutants is partially dependent on ABCB19 function, since loss of ABCB19 results in a partial rescue of the increased shoot branching phenotype of strigolactone mutants (Fig. 4.9). To test whether ABCB19 is involved in *BRC1*-mediated shoot branching, the *abcb19* mutation was introduced into the *brc1brc2* background through crossing and the effect on branching was assessed. The *abcb1* mutation was also introduced into the *brc1brc2* mutant background for completeness. Loss of ABCB1 in *brc1brc2* did not significantly affect the number of primary branches, compared to *brc1brc2*, irrespective of the growth regime used (Fig. 5.5A). In contrast, branching was significantly reduced in *brc1brc2abcb19* mutants, compared to *brc1brc2* and this reduction was clear in both long day grown and short day/long day shifted plants (Fig. 5.5A). The branching difference between long day and short day/long day shifted *brc1brc2abcb19* plants was markedly less than observed in *brc1brc2* mutants, further suggesting that loss of ABCB19 reduces the ability of *brc1brc2* mutants to activate their branches (Fig. 5.5B). Interestingly, branching in *abcb19* single mutants appeared to be reduced, compared to wild type under the short day/long day shifted growth conditions. Although this reduction in branching did not appear to be significant if all tested genotypes were compared to each other (Fig. 5.5A), a direct comparison between wild type and *abcb19* showed clear significant differences in all experiments ($p < 0.001$ for a pairwise Wilcoxon rank-sum test).

To further explore the effect of ABCB1 and ABCB19 on *brc1brc2* plants, additional shoot phenotypes were characterised at the terminal flowering stage in *brc1brc2abcb1* and *brc1brc2abcb19* mutants, grown under long day conditions (Fig. 5.6). Primary branching was reduced in *brc1brc2abcb19*, compared to *brc1brc2* mutants (Fig. 5.6A, reproduced from the same data set used for the branching under long days in Fig. 5.5A). Plant height was not affected by *abcb1* or *abcb19*, neither in a wild type background nor in the *brc1brc2* mutant background (Fig. 5.6B). Branch angles did not differ significantly in any of the tested genotypes (Fig. 5.6C). Loss of ABCB1 had no effect on stem diameter in wild type or *brc1brc2* mutant backgrounds. Loss of ABCB19 increased stem diameter slightly in *brc1brc2* mutant plants, whereas in wild type plants it had no measurable effect (Fig. 5.6D).

To test whether stem auxin transport is reduced by loss of ABCB1 or ABCB19 in *brc1brc2* mutants, bulk auxin transport assay was assessed in these mutant backgrounds. Loss of ABCB1 did not change bulk auxin transport, neither in a wild type nor in the *brc1brc2* mutant backgrounds (Fig. 5.7). In contrast, loss of ABCB19 reduced auxin transport in the *brc1brc2* mutant background to the same extent as seen in wild type (Fig. 5.7).

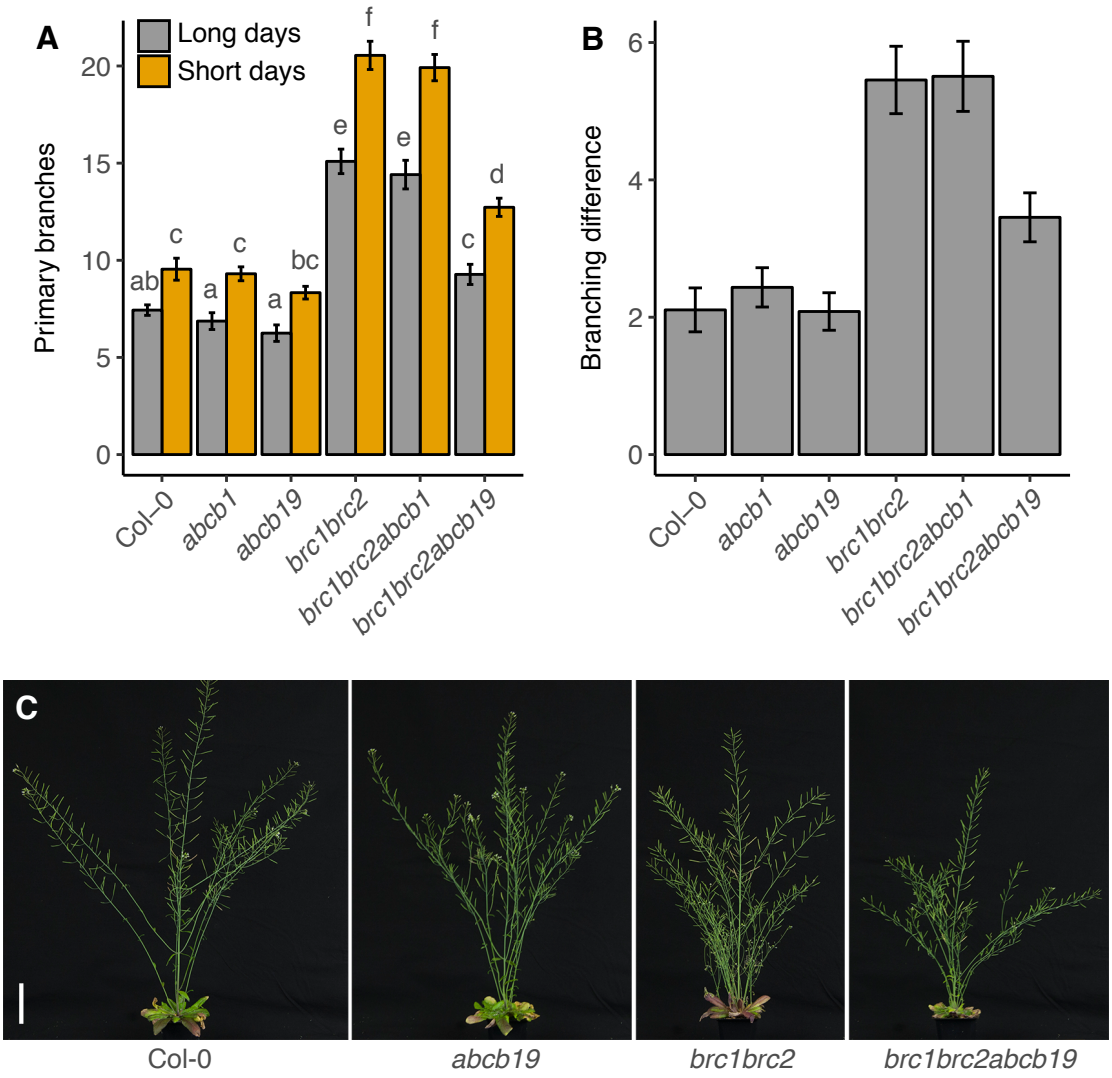

Fig. 5.5 Effect of growth conditions on branching in *brc1brc2* mutants lacking ABCB1/ABCB19. **(A)** Branching in *brc1brc2* mutants lacking functional ABCB1 or ABCB19, scored at terminal flowering. Plants were grown under long day growth conditions (grey bars) or under short day growth conditions for four weeks, prior to shifting to long day growth conditions (orange bars), n = 20-24. Data are representative for two independent experiments. Tukey's HSD test was carried out after obtaining the least-square means for a linear model fitting the data and different letters indicate statistically significant results at $p < 0.05$. **(B)** Difference in the mean number of branches between the different growth regimes of the plants depicted in **A**. Error bars indicate the standard error of the difference between the means of each two samples. **(C)** Photographs of selected genotypes shown in **A** at terminal flowering. Bar = 50 mm.

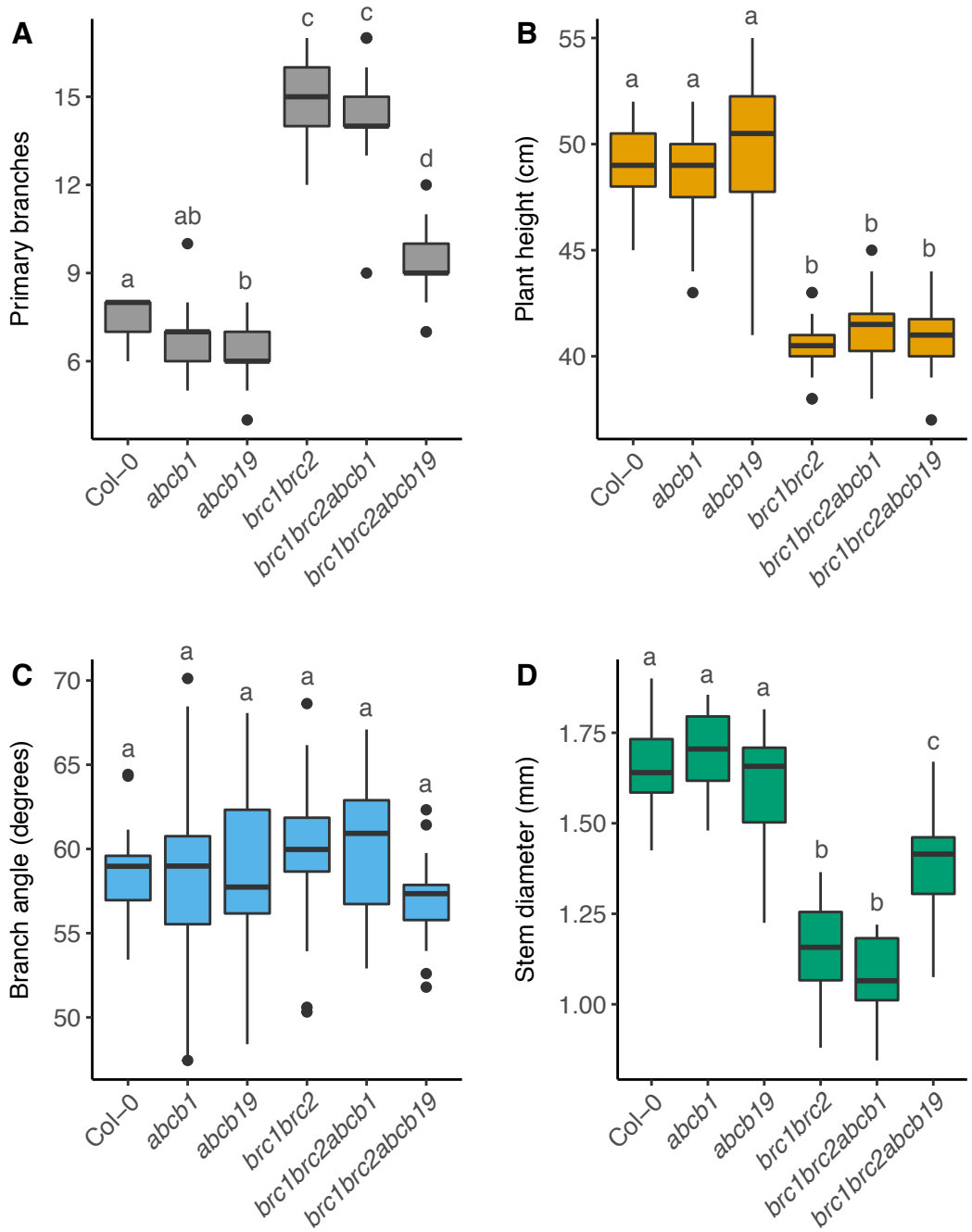

Fig. 5.6 Shoot phenotypes of *brc1brc2* plants lacking ABCB1/ABCB19.
(A) Primary branch number of plants grown under long days, scored at terminal flowering. Data are the same as the long day branching data presented in Fig. 5.5A. **(B)** Plant height at terminal flowering. **(C)** Branch angle at terminal flowering. **(D)** Stem diameter at terminal flowering. For **A**-**D** Tukey's HSD test was carried out after obtaining the least-square means for a linear model fitting the data and different letters indicate statistically significant results at $p < 0.05$. Data are representative of two independent experiments. n = 20-23.

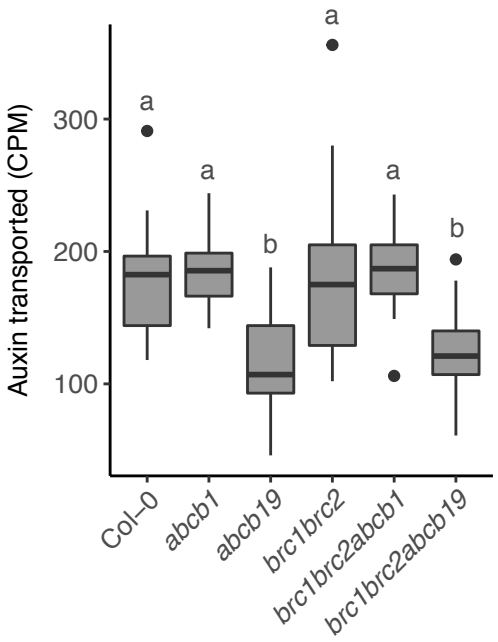

Fig. 5.7 Bulk auxin transport in *brc1brc2* mutants lacking ABCB1/ABCB19.
Bulk auxin transport in 6-week old basal internodes of *brc1brc2* plants lacking ABCB1 or ABCB19 functionality. Data are representative of two independent experiments, n = 21-24. Tukey's HSD test was carried out after obtaining the least-square means for a linear model fitting the data and different letters indicate statistically significant results at $p < 0.05$.

The data presented in Chapter 4 show that shoot branching control by strigolactones is partially dependent on PIN3/PIN4/PIN7 and ABCB19 function. This effect is evident when bud-bud competition is assessed in two-node explants lacking PIN3, PIN4, PIN7 or ABCB19. Addition of exogenous GR24 can restore competition between buds only partially (Fig. 4.7; 4.10). The *brc1brc2* mutant has previously been shown to respond to exogenous strigolactone application, although it is partially resistant (Seale et al., 2017). To assess whether competition between buds is further decreased in *brc1brc2* mutants by loss of PIN3, PIN4 and PIN7, two-node explants of *brc1brc2pin3pin4pin7* mutant plants were grown in a bud-bud competition assay and treated with exogenous GR24 (Fig. 5.8). These data are from a single experiment and should be treated with caution. The *d14* mutant was included as a negative control. In untreated explants, competition between *brc1brc2pin3pin4pin7* buds was decreased compared to wild type (Fig. 5.8). Addition of exogenous GR24 increased bud-bud competition in the *brc1brc2pin3pin4pin7* mutant explants to a comparable degree as seen in GR24-treated *pin3pin4pin7* and *brc1brc2* mutant explants. This was significantly less than the level of competition seen in GR24-treated wild type explants (Fig. 5.8). Consistent with published data, the *brc1brc2* mutant explants were responsive to GR24 (Seale et al., 2017). However, whereas untreated *brc1brc2* explants were reported to have decreased bud-bud competition compared to wild type (Seale et al., 2017), no significant difference was detected in this experiment (Fig. 5.8).

In the bud-bud competition assay, the *brc1brc2*, *pin3pin4pin7* and *brc1brc2pin3pin4pin7* mutants all show a similar GR24 response, which is less than that of wild type. There is no indication of additivity between *brc1brc2* and *pin3pin4pin7* (Fig. 5.8). To assess the response of whole-plant branching to GR24 in the *brc1brc2pin3pin4pin7* mutants, quintuple mutant plants were grown in long day conditions in sterile Weck jars containing agar-solidified ATS medium supplemented with 5 µM GR24 or solvent control (Fig. 5.9). The number of primary branches was scored 8 weeks after sowing. Because *brc1brc2abcb19* mutant plants showed a branching response on soil (Fig. 5.5), they were also included in this assay. The data from the *brc1brc2abcb19* are from a single experiment and should be treated with caution. The *d14* mutant was included as a negative control. Branching in the *brc1brc2pin3pin4pin7* mutant was unchanged compared to *brc1brc2* in the untreated controls (Fig. 5.9). Both *brc1brc2pin3pin4pin7* and *brc1brc2* mutants responded to GR24 treatment to a similar degree, resulting in reduced levels of branching. Branching in *brc1brc2abcb19* mutants was reduced under control conditions compared to *brc1brc2* (Fig. 5.9). This is consistent with the branching data from soil-grown plants. Branching in *brc1brc2abcb19* mutant plants grown on GR24-containing medium was unchanged, compared to plants grown under control conditions (Fig. 5.9).

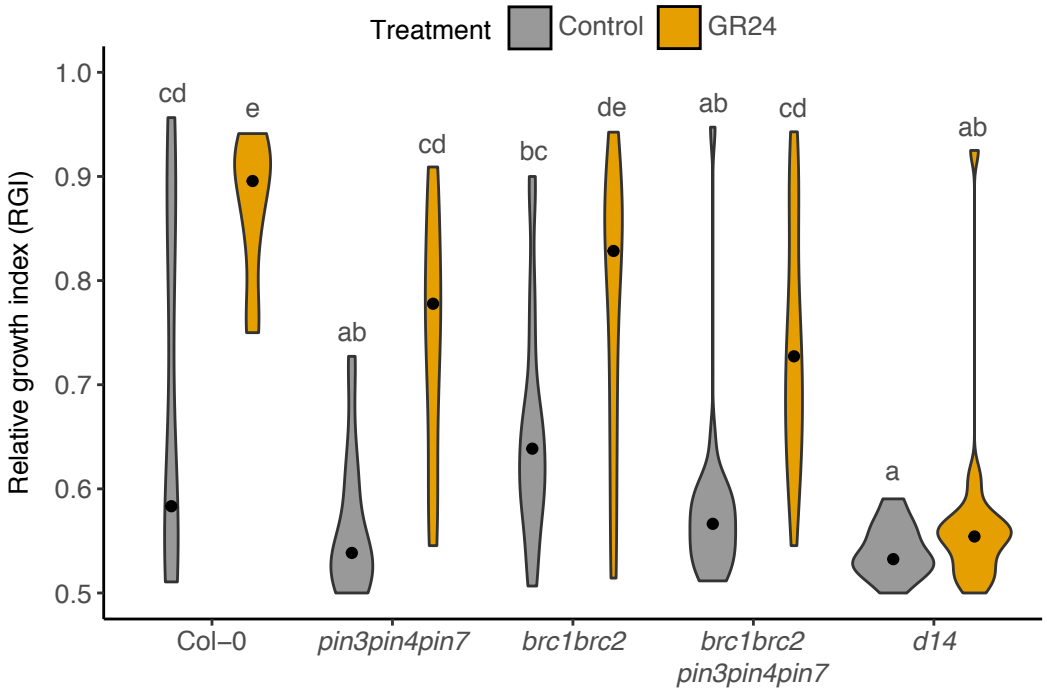

Fig. 5.8 Bud competition in *brc1brc2pin3pin4pin7* mutant two-node explants in response to GR24. Violin plot for the relative growth index (RGI) of two-node explants, treated with or without 5 µM basal GR24, 10 days post decapitation, n = 14-24. The RGI is the proportion of branch length in the longest branch. Black dots indicate the median value and the area of each plot represents the probability distribution of the values. Tukey's HSD test was carried out after obtaining the least-square means for a linear model fitting the data and different letters indicate statistically significant results at $p < 0.05$. Data are from a single experiment.

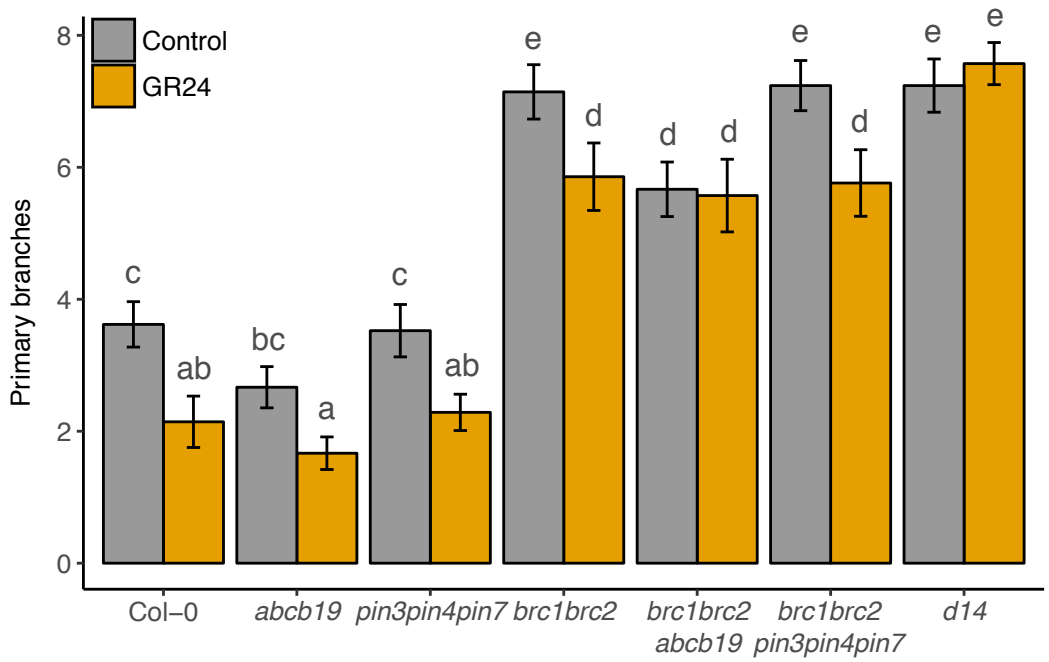

Fig. 5.9 Whole-plant responses to GR24 of *brc1brc2* mutants with impaired PIN3/PIN4/PIN7 or ABCB19 function.
Primary branch number of plants grown under axenic, long day growth conditions in jars, supplemented with ATS ± 5 µM GR24, scored after 8 weeks. Tukey's HSD test was carried out after obtaining the least-square means for a linear model fitting the data and different letters indicate statistically significant results at $p < 0.05$. Data are representative of two independent experiments for all genotypes apart from *brc1brc2abcb19*, which was included once, $n = 21$. Bars represent the 95 % confidence interval of the mean.

Taken together, these data show that *brc1brc2pin3pin4pin7* mutants are still able to respond to strigolactone. However, *brc1brc2abcb19* mutant plants are apparently unable to respond GR24 in a whole plant branching assay.

5.2.3 Environmental responses in *brc1brc2* mutants lacking PIN3/PIN4/PIN7 or ABCB19.

Plants lacking BRC1 have previously been shown to retain some ability to reduce branching in limiting environments. Wild type plants produce more branches when nitrate availability is sufficient, compared to conditions where nitrate availability is limiting (de Jong et al., 2014). The *brc1brc2* mutants display increased levels of branching compared to wild type under both high and low nitrate conditions (Seale et al., 2017). However, *brc1brc2* mutant plants produce significantly fewer branches under low nitrate conditions than under high nitrate availability, demonstrating that *brc1brc2* mutant plants are still able to respond to changing environmental conditions (Seale et al., 2017). Another environmental condition affecting branching is planting density. Plants grown under high planting density regimes produce fewer branches than when grown under low planting density regimes, a shading response which is at least partially mediated through *BRC1* (Gonzalez-Grandio et al., 2013). Although *brc1* mutants are branchy at both high and low planting densities, they retain some ability to reduce branching at high planting density (Aguilar-Martinez et al., 2007).

The branching phenotypes of the *brc1brc2pin3pin4pin7* and *brc1brc2abcb19* mutants show that, in the *brc1brc2* mutant background, loss of PIN3/PIN4/PIN7 and ABCB19 result in different branching responses. To further explore the effect of these mutations on *brc1brc2* branching under different growth regimes, plants were grown under different environmental conditions. To explore the effect of nitrate availability in these mutants, plants were grown on high (9 mM) and low (1.8 mM) nitrate conditions. Furthermore, plants were also subjected to different planting density regimes on soil, with low (1 plant per pot) and high (5 plants per pot) planting density. In both assays the number of primary branches was assessed at the terminal flowering stage. As expected, wild type plants produced more branches with high nitrate compared to low nitrate availability (Fig. 5.10A). The *abcb19* and *pin3pin4pin7* were still responsive to nitrate availability, showing similar responses to wild type (Fig. 5.10A). Consistent with published data (Seale et al., 2017), *brc1brc2* produced fewer branches under low nitrate conditions than under high nitrate. Branching levels of *brc1brc2pin3pin4pin7* mutant plants were similar to *brc1brc2* with both high and low nitrate availability. The *brc1brc2abcb19* mutant produced fewer branches than *brc1brc2* under high nitrate conditions and appeared unresponsive to nitrate limitation (Fig. 5.10A).

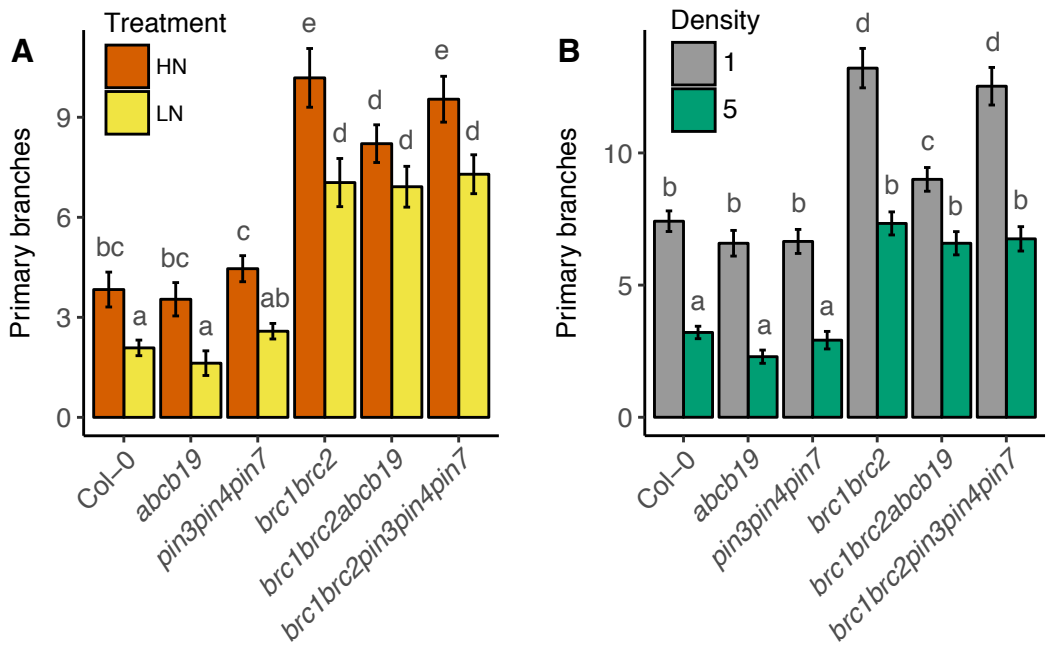

Fig. 5.10 Branching response to nitrate limitation and crowding in *brc1brc2abcb19* and *brc1brc2pin3pin4pin7* mutants.
(A) Primary branch number at terminal flowering of *brc1brc2 abcb19/pin3pin4pin7* mutants grown on high or low nitrate, n = 22-24. **(B)** Primary branch number at terminal flowering of *brc1brc2 abcb19/pin3pin4pin7* mutants grown under differing planting densities. Plants were soil-grown under low density (1 plant per pot) or high density (5 plants per pot), n = 21-24. For **A** and **B**, Tukey's HSD test was carried out after obtaining the least-square means for a linear model fitting the data and different letters indicate statistically significant results at $p < 0.05$. Data are representative of two independent experiments for all genotypes apart from *brc1brc2abcb19* in **B**, which was included once. Bars represent the 95 % confidence interval of the mean.

Increasing planting density had a clear effect on all tested genotypes, with fewer branches produced under high planting density regimes (Fig. 5.10B). Branching was reduced in *brc1brc2abcb19* mutant plants under low planting density, compared to *brc1brc2* (Fig. 5.10B). This is consistent with previous data (Fig. 5.5A). Increased planting density resulted in a small but significant decrease in branching in the *brc1brc2abcb19* mutant. The difference in branch numbers under low and high density planting was therefore much greater for *brc1brc2* and *brc1brc2pin3pin4pin7* than *brc1brc1abcb19*. However, there was no difference in branching level between any of the tested *brc1brc2* mutant combinations under high planting density (Fig. 5.10B).

Together, these data show that *brc1brc2* plants lacking PIN3, PIN4 and PIN7 are able to regulate their branch growth in response to nitrate availability and planting density. In contrast, *brc1brc2* plants lacking ABCB19 appear to have lost their ability to respond to nitrate availability, but are still able to respond weakly to planting density.

5.2.4 BRC1 protein function

Most of the published work on *BRC1* has focussed on the regulation of transcript abundance for this gene. The function of BRC1 is not specifically known, but other TCP transcription factors have been shown to include cell cycle genes among their transcriptional targets (Kosugi and Ohashi, 2002; Li et al., 2005; Schommer et al., 2014; Trémousaygue et al., 2003). A GFP-tagged overexpression line is available for BRC1, but growth of these plants is highly retarded and plants show many pleiotropic effects (Aguilar-Martinez et al., 2007). To better understand the biology of the BRC1 protein, a fluorescent-tagged reporter construct was generated. To avoid the pleiotropic effects of an overexpression line, a 2.5 kb fragment upstream of the *BRC1* START codon was used as a native promoter. The genomic DNA sequence for *BRC1* was amplified, minus the STOP codon. A 971 bp fragment downstream of the *BRC1* STOP codon was also amplified and these fragments were recombined with a Citrine fluorescent tag into a pH7m34GW plant destination vector (VIB, Ghent), using MultiSite Gateway Technology (Invitrogen) as described in Section 2.3.4, resulting in the *BRC1::BRC1:Citrine* construct (Fig. 5.11A).

To test whether the generated *BRC1::BRC1:Citrine* construct is functional, the construct was introduced into the *brc1* single mutant background, using the well-established floral dip method for Agrobacterium-mediated plant transformation (Clough and Bent, 1998). The pH7m34GW vector confers hygromycin resistance in plants, so the T1 seeds obtained after floral dipping were selected on hygromycin-containing growth medium using the selection method described in Section 2.3.8. Hygromycin-resistant plants were grown to maturity and a segregation analysis was performed in the following T2 generation. Individual lines that

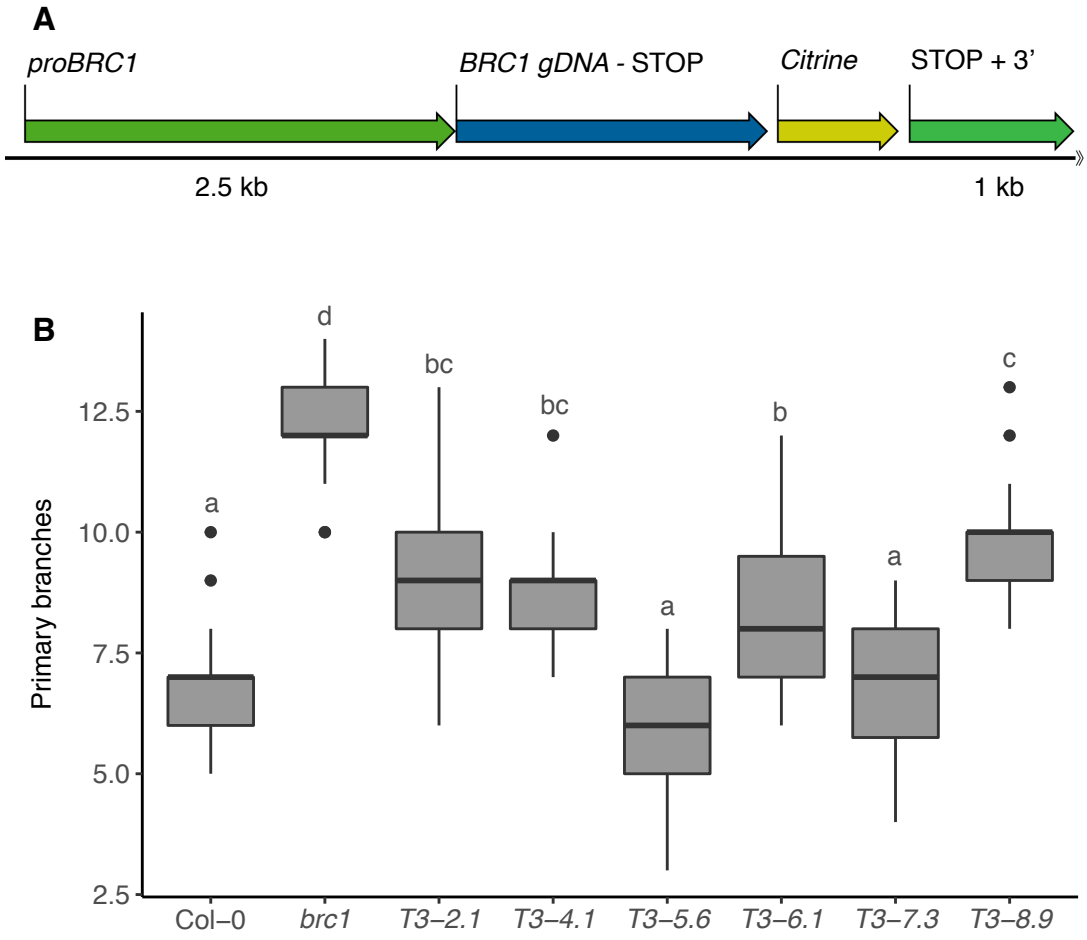

Fig. 5.11 BRC1 protein construct and complementation.
(A) Schematic illustrating the *BRC1::BRC1:Citrine* construct design. **(B)** Primary branching at terminal flowering of long-day-grown *brc1* mutant plants carrying single *BRC1::BRC1:Citrine* insertions, n = 17-24. Tukey's HSD test was carried out after obtaining the least-square means for a linear model fitting the data and different letters indicate statistically significant results at $p < 0.05$. Data are from a single experiment.

showed a 3:1 segregation were selected, in order to isolate single insertion site lines. Using the offspring of these lines, homozygous lines were selected in the T3 generation.

The functionality of the *BRC1::BRC1:Citrine* construct was assessed in planta by determining the ability of the single insertion lines to rescue the high branching phenotype of the *brc1* mutant. Branching was assessed in 6 independent homozygous transformation events, by determining the number of primary branches at terminal flowering of plants grown under long day conditions (Fig. 5.11B). All tested insertion lines activated fewer branches than *brc1* and two independent lines were able to restore branching to wild type levels, suggesting that in these two lines the *BRC1::BRC1:Citrine* construct is fully functional. The next step will be to further analyse the expression pattern of the *BRC1::BRC1:Citrine* construct in these lines. These lines provide a starting point for further investigation into the function of the BRC1 protein.

5.3 Summary

- Shoot branching control by *BRC1* is independent of PIN3, PIN4 and PIN7.
- Shoot branching control by *BRC1* is partially dependent on ABCB19, but not ABCB1.
- Branching response to strigolactone appears diminished in *brc1brc2abcb19* mutants.
- Branching response to nitrate is absent in *brc1brc2abcb19* mutants.
- A generated *BRC1::BRC1:Citrine* construct is able to rescue the branching in the *brc1* background

Chapter 6

The role of proton pumps in auxin transport and shoot branching

6.1 Introduction

The previous chapters have highlighted the importance of auxin export and import on the movement of auxin. These are active processes requiring energy. Whereas some transport proteins, such as ABCBs, are able to generate this energy themselves by binding and hydrolysing ATP, other proteins are not able to do this. These proteins, including PINs and AUX1/LAX proteins, rely on the proton motive force to energise them. The proton motive force is generated by the activity of plasma membrane H^+-ATPases, which create a membrane potential and a pH gradient across the plasma membrane.

Interestingly, plasma membrane H^+-ATPases themselves are affected by auxin. Auxin is able to activate plasma membrane proton pumps, which in some circumstances can lead to cell expansion (Hager, 2003). Furthermore, the proton gradients created by the H^+-ATPases might also create feedback on the transport of auxin that could contribute to the polarisation of auxin transport (Steinacher et al., 2012).

The main aim of the work presented in this chapter was to further investigate the role of plasma membrane H^+-ATPase activity in the context of auxin transport and shoot branching control. These processes were further explored using mutants in the two most abundantly expressed plasma membrane H^+-ATPases in Arabidopsis, AHA1 and AHA2 (Haruta et al., 2010). Auxin transport was analysed by measuring the bulk movement and pulse progression of auxin through stem segments lacking AHA1 or AHA2 function. Shoot branching was investigated by tracking the activation of rosette buds following decapitation, as well as branching in intact plants.

6.2 Results

6.2.1 The role of AHA proton ATPases in auxin movement in the stem

If AHA1 or AHA2 H^+-ATPase activity contributes to active transport of auxin, then it is possible that loss of function of these proteins will reduce auxin transport. To test whether this is the case in stems, bulk auxin transport was measured in *aha1* and *aha2* mutant stems. Bulk auxin transport was significantly reduced in *aha1* mutant stems, whereas *aha2* stems had wild type levels of stem auxin transport (Fig. 6.1A). To test whether the reduced stem auxin transport phenotype in *aha1* results from decreased accumulation of basal PIN1 on the plasma membrane of xylem parenchyma cells, *aha1* mutant lines homozygous for a *PIN1::PIN1:GFP* reporter construct (Benkova et al., 2003) were generated through crossing and PIN1-GFP levels were measured. No difference in PIN1 levels was detected between wild type and *aha1* mutant stems (Fig. 6.1B).

Together, these data suggest that bulk auxin transport in the stem is affected by AHA1 proton pump activity. The reduced stem auxin transport in *aha1* mutant stems is not caused by reduced basal PIN1 accumulation in xylem parenchyma cells.

As described above, the proton motive force energises both PIN and AUX/LAX activity. To assess the transport properties of *aha1* stems in more detail, the movement of an auxin pulse along stems was followed over time (Fig. 6.2). The profile of the auxin distribution in *aha1* mutant stems was not markedly different from wild type at any of the sampled time points (Fig. 6.2A). Rapid dampening and broadening occurred in both wild type and *aha1* stems, when the auxin distribution of the initial pulse was analysed after 30, 60 and 90 minutes. However, the auxin levels recovered in the *aha1* segments was consistently lower than in wild type. Assessing the total auxin uptake during the initial 10-minute pulse, equalling the sum of the counts of all segments within one sample, showed that *aha1* stems took up significantly less radiolabeled auxin than wild type (Fig. 6.2B).

To assess further auxin uptake in *aha* mutant stems, an auxin uptake experiment was performed (see Fig. 3.13A for a schematic overview of the method). These data are based on a single experiment, so they should be treated with caution. Auxin content of 15 mm long samples was determined after 0.5, 1, 3 and 5 hours incubation, at 2.5 mm intervals. After 0.5 hours incubation, total auxin uptake per genotype, determined as the sum of all the counts in each sample, was not significantly different between the three tested genotypes (Fig. 6.3A). After 1, 3 and 5 hours of incubation the total uptake of radiolabeled auxin was significantly reduced in *aha1* stems, compared to wild type, whereas uptake was similar to wild type in *aha2* stems (Fig. 6.3A). Analysing the auxin content per segment showed that the auxin content in the most apical segment was lower in *aha1* stems, an observation which

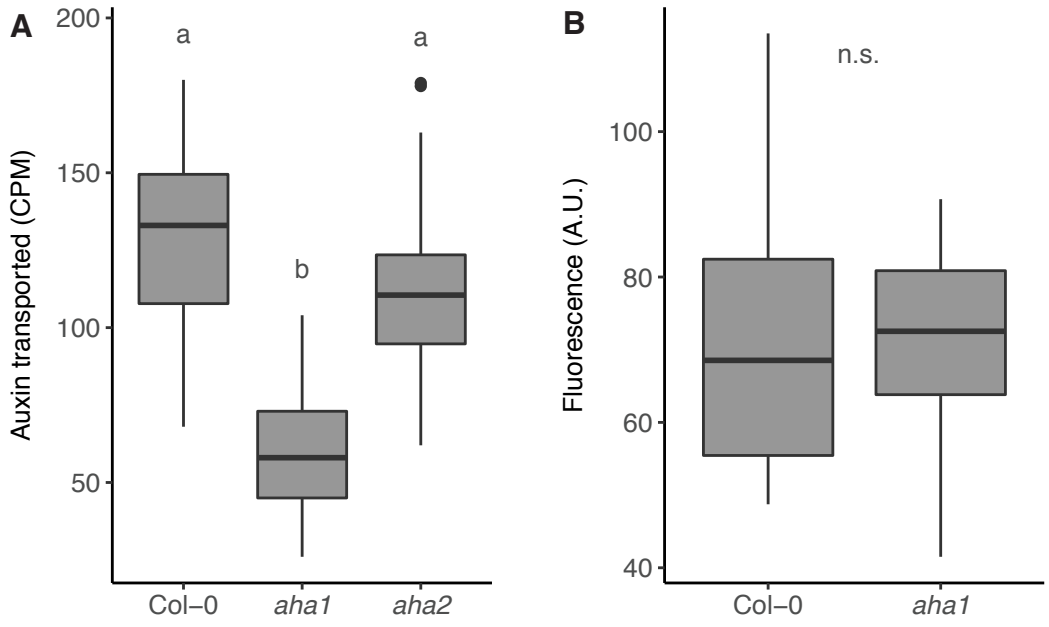

Fig. 6.1 Bulk auxin transport and PIN1 levels in *aha* stems.
(A) Bulk auxin transport in 6-week old basal internodes of plants lacking AHA1 or AHA2 functionality. Data are representative of five independent experiments, n = 23-24. Tukey's HSD test was carried out after obtaining the least-square means for a linear model fitting the data and different letters indicate statistically significant results at $p < 0.05$. **(B)** Quantification of PIN1-GFP levels at the basal plasma membrane of xylem parenchyma cells in basal internodes, at comparable stages as those used in **A**. For Col-0, n = 45; *aha1*, n = 40 membranes (mean of 5 per sample, 8-9 individual samples per line). Data are representative of three independent experiments. Student's t-test, $p < 0.05$, n.s. denotes non-significant differences.

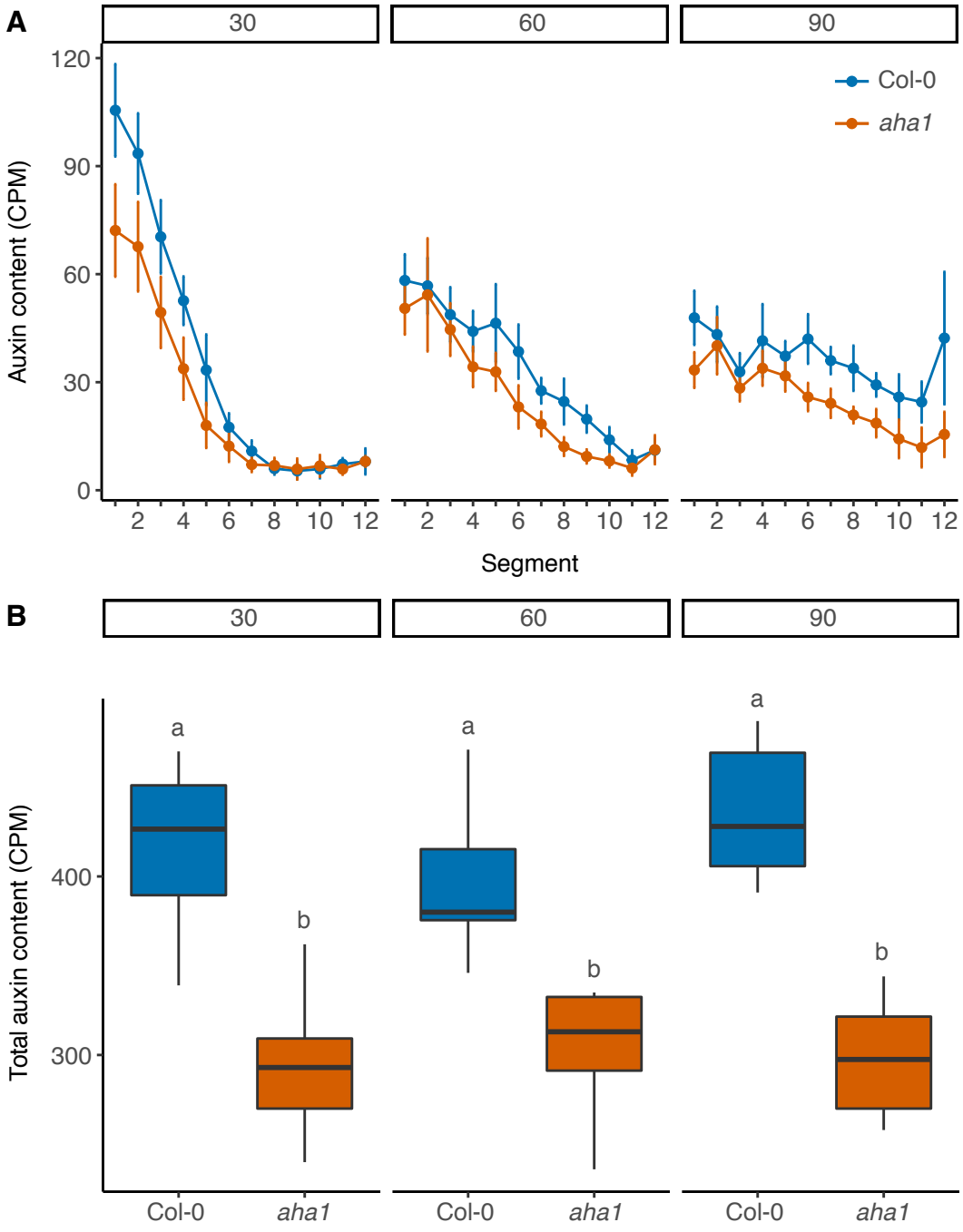

Fig. 6.2 Movement of an auxin pulse in the *aha1* mutant.
(A) Progression of a 10-minute pulse of 5 µM 14C-IAA through 24 mm long basal internodes of Col-0 and *aha1* stems at 30, 60 and 90 minutes after application (left to right), measured as counts per minute (CPM) in 2 mm segments. Bars represent the 95 % confidence interval of the mean. **(B)** Total auxin content per sample, equalling the sum of the counts of all segments within one sample. Tukey's HSD test was carried out after obtaining the least-square means for a linear model fitting the data and different letters indicate statistically significant results at $p < 0.05$. Data are representative of two independent experiments, $n = 8$.

was most pronounced at the later time points (Fig. 6.3B, C). Basal accumulation of auxin at the 3 and 5-hour time point was significantly reduced in *aha1* stems, compared to wild type ($p < 0.05$, Holm-Bonferroni-adjusted pairwise Wilcoxon rank-sum tests). This is consistent with observed reduction in bulk auxin transport in *aha1* stems (Fig. 6.1A).

Together, these data show that apical accumulation of auxin in *aha1* mutants is slower than in wild type, whereas this is unchanged in *aha2* mutant stems. Furthermore, in auxin pulse experiments less auxin moves along the stem in *aha1* mutants than in wild type, although the overall distribution appears similar.

6.2.2 The role of AHA proton ATPases in bud activation

The stem auxin transport phenotype in the *aha1* mutant raises the question as to whether loss of AHA1 function could affect bud outgrowth. To test this, rosette bud activation for wild type, *aha1* and *aha2* was investigated using a short day/long day decapitation assay. The number of rosette branches was scored 3, 5, 7, 10 and 14 days post decapitation, to follow bud activation dynamics (Fig. 6.4A). Bud activation in wild type and *aha2* was similar at all time points (Holm-Bonferroni-adjusted pairwise Wilcoxon rank-sum tests, not significant), with most branches activating by 5 days post decapitation and additional branch activation levelling off in the subsequent time points (Fig. 6.4A). In contrast, at 3 days post decapitation, the *aha1* mutant had significantly more active rosette branches than either wild type or *aha1* ($p < 0.001$, Holm-Bonferroni-adjusted pairwise Wilcoxon rank-sum tests). Branch activation in *aha1* plants also levelled off, as in wild type and *aha2* plants, but the number of active branches remained significantly higher at all sampled time points ($p < 0.001$, Holm-Bonferroni-adjusted pairwise Wilcoxon rank-sum tests).

The short day/long day decapitation assays show that rosette buds appear to activate more quickly in *aha1* mutants than in wild type (Fig. 6.4A). To test whether this could be attributed to an increased speed of outgrowth, the outgrowth of single cauline buds was assessed. Buds were released from inhibition by decapitation of the shoot apex and bud outgrowth was followed for 10 days (Fig. 6.4B). No difference in branch length between wild type and *aha1* could be detected at any time point in the experiment (Holm-Bonferroni-adjusted pairwise Wilcoxon rank-sum tests, not significant).

Together, these data show that rosette branching following decapitation is increased in *aha1* mutants. Furthermore, active *aha1* buds grow at a similar rate to wild type.

To further characterise the shoot phenotypes of the *aha1* and *aha2* mutants, plants were grown under long day growth conditions and scored at the terminal flowering stage (Fig. 6.5). These data are from a single experiment, and should be treated with caution. Under these conditions there was a slight, but significant, increase in primary branch number in *aha1*

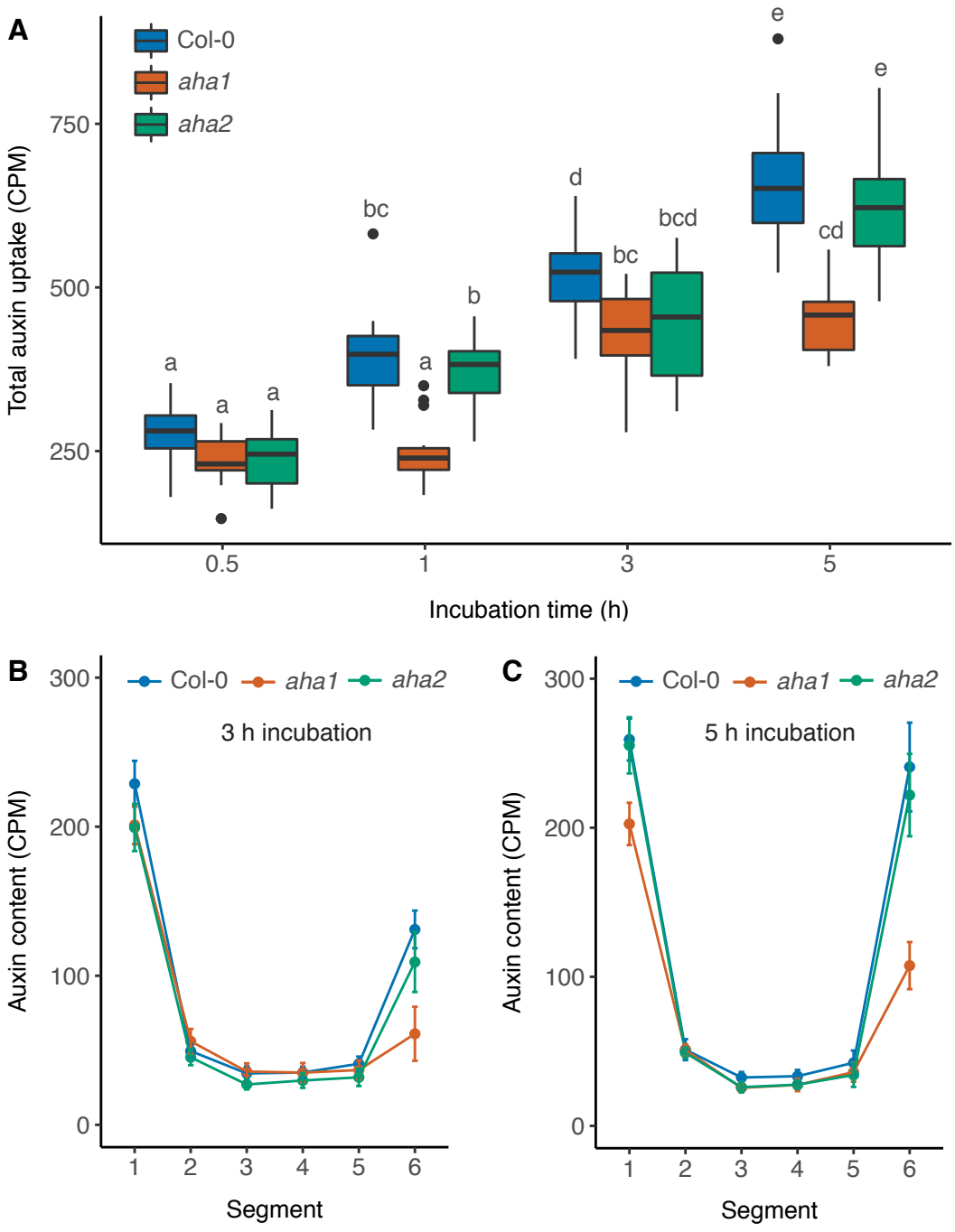

Fig. 6.3 Auxin uptake in *aha* stems.
(A) Total auxin uptake in *aha1* and *aha2* mutants after continuous incubation in 1 µM 14C-IAA for 0.5, 1, 3 or 5 hours. Uptake was determined as the sum of the counts of the six segments of each sample. **(B, C)** Mean auxin content per segment for each genotype after 3 **(B)** and 5 **(C)** hours of incubation. Bars represent the 95 % confidence interval of the mean. For **A**, Tukey's HSD test was carried out after obtaining the least-square means for a linear model fitting the data and different letters indicate statistically significant results at $p < 0.05$. Data are from a single experiment, $n = 16$.

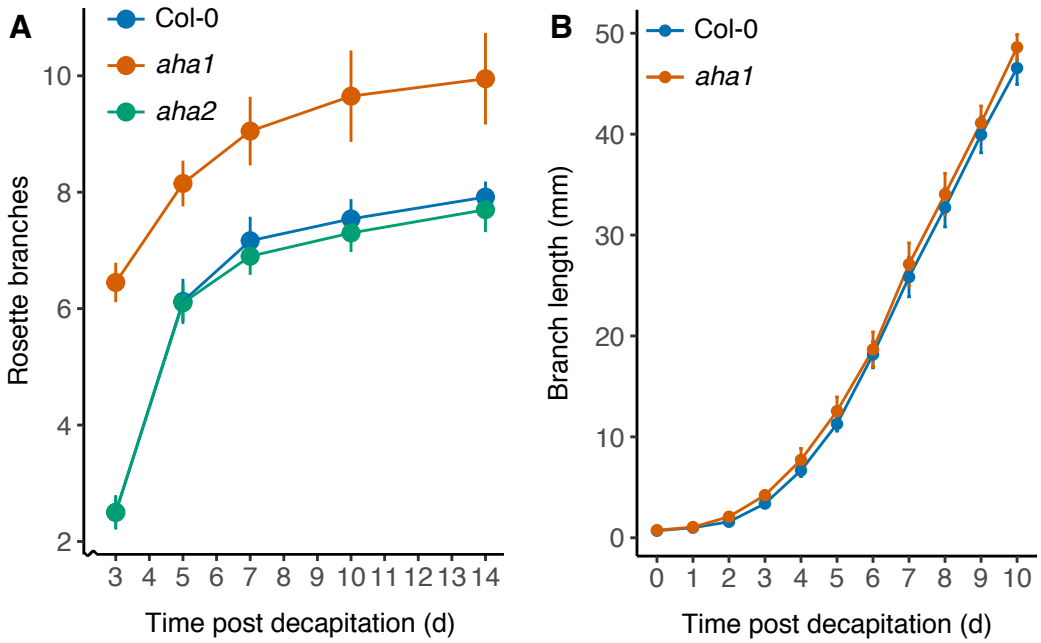

Fig. 6.4 Bud activation in *aha* mutants.
(A) Rosette branch activation dynamics of Col-0, *aha1* and *aha2* plants, using a standard short day/long day decapitation assay. The number of active rosette branches was scored 3, 5, 7, 10 and 14 days post decapitation. Tukey's HSD test was carried out after obtaining the least-square means for a linear model fitting the data and, using a threshold of $p < 0.05$. Rosette branch numbers for *aha1* were significantly increased across all time points, compared to Col-0 and *aha2*. No significant differences were found between Col-0 and *aha2*. Data are representative for four independent experiments, apart from the 14 day time point, which was sampled twice, n = 20-24. **(B)** Branch length of one-node Col-0 and *aha1* explants, followed for 10 days after decapitation. Tukey's HSD test was carried out after obtaining the least-square means for a linear model fitting the data and no significant differences were found at any time point. Data are representative of two independent experiments, n = 18.

mutant plants, compared to wild type and *aha2* (Fig. 6.5A). Plant height was decreased in *aha1*, but unchanged in *aha2* (Fig. 6.5B). A small, but significant decrease in branch angle was found in *aha1* mutants, whereas *aha2* was not different to wild type (Fig. 6.5C). Stems of *aha1* plants were also slightly thinner than in wild type, whereas no change was detected in *aha2* (Fig. 6.5D). Taken together, these data show that loss of AHA1 function leads to several subtle changes in auxin-related shoot phenotypes.

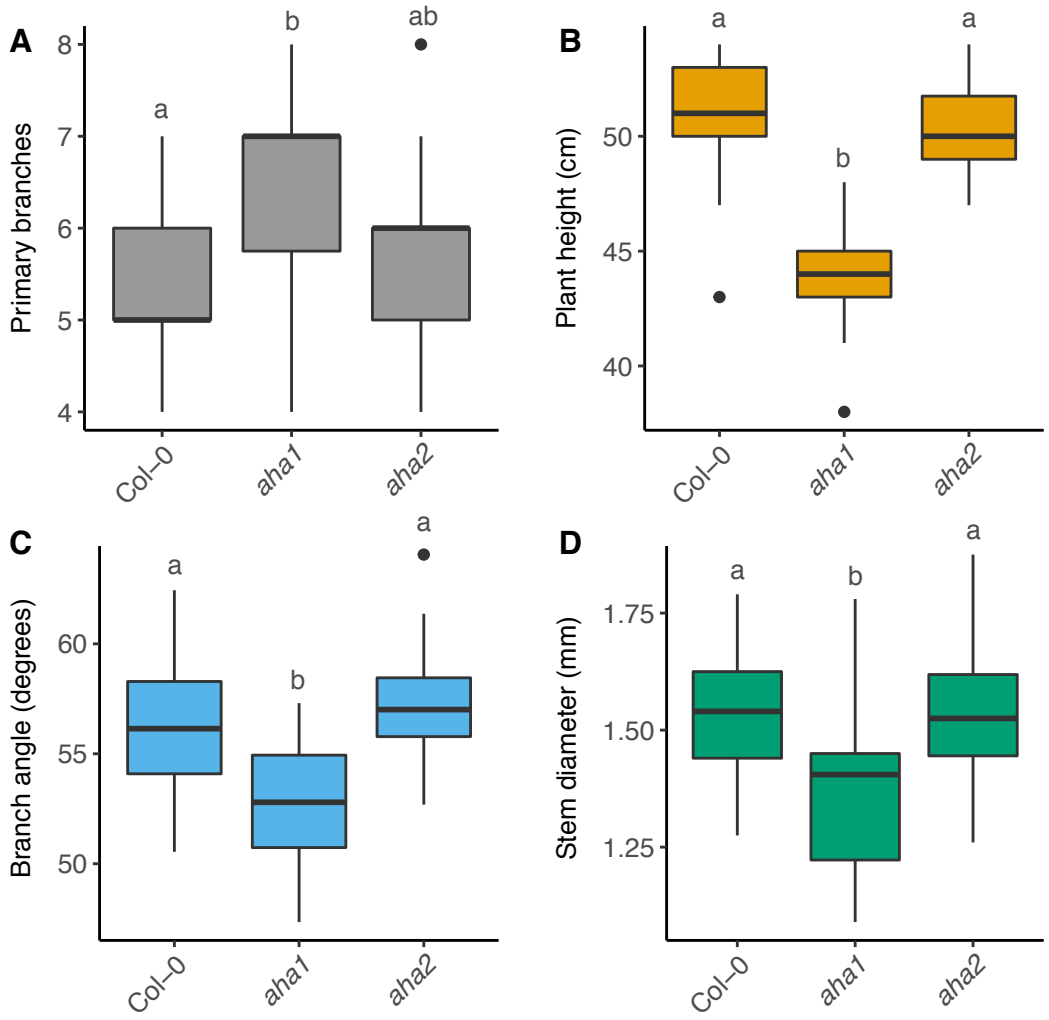

Fig. 6.5 Shoot phenotypes in *aha1* and *aha2* mutants.
(A) Primary branch number of plants grown under long days, scored at terminal flowering. **(B)** Plant height at terminal flowering. **(C)** Branch angle at terminal flowering. **(D)** Stem diameter at terminal flowering. Tukey's HSD test was carried out after obtaining the least-square means for a linear model fitting the data and different letters indicate statistically significant results at $p < 0.05$. Data are from a single experiment, n = 22-24. The wild type data are the same as presented in Fig. 4.12A.

The branching phenotype of *aha1* single mutants is subtle. It is possible that loss of H^+-ATPase activity would be more pronounced in a background with increased active auxin transport. To test this, the *aha1* and *aha2* mutants were crossed into the *d14* and *max4* strigolactone mutant backgrounds, which have high levels of auxin transport due to reduced PIN1 removal from the plasma membrane (Shinohara et al., 2013). Consistent with earlier data (Fig. 6.5A), the number of primary branches was increased in the *aha1* mutant, whereas branching was unchanged in *aha2* mutant plants (Fig. 6.6A). Interestingly, loss of AHA1 function strongly reduced branching in *d14* and *max4* mutant backgrounds (Fig. 6.6A, C). Branching in *aha2d14* and *aha2max4* was unchanged compared to *d14* and *max4*, respectively (Fig. 6.6A, C).

The *aha1* mutation also appeared to affect rosette leaf shape. Leaf blades of *aha1* plants appeared to be shorter and narrower than wild type leaves, and this was also visible in the *d14* and *max4* mutant backgrounds (Fig. 6.6B). The *aha2* mutations did not appear to affect leaf shape in any of the tested backgrounds (Fig. 6.6B). These data show that loss of AHA1 can lead to an increase or a decrease in branching, depending on the genetic background.

6.3 Summary

- AHA1 activity contributes to stem auxin transport.
- Basal PIN1 expression levels are unaffected by AHA1 in the stem.
- Auxin accumulation is impaired in *aha1* mutants.
- Rosette bud activation is increased in *aha1* mutants.
- Loss of AHA1 reduces branching in strigolactone mutants.

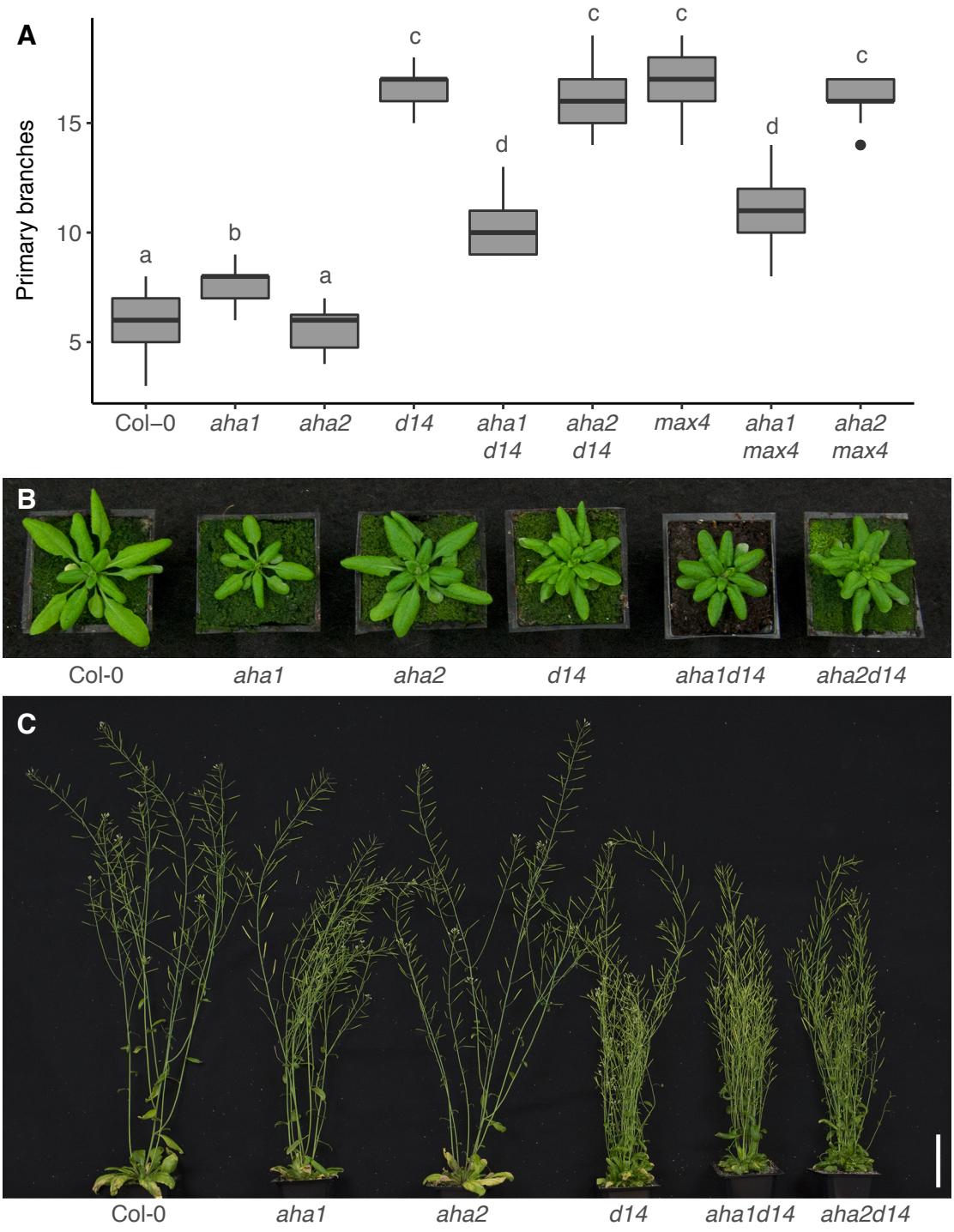

Fig. 6.6 Shoot branching in strigolactone mutants lacking AHA1/AHA2 function.
(A) Primary branch number of plants grown under long days, scored at terminal flowering. Tukey's HSD test was carried out after obtaining the least-square means for a linear model fitting the data and different letters indicate statistically significant results at $p < 0.05$. Data are representative of two independent experiments, n = 22-24. **(B)** Photographs of 4-week old plants grown under long days. **(C)** Photograph of representative plants of a subset of genotypes from **A**, bar = 50 mm.

Chapter 7

Discussion

7.1 Shoot branching and polar auxin transport

Growing shoot tips are able to communicate with each other, affecting each other's growth. This is clearly illustrated by apical dominance, where the main growing shoot is able to inhibit the outgrowth of buds in the leaf axils below it. Removal of the main shoot leads to activation of these buds, resulting in the growth of branches. For over 80 years it has been known that the plant hormone auxin plays a crucial role in this process, since auxin is able to imitate the inhibitory effect of the growing shoot tip (Thimann et al., 1934). Auxin is produced in the young, expanding leaves of the shoot tips and transported down the stem towards the root in the polar auxin transport stream (PATS). The polar manner in which auxin is transported has long been recognised (Went, 1928) and it has been observed in many different plant species by applying exogenous radiolabelled auxin to stem segments and tracking its movement (reviewed in Goldsmith, 1977). A crucial contributing factor to the polarity of auxin transport is the requirement for active export of auxin from the cell (Raven, 1975; Rubery and Sheldrake, 1974).

7.1.1 Polar auxin transport in the stem

Active auxin export is mediated by auxin efflux proteins, to which the PIN-FORMED (PIN) family in Arabidopsis make an important contribution. The PIN proteins give directionality to the auxin transport, because they are often localised in a polar manner (Chen et al., 1998; Gälweiler et al., 1998; Luschnig et al., 1998; Muller et al., 1998). In the stem, polar auxin transport is strongly associated with the vascular cambium and xylem parenchyma cells (reviewed in Goldsmith, 1977). The PIN1 protein accumulates to high levels in these tissues and is basally localised on the plasma membrane facing the root (Bennett et al.,

2006; Gälweiler et al., 1998). Polar auxin transport is significantly reduced in *pin1* mutants, indicating that the PIN1 protein plays a major role in the PATS (Fig. 3.2; Bennett et al., 1995; Okada et al., 1991). Addition of pharmacological inhibitors to wild type stems can reduce polar auxin transport to a greater extent than seen in *pin1* stems (Fig. 3.2; Bennett et al., 1995; Okada et al., 1991), suggesting that there are other auxin export proteins contributing to stem auxin movement. However, until recently little was known about the contribution of different auxin export proteins to auxin transport in the stem and generally PIN1 has been viewed as the main contributor through its major role in the PATS.

7.1.2 Stem auxin transport is multimodal

Much of the understanding of polar auxin transport, including in stems, comes from following the movement of radiolabelled auxin pulses in isolated plant segments. Early work in maize coleoptiles shows that an auxin pulse only moves basipetally and that it broadens as it moves through the sample (Goldsmith, 1967). This already suggests that, at least in maize coleoptiles, basipetal auxin movement does not occur with linear kinetics. If this were the case, it would be expected that an auxin pulse would retain its shape as it travels down the coleoptile. Modelling of these coleoptile data supports this non-linearity, because when the auxin transport network is represented as a single channel, the model poorly fits the data and is unable to capture the broadening observed experimentally (Mitchison, 2015). Instead, the modelling predicts that there must be exchange between a strong PATS channel and at least one additional auxin transporting channel in order to approximate the experimental data (Mitchison, 2015). Auxin pulses applied to Arabidopsis stems show an even more extreme dampening and broadening as the pulse moves through the segment (Fig. 3.4A; Bennett et al., 2016a; van Rongen, 2013). Direct measurements of endogenous auxin exported from the basal end of the stem are consistent with this. Here, auxin initially emerged from the base of freshly harvested stem segments at a high rate, but this rate is reduced progressively post harvesting, even though some auxin continues to drain. Furthermore, auxin continues to emerge for many hours, suggesting that while some auxin moves rapidly through the stem, there is also a pool of slower moving auxin (Bennett et al., 2016a). A computational framework was developed to further understand these auxin transport dynamics (Bennett et al., 2016a). The dynamics of the auxin pulse profiles, as well as the auxin drainage profiles were best captured in a model that included a high-conductance polar channel (such as the PATS), combined with a more widespread low-conductance and less polar channel, and third a non-polar channel (Bennett et al., 2016a). The inclusion of the third channel made only a modest improvement to the ability of the model to match the auxin transport data, but exchange of auxin between a high capacity high polarity transport route, and a lower

capacity less polar route was essential. This second route was termed connective auxin transport (CAT), since it is through CAT that auxin can be exchanged between the PATS and surrounding tissues, including axillary buds (Bennett et al., 2016a).

7.1.3 PIN3/PIN4/PIN7 contribute to connective auxin transport

Exchange of auxin between the PATS and its surrounding tissues is unlikely to be substantially mediated by PIN1, since the localisation of PIN1 is mainly restricted to the PATS (Gälweiler et al., 1998). This suggests that other auxin exporters may play a role in auxin exchange between these tissues. In accordance with this, other PIN proteins are expressed in the Arabidopsis stem, most notably PIN3, PIN4 and PIN7 (Bennett et al., 2016a; Boot et al., 2016). The expression domains of these proteins overlap with PIN1, but differ from it in two important ways. First, these PINs can be found in a much broader range of tissues in the stem than PIN1 and second, whereas PIN1 is predominantly basally localised and is highly polar, these PINs also accumulate on the lateral membranes of the cell and are in general less polar (Bennett et al., 2016a). As such, it is plausible that these PINs contribute to CAT. Consistent with a role in stem auxin transport, *pin3pin4pin7* mutant stems show a reduction in bulk auxin transport (Fig. 3.1). Importantly, the auxin transport dynamics in *pin3pin4pin7* are altered (Fig. 3.4A). If an auxin pulse is applied and left to progress through the stem for one hour, a proportion of the auxin moves slower through the stem than in wild type, whereas another proportion moves faster. These data are consistent with a reduced exchange of auxin between the PATS and CAT. Auxin already in the PATS is less likely to move out of it, due to the absence of PIN3, PIN4 and PIN7 and therefore it continues to move efficiently down the stem. Auxin in the surrounding tissues will move less efficiently, since auxin transport is less polar and of lower capacity, and it will be less efficiently transferred into the PATS. This results in a spreading and biphasic auxin distribution, compared to wild type. These observations can be captured using the same computational model used to simulate the wild type pulse dynamics. The *pin3pin4pin7* auxin pulse data were best captured if the permeability of the lateral membranes in each channel was lowered, thereby reducing the exchange of auxin between the channels (Bennett et al., 2016a).

7.2 Connective auxin transport allows communication between tissues

Auxin exchange is of particular relevance to understanding the control of shoot branching. The auxin transport canalisation model for shoot branching control proposes that buds need

to establish efficient auxin export into the main stem in order to activate and that this process occurs through auxin transport canalisation. The process of auxin transport canalisation is dynamic, involving auxin flowing from a source towards a sink upregulating and polarising its transport. This process provides a possible mechanism for the observation that buds on opposite sides of the stem are able to inhibit each other's growth and are able to do so despite exporting auxin into different vascular bundles (Ongaro et al., 2008; Snow, 1929). Because the PATS is limited to the vascular bundles, it is unlikely to be the only contributor to the process of auxin transport canalisation out of the bud. There is no expression of PIN1 in the peripheral regions of the stem and it is relatively slow to polarise and accumulate in the path from the bud apex to the PATS (Prusinkiewicz et al., 2009). Results in pea show that canalisation of PIN1 (PsPIN1) during bud activation can occur (Balla et al., 2011). In this study PsPIN1 marked channels between the bud and the stem become increasingly more polarised after decapitation of the apex. Polarised PsPIN1 is described as early as 6 hours post decapitation, and appears to be independent of transcription. Furthermore, export of radiolabelled auxin from axillary buds coincides with the polarising behaviour of PsPIN1 (Balla et al., 2011). The reported localisation data were obtained using an anti-*Arabidopsis*-PIN1 antibody, justified by homology between Arabidopsis *PIN1* and *PsPIN1*. However, recent data show that the phylogeny of the PIN1 clade in angiosperms is more complex than initially thought, with a closely related *Sister-of-PIN1* (*SoPIN1*) clade present in many angiosperms, including the Fabaceae family to which pea belongs (O'Connor et al., 2014). Furthermore, the anti-*Arabidopsis*-PIN1 antibody is polyclonal, raising the possibility that the different specificities of the antibodies might detect other PIN proteins, given the similarities in protein structure of the PINs. Nevertheless, these observations demonstrate that PINs are responsive to decapitation and are able to polarise during axillary bud activation.

7.2.1 PIN3/PIN4/PIN7 are required for rapid bud activation

The positive feedback between auxin flux and polarisation of active auxin transport is a crucial contributing factor in the process of canalisation, because it enables small fluxes of auxin to drive auxin transport canalisation (Sachs, 1981). In the context of shoot branching, if a bud is less able to export its auxin, it would negatively affect its ability to polarise auxin transport from the bud. This would affect its ability to successfully compete for outgrowth with other buds. The CAT plays an important role in mediating auxin exchange between the PATS and its surrounding tissues (Section 7.1.3), which connect the bud and the stem. While PIN1 is expressed in the PATS, PIN3, PIN4 and PIN7 accumulate in the stem periphery between the bud and the main stem PATS (Bennett et al., 2016a). As such these PINs may contribute more to the initial movement of auxin from the bud across the stem, aiding the bud

in canalising its auxin transport. In accordance with this, buds in the *pin3pin4pin7* mutant activate slowly following decapitation (Fig. 4.1B), which is expected if auxin transport canalisation is compromised. Further support for the slow activation of *pin3pin4pin7* comes from the bud activation dynamics of single, isolated, cauline buds. Compared to wild type, single *pin3pin4pin7* buds take around one day longer to activate, following release from inhibition by decapitation (Fig. 4.1C, D). This is consistent with a reduced ability to establish efficient auxin export from the bud towards the PATS, which is required for sustained growth.

7.2.2 PIN3/PIN4/PIN7 mediate bud-bud communication

The reduced ability of *pin3pin4pin7* buds to establish efficient auxin export is expected to have implications for their ability to compete for outgrowth, since this depends on access to the PATS (Prusinkiewicz et al., 2009). Bud competition relies on cross-stem communication, because buds vascularise into discrete vascular bundles and are thus unlikely to communicate directly through the PATS (Ongaro et al., 2008). Auxin exchange between the PATS and its surrounding tissues, as well as CAT-mediated cross-stem transport, may therefore be particularly important to communicate auxin status across the stem. Consistent with this, the movement of auxin across the stem is altered in *pin3pin4pin7* mutants (Bennett et al., 2016a). Movement of auxin across the stem can be measured by apically applying radiolabelled auxin to only half of the stem, by removing half of the stem at the stem apex (Bennett et al., 2016a). Cross-stem auxin movement can then be determined by measuring the basal accumulation of radiolabel at the opposite end of the stem. Significant amounts of auxin can still be recovered at the opposite side of the stem to the site of auxin application in wild type stems, consistent with appreciable movement of auxin across the stem tissues (Bennett et al., 2016a). In the *pin3pin4pin7* triple mutant bulk auxin transport is reduced (Fig. 3.1), but cross-stem movement of auxin in *pin3pin4pin7* stems is proportionally increased, compared to wild type (Bennett et al., 2016a). This may seem counter-intuitive if PIN3, PIN4 and PIN7 mediate cross-stem transport. However this can be explained by considering the role of these PINs in mediating exchange between the PATS and the surrounding tissues, such that in the triple mutant auxin is retained in the CAT domain, but can still move slowly down the stem due to the activity of other transporters (Bennett et al., 2016a).

Consistent with a role in mediating auxin transport across the stem, communication between *pin3pin4pin7* buds is impaired (Fig. 4.2). If two wild type buds on isolated stems are left to compete with each other for outgrowth, often one bud will grow to form a branch, inhibiting the outgrowth of the other (Fig. 4.2; Ongaro et al., 2008). In *pin3pin4pin7* mutants this inhibition is reduced, with both buds growing rapidly, consistent with reduced communication between the buds (Fig. 4.2).

7.3 Additional contributors to connective auxin transport

As discussed above, connective auxin transport is important for communication between shoot apices and contributes to the regulation of shoot branching. It is probable that, apart from PIN3, PIN4 and PIN7, other auxin export proteins also contribute to CAT. Likely candidates may be found in a class of non-PIN auxin transport proteins, the B-subfamily of ATP-binding cassette (ABC) transporters, since members of this class are known to affect stem auxin transport. ABCB proteins are able to transport various substrates across the plasma membrane and can function in uptake and export through the multiple transmembrane domains of the proteins. ATP provides energy for this process. ABCB proteins contain two cytoplasmic ATP-binding domains that bind and hydrolyse ATP to energise the movement of substrates. ABCB1 and ABCB19, two closely related homologues, appear to be particularly important since polar stem auxin transport is strongly reduced in *abcb1abcb19* double mutants (Noh et al., 2001). A possible explanation for the extreme reduction in polar auxin transport might lie in the interaction between ABCB19 and PIN1. Loss of ABCB19 in hypocotyls disrupts basal accumulation of PIN1, resulting in an increase in lateral auxin conductance (Noh et al., 2003). This is associated with defects in growth responses. For example, *abcb19* mutant plants display faster and stronger gravitropic responses and enhanced phototropism (Noh et al., 2003). ABCB1 and ABCB19 co-localise strongly with PIN1 in the root (Blakeslee et al., 2007). Further data presented suggest that ABCB19 also co-localises with PIN1 in the hypocotyl (Blakeslee et al., 2007), but these data are less clear. Nevertheless, ABCB19 appears to be able to interact with PIN1, since ABCB19 protein co-immunoprecipitates with PIN1 (Blakeslee et al., 2007). A possible function of this protein-protein interaction could be that ABCB19 stabilises plasma membrane microdomains that enhance the auxin export activity of PIN1 (Titapiwatanakun et al., 2009). However, PIN1 action does not strictly require ABCB1/ABCB19 function, since overexpression of PIN1 in *abcb1abcb19* roots still affects root gravitropism (Petrasek et al., 2006).

The expression domain of ABCB19 in the stem is much broader than that of PIN1, with ABCB19 expressed across almost all stem tissues (Bennett et al., 2016a). Interestingly, ABCB19 localisation in the stem is across all cell membranes, suggesting it may contribute to non-polar movement of auxin across the stem (Bennett et al., 2016a).

7.3.1 ABCB1 and ABCB19 contribute to stem auxin transport

Despite the predominantly non-polar localisation of ABCB1 and ABCB19 (Bennett et al., 2016a; Blakeslee et al., 2007; Geisler et al., 2005; Wu et al., 2007), loss of both ABCBs severely compromises polar movement of auxin in the stem, by up to 70 % (Fig. 3.8A; Bennett

et al., 2016a; Noh et al., 2001). Loss of ABCB19 alone has been reported to result in around 40-50 % less stem auxin transport than wild type (Noh et al., 2001). Given the overlap in expression domain of ABCB19 and PIN1 in the stem (Bennett et al., 2016a), it is possible that in the *abcb19* mutant, and to a greater extent in the *abcb1abcb19* double mutant, PIN1 is destabilised, resulting in a strong reduction in bulk auxin transport. However, the data on PIN1 localisation in *abcb* stems presented here do not seem to support this (Fig. 3.9A). Basal PIN1 levels in the *abcb1* mutant are reduced compared to wild type, but no difference is observed in the *abcb19* mutant and PIN1 does not appear to be destabilised in these tissues (Fig. 3.9B). The tissues used here are more mature than those used for the published stem auxin transport defects (Noh et al., 2001), so it is possible that effects on PIN1 localisation are only prevalent in younger tissues. Furthermore, it is also possible that there is functional redundancy between ABCB1 and ABCB19 in this process.

The reported strong reduction in polar auxin transport in *abcb19* inflorescences (Noh et al., 2001) was less obvious in the experiments presented here. A consistent reduction could only be observed in *abcb19* mutant stems when auxin transport was measured over longer time periods (Fig. 3.9C). In the standard assay where transport is measured over a 6-hour period, *abcb19* mutants did not always show significant differences in polar stem auxin transport, compared to wild type (Fig. 3.8A). The modest effect of *abcb19* on stem auxin transport is further exemplified by the auxin pulse data, where no differences are detected between *abcb19* mutants and wild type (Fig. 3.10). It is likely that other auxin transporters are able to compensate for the loss of ABCB19.

It seems that, at least in combination, ABCB1 and ABCB19 make a substantial contribution to polar auxin transport in the stem (Fig. 3.8A). Meaningful interpretation of these data is difficult because of the phenotype of the double mutant (Fig. 4.8D; Noh et al., 2001). The reduction in stem auxin transport could be a direct result of the loss of auxin transport proteins, but altered stem anatomy may also contribute, or both. Furthermore, comparisons between the double mutant and other genotypes are problematic. Given the short length of the internode, stem segments used for auxin transport measurements span multiple nodes, where normally this is measured within a single, basal internode.

7.3.2 ABCB1 and ABCB19 may contribute to rapid bud activation

The strong combined effect of ABCB1 and ABCB19 has also been implicated in shoot branching, based on the higher number of secondary inflorescences observed in mature *abcb1abcb19* double mutants (Noh et al., 2001). This phenotype was attributed to a reduction of apical dominance, presumably caused by reduced auxin export from active apices (Noh et al., 2001). If apical dominance is causative for the bushy appearance of *abcb1abcb19*

mutants, then this should be detectable at early stages of development, which was not the case (Fig. 4.8D). Furthermore, removal of the primary shoot apex should lead to profuse branching. However, upon decapitation, *abcb1abcb19* double mutants activate fewer buds than wild type and the buds that do activate do so more slowly (Fig. 4.8A). There appears to be a synergistic effect of *abcb1* and *abcb19*, since bud activation is not different from wild type in the single mutants (Fig. 4.8A). Some caution is needed in interpreting these results since the double mutants formed significantly fewer leaves than wild type and also had significantly more empty axils, suggesting that axillary bud formation is impaired in this mutant (Fig. 4.8B). Nonetheless the slow activation of buds is striking and suggests that ABCB1 and ABCB19 could regulate bud outgrowth by contributing to the initial flow of auxin from the bud towards the stem. Consistent with this idea, ABCB19, at least, is expressed in the stem periphery (Bennett et al., 2016a).

These results appear to be inconsistent with the previously reported bushy phenotype, but the bushy phenotype was reported to occur late into development and quantification was absent (Noh et al., 2001). It is likely that this phenotype is an indirect effect of the low fertility of the double mutant, which is expected to delay senescence and reduce auxin supply from developing seeds (Hensel et al., 1994).

7.3.3 ABCB19 mediates bud-bud communication

The slow activation of *abcb1abcb19* buds upon decapitation raises the question whether these proteins could mediate communication between buds. If so, then bud-bud communication between two isolated buds is expected to be impaired, in a similar way as observed for the *pin3pin4pin7* mutant (Fig. 4.2, Section 7.2.2). However, the strong reduction in internode length of the *abcb1abcb19* double mutants did not allow collection of suitable two-node material.

Although the *abcb1* and *abcb19* single mutants did not show any defects in bud activation (Fig. 4.8A), the subtle effects of *abcb19*, at least, on stem auxin transport, combined with the expression domain of ABCB19 in the stem periphery and the synergistic effects observed in *abcb1abcb19* double mutants, suggest that ABCB19 could contribute to communication between buds. Consistent with this, competition between two isolated buds is reduced in *abcb19* mutants (Fig. 4.8C).

7.3.4 PIN3/PIN4/PIN7 and ABCB19 can act synergistically in shoot branching control

The data discussed so far suggest that PIN3, PIN4 and PIN7 contribute to connective auxin transport and that these PINs play an important role in mediating both bud activation and bud-bud communication. Similarly, ABCB19 appears to have a modest effect on stem auxin transport and clearly affects bud-bud communication. Thus it appears that the PINs and ABCB19 have partially overlapping roles in the regulation of shoot branching. Both the PINs and ABCB19 are expressed in the tissues surrounding the PATS. Therefore it could be that they have a synergistic effect on auxin exchange between the PATS and its surrounding tissues. The bulk auxin transport data of the *abcb19pin3pin4pin7* mutant does not seem to support this (Fig. 3.11). Polar auxin transport in the quadruple mutant is reduced, but to the same extent as in the *pin3pin4pin7* triple mutant, suggesting that loss of ABCB19 does not exacerbate the stem auxin transport defect of the PIN triple mutant. It should be noted that the bulk auxin transport experiments do not provide information on the dynamics of auxin movement. It will be useful to assess this by following the progression of an auxin pulse and measuring cross-stem auxin transport in the *abcb19pin3pin4pin7* mutant.

An overlapping role for PIN3, PIN4, PIN7 and ABCB19 in the regulation of shoot branching is supported by the synergistic effect of these transporters on bud activation dynamics following decapitation (Fig. 4.11). Plants lacking ABCB19 activate their rosette buds normally, whereas plants lacking PIN3, PIN4 and PIN7 activate their rosette buds slowly (Fig. 4.1B, 4.8A). However, loss of all four transporters has a profound effect on the ability of rosette buds to activate, demonstrated by the severely reduced bud activation in the *abcb19pin3pin4pin7* mutant (Fig. 4.11). To provide an explanation for these observations, it is important to consider the possible effects the loss of these proteins could have on auxin transport canalisation. The ABCB19 protein is widely expressed throughout the shoot (Bennett et al., 2016a) and could be regarded as a general auxin efflux carrier, which exports auxin at a basal level (Sieberer and Leyser, 2006). In *abcb19* single mutants the basal level of auxin transport is thus reduced, but this would have little effect on the overall balance of the auxin transport network. Since PIN3, PIN4 and PIN7 are still present in the *abcb19* mutant, an initial flux of auxin from the bud towards the stem would ensure wild-type-like bud activation. In the *pin3pin4pin7* mutant bud activation is slow because this initial auxin flux is impaired, but *pin3pin4pin7* buds are still able to activate eventually, presumably because they can still export auxin through other auxin transport proteins, such as ABCB19. If ABCB19 is predominantly involved in the CAT, then auxin movement between the bud and the stem is likely increasingly impaired in the *abcb19pin3pin4pin7* mutant auxin movement. If so, then it is expected that *abcb19pin3pin4pin7* single buds will activate slowly, additively

to the delay in activation observed in *pin3pin4pin7* (Fig. 4.1C). Another possibility is that, instead of affecting CAT, ABCB19 is more important for driving auxin export away from the bud apex. This could lead to synergistic effects on bud activation, without any additive effects on bulk auxin transport. These possibilities remain to be investigated.

The PIN3/PIN4/PIN7 and ABCB19 proteins all contribute to bud-bud communication and, in accordance with this, bud-bud competition in both *pin3pin4pin7* and *abcb19* mutant explants is essentially abolished (Fig. 4.2B, 4.8C). Because of this, it is not possible to assess synergistic interactions between these mutations, and unsurprisingly bud-bud competition in the quadruple mutant does not differ significantly from the *pin3pin4pin7* and *abcb19* mutants (Fig. 4.11C).

Despite the clear effects of PIN3, PIN4, PIN7 and ABCB19 on bud outgrowth responses, little effect is observed in intact plants. Primary branching in *pin3pin4pin7*, *abcb19* and *abcb19pin3pin4pin7* mutant plants is comparable to wild type when plants are grown under long day conditions (Fig. 4.12). Increasing the number of nodes, by growing plants under short day conditions for 4 weeks prior to shifting to long day growth conditions, does not lead to observable branching differences in the *pin3pin4pin7* background, compared to wild type (Fig. 5.2). In *abcb19* mutants branching appears to be significantly reduced, if directly compared to wild type (see Section 5.2). Whether branching in *abcb19pin3pin4pin7* mutant plants is further reduced under these growth conditions remains to be tested.

7.3.5 Auxin importers contribute to stem auxin transport

Auxin movement and exchange of auxin across the stem depends on efficient cell-to-cell transport, which is at least in part mediated by PIN3, PIN4 and PIN7 auxin exporters. Efficient cell-to-cell movement has also been suggested to rely on active import of auxin into the cell. Even though protonated IAA is able to freely cross the plasma membrane, active auxin import has been argued to be play a dominant role in auxin influx (Kramer and Bennett, 2006). Consistent with this, the AUX1 auxin influx carrier dominates the auxin uptake into Arabidopsis protoplasts, whilst diffusive influx of auxin appears to be negligible (Rutschow et al., 2014). AUX1 can also mediate auxin uptake in *Xenopus* oocytes and this uptake is both saturable and pH dependent (Yang et al., 2006). AUX1 is part of a four-member gene family in Arabidopsis, along with LAX1-LAX3. Most of the research on AUX1/LAX auxin importers has focussed on root growth, where, for example AUX1 strongly affects root gravitropism (Bennett et al., 1996).

Auxin importers do appear to play a role in the development of the inflorescence. Vascular bundle formation is reduced in the *aux1lax1lax2lax3* mutant (Fabregas et al., 2015). This effect is only observed if plant longevity is increased by growth under short day conditions,

whereas plants grown under long days develop normal vascular bundles (Fabregas et al., 2015). Furthermore, the effect is not observed under either growth condition in the *aux1* single mutant (Fabregas et al., 2015). AUX1/LAX proteins are expressed in inflorescence stems, with AUX1, LAX1 and LAX2 expression visible in procambial and protoxylem cells of long-day-grown plants and LAX3 expression in the phloem (Fabregas et al., 2015). However, these data are from transverse sections, making it difficult to accurately assess the localisation pattern on the plasma membrane. Analysis of an *AUX1-YFP* reporter construct in longitudinal stem segments shows that AUX1 is non-polarly expressed in the vascular bundles, in a domain that is broader than PIN1 but less broad than PIN7 (Dr. T. Bennett, pers. comm.). This suggests that AUX1 could mediate some aspects of auxin transport in the PAT/CAT streams.

The contribution of AUX1/LAX import proteins to stem auxin transport has been recently explored by fitting mathematical models to experimental data (Boot et al., 2016). In these experiments, auxin from a donor well was allowed to progress through an isolated stem segment in an apical to basal direction and collected in a receiver well. In these experiments the basal accumulation of auxin in the receiver well was strongly reduced for the *aux1lax1lax2lax3* quadruple mutant, as was the transport capacity in the mutant (Boot et al., 2016). Consistent with this, bulk auxin transport through *aux1* and *aux1lax1lax2lax3* mutant stems is reduced (Fig. 3.12). Further support for a role of AUX1/LAX in stem auxin transport comes from the auxin uptake experiments (Fig. 3.13). The cumulative amount of auxin entering the stem during the experiment is significantly reduced in the *aux1* and *aux1/lax* mutants (Fig. 3.13B), suggesting a reduction in uptake of auxin. However, this is apparently not caused by defects in initial auxin uptake, because the most apical segment in contact with the radiolabelled buffer solution in *aux1* and *aux1/lax* mutants accumulates auxin to a similar extent as wild type (Fig. 3.13D, segment 1). This was also observed in the donor-receiver transport assays conducted with the *aux1/lax* mutant, where auxin was still able to move from the donor well into the apical part of the stem segment (Boot et al., 2016). It is possible that auxin uptake at the cut surface does not require AUX1/LAX and that auxin diffuses freely into the uppermost cells. However, AUX1/LAX are clearly required for efficient further transport down the stem, since basal accumulation is impaired in the *aux1* and *aux1/lax* mutants, both in absolute and relative terms (Fig. 3.12, 3.13C). This is in accordance with the reported reduction in auxin transport capacity of the *aux1lax1lax2lax3* (Boot et al., 2016). Interestingly, the *aux1lax1lax2lax3* mutant did not show any apparent changes in the velocity of auxin transport in the donor-receiver transport experiments (Boot et al., 2016). It will be useful to further explore these dynamics using auxin pulse assays.

7.3.6 Auxin importers are unlikely to be regulators of bud activation

The reduced auxin transport capacity observed in the *aux1* and *aux1/lax* mutants raises the possibility that auxin importers might affect bud outgrowth. A possible mechanism for how auxin importers would accomplish this could be through regulating the efficiency at which auxin is able to reach the PATS or CAT tissues. Assessing bud outgrowth in *aux1/lax* mutants can be challenging. Axillary bud formation in the *aux1lax1lax2* triple mutant is strongly impaired (Wang et al., 2014a). Consistent with this, *aux1lax1lax2lax3* quadruple mutants also display strong defects in axillary bud formation (Fig. 4.13B). A substantial proportion of rosette leaf axils and cauline leaf axils are empty, which makes it difficult to assess bud outgrowth. The reduced activation of rosette branches in the *aux1lax1lax2lax3* quadruple mutant (Fig. 4.13A) could be the result of decreased activation or the reduced number of buds available for outgrowth, or both. The *aux1* single mutant shows no apparent defects in axillary bud formation (Fig. 4.13B) but has a significant effect on auxin transport through stems (Fig. 3.12), making this a more suitable line for assessing the contribution of auxin import to shoot branching control. The branching response following decapitation as well as branching under standard long day growth conditions show no difference between *aux1* and wild type plants, suggesting that the AUX1 protein does not play an important role in mediating bud outgrowth (Fig. 4.13A, 4.13C).

As mentioned above, the AUX1 protein is expressed non-polarly in a domain that extends beyond that of PIN1. It is therefore possible that it contributes to efficient cross-stem movement of auxin. If this were the case, a reduction in communication across the stem would be expected in *aux1* mutants. However, *aux1* two-node explants were able to compete effectively for outgrowth (Fig. 4.13D), suggesting that AUX1-mediated auxin import does not contribute to bud-bud communication. It is interesting to note that a clear reduction in bulk auxin transport caused by auxin import defects, as observed in the *aux1* single mutant (Fig. 3.12), does not appear to have any effect on bud activation. In contrast, a comparable reduction caused by auxin export defects, as observed in the *pin3pin4pin7* mutant (Fig. 3.1A), does lead to branching defects. Whether this has implications for understanding auxin transport canalisation remains to be tested.

7.4 Regulation of shoot branching by strigolactone

Strigolactones are central to understanding the role of auxin transport canalisation in shoot branching control. Buds compete for access to the auxin transport stream of the stem, thereby affecting each other's ability to activate (Bennett et al., 2006; Crawford et al., 2010; Prusinkiewicz et al., 2009; Shinohara et al., 2013). In this context strigolactones modulate the

competition between buds. Competition between buds is impaired in strigolactone mutants and effects of PIN1 accumulation on the plasma membrane can at least in part explain this. In strigolactone mutants PIN1 overaccumulates on the plasma membrane of xylem parenchyma cells in the PATS (Bennett et al., 2006; Crawford et al., 2010; Shinohara et al., 2013). Strigolactone triggers the rapid depletion of PIN1 from the basal plasma membrane of xylem parenchyma cells. This process is independent of protein synthesis, but is dependent on clathrin-mediated membrane trafficking (Shinohara et al., 2013). Thus the increased accumulation of PIN1 in strigolactone mutants is likely the result of a decrease in PIN1 removal from the plasma membrane. This decrease in the removal of PIN1 from the plasma membrane affects the ability of strigolactone mutant buds to activate in at least three ways. First, the increased PIN1 levels lead to higher levels of stem auxin transport which, despite the higher levels of auxin in strigolactone mutant stems (Prusinkiewicz et al., 2009), could make the stem a better sink because more PIN1 protein is available to transport auxin towards the root. Second, the increased levels of PIN1 protein in the bud can influence the source strength, since more auxin exporter protein is available to export, and canalise, auxin from the bud towards the stem. Third, the decreased removal of PIN1 could contribute to increased feedback between auxin flux and auxin transport, making it easier for buds to canalise their auxin transport into the main stem. Combined, this enables strigolactone mutant buds to activate more easily than wild type buds. Consistent with this mode of action, strigolactone acts to enhance competition between growing shoot apices, rather than straightforwardly inhibiting the growth of buds (Crawford et al., 2010).

7.4.1 Stem auxin transport in strigolactone mutants

The reduced removal of basal PIN1 in strigolactone mutants clearly leads to an increase in stem polar auxin transport, but it was less well understood what effect this has on stem auxin transport dynamics. When *max4* mutant stems are provided with a one-hour pulse of radiolabelled auxin and auxin emergence is measured over time at the basal end, the emergence profile is comparable to wild type but for each time point more auxin is collected from *max4* mutant stems (Bennett et al., 2006). This suggests that the rate of auxin movement in strigolactone mutants is unchanged. In accordance with this, the dynamics of an auxin pulse in *max2* mutants are comparable to wild type (Fig. 3.5).

In contrast to the *max4* experiment described above, the *max2* transport profiles presented here were not higher than wild type (Fig. 3.5). This difference may be explained by the difference in pulse length and experimental setup. The *max4* profiles were obtained by incubating the stems for 1 hour in radiolabelled auxin, whereas the pulse assays presented here use a 10 minute pulse. Modelling of these differences suggests that when influx of auxin

into the stem segment is a limiting factor, then only a certain amount of auxin will enter the stem segment, regardless of the genotype (Dr. G. Hines, pers. comm.). This situation might arise at short treatment durations, such as during an auxin pulse experiment. Here wild type and *max* mutant stems are expected to contain similar amounts of auxin. In contrast, if the concentration instead of influx of auxin at the apex is limiting, then the amount of radiolabelled auxin present in the stem segment is expected to depend on the rate at which auxin can be drawn from this pool of auxin and transported basally (Dr. G. Hines, pers. comm.). This situation might arise during longer treatment durations, such as during bulk auxin transport assays or long pulse applications. In these experiments the rate of export may be become limiting in wild type stems whereas in *max* mutants, which have increased accumulation of PIN1, the rate of export is less limited, resulting in increased transport.

Interestingly, the *max2* pulse dynamics can be reproduced by the computational model used to capture the pulse dynamics observed in Bennett et al. (2016a) if, in addition to increased PATS, the lateral exchange between the PATS and CAT is increased (Dr. G. Hines, pers. comm.). This suggests that the increased auxin transport in the *max* mutants depends in part on CAT activity. In accordance with this, bulk auxin transport in strigolactone mutants stems with impaired CAT is reduced (Fig. 4.3A), apparently without affecting basal accumulation of PIN1 on the plasma membrane (Fig. 4.3B). When the movement of a pulse of radiolabelled auxin is followed over time, strikingly, the pulse shape is retained much more clearly than in wild type stems, where broadening and dampening of the pulse traces is evident (Fig. 3.6B; 3.7). In comparison with the *pin3pin4pin7* pulse, where some auxin moves faster than wild type and some slower, in *max2pin3pin4pin7* a single pulse is retained. As described, according to modelling results this is consistent with a single transport mode dominating in this genotype (Bennett et al., 2016a; Mitchison, 2015). One possibility is that the increased accumulation of PIN1 increases PATS but also contributes to lateral movement of auxin, creating a wider PATS-type channel than in the wild type.

7.4.2 PIN3/PIN4/PIN7 contribute to strigolactone-mediated shoot branching control

The effects of PIN3, PIN4 and PIN7 on bud activation and bud-bud communication provide strong support for the role of CAT in bud outgrowth. The effects of CAT and auxin exchange between the PATS and CAT could affect strigolactone-mediated shoot branching in different ways. The rapid accumulation of PIN1 on the plasma membrane is predicted to make it easier for buds to canalise their auxin, leading to increased branch activation. In the *pin3pin4pin7* triple mutant bud activation following decapitation is delayed (Fig. 4.1). This is consistent

with a role of these PINs in the initial movement of auxin out of the bud into the stem, and decreased ability to canalise their auxin transport from the bud towards the stem. Consistent with this, rosette bud activation following decapitation is decreased in *max2pin3pin4pin7* and *max4pin3pin4pin7* mutants, compared to their *max* controls (Fig. 4.4A, B). Furthermore, shoot branching in intact plants is also significantly reduced in *max2pin3pin4pin7*, *max4pin3pin4pin7* and *d14pin3pin4pin7* mutants (Fig. 4.5A; 5.3A) compared to their controls, demonstrating that these PINs are required for the some of the increased shoot branching phenotype in strigolactone-deficient mutants.

Communication between adjacent *pin3pin4pin7* mutant buds is reduced, resulting in reduced competition for outgrowth, which is likely to be due to slow movement of auxin across the stem (Fig. 4.2B). Bud-bud competition in strigolactone mutants is also reduced, but this is likely to be for the contrasting reason that canalisation of auxin transport from the bud to the stem in strigolactone mutants is so rapid that there is insufficient time for bud-bud communication (Crawford et al., 2010). Loss of PIN3, PIN4 and PIN7 is thus not expected to affect bud-bud competition in a strigolactone mutant background, but addition of GR24 should still be able to restore competition. In accordance with this prediction, the competition between *maxpin3pin4pin7* mutant two-node explants was similar to that observed in the *max* and the *pin3pin4pin7* triple mutants (Fig. 4.7). Addition of GR24 was able to increase bud-bud competition in wild type, *pin3pin4pin7* and *max4pin3pin4pin7* two-nodes, but not in *max2* and *max2pin3pin4pin7* nodes (Fig. 4.7). This is consistent with the known role of MAX2 in strigolactone signalling (see Section 1.2.3). Interestingly, bud-bud competition was only partially restored in *pin3pin4pin7* and *max4pin3pin4pin7* two-node explants, compared to their controls. This highlights the importance of these PINs in cross-stem communication, because even in this highly competitive environment, where auxin transport canalisation between buds and stems is slow, buds are less able to inhibit each other. The reduced response of *pin3pin4pin7* two-node explants could arise if strigolactone affects the removal of PIN3, PIN4 or PIN7 from the basal plasma membrane, in a similar manner as with PIN1. Indeed this appears to be the case for PIN7, which shows reduced levels of basal accumulation in the stem upon treatment with GR24, whereas PIN3 and PIN4 appear to be unresponsive (F. Ticchiarelli, pers. comm.). However, this does not appear to have a major impact on strigolactone response, because whole plant responses of *pin3pin4pin7* mutants to GR24 are comparable to wild type (Fig. 4.6).

7.4.3 ABCB19 contributes to strigolactone-mediated shoot branching control

The pronounced reduction in branching in *maxpin3pin4pin7* mutants demonstrates that the mild effects of impaired CAT in wild type plants can be exaggerated in high branching backgrounds. Similar to *pin3pin4pin7*, the effects of loss of ABCB1 or ABCB19 on shoot branching are mild. Bud activation dynamics and shoot branching in intact plant is unchanged in *abcb1* and *abcb19* single mutants under long day growth conditions (Fig. 4.8; 4.9). However, as previously mentioned, ABCB19 does appear to play some role in shoot branching control, because branching in intact plants is reduced when the number of available nodes is increased (see Section 5.2). Furthermore, bud-bud communication is also impaired in the *abcb19* single mutant (Fig. 4.8C) and *abcb19* also has a synergistic effect on bud activation dynamics in the *pin3pin4pin7* mutant background (Fig. 4.11A).

Comparable to the effects observed for *pin3pin4pin7*, loss of ABCB19 in the high branching strigolactone mutant background has a much stronger effect on branching than in the wild type background, with a significant reduction in branching in *max2abcb19* and *max4abcb19* mutants, compared to their *max* controls (Fig. 4.9A). Loss of ABCB1 does not appear to affect strigolactone mutant branching (Fig. 4.9A). Given the synergistic effects of *abcb19* and *pin3pin4pin7* on bud activation dynamics after decapitation, it will be interesting to test if they also synergistically affect these dynamics in a strigolactone-deficient background.

As previously mentioned, PIN1-ABCB19 interaction might stabilise plasma membrane microdomains which enhance the auxin export activity of PIN1 (Titapiwatanakun et al., 2009; Section 7.3. Thus it is possible that loss of ABCB19 leads to destabilisation of PIN1. Although there was no obvious change in basal plasma membrane PIN1 stability in *abcb19* single mutants (Fig. 3.9) it is possible that effects are more prevalent in the strigolactone mutant background where PIN1 overaccumulates and this remains to be tested.

The reduction in branching in *maxabcb19* mutants shows that ABCB19 is involved in strigolactone-mediated shoot branching control. The mechanism through which it acts is less clear. Given its expression domain and the reduced bud-bud communication in *abcb19* single mutants, it is possible that ABCB19 contributes to CAT. However, wild type behaviour of auxin pulses (Fig. 3.10) and cross-stem auxin transport (Dr. T. Bennett, pers. comm.) in *abcb19* mutant stems suggest that ABCB19 does not affect stem auxin transport in the same manner as PIN3, PIN4 and PIN7 do. The *max2pin3pin4pin7* auxin pulse dynamics show that disrupting CAT in a high PATS background can help further the understanding of the auxin transport network in the stem (Fig. 3.6B; 3.7), especially when the observations are modelled. A similar approach for *maxabcb19* mutants might help to better understand

the differences between ABCB19 and PIN3, PIN4, PIN7 in stem auxin transport. As mentioned in Section 7.3.4, it is also possible that the effect of ABCB19 might be more related to contributions to auxin movement in the bud itself, rather than to CAT. If ABCB19 is important for driving auxin from the bud towards the stem, then it could effectively contribute to the auxin source strength of the bud. This remains to be investigated.

Plants lacking ABCB19 are still responsive to exogenous GR24 (Fig. 4.10). This is not surprising, since PIN1 is still present at wild type levels in *abcb19* (Fig. 3.9) and presumably the addition of GR24 is able to increase the rate of PIN1 removal from the basal plasma membrane in these plants, resulting in decreased branching (Fig. 4.10A). The *abcb19* single mutant produces consistently fewer branches than wild type when grown under axenic conditions (Fig. 4.10A), presumably because growth conditions are more challenging than on soil, where no obvious branching difference is found, unless the vegetative phase is extended (see Section 5.2). Interestingly, GR24 is unable to fully restore bud-bud competition in *abcb19* two-node explants (Fig. 4.10B). This is similar to the effect of GR24 on *pin3pin4pin7* bud-bud competition (Fig. 4.7). However, in the *pin3pin4pin7* mutant cross-stem auxin transport is clearly impaired (Bennett et al., 2016a), whereas it appears to be unchanged in *abcb19* mutants (Dr. T. Bennett, pers. comm.). Even so, ABCB19 is apparently needed for effective bud-bud communication. It is possible that cross-stem movement in *abcb19* mutants is only subtly altered and that its effects are not detected in the cross-stem auxin transport assay or that the effects of *abcb19* are more directly related to auxin transport from the bud, rather than the stem. A good strategy to further explore the contribution of ABCB19 on bud-bud communication would be to test bud-bud competition in *maxabcb19* mutants. However, initial internode elongation in these mutant backgrounds is slow, making it difficult to collect useable plant material to test bud-bud competition.

7.5 Providing energy for auxin transport and shoot branching

The active import and export of auxin requires energy. ABCB proteins are able to energise their own transport through ATP hydrolysis. In contrast, energy for the AUX1/LAX and PIN proteins relies on the proton motive force. The proton motive force is generated through the activity of plasma membrane H^+-ATPases, which pump protons out of the cell, resulting in a membrane potential and pH gradient across the plasma membrane, which in turn is able to energise secondary transporters, such as PIN proteins. The AUX1/LAX proteins form a sub-class within the super family of amino acid/auxin permeases, which are predicted to

rely on proton symport for their function (Young et al., 1999). Therefore, a reduction in proton movement across the plasma membrane could also reduce the ability of AUX1/LAX protein function. In addition, such a reduction in proton flux could affect the passive influx of auxin by shifting the balance between protonated IAA (IAAH) and disassociated IAA (IAA^-). However, this is unlikely to have a large effect if auxin importers are present on the plasma membrane, since they appear to contribute most of the auxin import into the cell (Rutschow et al., 2014). The activity of the H^+-ATPases thus has the potential to affect auxin transport in multiple ways.

7.5.1 AHA1 contributes to stem auxin transport

Mathematical modelling of the feedback between auxin and apoplastic pH predicts that an increased movement of protons into the apoplast results in increased carrier-mediated auxin transport rates (Steinacher et al., 2012). In accordance with this, stem auxin transport is reduced in the *aha1* H^+-ATPase mutant (Fig. 6.1A), which has impaired proton pump activity. Auxin transport rates in *aha2* mutant stems are unchanged, which corresponds well with the expression profiles for these two H^+-ATPases, since *AHA1* is more strongly expressed in developing aerial tissues than *AHA2* (Haruta et al., 2010). Although the proton secreting activity of *aha1* roots is reduced compared to wild type (Haruta et al., 2010), it is unclear whether loss of *AHA1* results in marked changes in apoplastic pH in the stem, and this remains to be tested.

Changes in proton gradients across the plasma membrane are predicted to affect both auxin import and export processes. Consistent with this, the pattern of auxin accumulation over time in *aha1* stems fed radiolabelled auxin at the apical end is complex. In wild type stems, the amount of auxin accumulates steadily over time, with auxin levels continuing to build over time at both the apical and basal ends (Fig. 6.2; 6.3). In contrast, auxin is slow to accumulate in *aha1* stems. Over time auxin does build up to levels not far below wild type, but it plateaus. This is likely due to a combination of limited transport of auxin along the stem and limited accumulation of auxin at the apex in comparison to wild type. This pattern is different from the auxin accumulation properties observed in the *aux1/lax* mutants, where total uptake during the experiment is reduced, but initial accumulation at the apical end appears unimpaired (Fig. 3.13D). Auxin accumulation in *aha1* mutant stems also appears to be affected during the short accumulation period in auxin pulse assays, where less auxin enters *aha1* mutant stems during the 10 minute pulse (Fig. 6.2B). The overall distribution of auxin broadly follows a similar profile to wild type (Fig. 6.2A), but less auxin moves along the stem such that the *aha1* and wild type profiles run largely in parallel. Thus it appears

that AHA1 is important for efficient auxin uptake into and progression along the stem auxin transport network.

In combination with the results for strigolactone mutants, these data suggest that the ability of stems to transport auxin efficiently to the basal end is dependent on both active influx and efflux. However, the amount of auxin that accumulates at the apical end of the stem is dependent more on efficient auxin efflux away from the apex than it is on efficient auxin uptake. Interestingly, it is the efficient efflux of auxin that appears to be more important for the control of shoot branching. This might be of relevance for understanding critical aspects of the bud activation process, such as the ability of auxin from young expanding leaves at the bud apex to enter the bud stem auxin transport network.

7.5.2 AHA1 affects shoot branching

An important factor affecting auxin transport canalisation is the positive feedback of auxin on its own transport. Changes to this feedback are likely to affect the balance of auxin transport canalisation and in turn, shoot branching. Proton gradients have been suggested to provide feedback on the polarisation of auxin transport in models that explore the effects of auxin-induced apoplastic acidification (Steinacher et al., 2012). A reduced proton gradient, as might be expected in mutants with impaired proton pump activity, may thus lead to changes in shoot branching. Consistent with this, branching is increased in intact *aha1* mutant plants (Fig. 6.4A; 6.5). Although intuitively it might be expected that a reduction in proton gradients would lead to a reduction in branch activation, possibly resulting from reduced auxin transport canalisation, this is not necessarily the only outcome. Increased branching can occur in at least two ways. One is in an environment where auxin transport canalisation can readily occur, such as in strigolactone mutants, where PIN1 removal is reduced (Crawford et al., 2010; Prusinkiewicz et al., 2009; Shinohara et al., 2013). The other is in a low auxin transport environment, such as observed in the *tir3* mutant, where less auxin is exported from each apex (Prusinkiewicz et al., 2009; Shinohara et al., 2013). If auxin transport canalisation from the bud is impaired, then buds may activate slower, an effect observed in the *pin3pin4pin7* mutant (Fig. 4.1). However, single *aha1* buds are able to activate normally (Fig. 6.4B), suggesting that canalisation is unaffected. Instead, it appears that the reduced auxin transport in the *aha1* mutant affects the ability of buds to inhibit each other. Consistent with this, *aha1* buds activate rapidly following decapitation (Fig. 6.4A). It will be interesting to test if this effect is also observed in the two-node explant bud-bud competition assay, where *aha1* two-nodes are expected to display reduced competition.

Shoot branching in strigolactone mutants can be reduced by changes in auxin transport, as observed in *maxabcb19* and *maxpin3pin4pin7* mutants (Fig. 4.5; 4.9). In accordance

with this, loss of AHA1 function is also able to suppress branching in strigolactone mutants (Fig. 6.6). Which aspects of the auxin transport network are affected in these mutants is currently unclear, because no information is available on auxin transport in these mutants. Reduced proton pump activity appears to affect both auxin import and export. This could have disproportionate effects on auxin transport and/or auxin transport canalisation in mutants where either of these processes is increased, such as in strigolactone mutants. How proton pump activity affects the self-organising properties of the auxin transport network in these mutant backgrounds remains to be tested.

7.6 Interaction between *BRC1* and connective auxin transport

The self-organising properties of the auxin transport network are not the only proposed mechanism for the regulation of bud outgrowth control. Outgrowth has also been suggested to occur via the regulation of *BRC1* transcription, where changes in *BRC1* result in bud outgrowth responses (Aguilar-Martinez et al., 2007; Braun et al., 2012; Dun et al., 2012). However, the recent demonstration that strong *BRC1* expression is neither necessary nor sufficient for bud inhibition casts doubts on the straightforward relationship between *BRC1* expression levels and bud outgrowth (Seale et al., 2017). Instead, *BRC1* may act more as a modulator of bud activation potential within an auxin transport-based framework of bud activation control (Seale et al., 2017). The effect of *BRC1* on bud activation potential corresponds well to bud activation patterns. Buds activate in a basipetal sequence upon floral transition, an effect likely caused by reduced auxin production and export from floral apices (Prusinkiewicz et al., 2009). In *BRC1*-deficient plants buds that remain inhibited are at the more basal end of this sequence (Aguilar-Martinez et al., 2007; Seale, 2016). Buds at the apical end activate even in the presence of high *BRC1* transcript levels (Seale et al., 2017). This suggests that buds with high levels of *BRC1* are only able to activate in an environment where auxin transport canalisation from the bud can easily occur. In contrast, inhibition of *brc1* buds is only likely to occur when canalisation conditions are inhibitory, such as when stem auxin concentrations are high (Seale et al., 2017). This raises interesting questions about the relationship between *BRC1* and auxin transport, particularly in the context of strigolactone-mediated shoot branching control.

BRC1 has been suggested to be a transcriptional target of strigolactone signalling. In agreement with this strigolactone is unable to rescue the increased branching phenotype of *brc1* mutants and *BRC1* is downregulated in strigolactone mutants (Aguilar-Martinez

et al., 2007; Braun et al., 2012; Brewer et al., 2009). However, loss of *BRC1* and its closest relative *BRC2*, which has slight additive effects on branching (Aguilar-Martinez et al., 2007), does not increase branching to the same extent as observed in strigolactone mutants. This is particularly clear in growth conditions where the number of vegetative nodes is increased (Fig. 5.2; Bennett et al., 2016b; Seale et al., 2017). Furthermore, there is also some additivity in the control of branching control *brc1brc2* and strigolactone mutants (Bennett et al., 2016b; Chevalier et al., 2014; Seale et al., 2017), and *brc1brc2* mutants retain some strigolactone response. For example, when *brc1brc2* mutant plants are grown on GR24-containing media, they still show a partial suppression of branching (Fig. 5.9; Seale et al., 2017), demonstrating that strigolactone and *BRC1* regulate shoot branching at least partially independently of each other.

7.6.1 Shoot branching control by *BRC1* is independent of PIN3/PIN4/PIN7

The partially independent mechanisms through which strigolactone and *BRC1* regulate shoot branching are further exemplified by the observation that PIN1 does not overaccumulate in *brc1* mutant stems (Bennett et al., 2016b). Consistent with this, polar stem auxin transport in *brc1brc2* mutants is comparable to wild type (Fig. 5.4; Bennett et al., 2016b). This is in contrast to shoot branching control by strigolactones, which is at least partly mediated by effects on PIN1, which correlate with increased levels of polar stem auxin transport (Fig. 5.4; Bennett et al., 2006). CAT also contributes significantly to strigolactone-mediated shoot branching control, with significant suppression of the highly branched phenotype of strigolactone mutants in the *pin3pin4pin7* triple mutant (Fig. 4.5A). In contrast, loss of PIN3, PIN4 and PIN7 does not affect shoot branching in intact *brc1brc2* mutant plants (Fig. 5.2). This is even the case when branch suppression is promoted by challenging environmental conditions such as nitrate limitation or crowding (Fig. 5.10A, B) or by addition of exogenous GR24 (Fig. 5.9).

Competition between two isolated *brc1brc2* buds has previously been shown to be reduced, but still fully sensitive to strigolactone (Seale et al., 2017). In the single experiment presented here this reduction in competition was not observed, but competition was still clearly increased upon treatment with strigolactone, to a comparable degree as in wild type (Fig. 5.8). This demonstrates that these buds were still responsive to strigolactone. Responses to GR24 in *brc1brc2pin3pin4pin7* two-node explants were indistinguishable from *pin3pin4pin7* (Fig. 5.9), consistent with the independent roles of *BRC1* and PIN3, PIN4 and PIN7 in mediating bud outgrowth. However, *brc1brc2pin3pin4pin7* two-node responses

were also not significantly different from *brc1brc2*, and further experiments are needed to clarify bud competition responses in these mutant backgrounds.

7.6.2 Shoot branching control by *BRC1* is partially dependent on ABCB19

In contrast to loss of PIN3, PIN4 and PIN7, loss of ABCB19 is able to reduce shoot branching in the *brc1brc2* mutant background (Fig. 5.5). This raises the possibility that ABCB19 acts downstream of *BRC1* to regulate shoot branching. However, the ability of *abcb19* to suppress branching in *brc1brc2* is nitrate sensitive. Loss of ABCB19 in *brc1brc2* mutant plants reduces the number of branches when nitrate availability is high (Fig. 5.10), but branching under low nitrate availability in the *brc1brc2abcb19* mutants is no different to *brc1brc2*. This argues against a simple linear pathway from *BRC1* to ABCB19. When nitrate availability is low, active shoot apices appear to export more auxin into the main stem PATS, thereby preventing the activation of more basal branches (de Jong et al., 2014). In addition, low nitrate reduces cytokinin supply from the root (Miyawaki et al., 2004; Takei et al., 2004), which could further reduce bud activation. Thus *abcb19* appears to suppress branching in *brc1brc2* mutants in a low auxin, high cytokinin environment, but not in a high auxin, low cytokinin environment. Similarly, *abcb19* cannot suppress branching in *brc1brc2* mutants where branching is reduced by treatment with GR24 (Fig. 5.9). Thus the ability of *abcb19* to suppress branching in the *brc1brc2* mutant background seems to be limited to branching-permissive situations.

One possibility that could account for these results is that ABCB19 is generically required for high levels of branching. For example, in its absence, overall auxin mobility in the plant is compromised and this in turn limits the number of active buds that can be supported. Consistent with this idea, *abcb19* is also able to suppress branching in strigolactone deficient mutants. Alternatively, a role for ABCB19 in bud activation by driving auxin from the bud could conceivably have similar effects on both *brc1brc2* and strigolactone-deficient mutants.

7.7 Conclusions and further directions

To summarise, the data in this thesis demonstrate that the auxin transport network in the stem is complex and multimodal (Fig. 7.1). Stem auxin transport is shown to consist of a high capacity highly polar auxin transport mode (PATS), as well as a less polar lower capacity transport mode (CAT), with exchange between them. The CAT is shown to play an important role in bud activation and appears to be particularly important for buds to effectively communicate across the stem. The PIN3/PIN4/PIN7 proteins are important contributors to

CAT and ABCB19 may contribute as well. Loss of CAT is able to partially suppress the high branching phenotype of strigolactone mutants. This ability to suppress branching does not appear to be a generic effect, because loss of PIN3/PIN4/PIN7 is unable to suppress the high branching phenotype observed in *brc1brc2* mutants.

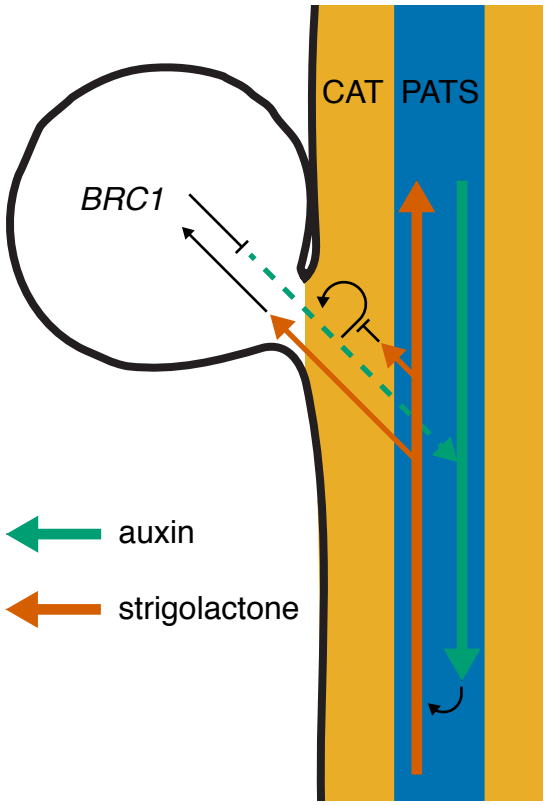

Fig. 7.1 Model for auxin transport-mediated bud activation.
Schematic illustration of an Arabidopsis stem segment bearing one bud. The coloured arrows indicate flow of auxin (green) and strigolactone (red). The blue shading indicates the polar auxin transport stream (PATS) and the orange shading represents the connective auxin transport (CAT). The black lines indicate either promotion (arrowheads) or repression (end lines).

The loss of ABCB19 function is able to partially suppress the high branching phenotypes in both the strigolactone mutants and *brc1brc2* mutants. Although this suggests that ABCB19 might be downstream of *BRC1* and strigolactone signalling, not all the data are in accordance with this. Further investigation of the response of *brc1brc2abcb19* mutant plants to strigolactone might help resolve this question.

Although low levels of BRC1 apparently make it easier for buds to activate, little is known about BRC1 function. Therefore, progress toward better understanding the role of *BRC1* in shoot branching should come from understanding the biology of the BRC1 protein.

The generation of the reporter construct presented here will likely aid in this process, because it enables studying dynamic protein responses in planta. Furthermore, it allows biochemical experiments that may help identify proteins that interact with BRC1 during bud activation.

The effects of H^+-ATPase activity on auxin transport and shoot branching presented in this thesis suggest that H^+-ATPase activity is able to affect both these processes. However, the mechanism underlying this is still very unclear. A first step to a better understanding should come from comparing the effects of H^+-ATPase activity on stem auxin transport in backgrounds with normal and increased levels of auxin transport. Furthermore, exploring the effects of altered H^+-ATPase activity on bud competition may help to better understand its effects on bud activation.

The questions which have been answered in this thesis have inevitably led to new, exciting questions, as discussed above. The findings presented provide a useful framework for exploring the answers to them.

References

Abe, S., Sado, A., Tanaka, K., Kisugi, T., Asami, K., Ota, S., Kim, H. I., Yoneyama, K., Xie, X., Ohnishi, T., Seto, Y., Yamaguchi, S., Akiyama, K., Yoneyama, K., and Nomura, T. (2014). Carlactone is converted to carlactonoic acid by MAX1 in Arabidopsis and its methyl ester can directly interact with AtD14 in vitro. *Proc Natl Acad Sci U S A*, 111(50):18084–9.

Aguilar-Martinez, J. A., Poza-Carrion, C., and Cubas, P. (2007). Arabidopsis BRANCHED1 acts as an integrator of branching signals within axillary buds. *Plant Cell*, 19(2):458–72.

Agusti, J., Herold, S., Schwarz, M., Sanchez, P., Ljung, K., Dun, E. A., Brewer, P. B., Beveridge, C. A., Sieberer, T., Sehr, E. M., and Greb, T. (2011). Strigolactone signaling is required for auxin-dependent stimulation of secondary growth in plants. *Proceedings of the National Academy of Sciences of the United States of America*, 108(50):20242–7.

Akiyama, K., Matsuzaki, K., and Hayashi, H. (2005). Plant sesquiterpenes induce hyphal branching in arbuscular mycorrhizal fungi. *Nature*, 435(7043):824–7.

Alder, A., Jamil, M., Marzorati, M., Bruno, M., Vermathen, M., Bigler, P., Ghisla, S., Bouwmeester, H., Beyer, P., and Al-Babili, S. (2012). The path from β-carotene to carlactone, a strigolactone-like plant hormone. *Science*, 335(6074):1348–51.

Axelsen, K. B. and Palmgren, M. G. (2001). Inventory of the superfamily of P-type ion pumps in Arabidopsis. *Plant Physiol*, 126(2):696–706.

Bainbridge, K., Guyomarc'h, S., Bayer, E., Swarup, R., Bennett, M., Mandel, T., and Kuhlemeier, C. (2008). Auxin influx carriers stabilize phyllotactic patterning. *Genes and Development*, 22(6):810–23.

Balla, J., Kalousek, P., Reinohl, V., Friml, J., and Prochazka, S. (2011). Competitive canalization of PIN-dependent auxin flow from axillary buds controls pea bud outgrowth. *Plant Journal*, 65(4):571–7.

Bartel, B. and Fink, G. R. (1995). ILR1, an amidohydrolase that releases active indole-3-acetic acid from conjugates. *Science*, 268(5218):1745–8.

Bayer, E. M., Smith, R. S., Mandel, T., Nakayama, N., Sauer, M., Prusinkiewicz, P., and Kuhlemeier, C. (2009). Integration of transport-based models for phyllotaxis and midvein formation. *Genes and Development*, 23(3):373–84.

Benkova, E., Michniewicz, M., Sauer, M., Teichmann, T., Seifertova, D., Jurgens, G., and Friml, J. (2003). Local, efflux-dependent auxin gradients as a common module for plant organ formation. *Cell*, 115(5):591–602.

Bennett, M. J., Marchant, A., Green, H. G., May, S. T., Ward, S. P., Millner, P. A., Walker, A. R., Schulz, B., and Feldmann, K. A. (1996). Arabidopsis *AUX1* gene: A permease-like regulator of root gravitropism. *Science*, 273(5277):948–50.

Bennett, S. R. M., Alvarez, J., Bossinger, G., and Smyth, D. R. (1995). Morphogenesis in *pinoid* mutants of Arabidopsis thaliana. *The Plant Journal*, 8(4):505–20.

Bennett, T., Hines, G., van Rongen, M., Waldie, T., Sawchuk, M. G., Scarpella, E., Ljung, K., and Leyser, O. (2016a). Connective auxin transport in the shoot facilitates communication between shoot apices. *PLoS Biol*, 14(e1002446).

Bennett, T. and Leyser, O. (2014). *The Auxin Question: A Philosophical Overview*, pages 3–19. Springer Vienna, Vienna.

Bennett, T., Liang, Y., Seale, M., Ward, S., Muller, D., and Leyser, O. (2016b). Strigolactone regulates shoot development through a core signalling pathway. *Biol Open*, 5(12):1806–20.

Bennett, T., Sieberer, T., Willett, B., Booker, J., Luschnig, C., and Leyser, O. (2006). The Arabidopsis MAX pathway controls shoot branching by regulating auxin transport. *Current Biology*, 16(6):553–63.

Besserer, A., Puech-Pagès, V., Kiefer, P., Gomez-Roldan, V., Jauneau, A., Roy, S., Portais, J.-C., Roux, C., Bécard, G., and Séjalon-Delmas, N. (2006). Strigolactones stimulate arbuscular mycorrhizal fungi by activating mitochondria. *PLoS Biol*, 4(7):e226.

Blakeslee, J. J., Bandyopadhyay, A., Lee, O. R., Mravec, J., Titapiwatanakun, B., Sauer, M., Makam, S. N., Cheng, Y., Bouchard, R., Adamec, J., Geisler, M., Nagashima, A., Sakai, T., Martinoia, E., Friml, J., Peer, W. A., and Murphy, A. S. (2007). Interactions among PIN-FORMED and P-glycoprotein auxin transporters in Arabidopsis. *Plant Cell*, 19(1):131–47.

Blilou, I., Xu, J., Wildwater, M., Willemsen, V., Paponov, I., Friml, J., Heidstra, R., Aida, M., Palme, K., and Scheres, B. (2005). The PIN auxin efflux facilitator network controls growth and patterning in Arabidopsis roots. *Nature*, 433(7021):39–44.

Booker, J., Auldridge, M., Wills, S., McCarty, D., Klee, H., and Leyser, O. (2004). MAX3/CCD7 is a carotenoid cleavage dioxygenase required for the synthesis of a novel plant signaling molecule. *Current Biology*, 14(14):1232–8.

Booker, J., Chatfield, S., and Leyser, O. (2003). Auxin acts in xylem-associated or medullary cells to mediate apical dominance. *Plant Cell*, 15(2):495–507.

Booker, J., Sieberer, T., Wright, W., Williamson, L., Willett, B., Stirnberg, P., Turnbull, C., Srinivasan, M., Goddard, P., and Leyser, O. (2005). MAX1 encodes a cytochrome P450 family member that acts downstream of MAX3/4 to produce a carotenoid-derived branch-inhibiting hormone. *Developmental Cell*, 8(3):443–9.

Boot, K. J., Hille, S. C., Libbenga, K. R., Peletier, L. A., van Spronsen, P. C., van Duijn, B., and Offringa, R. (2016). Modelling the dynamics of polar auxin transport in inflorescence stems of Arabidopsis thaliana. *Journal of Experimental Botany*, 67(3):649–66.

Braun, N., de Saint Germain, A., Pillot, J. P., Boutet-Mercey, S., Dalmais, M., Antoniadi, I., Li, X., Maia-Grondard, A., Le Signor, C., Bouteiller, N., Luo, D., Bendahmane, A., Turnbull, C., and Rameau, C. (2012). The pea TCP transcription factor PsBRC1 acts downstream of strigolactones to control shoot branching. *Plant Physiology*, 158(1):225–38.

Brewer, P. B., Dun, E. A., Ferguson, B. J., Rameau, C., and Beveridge, C. A. (2009). Strigolactone acts downstream of auxin to regulate bud outgrowth in pea and Arabidopsis. *Plant Physiology*, 150(1):482–93.

Brewer, P. B., Dun, E. A., Gui, R., Mason, M. G., and Beveridge, C. A. (2015). Strigolactone inhibition of branching independent of polar auxin transport. *Plant Physiol*, 168(4):1820–9.

Brewer, P. B., Yoneyama, K., Filardo, F., Meyers, E., Scaffidi, A., Frickey, T., Akiyama, K., Seto, Y., Dun, E. A., Cremer, J. E., Kerr, S. C., Waters, M. T., Flematti, G. R., Mason, M. G., Weiller, G., Yamaguchi, S., Nomura, T., Smith, S. M., Yoneyama, K., and Beveridge, C. A. (2016). LATERAL BRANCHING OXIDOREDUCTASE acts in the final stages of strigolactone biosynthesis in Arabidopsis. *Proc Natl Acad Sci U S A*, 113(22):6301–6.

Calderón Villalobos, L. I. A., Lee, S., De Oliveira, C., Ivetac, A., Brandt, W., Armitage, L., Sheard, L. B., Tan, X., Parry, G., Mao, H., Zheng, N., Napier, R., Kepinski, S., and Estelle, M. (2012). A combinatorial TIR1/AFB–Aux/IAA co-receptor system for differential sensing of auxin. *Nat Chem Biol*, 8(5):477–85.

Chatfield, S. P., Stirnberg, P., Forde, B. G., and Leyser, O. (2000). The hormonal regulation of axillary bud growth in Arabidopsis. *Plant Journal*, 24(2):159–69.

Chen, R., Hilson P Fau Sedbrook, J., Sedbrook J Fau Rosen, E., Rosen E Fau Caspar, T., Caspar T Fau Masson, P. H., and Masson, P. H. (1998). The Arabidopsis thaliana AGRAVITROPIC 1 gene encodes a component of the polar-auxin-transport efflux carrier. *Proceedings of the National Academy of Sciences*, 95:15112–7.

Chevalier, F., Nieminen, K., Sanchez-Ferrero, J. C., Rodriguez, M. L., Chagoyen, M., Hardtke, C. S., and Cubas, P. (2014). Strigolactone promotes degradation of DWARF14, an α/β hydrolase essential for strigolactone signaling in Arabidopsis. *Plant Cell*, 26(3):1134–50.

Clough, S. J. and Bent, A. F. (1998). Floral dip: a simplified method for Agrobacterium-mediated transformation of Arabidopsis thaliana. *Plant J*, 16(6):735–43.

Cook, C. E., Whichard, L. P., Turner, B., Wall, M. E., and Egley, G. H. (1966). Germination of witchweed (Striga lutea Lour.): Isolation and properties of a potent stimulant. *Science*, 154(3753):1189–90.

Crawford, S., Shinohara, N., Sieberer, T., Williamson, L., George, G., Hepworth, J., Muller, D., Domagalska, M. A., and Leyser, O. (2010). Strigolactones enhance competition between shoot branches by dampening auxin transport. *Development*, 137(17):2905–13.

Dal Bosco, C., Dovzhenko, A., Liu, X., Woerner, N., Rensch, T., Eismann, M., Eimer, S., Hegermann, J., Paponov, I. A., Ruperti, B., Heberle-Bors, E., Touraev, A., Cohen, J. D., and Palme, K. (2012). The endoplasmic reticulum localized PIN8 is a pollen-specific auxin carrier involved in intracellular auxin homeostasis. *Plant J*, 71(5):860–70.

de Jong, M., George, G., Ongaro, V., Williamson, L., Willetts, B., Ljung, K., McCulloch, H., and Leyser, O. (2014). Auxin and strigolactone signaling are required for modulation of Arabidopsis shoot branching by nitrogen supply. *Plant Physiol*, 166(1):384–95.

de Saint Germain, A., Clave, G., Badet-Denisot, M. A., Pillot, J. P., Cornu, D., Le Caer, J. P., Burger, M., Pelissier, F., Retailleau, P., Turnbull, C., Bonhomme, S., Chory, J., Rameau, C., and Boyer, F. D. (2016). An histidine covalent receptor and butenolide complex mediates strigolactone perception. *Nat Chem Biol*, 12(10):787–94.

Dharmasiri, N., Dharmasiri, S., and Estelle, M. (2005). The F-box protein TIR1 is an auxin receptor. *Nature*, 435(7041):441–5.

Doebley, J., Stec, A., and Hubbard, L. (1997). The evolution of apical dominance in maize. *Nature*, 386(6624):485–8.

Dun, E. A., de Saint Germain, A., Rameau, C., and Beveridge, C. A. (2012). Antagonistic action of strigolactone and cytokinin in bud outgrowth control. *Plant Physiology*, 158(1):487–98.

Fabregas, N., Formosa-Jordan, P., Confraria, A., Siligato, R., Alonso, J. M., Swarup, R., Bennett, M. J., Mahonen, A. P., Cano-Delgado, A. I., and Ibanes, M. (2015). Auxin influx carriers control vascular patterning and xylem differentiation in Arabidopsis thaliana. *PLoS Genet*, 11(4):e1005183.

Finlayson, S. A. (2007). Arabidopsis TEOSINTE BRANCHED1-LIKE 1 regulates axillary bud outgrowth and is homologous to monocot TEOSINTE BRANCHED1. *Plant and Cell Physiology*, 48(5):667–77.

Foo, E., Buillier, E., Goussot, M., Foucher, F., Rameau, C., and Beveridge, C. A. (2005). The branching gene RAMOSUS1 mediates interactions among two novel signals 464 and auxin in pea. *Plant Cell*, 17(2):464–74.

Friml, J., Benkova, E., Blilou, I., Wisniewska, J., Hamann, T., Ljung, K., Woody, S., Sandberg, G., Scheres, B., Jurgens, G., and Palme, K. (2002a). AtPIN4 mediates sink-driven auxin gradients and root patterning in Arabidopsis. *Cell*, 108(5):661–73.

Friml, J., Vieten, A., Sauer, M., Weijers, D., Schwarz, H., Hamann, T., Offringa, R., and Jurgens, G. (2003). Efflux-dependent auxin gradients establish the apical-basal axis of Arabidopsis. *Nature*, 426(6963):147–53.

Friml, J., Wisniewska, J., Benkova, E., Mendgen, K., and Palme, K. (2002b). Lateral relocation of auxin efflux regulator PIN3 mediates tropism in Arabidopsis. *Nature*, 415(6873):806–9.

Geisler, M., Blakeslee, J. J., Bouchard, R., Lee, O. R., Vincenzetti, V., Bandyopadhyay, A., Titapiwatanakun, B., Peer, W. A., Bailly, A., Richards, E. L., Ejenda, K. F. K., Smith, A. P., Baroux, C., Grossniklaus, U., Muller, A., Hrycyna, C. A., Dudler, R., Murphy, A. S., and Martinoia, E. (2005). Cellular efflux of auxin catalyzed by the Arabidopsis MDR/PGP transporter AtPGP1. *Plant Journal*, 44(2):179–94.

Geisler, M., Kolukisaoglu, H., Bouchard, R., Billion, K., Berger, J., Saal, B., Frangne, N., Koncz-Kálmán, Z., Koncz, C., Dudler, R., Blakeslee, J. J., Murphy, A. S., Martinoia, E., and Schulz, B. (2003). TWISTED DWARF1, a unique plasma membrane-anchored immunophilin-like protein, interacts with Arabidopsis Multidrug Resistance-like Transporters AtPGP1 and AtPGP19. *Molecular Biology of the Cell*, 14(10):4238–49.

Geldner, N., Friml, J., Stierhof, Y. D., Jurgens, G., and Palme, K. (2001). Auxin transport inhibitors block PIN1 cycling and vesicle trafficking. *Nature*, 413(6854):425–8.

Gillissen, B., Burkle, L., Andre, B., Kuhn, C., Rentsch, D., Brandl, B., and Frommer, W. B. (2000). A new family of high-affinity transporters for adenine, cytosine, and purine derivatives in Arabidopsis. *Plant Cell*, 12(2):291–300.

Goldsmith, M. H. M. (1967). Movement of pulses of labeled auxin in corn coleoptiles. *Plant Physiology*, 42:258–63.

Goldsmith, M. H. M. (1977). The polar transport of auxin. *Annual Review of Plant Physiology*, 28(1):439–78.

Gomez-Roldan, V., Fermas, S., Brewer, P. B., Puech-Pages, V., Dun, E. A., Pillot, J. P., Letisse, F., Matusova, R., Danoun, S., Portais, J. C., Bouwmeester, H., Becard, G., Beveridge, C. A., Rameau, C., and Rochange, S. F. (2008). Strigolactone inhibition of shoot branching. *Nature*, 455(7210):189–U22.

Gonzalez-Grandio, E., Poza-Carrion, C., Sorzano, C. O., and Cubas, P. (2013). BRANCHED1 promotes axillary bud dormancy in response to shade in Arabidopsis. *Plant Cell*, 25(3):834–50.

Gray, W. M., Kepinski, S., Rouse, D., Leyser, O., and Estelle, M. (2001). Auxin regulates SCF(TIR1)-dependent degradation of AUX/IAA proteins. *Nature*, 414(6861):271–6.

Grbic, B. and Bleecker, A. B. (1996). An altered body plan is conferred on Arabidopsis plants carrying dominant alleles of two genes. *Development*, 122(8):2395–403.

Greb, T., Clarenz, O., Schafer, E., Muller, D., Herrero, R., Schmitz, G., and Theres, K. (2003). Molecular analysis of the LATERAL SUPPRESSOR gene in Arabidopsis reveals a conserved control mechanism for axillary meristem formation. *Genes and Development*, 17(9):1175–87.

Guan, J. C., Suzuki, M., Wu, S., Latshaw, S. P., Petruff, T., Goulet, C., Klee, H. J., Koch, K. E., and McCarty, D. R. (2012). Diverse roles of strigolactone signaling in maize architecture and the uncoupling of a branching-specific sub-network. *Plant Physiology*.

Guilfoyle, T. J. and Hagen, G. (2007). Auxin response factors. *Curr Opin Plant Biol*, 10(5):453–60.

Guilfoyle, T. J., Ulmasov, T., and Hagen, G. (1998). The ARF family of transcription factors and their role in plant hormone-responsive transcription. *Cell Mol Life Sci*, 54(7):619–27.

Gälweiler, L., Guan, C., Müller, A., Wisman, E., Mendgen, K., Yephremov, A., and Palme, K. (1998). Regulation of polar auxin transport by AtPIN1 in Arabidopsis vascular tissue. *Science*, 282(5397):2226–30.

Hager, A. (2003). Role of the plasma membrane H+-ATPase in auxin-induced elongation growth: historical and new aspects. *J Plant Res*, 116(6):483–505.

Hamiaux, C., Drummond, R. M., Janssen, B., Ledger, S., Cooney, J., Newcomb, R., and Snowden, K. (2012). DAD2 is an α/β hydrolase likely to be involved in the perception of the plant branching hormone, strigolactone. *Current Biology*, 22(21):2032–6.

Harrison, S. J., Mott, E. K., Parsley, K., Aspinall, S., Gray, J. C., and Cottage, A. (2006). A rapid and robust method of identifying transformed Arabidopsis thaliana seedlings following floral dip transformation. *Plant Methods*, 2(1):19.

Haruta, M., Burch, H. L., Nelson, R. B., Barrett-Wilt, G., Kline, K. G., Mohsin, S. B., Young, J. C., Otegui, M. S., and Sussman, M. R. (2010). Molecular characterization of mutant Arabidopsis plants with reduced plasma membrane proton pump activity. *J Biol Chem*, 285(23):17918–29.

Hayward, A., Stirnberg, P., Beveridge, C., and Leyser, O. (2009). Interactions between auxin and strigolactone in shoot branching control. *Plant Physiology*, 151(1):400–12.

Heisler, M. G., Ohno, C., Das, P., Sieber, P., Reddy, G. V., Long, J. A., and Meyerowitz, E. M. (2005). Patterns of auxin transport and gene expression during primordium development revealed by live imaging of the Arabidopsis inflorescence meristem. *Current Biology*, 15(21):1899–911.

Hempel, F. D. and Feldman, L. J. (1994). Bi-directional inflorescence development in Arabidopsis thaliana: Acropetal initiation of flowers and basipetal initiation of paraclades. *Planta*, 192(2):276–86.

Hensel, L. L., Nelson, M. A., Richmond, T. A., and Bleecker, A. B. (1994). The fate of inflorescence meristems is controlled by developing fruits in Arabidopsis. *Plant Physiology*, 106(3):863.

Hirose, N., Takei, K., Kuroha, T., Kamada-Nobusada, T., Hayashi, H., and Sakakibara, H. (2008). Regulation of cytokinin biosynthesis, compartmentalization and translocation. *Journal of Experimental Botany*, 59(1):75–83.

Hubbard, L., McSteen, P., Doebley, J., and Hake, S. (2002). Expression patterns and mutant phenotype of *teosinte branched1* correlate with growth suppression in maize and teosinte. *Genetics*, 162(4):1927–35.

Hwang, I., Sheen, J., and Muller, B. (2012). Cytokinin signaling networks. *Annual Review of Plant Biology*, 63:353–80.

Jackson, R. G., Lim, E. K., Li, Y., Kowalczyk, M., Sandberg, G., Hoggett, J., Ashford, D. A., and Bowles, D. J. (2001). Identification and biochemical characterization of an Arabidopsis indole-3-acetic acid glucosyltransferase. *J Biol Chem*, 276(6):4350–6.

Jakubowska, A. and Kowalczyk, S. (2005). A specific enzyme hydrolyzing 6-O(4-O)-indole-3-ylacetyl-beta-D-glucose in immature kernels of *Zea mays*. *J Plant Physiol*, 162(2):207–13.

Jönsson, H., Heisler, M. G., Shapiro, B. E., Meyerowitz, E. M., and Mjolsness, E. (2006). An auxin-driven polarized transport model for phyllotaxis. *Proceedings of the National Academy of Sciences*, 103(5):1633–8.

Kagiyama, M., Hirano, Y., Mori, T., Kim, S.-Y., Kyozuka, J., Seto, Y., Yamaguchi, S., and Hakoshima, T. (2013). Structures of D14 and D14L in the strigolactone and karrikin signaling pathways. *Genes to Cells*, 18(2):147–60.

Kamimoto, Y., Terasaka, K., Hamamoto, M., Takanashi, K., Fukuda, S., Shitan, N., Sugiyama, A., Suzuki, H., Shibata, D., Wang, B., Pollmann, S., Geisler, M., and Yazaki, K. (2012). Arabidopsis ABCB21 is a facultative auxin importer/exporter regulated by cytoplasmic auxin concentration. *Plant Cell Physiol*, 53(12):2090–100.

Kepinski, S. and Leyser, O. (2005). The arabidopsis F-box protein TIR1 is an auxin receptor. *Nature*, 435(7041):446–51.

Kierzkowski, D., Lenhard, M., Smith, R., and Kuhlemeier, C. (2013). Interaction between meristem tissue layers controls phyllotaxis. *Developmental Cell*, 26(6):616–28.

Ko, D., Kang, J., Kiba, T., Park, J., Kojima, M., Do, J., Kim, K. Y., Kwon, M., Endler, A., Song, W. Y., Martinoia, E., Sakakibara, H., and Lee, Y. (2014). Arabidopsis ABCG14 is essential for the root-to-shoot translocation of cytokinin. *Proc Natl Acad Sci U S A*, 111(19):7150–5.

Kohlen, W., Charnikhova, T., Liu, Q., Bours, R., Domagalska, M. A., Beguerie, S., Verstappen, F., Leyser, O., Bouwmeester, H., and Ruyter-Spira, C. (2011). Strigolactones are transported through the xylem and play a key role in shoot architectural response to phosphate deficiency in nonarbuscular mycorrhizal host Arabidopsis. *Plant Physiology*, 155(2):974–87.

Kosugi, S. and Ohashi, Y. (2002). DNA binding and dimerization specificity and potential targets for the TCP protein family. *Plant Journal*, 30(3):337–48.

Kramer, E. M. and Ackelsberg, E. M. (2015). Auxin metabolism rates and implications for plant development. *Front Plant Sci*, 6.

Kramer, E. M. and Bennett, M. J. (2006). Auxin transport: a field in flux. *Trends Plant Sci*, 11(8):382–6.

Krecek, P., Skupa, P., Libus, J., Naramoto, S., Tejos, R., Friml, J., and Zazimalova, E. (2009). The PIN-FORMED (PIN) protein family of auxin transporters. *Genome Biol*, 10(12):249.

Kretzschmar, T., Kohlen, W., Sasse, J., Borghi, L., Schlegel, M., Bachelier, J. B., Reinhardt, D., Bours, R., Bouwmeester, H. J., and Martinoia, E. (2012). A petunia ABC protein controls strigolactone-dependent symbiotic signalling and branching. *Nature*, 483(7389):341–4.

Kubes, M., Yang, H., Richter, G. L., Cheng, Y., Mlodzinska, E., Wang, X., Blakeslee, J. J., Carraro, N., Petrasek, J., Zazimalova, E., Hoyerova, K., Peer, W. A., and Murphy, A. S. (2012). The Arabidopsis concentration-dependent influx/efflux transporter ABCB4 regulates cellular auxin levels in the root epidermis. *Plant J*, 69(4):640–54.

Kudo, T., Kiba, T., and Sakakibara, H. (2010). Metabolism and long-distance translocation of cytokinins. *J Integr Plant Biol*, 52(1):53–60.

Kurakawa, T., Ueda, N., Maekawa, M., Kobayashi, K., Kojima, M., Nagato, Y., Sakakibara, H., and Kyozuka, J. (2007). Direct control of shoot meristem activity by a cytokinin-activating enzyme. *Nature*, 445(7128):652–5.

Kuroha, T., Tokunaga, H., Kojima, M., Ueda, N., Ishida, T., Nagawa, S., Fukuda, H., Sugimoto, K., and Sakakibara, H. (2009). Functional analyses of LONELY GUY cytokinin-activating enzymes reveal the importance of the direct activation pathway in Arabidopsis. *The Plant Cell*, 21(10):3152–69.

Lazar, G. and Goodman, H. M. (2006). MAX1, a regulator of the flavonoid pathway, controls vegetative axillary bud outgrowth in Arabidopsis. *Proceedings of the National Academy of Sciences of the United States of America*, 103(2):472–6.

Li, C., Potuschak, T., Colón-Carmona, A., Gutiérrez, R. A., and Doerner, P. (2005). Arabidopsis TCP20 links regulation of growth and cell division control pathways. *Proceedings of the National Academy of Sciences of the United States of America*, 102(36):12978–83.

Li, C.-J. and Bangerth, F. (1999). Autoinhibition of indoleacetic acid transport in the shoots of two-branched pea (*Pisum sativum*) plants and its relationship to correlative dominance. *Physiologia Plantarum*, 106(4):415–20.

Li, S. (2015). The Arabidopsis thaliana TCP transcription factors: A broadening horizon beyond development. *Plant Signal Behav*, 10(7).

Lin, R. and Wang, H. (2005). Two homologous ATP-binding cassette transporter proteins, AtMDR1 and AtPGP1, regulate Arabidopsis photomorphogenesis and root development by mediating polar auxin transport. *Plant Physiology*, 138(2):949–64.

Luschnig, C., Gaxiola Ra Fau Grisafi, P., Grisafi P Fau Fink, G. R., and Fink, G. R. (1998). EIR1, a root-specific protein involved in auxin transport, is required for gravitropism in Arabidopsis thaliana. *Genes and Development*, 12(0890-9369 (Print)):2175–87.

Maraschin F dos, S., Memelink, J., and Offringa, R. (2009). Auxin-induced, SCF (TIR1)-mediated poly-ubiquitination marks Aux/IAA proteins for degradation. *Plant J*, 59(1):100–9.

Marchant, A. and Bennett, M. J. (1998). The Arabidopsis AUX1 gene: a model system to study mRNA processing in plants. *Plant Mol Biol*, 36(3):463–71.

Mashiguchi, K., Tanaka, K., Sakai, T., Sugawara, S., Kawaide, H., Natsume, M., Hanada, A., Yaeno, T., Shirasu, K., Yao, H., McSteen, P., Zhao, Y., Hayashi, K., Kamiya, Y., and Kasahara, H. (2011). The main auxin biosynthesis pathway in Arabidopsis. *Proc Natl Acad Sci U S A*, 108(45):18512–7.

Mitchison, G. (2015). The shape of an auxin pulse, and what it tells us about the transport mechanism. *PLoS Comput Biol*, 11(10):e1004487.

Miyawaki, K., Matsumoto-Kitano, M., and Kakimoto, T. (2004). Expression of cytokinin biosynthetic isopentenyltransferase genes in Arabidopsis: tissue specificity and regulation by auxin, cytokinin, and nitrate. *Plant J*, 37(1):128–38.

Morffy, N., Faure, L., and Nelson, D. C. (2016). Smoke and hormone mirrors: Action and evolution of karrikin and strigolactone signaling. *Trends Genet*, 32(3):176–88.

Morris, D. A. (1977). Transport of exogenous auxin in 2-branched dwarf pea-seedlings (*Pisum sativum* l.) - some implications for polarity and apical dominance. *Planta*, 136(1):91–6.

Mravec, J., Skupa, P., Bailly, A., Hoyerova, K., Krecek, P., Bielach, A., Petrasek, J., Zhang, J., Gaykova, V., Stierhof, Y. D., Dobrev, P. I., Schwarzerova, K., Rolcik, J., Seifertova, D., Luschnig, C., Benkova, E., Zazimalova, E., Geisler, M., and Friml, J. (2009). Subcellular homeostasis of phytohormone auxin is mediated by the ER-localized PIN5 transporter. *Nature*, 459(7250):1136–U127.

Muller, A., Guan C Fau Galweiler, L., Galweiler L Fau Tanzler, P., Tanzler P Fau Huijser, P., Huijser P Fau Marchant, A., Marchant A Fau Parry, G., Parry G Fau Bennett, M., Bennett M Fau Wisman, E., Wisman E Fau Palme, K., and Palme, K. (1998). AtPIN2 defines a locus of Arabidopsis for root gravitropism control. *The EMBO Journal*, 17(0261-4189 (Print)):6903–11.

Muller, D., Waldie, T., Miyawaki, K., To, J. P., Melnyk, C. W., Kieber, J. J., Kakimoto, T., and Leyser, O. (2015). Cytokinin is required for escape but not release from auxin mediated apical dominance. *Plant J*, 82(5):874–86.

Noh, B., Bandyopadhyay, A., Peer, W., Spalding, E. P., and Murphy, A. (2003). Enhanced gravi- and phototropism in plant *mdr* mutants mislocalizing the auxin efflux protein PIN1. *Nature*, 423(6943):999–1002.

Noh, B., Murphy, A. S., and Spalding, E. P. (2001). Multidrug resistance-like genes of Arabidopsis required for auxin transport and auxin-mediated development. *Plant Cell*, 13(11):2441–54.

Nordstrom, A., Tarkowski, P., Tarkowska, D., Norbaek, R., Astot, C., Dolezal, K., and Sandberg, G. (2004). Auxin regulation of cytokinin biosynthesis in Arabidopsis thaliana: A factor of potential importance for auxin-cytokinin-regulated development. *Proceedings of the National Academy of Sciences of the United States of America*, 101(21):8039–44.

O'Connor, D. L., Runions, A., Sluis, A., Bragg, J., Vogel, J. P., Prusinkiewicz, P., and Hake, S. (2014). A division in PIN-mediated auxin patterning during organ initiation in grasses. *PLoS Comput Biol*, 10(1):e1003447.

Okada, K., Ueda, J., Komaki, M. K., Bell, C. J., and Shimura, Y. (1991). Requirement of the auxin polar transport system in early stages of Arabidopsis floral bud formation. *Plant Cell*, 3(7):677–84.

Ongaro, V., Bainbridge, K., Williamson, L., and Leyser, O. (2008). Interactions between axillary branches of Arabidopsis. *Molecular Plant*, 1(2):388–400.

Paciorek, T., Zazimalova, E., Ruthardt, N., Petrasek, J., Stierhof, Y.-D., Kleine-Vehn, J., Morris, D. A., Emans, N., Jurgens, G., Geldner, N., and Friml, J. (2005). Auxin inhibits endocytosis and promotes its own efflux from cells. *Nature*, 435(7046):1251–6.

Paponov, I. A., Teale, W. D., Trebar, M., Blilou, I., and Palme, K. (2005). The PIN auxin efflux facilitators: evolutionary and functional perspectives. *Trends Plant Sci*, 10(4):170–7.

Peer, W. A., Cheng, Y., and Murphy, A. S. (2013). Evidence of oxidative attenuation of auxin signalling. *J Exp Bot*, 64(9):2629–39.

Peret, B., Swarup, K., Ferguson, A., Seth, M., Yang, Y., Dhondt, S., James, N., Casimiro, I., Perry, P., Syed, A., Yang, H., Reemmer, J., Venison, E., Howells, C., Perez-Amador, M. A., Yun, J., Alonso, J., Beemster, G. T., Laplaze, L., Murphy, A., Bennett, M. J., Nielsen, E., and Swarup, R. (2012). AUX/LAX genes encode a family of auxin influx transporters that perform distinct functions during Arabidopsis development. *Plant Cell*, 24(7):2874–85.

Perrot-Rechenmann, C. (2010). Cellular responses to auxin: division versus expansion. *Cold Spring Harb Perspect Biol*, 2(5):a001446.

Petrasek, J., Mravec, J., Bouchard, R., Blakeslee, J. J., Abas, M., Seifertova, D., Wisniewska, J., Tadele, Z., Kubes, M., Covanova, M., Dhonukshe, P., Skupa, P., Benkova, E., Perry, L., Krecek, P., Lee, O. R., Fink, G. R., Geisler, M., Murphy, A. S., Luschnig, C., Zazimalova, E., and Friml, J. (2006). PIN proteins perform a rate-limiting function in cellular auxin efflux. *Science*, 312(5775):914–8.

Prasad, T. K., Li, X., Abdel-Rahman, A. M., Hosokawa, Z., Cloud, N. P., Lamotte, C. E., and Cline, M. G. (1993). Does auxin play a role in the release of apical dominance by shoot inversion in *Ipomoea nil*? *Annals of Botany*, 71(3):223–9.

Prusinkiewicz, P., Crawford, S., Smith, R. S., Ljung, K., Bennett, T., Ongaro, V., and Leyser, O. (2009). Control of bud activation by an auxin transport switch. *Proceedings of the National Academy of Sciences of the United States of America*, 106(41):17431–6.

Pěnčík, A., Simonovik, B., Petersson, S. V., Henyková, E., Simon, S., Greenham, K., Zhang, Y., Kowalczyk, M., Estelle, M., Zažímalová, E., Novák, O., Sandberg, G., and Ljung, K. (2013). Regulation of auxin homeostasis and gradients in Arabidopsis roots through the formation of the indole-3-acetic acid catabolite 2-oxindole-3-acetic acid. *The Plant Cell*, 25(10):3858–70.

Rampey, R. A., LeClere, S., Kowalczyk, M., Ljung, K., Sandberg, G., and Bartel, B. (2004). A family of auxin-conjugate hydrolases that contributes to free indole-3-acetic acid levels during Arabidopsis germination. *Plant Physiology*, 135(2):978–88.

Rashotte, A. M., Mason, M. G., Hutchison, C. E., Ferreira, F. J., Schaller, G. E., and Kieber, J. J. (2006). A subset of Arabidopsis AP2 transcription factors mediates cytokinin responses in concert with a two-component pathway. *Proc Natl Acad Sci U S A*, 103(29):11081–5.

Rashotte, A. M., Poupart, J., Waddell, C. S., and Muday, G. K. (2003). Transport of the two natural auxins, indole-3-butyric acid and indole-3-acetic acid, in Arabidopsis. *Plant Physiology*, 133(2):761–72.

Raven, J. A. (1975). Transport of indoleacetic acid in plant cells in relation to pH and electrical potential gradients, and its significance for polar IAA transport. *New Phytologist*, 74(2):163–72.

Rayle, D. L. and Cleland, R. E. (1992). The Acid Growth Theory of auxin-induced cell elongation is alive and well. *Plant Physiol*, 99(4):1271–4.

Reinhardt, D., Pesce, E.-R., Stieger, P., Mandel, T., Baltensperger, K., Bennett, M., Traas, J., Friml, J., and Kuhlemeier, C. (2003). Regulation of phyllotaxis by polar auxin transport. *Nature*, 426(6964):255–60.

Roman, G., Lubarsky, B., Kieber, J. J., Rothenberg, M., and Ecker, J. R. (1995). Genetic analysis of ethylene signal transduction in Arabidopsis thaliana: Five novel mutant loci integrated into a stress response pathway. *Genetics*, 139(3):1393–409.

Rubery, P. H. and Sheldrake, A. R. (1974). Carrier-mediated auxin transport. *Planta*, 118(2):101–21.

Ruegger, M., Dewey, E., Gray, W. M., Hobbie, L., Turner, J., and Estelle, M. (1998). The TIR1 protein of Arabidopsis functions in auxin response and is related to human SKP2 and yeast Grr1p. *Genes and Development*, 12(2):198–207.

Ruegger, M., Dewey, E., Hobbie, L., Brown, D., Bernasconi, P., Turner, J., Muday, G., and Estelle, M. (1997). Reduced naphthylphthalamic acid binding in the *tir3* mutant of Arabidopsis is associated with a reduction in polar auxin transport and diverse morphological defects. *Plant Cell*, 9(5):745–57.

Rutschow, H. L., Baskin, T. I., and Kramer, E. M. (2014). The carrier AUXIN RESISTANT (AUX1) dominates auxin flux into arabidopsis protoplasts. *New Phytologist*, 204(3):536–44.

Sachs, T. (1981). The control of the patterned differentiation of vascular tissues. *Advances in Botanical Research Incorporating Advances in Plant Pathology*, 9:151–262.

Sachs, T. and Thimann, V. (1967). Role of auxins and cytokinins in release of buds from dominance. *American Journal of Botany*, 54(1):136–144.

Sauer, M., Balla, J., Luschnig, C., Wisniewska, J., Reinohl, V., Friml, J., and Benkova, E. (2006). Canalization of auxin flow by Aux/IAA-ARF-dependent feedback regulation of PIN polarity. *Genes and Development*, 20(20):2902–11.

Sawchuk, M. G., Edgar, A., and Scarpella, E. (2013). Patterning of leaf vein networks by convergent auxin transport pathways. *PLoS Genet*, 9(2):e1003294.

Scarpella, E., Marcos, D., Friml, J., and Berleth, T. (2006). Control of leaf vascular patterning by polar auxin transport. *Genes and Development*, 20(8):1015–27.

Scarpella, E. and Meijer, A. H. (2004). Pattern formation in the vascular system of monocot and dicot plant species. *New Phytologist*, 164(2):209–42.

Schommer, C., Debernardi, J. M., Bresso, E. G., Rodriguez, R. E., and Palatnik, J. F. (2014). Repression of cell proliferation by miR319-regulated TCP4. *Molecular Plant*, 7(10):1533–44.

Seale, M. (2016). *The role of transcriptional targets in the hormonal regulation of shoot branching*. PhD thesis.

Seale, M., Bennett, T., and Leyser, O. (2017). *BRC1* expression regulates bud activation potential but is not necessary or sufficient for bud growth inhibition in Arabidopsis. *Development*, 144(9):1661–73.

Shinohara, N., Taylor, C., and Leyser, O. (2013). Strigolactone can promote or inhibit shoot branching by triggering rapid depletion of the auxin efflux protein PIN1 from the plasma membrane. *PLoS Biol*, 11(1):e1001474.

Sieberer, T. and Leyser, O. (2006). Auxin transport, but in which direction? *Science*, 312(5775):858–60.

Smith, R. S., Guyomarc'h, S., Mandel, T., Reinhardt, D., Kuhlemeier, C., and Prusinkiewicz, P. (2006). A plausible model of phyllotaxis. *Proceedings of the National Academy of Sciences*, 103(5):1301–6.

Snow, R. (1929). The transmission of inhibition through dead stretches of stem. *Annals of Botany*, os-43(2):261–7.

Sorefan, K., Booker, J., Haurogne, K., Goussot, M., Bainbridge, K., Foo, E., Chatfield, S., Ward, S., Beveridge, C., Rameau, C., and Leyser, O. (2003). MAX4 and RMS1 are orthologous dioxygenase-like genes that regulate shoot branching in Arabidopsis and pea. *Genes and Development*, 17(12):1469–74.

Soundappan, I., Bennett, T., Morffy, N., Liang, Y., Stanga, J. P., Abbas, A., Leyser, O., and Nelson, D. C. (2015). SMAX1-LIKE/D53 family members enable distinct MAX2-dependent responses to strigolactones and karrikins in Arabidopsis. *Plant Cell*, 27(11):3143–59.

Spartz, A. K., Lee, S. H., Wenger, J. P., Gonzalez, N., Itoh, H., Inze, D., Peer, W. A., Murphy, A. S., Overvoorde, P. J., and Gray, W. M. (2012). The SAUR19 subfamily of SMALL AUXIN UP RNA genes promote cell expansion. *Plant J*, 70(6):978–90.

Spartz, A. K., Lor, V. S., Ren, H., Olszewski, N. E., Miller, N. D., Wu, G., Spalding, E. P., and Gray, W. M. (2017). Constitutive expression of Arabidopsis sMALL AUXIN UP RNA19 (SAUR19) in tomato confers auxin-independent hypocotyl elongation. *Plant Physiol*, 173(2):1453–62.

Spartz, A. K., Ren, H., Park, M. Y., Grandt, K. N., Lee, S. H., Murphy, A. S., Sussman, M. R., Overvoorde, P. J., and Gray, W. M. (2014). SAUR inhibition of PP2C-D phosphatases activates plasma membrane H+-ATPases to promote cell expansion in Arabidopsis. *Plant Cell*, 26(5):2129–42.

Staswick, P. E., Serban, B., Rowe, M., Tiryaki, I., Maldonado, M. T., Maldonado, M. C., and Suza, W. (2005). Characterization of an Arabidopsis enzyme family that conjugates amino acids to indole-3-acetic acid. *The Plant Cell*, 17(2):616–27.

Steinacher, A., Leyser, O., and Clayton, R. H. (2012). A computational model of auxin and pH dynamics in a single plant cell. *J Theor Biol*, 296:84–94.

Stepanova, A. N., Robertson-Hoyt, J., Yun, J., Benavente, L. M., Xie, D. Y., Dolezal, K., Schlereth, A., Jurgens, G., and Alonso, J. M. (2008). TAA1-mediated auxin biosynthesis is essential for hormone crosstalk and plant development. *Cell*, 133(1):177–91.

Stepanova, A. N., Yun, J., Robles, L. M., Novak, O., He, W., Guo, H., Ljung, K., and Alonso, J. M. (2011). The Arabidopsis YUCCA1 flavin monooxygenase functions in the indole-3-pyruvic acid branch of auxin biosynthesis. *Plant Cell*, 23(11):3961–73.

Stirnberg, P., Chatfield, S. P., and Leyser, H. M. (1999). AXR1 acts after lateral bud formation to inhibit lateral bud growth in Arabidopsis. *Plant Physiology*, 121(3):839–47.

Stirnberg, P., Furner, I. J., and Leyser, H. M. O. (2007). MAX2 participates in an SCF complex which acts locally at the node to suppress shoot branching. *Plant Journal*, 50(1):80–94.

Stirnberg, P., van De Sande, K., and Leyser, H. M. (2002). MAX1 and MAX2 control shoot lateral branching in Arabidopsis. *Development*, 129(5):1131–41.

Swarup, R., Friml, J., Marchant, A., Ljung, K., Sandberg, G., Palme, K., and Bennett, M. (2001). Localization of the auxin permease AUX1 suggests two functionally distinct hormone transport pathways operate in the Arabidopsis root apex. *Genes and Development*, 15(20):2648–53.

Szerszen, J. B., Szczyglowski, K., and Bandurski, R. S. (1994). *iaglu*, a gene from *Zea mays* involved in conjugation of growth hormone indole-3-acetic acid. *Science*, 265(5179):1699–701.

Takahashi, K., Hayashi, K., and Kinoshita, T. (2012). Auxin activates the plasma membrane H+-ATPase by phosphorylation during hypocotyl elongation in Arabidopsis. *Plant Physiol*, 159(2):632–41.

Takei, K., Ueda, N., Aoki, K., Kuromori, T., Hirayama, T., Shinozaki, K., Yamaya, T., and Sakakibara, H. (2004). AtIPT3 is a key determinant of nitrate-dependent cytokinin biosynthesis in Arabidopsis. *Plant Cell Physiol*, 45(8):1053–62.

Tan, X., Calderon-Villalobos, L. I. A., Sharon, M., Zheng, C. X., Robinson, C. V., Estelle, M., and Zheng, N. (2007). Mechanism of auxin perception by the TIR1 ubiquitin ligase. *Nature*, 446(7136):640–5.

Tanaka, M., Takei, K., Kojima, M., Sakakibara, H., and Mori, H. (2006). Auxin controls local cytokinin biosynthesis in the nodal stem in apical dominance. *Plant Journal*, 45(6):1028–36.

Tao, Y., Ferrer, J. L., Ljung, K., Pojer, F., Hong, F., Long, J. A., Li, L., Moreno, J. E., Bowman, M. E., Ivans, L. J., Cheng, Y., Lim, J., Zhao, Y., Ballare, C. L., Sandberg, G., Noel, J. P., and Chory, J. (2008). Rapid synthesis of auxin via a new tryptophan-dependent pathway is required for shade avoidance in plants. *Cell*, 133(1):164–76.

Thimann, K. V. and Skoog, F. (1933). Studies on the growth hormone of plants III: The inhibiting action of the growth substance on bud development. *Proceedings of the National Academy of Sciences of the United States of America*, 19:714–6.

Thimann, K. V., Skoog, F., and Kerckhoff, W. G. (1934). On the inhibition of bud development and other functions of growth substance in *Vicia faba*. *Proceedings of the Royal Society of London Series B-Containing Papers of a Biological Character*, 114(789):317–39.

Tissier, A. F., Marillonnet S Klimyuk, V., Patel, K., Torres, M. A., Murphy, G., and Jones, J. D. (1999). Multiple independent defective suppressor-mutator transposon insertions in Arabidopsis: a tool for functional genomics. *The Plant Cell*, 11:1841–52.

Titapiwatanakun, B., Blakeslee, J. J., Bandyopadhyay, A., Yang, H., Mravec, J., Sauer, M., Cheng, Y., Adamec, J., Nagashima, A., Geisler, M., Sakai, T., Friml, J., Peer, W. A., and Murphy, A. S. (2009). ABCB19/PGP19 stabilises PIN1 in membrane microdomains in Arabidopsis. *Plant Journal*, 57(1):27–44.

Trémousaygue, D., Garnier, L., Bardet, C., Dabos, P., Hervé, C., and Lescure, B. (2003). Internal telomeric repeats and 'TCP domain' protein-binding sites co-operate to regulate gene expression in Arabidopsis thaliana cycling cells. *The Plant Journal*, 33(6):957–66.

Ulmasov, T., Hagen, G., and Guilfoyle, T. J. (1997). ARF1, a transcription factor that binds to Auxin Response Elements. *Science*, 276(5320):1865–8.

Umehara, M., Hanada, A., Yoshida, S., Akiyama, K., Arite, T., Takeda-Kamiya, N., Magome, H., Kamiya, Y., Shirasu, K., Yoneyama, K., Kyozuka, J., and Yamaguchi, S. (2008). Inhibition of shoot branching by new terpenoid plant hormones. *Nature*, 455(7210):195–U29.

van Rongen, M. (2013). *The role of PIN1-dependent auxin flux in Arabidopsis bud activation*. Master's thesis.

Vernoux, T., Brunoud, G., Farcot, E., Morin, V., Van den Daele, H., Legrand, J., Oliva, M., Das, P., Larrieu, A., Wells, D., Guédon, Y., Armitage, L., Picard, F., Guyomarc'h, S., Cellier, C., Parry, G., Koumproglou, R., Doonan, J. H., Estelle, M., Godin, C., Kepinski, S., Bennett, M., De Veylder, L., and Traas, J. (2011). The auxin signalling network translates dynamic input into robust patterning at the shoot apex. *Molecular Systems Biology*, 7(1).

Wang, L., Wang, B., Jiang, L., Liu, X., Li, X., Lu, Z., Meng, X., Wang, Y., Smith, S. M., and Li, J. (2015). Strigolactone signaling in Arabidopsis regulates shoot development by targeting D53-Like SMXL repressor proteins for ubiquitination and degradation. *Plant Cell*, 27(11):3128–42.

Wang, Q., Kohlen, W., Rossmann, S., Vernoux, T., and Theres, K. (2014a). Auxin depletion from the leaf axil conditions competence for axillary meristem formation in Arabidopsis and tomato. *Plant Cell*, 26(5):2068–79.

Wang, Y., Wang, J., Shi, B., Yu, T., Qi, J., Meyerowitz, E. M., and Jiao, Y. (2014b). The stem cell niche in leaf axils is established by auxin and cytokinin in Arabidopsis. *Plant Cell*, 26(5):2055–67.

Waters, M. T., Nelson, D. C., Scaffidi, A., Flematti, G. R., Sun, Y. K., Dixon, K. W., and Smith, S. M. (2012). Specialisation within the DWARF14 protein family confers distinct responses to karrikins and strigolactones in Arabidopsis. *Development*, 139(7):1285–95.

Went, F. (1928). Wuchstoff und wachstum. *Recueil des travaux botaniques néerlandais*, 25:1–116.

Werner, T., Motyka, V., Laucou, V., Smets, R., Van Onckelen, H., and Schmülling, T. (2003). Cytokinin-deficient transgenic Arabidopsis plants show multiple developmental alterations indicating opposite functions of cytokinins in the regulation of shoot and root meristem activity. *Plant Cell*, 15(11):2532–50.

Wickson, M. and Thimann, K. (1958). The antagonism of auxin and kinetin in apical dominance. *Physiologia Plantarum*, 11(1):62–74.

Wilson, A. K., Pickett, F. B., Turner, J. C., and Estelle, M. (1990). A dominant mutation in Arabidopsis confers resistance to auxin, ethylene and abscisic acid. *Mol Gen Genet*, 222(2-3):377–83.

Won, C., Shen, X., Mashiguchi, K., Zheng, Z., Dai, X., Cheng, Y., Kasahara, H., Kamiya, Y., Chory, J., and Zhao, Y. (2011). Conversion of tryptophan to indole-3-acetic acid by TRYPTOPHAN AMINOTRANSFERASES OF ARABIDOPSIS and YUCCAs in Arabidopsis. *Proc Natl Acad Sci U S A*, 108(45):18518–23.

Wu, G., Lewis, D. R., and Spalding, E. P. (2007). Mutations in Arabidopsis multidrug resistance-like ABC transporters separate the roles of acropetal and basipetal auxin transport in lateral root development. *Plant Cell*, 19(6):1826–37.

Wulfetange, K., Lomin, S. N., Romanov, G. A., Stolz, A., Heyl, A., and Schmülling, T. (2011). The cytokinin receptors of Arabidopsis are located mainly to the endoplasmic reticulum. *Plant Physiol*, 156(4):1808–18.

Xu, J., Hofhuis, H., Heidstra, R., Sauer, M., Friml, J., and Scheres, B. (2006). A molecular framework for plant regeneration. *Science*, 311(5759):385–8.

Yang, Y., Hammes, U. Z., Taylor, C. G., Schachtman, D. P., and Nielsen, E. (2006). High-affinity auxin transport by the AUX1 influx carrier protein. *Current Biology*, 16(11):1123–7.

Yao, R., Ming, Z., Yan, L., Li, S., Wang, F., Ma, S., Yu, C., Yang, M., Chen, L., Chen, L., Li, Y., Yan, C., Miao, D., Sun, Z., Yan, J., Sun, Y., Wang, L., Chu, J., Fan, S., He, W., Deng, H., Nan, F., Li, J., Rao, Z., Lou, Z., and Xie, D. (2016). DWARF14 is a non-canonical hormone receptor for strigolactone. *Nature*, 536(7617):469–73.

Young, G., Jack, D., Smith, D., and Saier, M. (1999). The amino acid/auxin:proton symport permease family. *Biochimica et Biophysica Acta (BBA) - Biomembranes*, 1415(2):306–22.

Zhang, K., Novak, O., Wei, Z., Gou, M., Zhang, X., Yu, Y., Yang, H., Cai, Y., Strnad, M., and Liu, C. J. (2014). Arabidopsis ABCG14 protein controls the acropetal translocation of root-synthesized cytokinins. *Nat Commun*, 5:3274.

Zhao, L.-H., Zhou, X. E., Wu, Z.-S., Yi, W., Xu, Y., Li, S., Xu, T.-H., Liu, Y., Chen, R.-Z., Kovach, A., Kang, Y., Hou, L., He, Y., Xie, C., Song, W., Zhong, D., Xu, Y., Wang, Y., Li, J., Zhang, C., Melcher, K., and Xu, H. E. (2013). Crystal structures of two phytohormone signal-transducing α/β hydrolases: karrikin-signaling KAI2 and strigolactone-signaling DWARF14. *Cell Research*, 23(3):436–9.

Zhao, L.-H., Zhou, X. E., Yi, W., Wu, Z., Liu, Y., Kang, Y., Hou, L., de Waal, P. W., Li, S., Jiang, Y., Scaffidi, A., Flematti, G. R., Smith, S. M., Lam, V. Q., Griffin, P. R., Wang, Y., Li, J., Melcher, K., and Xu, H. E. (2015). Destabilization of strigolactone receptor DWARF14 by binding of ligand and E3-ligase signaling effector DWARF3. *Cell Research*, 25(11):1219–36.

Zhao, Y. (2010). Auxin biosynthesis and its role in plant development. *Annu Rev Plant Biol*, 61:49–64.

Zhao, Y. (2012). Auxin biosynthesis: A simple two-step pathway converts tryptophan to indole-3-acetic acid in plants. *Molecular Plant*, 5(2):334–8.

Zurcher, E., Liu, J., di Donato, M., Geisler, M., and Muller, B. (2016). Plant development regulated by cytokinin sinks. *Science*, 353(6303):1027–30.

Östin, A., Kowalyczk, M., Bhalerao, R. P., and Sandberg, G. (1998). Metabolism of indole-3-acetic acid in Arabidopsis. *Plant Physiology*, 118(1):285–96.

Appendix A

Plant lines and sources

Table A.1 Plant line sources

Genotype	Locus	Origin	Published in
Col-0	Ecotype	Leyser lab stock	
abcb1-100	At2g36910	National Arabidopsis Stock Centre, Nottingham, UK	Li et al. (2005)
abcb19-101	At3g28860	National Arabidopsis Stock Centre, Nottingham, UK	Li et al. (2005)
aha1-7	At2g18960	National Arabidopsis Stock Centre, Nottingham, UK	Haruta et al. (2010)
aha2-4	At4g30190	National Arabidopsis Stock Centre, Nottingham, UK	Haruta et al. (2010)
aux1lax1 lax2lax3 quadruple	At2g38120; At5g01240; At2g21050; At1g77690	Braybrook lab, University of Cambridge, UK.	Bainbridge et al. (2008)
aux1-21	At2g38120	Braybrook lab, University of Cambridge, UK.	Marchant and Bennett, (1998)
brc1-2	At3g18550	Pilar Cubas, Centro Nacional de Biotecnologia, Madrid, Spain	Aguilar-Martinez et al., (2007)
brc2-1	At1g68800	Pilar Cubas, Centro Nacional de Biotecnologia, Madrid, Spain	Aguilar-Martinez et al., (2007)
d14-1	At3g03990	Mark Waters, University of Western Australia, Crawley, Australia	Waters et al. (2012)

Continued on next page

Table A.1 – continued from previous page

Genotype	Locus	Origin	Published in
max2-1	At2g42620	Leyser lab stock	Stirnberg et al. (2002)
max4-5	At4g32810	Leyser lab stock	Bennett et al. (2006)
pin1-613	At1g73590	Leyser lab stock	Bennett et al. (2006)
pin2 (*eir1-1*)	At5g57090	Leyser lab stock	Luschnig et al. (1998); Roman et al. (1995)
pin3-3	At1g70940	Ben Scheres, Wageningen University, The Netherlands	Friml et al. (2002b)
pin4-3	At2g01420	Ben Scheres, Wageningen University, The Netherlands	Friml et al. (2002a)
pin5-4	At5g16530	Enrico Scarpella, University of Alberta, Canada	Mravec et al. (2009)
pin6	At1g77110	Enrico Scarpella, University of Alberta, Canada	Tissier et al. (1999)
pin7-1	At1g23080	Ben Scheres, Wageningen University, The Netherlands	Friml et al. (2003)
pin8-1	At5g15100	Enrico Scarpella, University of Alberta, Canada	Dal Bosco et al. (2012)
PIN1:GFPb	At1g73590	Eva Benkova, Institute of Science and Technology, Vienna, Austria	Benkova et al. (2003)
PIN1:GFPs	At1g73590	Ben Scheres, Wageningen University, The Netherlands	Xu et al. (2006)

Table A.2 Plant line descriptions

Genotype	Description
Col-0	Wild type, all plant lines are in this background
abcb1-100	T-DNA insertion, SALK_083649, in exon 9
abcb19-101	T-DNA insertion, SALK_033455, in exon 6
aha1-7	T-DNA insertion, SALK_065288, in exon 13
aha2-4	T-DNA insertion, SALK_082786, in intron 3
aux1 lax1 lax2 lax3	T-DNA insertions in AUX1 and three LIKE-AUX1 genes
aux1-21	Deletion of nucleotide A823 in exon 5
brc1-2	T-DNA insertion, SALK_091920, in exon 3.
brc2-1	T-DNA insertion, SALK_023116, in exon 1.
d14-1	WiscDsLox transposon insertion, WiscDsLoxHs137_07E
max2-1	EMS mutant, with guanine to adenine substitution leading to a non-functional protein
max4-5	Point mutation in exon 2, leading to a premature STOP-codon
pin1-613	T-DNA insertion, SALK_047613, in intron 3
pin2 (*eir1-1*)	Diepoxybutane mutagenesis mutant. Mutation unknown, but allelic to null mutant eir1-3
pin3-3	2 bp deletion in exon 1, producing a frameshift mutation
pin4-3	En-1 transposon insertion 1578 bp from ATG in exon 2
pin5-4	T-DNA insertion, SALK_042994, in intron 2
pin6	Single dSpm transposable element 183 bp upstream from ATG, SM_3_15050
pin7-1	En-1 transposon insertion 702 bp from ATG in exon 1 (resequenced)
pin8-1	T-DNA insertion, SALK_107965, in exon 1
PIN1:GFPb	PIN1-GFP fusion construct under native promoter. GFP insertion at amino acid 443.
PIN1:GFPs	PIN1-GFP fusion construct under native promoter. GFP insertion at amino acid 217.

Appendix B

Primers and genotyping strategies

Table B.1 Genotyping primer sequences

ID	Gene	Sequence	Direction
MVR098	*abcb1-100*	GAAGACTGCGACAAGGACAAG	forward
MVR099	*abcb1-100*	GCAAGAGCGATGTTGAAGAAC	reverse
MVR100	*abcb19-101*	GCAATTGCAATTCTCTGCTTC	forward
MVR101	*abcb19-101*	CTCAGGCAATTGCTCAAGTTC	reverse
MVR080	*aha1-7*	GCGTTGTAACTCTTGCAGTTTG	forward
MVR081	*aha1-7*	CATCTTCTTTTGGCTGCAGAC	reverse
MVR082	*aha2-4*	TTGAAAAGGCTGATGGATTTG	forward
MVR083	*aha2-4*	CTCCAGGACGTTCAACAAAAG	reverse
MVR221	*aux1-21*	CATTTAATTGCACTTTCCTCTTGTT	forward
MVR222	*aux1-21*	CATATACTGTCACCTCAATGCAAAG	reverse
MVR228	*brc1-2*	AACCAAACCATCCCAAAC	forward
MVR229	*brc1-2*	ACCAAGTACCAATCCACA	reverse
MVR230	*brc2-1*	CTTTTCTCCTCATCCACC	forward
MVR231	*brc2-1*	CCTTCTTTTCCTTTCTCTTC	reverse
MVR225	*d14-1*	AAGAATATGGCAAGTGCAAC	forward
MVR226	*d14-1*	GATGATTCCGATCATAGCG	reverse
MVR094	En8130	GAGCGTCGGTCCCCACACTTCTATAC	forward
MVR227	L4 WiscLoxHS	TGATCCATGTAGATTTCCCGGACATGAAG	forward
MVR223	*max2-1*	CCGAATTTGGAAGAGATTAG	forward
MVR224	*max2-1*	CTCAAGCTTCCAATTCCGGT	reverse
MVR248	*max4-5*	GGCGGGTGAGGTGTCGAAGTGGGTCCT	forward

Continued on next page

Table B.1 – continued from previous page

ID	Gene	Sequence	Direction
MVR249	*max4-5*	ATCACTTACGACTTCTCC	reverse
MVR086	*pin1-613*	CAAAAACACCCCCAAAATTTC	forward
MVR087	*pin1-613*	AATCATCACAGCCACTGATCC	reverse
MVR088	*pin3-3*	GGAGCTCAAACGGGTCACC	forward
MVR089	*pin3-3*	TAACCGGAAAGCGACGAGA	reverse
MVR090	*pin4-3*	CCTAAAGAAAACCAACAGCA	forward
MVR091	*pin4-3*	AATTAAACACACAGACCCAC	reverse
MVR144	*pin5-4*	TGTGGTTGTGGGAGAGAAGTC	forward
MVR145	*pin5-4*	AAATTTGGACTTACGCTGTGC	reverse
MVR216	*pin6*	CATAACGAAGCTAACTAAGGGGTAATCTC	forward
MVR217	*pin6*	GGAGTTCAAAGAGGAATAGTAGCAGAG	reverse
MVR092	*pin7-1*	TCCTCGTCCGTCTAATCT	forward
MVR095	*pin7-1*	CCACATCCCACCTTCATATC	reverse
MVR146	*pin8-1*	TGAAAGACATTTTGATGGCATC	forward
MVR147	*pin8-1*	CCAAATCAAGCTTTGCAAGAC	reverse
MVR036	SALK LBb1.3	ATTTTGCCGATTTCGGAAC	forward
MVR218	Spm	TACGAATAAGAGCGTCCATTTTAGAGTG	forward

Table B.2 Sequencing primer sequences

ID	Gene	Sequence	Direction
MVR254	BRC1 fragment 1	CTTCTTTTCTTAGGGCTTC	forward
MVR261	BRC1 fragment 1	CAAACTACAAAGACCAACAG	reverse
MVR255	BRC1 fragment 2	CTTAGTTCTTTCTTACGGTG	forward
MVR262	BRC1 fragment 2	CATATCTCTCTCACCAAAC	reverse
MVR256	BRC1 fragment 3	TTTCTCTCTCTTTCTCTCCA	forward
MVR263	BRC1 fragment 3	GGAGTAATGAAGATCCGT	reverse
MVR257	BRC1 fragment 4	CAAGATCAAAACGGCCAA	forward
MVR264	BRC1 fragment 4	TCTTGTCTTCGCAGTGTGT	reverse
MVR258	BRC1 fragment 5	GACACACTGCGAAGACAA	forward
MVR265	BRC1 fragment 5	CTTTGGCCGTTTTGATCT	reverse
MVR259	BRC1 fragment 6	AGCAGCATCAGTTTACGG	forward
MVR266	BRC1 fragment 6	GGAGAGAAAGAGAGAGAA	reverse
MVR260	BRC1 fragment 7	GTTTGGTGAGAGAGATATG	forward
MVR267	BRC1 fragment 7	CACCGTAAGAAAGAACTAAG	reverse
MVR142	M13	TGTAAAACGACGGCCAGT	forward
MVR143	M13	CAGGAAACAGCTATGACCATG	reverse

Table B.3 Cloning primer sequences

ID	Gene	Sequence	Direction
MVR269	BRC1 (attB1r)	GGGGACTGCTTTTTTGTACAAACTTGCATA CATGTTTTGATAGTTGTGCATGAGG	reverse
MVR270	BRC1 (attB2r)	GGGGACAGCTTTCTTGTACAAAGTGGCGT GAAACTGATTTCATTTAACATTAATAT	forward
MVR271	BRC1 (attB3)	GGGGACAACTTTGTATAATAAAGTTGGAA CAACAACGACCACCCA	reverse
MVR268	BRC1 (attB4)	GGGGACAACTTTGTATAGAAAAGTTGCGG AGAGTGTGTGTGTGAGAG	forward

Table B.4 Genotyping strategies

Gene	Wild type	Insertion/digest
abcb1-100	MVR098 + MVR099	MVR036 + MVR099
abcb19-101	MVR100 + MVR101	MVR036 + MVR101
aha1-7	MVR080 + MVR081	MVR036 + MVR081
aha2-4	MVR082 + MVR083	MVR036 + MVR083
aux1-21	MVR221 + MVR222	Digest with ApaLI
brc1-2	MVR228 + MVR229	MVR036 + MVR229
brc2-1	MVR230 + MVR231	MVR036 + MVR231
d14-1	MVR225 + MVR226	MVR226 + MVR227
max2-1	MVR223 + MVR224	Digest with BccI
max4-5	MVR248 + MVR249	Digest with StyI
pin1-613	MVR086 + MVR087	MVR036 + MVR087
pin3-3	MVR088 + MVR089	Digest with StyI
pin4-3	MVR090 + MVR091	MVR094 + MVR091
pin5-4	MVR144 + MVR145	MVR036 + MVR145
pin6	MVR216 + MVR217	MVR217 + MVR218
pin7-1	MVR092 + MVR095	MVR094 + MVR095
pin8-1	MVR146 + MVR147	MVR036 + MVR147

Appendix C

List of abbreviations

Table C.1 List of abbreviations

Abbreviation	Description
ABC	ATP-binding cassette
ATP	adenosine triphosphate
ATS	Arabidopsis thaliana salt
bp	base pairs
CAT	connective auxin transport
cDNA	complementary DNA
Citrine	a YFP-variant
CPM	counts per minute
DNA	deoxyribonucleic acid
EDTA	ethylenediaminetetraacetic acid
GFP	green fluorescent protein
GR24	racemic mixture of synthetic strigolactones
HSD	honest significant difference
IAA	indole-3-acetic acid
iP	isopentenyladenine
IPA	indole-3-pyruvate
LB	lysogeny broth
NAA	1-naphthaleneacetic acid
NaCl	sodium chloride
NPA	1-N-naphthylphthalamic acid
oxIAA	2-oxindole-3-acetic acid

Continued on next page

Table C.1 – continued from previous page

Abbreviation	Description
PAGE	polyacrylamide gel electrophoresis
PATS	polar auxin transport stream
PCR	polymerase chain reaction
RGI	relative growth index
RNA	ribonucleic acid
RPM	revolutions per minute
SAM	shoot apical meristem
SCF	Skp, Cullin, F-box
SDS	sodium dodecyl sulfate
SOC	super optimal broth with catabolite repression
TBE	Tris/Borate/EDTA
T-DNA	transfer DNA
TIBA	2,3,5-triiodobenzoic acid
Tris-HCl	tris hydrochloride
tZ	*trans*-Zeatin
YFP	yellow fluorescent protein